Genomic Implications of Gene Dosage Imbalance in Autosomal Trisomy during Neurogenesis

Chi Chiu Wang

DOCTOR OF PHILOSOPHY

Center for Information Biology & DNA Data Bank of Japan

National Institute of Genetics

at

Department of Genetics

School of Life Science

The Graduate University for Advanced Studies

Japan

2011

Acknowledgements

This dissertation has only been possible because of the goodwill and generosity of many people and their institutions.

In particular, a very special acknowledgement is made to Professor Takashi Gojobori, my inspiring supervisor, from Center for Information Biology and DNA Data Bank of Japan, National Institute of Genetics, Japan, for his highly inspiration, warm-hearted encouragement, never-ending support, and invaluable assistance in my postdoctoral training in microarray, comparative genomics and molecular evolution and herein my PhD study in Genetics; to Professor Kazuho Ikeo, for his persistent enthusiastism, perpetual willingness, administrative help, and philosophical suggestion during preparation of the dissertation and application of JSPS scholarships; and also to Professor Michael Scott Rogers, my motivating advisor, from Department of Obstetrics and Gynaecology, The Chinese University of Hong Kong, for his constant advice, academic support and clinical guidance since my first PhD study in Surgical Sciences.

I should thank Professor Mitsuo Oshimura and his associates and students for their assistance in conducting the chromosome transfer experiments and stem cell research over their advanced research establishment in the Department of Molecular and Cell Genetics, School of Life Sciences, Tottori University, Japan.

The studies were supported in part by several research scholarships and grants, including Postdoctoral Fellowship for Foreign Researchers for FY 2001 (P-01104) & RONPAKU (Dissertation PhD) Program for FY 2009, FY 2010 & FY 2011 (CHN-10902) from Japan Society for the Promotion of Science (JSPS); Li Ka Shing Institute of Health Sciences Grant for Embryonic Stem Cell Research (6901988), Medicine Panel Direct Grant (2008.1.052 & 2002.2.024), Special Grant for Teaching Staff to Conduct Research Outside Hong Kong (2004) from The Chinese University of Hong Kong.

Last but not least I would like to thank all the supports from my department and university and also specially dedicate this thesis to my respected parents and my beloved Sally and Nicole for their greatest understanding, patience and love.

Table of Contents

Abstract

Autosomal trisomy is a numerical chromosomal anomaly with an extra single copy of an autosomal chromosome. It is associated with general developmental failure followed by processes of neurodegeneration. Moreover, variable cognitive impairment and behavioural phenotypes are markedly presented, although relationship between learning difficulty and autosomal trisomic conditions is still unclear.

The most common and important autosomal trisomy at live birth in human is trisomy 21, 3 copies of human chromosome 21. It attributes to over 95% of Down syndrome. Many efforts had been made to identify loci and genes on human chromosome 21 in association with the neurodevelopmental pathology through such methods as gene cloning, locus mapping, animal modelling and chromosome sequencing. However, only very few critical genomic regions and genes in the human chromosome 21 can be linked with neurological manifestations in Down syndrome. Thus, it is quite unlikely that neurological manifestations in Down syndrome are due to only a few numbers of specific genomic regions and genes through autosomal trisomy. Instead, currently prevalent working hypothesis of autosomal trisomy is the global (namely genome-wide) dosage imbalance of increased gene products in the extra chromosome.

A direct link of the cognitive conditions of Down syndrome to the global gene dosage imbalance is complexly difficult because of its multiply underlying genetic causes and the large number of genes affected by the aneuploidy itself. Taking an advantage of technological advancements of genomic approaches, however, a large-scale analysis of transcriptomic and proteomic profiling have been conducted for understanding the gene dosage imbalance of autosomal trisomy. In most of those studies, unfortunately, neural tissues and neurogenesis-related cells have been never used: Indeed, the studies were carried out mostly on adult materials, even amniocytes, placental or fibroblast cells. Moreover, it is known that many of the pathological traits of autosomal trisomy are likely to be linked to the alteration of neural pathways during an early stage of embryonic development. In particular, abnormalities in brain developments contributing to the cognition phenotypes in autosomal trisomy are likely to arise during embryogenesis. Thus, it is

critically important to conduct genome-wide investigation at early stages during neurogenesis and neural differentiation.

The aim of the present thesis is to clarify the genomic features of autosomal trisomy by examining the working hypothesis that autosomal trisomy causes the global dosage imbalance of increased gene products in the extra chromosome. To attain the aim, I conducted genome-wide analyses of transcriptomic and proteomic profiling for understanding the genomic features of gene dosage imbalance of autosomal trisomy, using mouse embryonic stem cell lines containing either extra human or mouse autosomal chromosome(s). Establishing these chromosomally engineered embryonic stem cell lines of mouse by chromosome transfer technologies, I used the aneuploid neurons to which the engineered embryonic stem cells were differentiated *in vitro*. In particular, I focused upon chromosome 21 trisomy in this study because of its apparent connection to Down syndrome.

For a large scale analysis of gene expression profiling, I employed microarray and two-dimensional electrophoresis for transcriptomic and proteomic examinations, respectively. The profiling data obtained was subjected to data mining by bioinformatics analysis that I conducted, in order to study molecular mechanisms of autosomal imbalance and its genomic implications in early development of the nervous system.

Once I obtained candidate genes associated with autosomal trisomy from the data mining, I further carried out quantitative and functional analyses of those genes by embryoid body formation assay and RNA interference *in vitro* and teratoma and chimeric models of mouse *in vivo*. These analyses were conducted to identify possible roles of those genes in the autosomal trisomy at early stages of neuron differentiation and brain developments.

In the present study, I obtained the following results:
First, my transcriptomic analysis of microarray demonstrated that for the trisomic genes (on chromosome 21) in the differentiating aneuploid neurons, there were three categorical gene classes of up-regulated, no changed and down-regulated gene expressions: (1) 30 genes showed the 1.5-fold increased level of expression (primary gene dosage effect), which occupied 54%, (2)

14 genes indicated no changes (dosage compensation), which corresponded to 25%, and (3) 12 genes manifested 1.5-fold decreased level (reverse gene dosage effect), which was 21%. Thus, I found that the significant imbalance of gene dosage of autosomal trisomy was taking place in the genome-wide fashion at early stages of the developing neurons and brains.

Second, I focused upon the genes of primary dosage effect, namely up-regulated genes, because they occupied a largest proportion in the trisomic genes examined. Then, I found that 118 disomic genes (on all the autosomal chromosomes except chromosome 21) manifested significantly positive correlation with the trisomic genes (on chromosome 21) whereas 47 other disomic gens showed significantly negative correlation. Thus, I found a total of 165 genes that are located on all the autosomal chromosomes other than chromosome 21 and that are possibly influenced by the secondary or trans-acting effects of the genes on additional chromosome 21. Moreover, those 165 disomic genes are rather evenly distributed over the entire genome, implying that there exists genome-wide background association with the trisomic genes of primary gene dosage effect.

Third, from my gene ontology analysis, I showed that the trisomic genes of primary gene dosage effect are mainly involved in the molecular function of proteins such as translational regulators and nuclear transcriptional factors. When I conducted further a comparative proteomic analysis, I made the observations indicating a possibility that the post-transcriptional and translational machineries are working as a underlying mechanism of gene products manifested during the neurogenesis in autosomal trisomy. This is also good indication for supporting genome-wide association of the trisomic genes of primary gene dosage.

Fourth and the last, I successfully identified a few of gene sets that show clear association with the enhanced apoptosis during early neural differentiation *in vitro* and in aneuploid neurons *in vitro* as well as fetal brains *in vivo*. Those gene set may be the candidate genes that are responsible for possible link of the cognitive conditions of Down syndrome to the genome-wide gene dosage imbalance.

In conclusion, I found that the gene dosage imbalance of autosomal trisomy globally (genome-widely) affects gene expression and protein expression of the disomic genes early in neurogenesis. The autosomal imbalance is associated with general neuronal loss possibly through underlying of neural apoptosis during neural differentiation. The understanding of the molecular mechanisms of the neural development in autosomal trisomy relies on the integration of multilevel molecular data such as transcriptomic, proteomic, and metabolomic data. From these reasons, I concluded that massive data mining and its further systematic analysis by bioinformatics approaches are essential for understanding the genomic implication of the gene dosage imbalance in autosomal trisomy.

List of Figures

List of Tables

Publications

Journal publications in developmental genomics, gene expression profile and bioinformatics

collaborations with host institution (National Institute of Genetics, Japan):

1. **Wang CC**, Shum ASW, Leung MBW, Hwang JS, Rogers MS, Gojobori T, Ikeo K. 2003 Microarray analysis of differential gene expression in embryos of diabetic mice. *In*: *EUROMEDLAB 2003*. Monduzzi Editore S.p.A., MEDIMOND Inc., Italy. pp 979-981.
2. **Wang CC**, Hwang JS, Rogers MS, Gojobori T, Ikeo K. 2003 Triple hybridization: a new implementation of microarray profiling. *In: EUROMEDLAB 2003*. Monduzzi Editore S.p.A., MEDIMOND Inc., Italy. pp.975-978.
3. **Wang CC**, Kadota M, Nishigaki R, Shirayoshi Y, Rogers MS, Gojobori T, Ikeo K, Oshimura M. 2004 Molecular hierarchy in neurons differentiated from mouse ES cells containing a single human chromosome 21. *Biochem Biophy Res Commun* 314: 335-350.
4. Kadota M, Nishigaki R, **Wang CC**, Toda T, Shirayoshi Y, Gojobori T, Ikeo K, Rogers MS, Oshimura M. 2004 Proteomic signatures and aberrations of mouse embryonic stem cells containing a single human chromosome 21 in neuronal differentiation: an *in vitro* model of Down syndrome. *Neuroscience* 129: 325-335.
5. **Wang CC**, Tang LY, Choy KW, Rogers MS, Gojobori T, Ikeo K, Lam DSC, Pang CP. 2005 New transcription factors for early eye formation in mouse. *Genes Genet Syst* 80: 427.
6. **Wang CC**, Hwang JS, Gojobori T, Ikeo K. 2005 New Implementation of microarray profiling by triple hybridization. *Clin Chem 51*: A196-197, D-129.
7. Choy KW, **Wang CC**, Ogura A, Lau TK, Rogers MS, Ikeo K, Gojobori T, Lam DSC, Pang CP. 2006 Genomic annotation of 15,809 ESTs identified from pooled early gestation human eyes. *Physiol Genomics* 25(1): 9-15.
8. Choy KW, **Wang CC**, Ogura A, Lau TK, Rogers MS, Ikeo K, Gojobori T, Tang LY, Lam DSC, TKH Chung, Pang CP. 2006 Molecular characterization of developmental gene in eyes: through data-mining on integrated transcriptome databases. *Clin Biochem* 39(3): 224-230.
9. **Wang CC**, Tang LY, Choy KW, Gojobori T, Ikeo K, Pang CP. 2007 A novel transcription factor for optic vesicle induction and neuroepithelium differentiation during eye development in mouse. Asian J Ophthalmol 9(1) S1: 81 (100).
10. Uehara S, Izumi Y, Kubo Y, **Wang CC**, Mineta K, Ikeo K, Gojobori T, Tachibana M, Shiroishi T, Yamamoto H. 2008 A characteristic role for anti-oxidant responses of the inner ear melanocytes essential for hearing acuity. *Pigm Cell Melanoma Res* 21(2): 310-311, 2008.
11. Uehara S, Izumi Y, Kubo Y, **Wang CC**, Mineta K, Ikeo K, Gojobori T, Tachibana M, Kikuchi T, Kabayashi T, Shibahara S, Taya C, Yonekawa H, Shiroishi T, Yamamoto H. 2009 Specific expression of Gsta4 in mouse cochlear melanocytes: A novel role for hearing and melanocyte differentiation. *Pigm Cell Melanoma Res* 22(1): 111-119.
12. **Wang CC**, Kazuki Y, Oshimura M, Ikeo K, Gojobori T. 2011 Gene dosage imbalance of human chromosome 21 in mouse embryonic stem cells differentiating to neurons. *Gene* 481: 93-101.

collaborations with home institution (The Chinese University of Hong Kong, Hong Kong) and others:

1. **黃志超**。 2004 唐氏綜合征胚胎幹細胞神經元分化過程中的基因劑量失衡：轉錄組學、蛋白組學表達和生物信息學分析。*中國科協第五屆青年學術年會文集: 科技工程與經濟社會協調發*

展。張玉台主編, 中國科學技術出版社, 分5生命科學與生物技術前沿。

2. **Wang CC**. 2005 Development of rhombencephalon: molecular evolution and genetic regulation. *Neuroembryology & Aging* 3: 78-91.
3. Chu CY, Xiao X, Zhou XG, Lau TK, Rogers MS, Fok TF, Law LK, Pang CP, **Wang CC**. 2006 Metabolomic and bioinformatics analyses in asphyxiated neonates. *Clin Biochem* 39(3): 203-209.
4. Borchert A, **Wang CC**, Ufer C, Schiebel H, Savaskan NE, Kuhn H. 2006 The role of phospholipids hydroperoxide glutathione peroxidase (GPx4) isoforms in murine embryogenesis. *J Biol Chem* 281(28): 19655-19664.
5. Choy KW, Wong HK, Tang LY, **Wang CC**, Lau TK, Pang CP. 2007 Gene expression of human fetal retinal ganglion cell during early eye development. *Asian J Ophthalmol* 9(1) S1: 81-82.
6. Han Y, **Wang CC**, Feng HL, Haines CJ. 2007 Genomic and proteomic controls of infertility in sterile partial t-haplotype mice. *Fertil Steril* 88; S373.
7. Kurosaki H, Kazuki Y, Hiratsuka M, Inoue T, Matsui Y, **Wang CC**, Kanatsu-Shinohara M, Shinohara T, Toda T, Oshimura M. 2007 A comparison study in the proteomic signatures of multipotent germline stem cells, embryonic stem cells, and germline stem cells. *Biochem Biophys Res Commun* 353(2): 259-267.
8. Ufer C, **Wang CC**, Fahling M, Schiebel H, Thiele BJ, Billett EE, Kuhn H, Borhert A. 2008 Translational regulation of glutathione peroxidase 4 expression through guanine-rich sequence binding factor 1 is essential for embryonic brain development. *Gene Dev* 1835-1850. (equal 1st author)
9. Choy KW, Tsang PT, Leung TY, **Wang CC**, Lau TK. 2008 The application of microarray based comparative genomic hybridization in prenatal diagnosis. *Fetal Matern Med Rev* 19(2): 119-133.
10. Law LW, Lau TK, Fung TY, Leung TY, **Wang CC**, Choy KW. 2009 De novo 16p13.11 microdeletion identified by high resolution array CGH in a fetus with increased nuchal translucency. *Br J Obstet Gynaecol* 116(2): 339-343.
11. Wong HK, **Wang CC**, Pang CP, Choy KW. 2009 Identification of coding and non-coding RNA(s) specific for early human retina development. *Mech Dev* 126: S169.
12. Kai Y, **Wang CC**, Kishigami S, Kazuki Y, Abe S, Takiguchi M, Wakayama T, Shirayoshi Y, Inoue T, Ito H, Oshimura M. 2009 Enhanced apoptosis during early neuronal differentiation in mouse ES cells with autosomal imbalance. *Cell Research* 19(2): 247-258.
13. Ufer C, **Wang CC**, Borchert A, Heydeck D, Kuhn H. 2010 Redox control in mammalian embryo development. *Antioxid Redox Sign* 13(6): 833-875.

Journal publications in areas other than developmental genomics

as first or senior author:

1. **Wang CC**, Rogers MS. 1997 Lipid peroxidation in cord blood: the effects of umbilical nuchal cord. Br J Obstet Gynecol. 104: 251-255.
2. **Wang CC**, Rogers MS. 1997 Lipid peroxide in cord blood: the effect of amniotic fluid volume during labour. Br J Obstet Gynecol 104: 1140-1144.
3. **Wang CC**, Rogers MS. 1997 Lipid peroxide in cord blood: a randomised sequential pairs study of prophylactic saline amnioinfusion for intrapartum oligohydramnios. Br J Obstet Gynecol 104: 1145-

1151.

4. Rogers MS, Mongellia JM, Tsang B, **Wang CC**. 1999 Fetal and maternal level of lipid peroxidation in term pregnancies. Acta Obstet Gynecol Scand 78: 120-124.
5. Rogers MS, **Wang CC**. 1999 A comparison of three ultrasound estimates of intrapartum oligohydramnios for prediction of fetal hypoxia-reperfusion injury. Early Human Development 56: 117-126.
6. **Wang CC**, Chu CY, Chu KO, Choy KW, Rogers MS, Khaw KS, Pang CP. 2004 Trolox-equivalent antioxidant capacity (TEAC) assay versus oxygen radical absorbance capacity (ORAC) assay in plasma. Clin Chem 50: 952-954.
7. **Wang CC**, Rogers MS, Pang CP. 2006 Measurements of Total Antioxidant Capacity. In: Antioxidants: New Research. Columbus F Ed. Nova Science, New York. pp.153-175.
8. **Wang CC**, Rogers MS. 2007 Oxidative Stress and Fetal Hypoxia. In Reactive Oxygen Species and Disease. Goth Laszlo Ed. Research Signpost, India. pp.257-282 .
9. **Wang CC**, Yim KW, Poon TCW, Choy KW, Chu CY, Lui WT, Lau TK, Rogers MS, Leung TN. 2007 Innate immune response by ficolin binding in apoptotic placenta is associated with the clinical syndrome of preeclampsia. Clin Chem 53: 42-52.
10. **Wang CC**, Yim KW, Poon TCW, Choy KW, Chu CY, Lui WT, Leung TN, Lau TK, Rogers MS. 2007 The role of lectin-complement pathway in innate immune responses in clinical preeclampsia. Am J Reprod Immunol 57, 467.
11. **Wang CC**, Chu KO, Chong WS, Li WY, Pang CP, Shum ASW, Lau TK, Rogers MS. 2007 Tea epigallocatechin-3-gallate increased 8-isoprostane level and induced caudal regression in developing rat embryos. Free Radic Biol Med 43, 519-527.
12. Xu H, Lui WT, Chu CY, Ng PS, **Wang CC**, Rogers MS. 2009 Anti-angiogenic effects of green tea catechin on an experimental endometriosis mouse model. Human Reprod 24(3): 608-618.
13. Chu CY, Poon CW, Pong JCF, Pang CP, **Wang CC**. 2009 Human normal tear Proteome. Graef Arch Clin Exp 247, 725-727.
14. Pong JCF, Chu CY, Chu KO, Poon TCW, Ngai SM, Pang CP, **Wang CC**. 2010 Identification of Hemopexin in Tear Film. Anal Biochem 404(1): 82-85.
15. **Wang CC**. 2010 Therapeutic values of Vitamin E in clinical practice. In: Vitamin E: Nutrition, Side Effects and Supplements. Columbus F Ed. Nova Science, New York.
16. Xu H, **Wang CC**. 2010Angiogenesis and Anti-angiogenesis Therapy of Endometriosis. In: Endometriosis: Symptoms, Diagnosis and Treatments. Columbus F Ed. Nova Science, New York. Chapter 1, pp. 1-40.
17. Khaw KS, Ngan Kee WD, Chu CY, Ng FF, Tam WH, Critchley LAH, Rogers MS, **Wang CC**. 2010 The effect of different inspired oxygen fractions on lipid peroxidation during general anaesthesia for elective Caesarean section. Br J Anaesth 105(3): 355-360.

Conference Abstracts related to the thesis:

1. **Wang CC**. Bioinformatics and application of microarray biotechnology in medical research. *Faculty Research Day 2004*. Faculty of Medicine, The Chinese University of Hong Kong, Hong Kong. 7 February 2004. (**Invited Speaker**)
2. **Wang CC**. Gene dosage imbalance in mouse genome with an extra human Chr21. *Biosciences*

Alumin Network China, Shanghai, China. 7-9 May 2004. (Poster)

3. **Wang CC**. Transcriptomic to proteomic: microarray and 2D-PAGE/MALDI-TOF MS in TT2F/hChr21 neuronal differentiation. *Biosciences Alumin Network China.* Shanghai, China. 7-9 May 2004. (**DAAD Travel Grant**, **Invited Speaker**)

4. **Wang CC**. A mouse ES neuronal differentiation model for gene dosage imbalance in Down syndrome. *2004 Sir Edward Memorial Fund Postgraduate Conference*. The Chinese University of Hong Kong, Hong Kong. 14-15 June 2004. (Poster)

5. **Wang CC**. An in silico system biology approach for integrating and evaluating complex brain development in mouse embryos. *Beyond Genome 2004*. San Francisco, USA. 21-24 June 2004. (Poster)

6. **Wang CC**. Gene dosage imbalance in Down syndrome ES neuron differentiation: transcriptomic and proteomic expression and bioinformatic analyses. *5th China Association of Science and Technology Conference of Young Scientists*. Shanghai, China. 1-5 November 2004. (**CAST Travel Award**, **Invited Speaker**)

7. **Wang CC**. Neuron differentiation in mouse ES cells containing a single human chromosome 21: an *in vitro* model of neurogenesis in Down's syndrome. *Frontiers in Biomedical Research HKU 2004*. The University of Hong Kong, Hong Kong. 3 December 2004. (**Invited Speaker**)

8. **Wang CC**. *In vitro* neurogenesis and cardiogenesis in mouse ES cells containing a single hChr21. *Stem Cell Symposium*. Faculty of Medicine, The Chinese University of Hong Kong. 14 January 2005. (**Invited Speaker**)

9. **Wang CC**, Rogers MS, Gojobori T, Ikeo K. Microarray bioinformatics in developmental biology and medicine. *Symposium in Developmental Genomics and Bioinformatics*. The Chinese University of Hong Kong, Hong Kong. 7 April 2005. (**Invited speaker**)

10. **Wang CC**, Kadota M, Nishigaki R, Oshimura M, Rogers MS, Gojobori T, Ikeo K. Transcriptomic and proteomic aberration in Down's neurogenesis. *The 3rd Hong Kong Medical Genetics Conference*. Hong Kong Society of Medical Genetics. Hong Kong. 8-10 April 2005. (Poster, **Outstanding Poster Award**)

11. **Wang CC**, Rogers MS, Gojobori T, Ikeo K. Microarray bioinformatics in developmental biology and biomedicine. *The 3rd Hong Kong Medical Genetics Conference*. Hong Kong Society of Medical Genetics. Hong Kong. 8-10 April 2005. (**Invited speaker**)

12. **Wang CC**. An *in vitro* neuronal differentiation model for gene dosage imbalance in Down syndrome. *Mount Desert Island Stem cell Symposium*. The Mount Desert Island Biological Laboratory and The Jackson Laboratory, Maine, USA. 12-14 August, 2005. (Selected Oral)

13. **Wang CC**. Developmental Genomics and Bioinformatics in Brain and Eye Development. *The 21st Century of COE Program. Department of Biomedical Science*, Regenerative Medicine and Biofunction, Graduate School of Medical Science, Tottori University, Yonago, Japan. 21 April 2006. (**Visiting Professorship**)

14. **Wang CC**. Establishing trisomy human embryonic cell lines by chromosome transfer technology. *5th International Society of Stem Cell Research*, Queensland, Australia, 17-20 June 2007. (**ISSCR Travel Award**, Poster)

15. **Wang CC**, Kai Y, Oshimura M. A novel molecular pathway responsible for the defective neuronal differentiation and neurodegeneration in aneuploidy mouse embryonic stem cell lines and transgenic mice. *5th International Society of Stem Cell Research*, Queensland, Australia, 17-20 June 2007. (**ISSCR Travel Award**, Poster)

Awards

2000 Dec

Postdoctoral Fellowship for Foreign Researchers for FY 2001 (P 01104), Japan Society for the Promotion of Science (JSPS), Japan studying at Center for Information Biology (CIB) & DNA Data Bank of Japan (DDBJ), National Institute of Genetics (NIG), Mishima, Japan. 7 May 2001 - 6 May 2002.

2002 Mar

Grant-in-Aids for FY 2001 (P 01104), Japan Society for the Promotion of Science (JSPS), Japan attending Microarray Bioinformatics Course in University of Oxford, Oxford, United Kingdom. 18-22 March 2002.

2004 May

Travel Grant, Deutscher Akademischer Austausch Dienst (DAAD), German Academic Exchange Service, Germany presenting at the Biosciences Alumni Network China, Shanghai Institutes for Biological Sciences (SIBS) of the Chinese Academy of Sciences (CAS), Shanghai, China. 7-9 May 2004.

2004 Nov

Travel Grant, China Association for Science and Technology (CAST), Beijing presenting at the 5th CAST Conference of Young Scientists, Shanghai, China. 1-5 November 2004.

2005 Apr

Outstanding Poster Award, Hong Kong Society of Medical Genetics (HKSMG), Hong Kong presenting at the 3rd Hong Kong Medical Genetics Conference, Hong Kong. 8-10 April 2005.

2006 Aug

HUGO Travel Award, The Human Genome Organisation (HUGO), United Kingdom attending the 5th HUGO Mutation Detection Training Course in Leiden, Netherlands. 31 Aug - 4 Sept 2006.

2006 Aug

Visiting Professorship, 21st Century COE Programme in Chromosome Engineering Technology, Ministry of Education, Culture, Sports, Science and Technology (MEXT), Japan visiting School of Life Sciences, Faculty of Medicine, Totorri University. Yonago, Japan. 13-23 April 2006.

2007 Jun

Travel Award, International Society for Stem Cell Research (ISSCR), USA presenting at the 5th International Society of Stem Cell Research, Queensland, Australia, 17-20 June 2007.

2008 Dec

Ronpaku Fellowship for FY 2009, 2010 & 2011 (CHN-10902), Japan Society for the Promotion of Science (JSPS), Japan studying at Department of Genetics, School of Life Science, The Graduate University for Advanced Studies, c/o Center for Information Biology (CIB) & DNA Data Bank of Japan (DDBJ), National Institute of Genetics (NIG), Mishima, Japan.

2011 Jan

Staff Development Grant 2011/2012. C.Y. Kwan/Lee Hysan Foundation Endowment Funds/Sino-British Fellowship Trust Fund for Staff Development, The Chinese University of Hong Kong.

Chapter 1

Genetics of Autosomal Trisomy

1.1. Chromosomes and Karyotypes

A chromosome is an organized structure of DNA and protein in cells. It is a single piece of coiled DNA containing many genes, regulatory elements and other nucleotide sequences. Chromosomes also contain DNA-bound proteins, which serve to package the DNA and control its functions. The word chromosome comes from the Greek χρῶμα (chroma, color) and σῶμα (soma, body) due to their property of being very strongly stained by particular dyes.

A karyotype is the number and appearance of chromosomes in the nucleus of a eukaryote cell (White MJD 1973, Stebbins GL 1950). The term is also used for the complete set of chromosomes in a species, or an individual organism. Karyotypes describe the characteristics of chromosomes under a light microscope, including their number, length, position of the centromeres, differences between the chromosomes, and other physical characteristics (King et al 2006).

Chromosomes can be divided into two types: autosomes and sex chromosomes. Normal human cells have 23 pairs of large linear nuclear chromosomes, include 22 pairs of autosomes and 1 pair of sex chromosomes (Miller & Therman 2001). The basic number of chromosomes in the somatic cells of an individual or a species is called the somatic number and is designated as 2n. Thus, in humans 2n = 46. In the germ-line (the sex cells) the chromosome number is n (humans: n = 23). Closer to Homo sapiens, the great apes have 2n = 48 chromosomes. Studies in chromosomes and karyotypes can be used for many purposes, such as chromosomal aberrations, cellular function, taxonomic relationships, and past evolutionary events.

1.2. Diversity and Evolution

Chromosomes vary widely between different organisms. The DNA molecules may be circular or linear, and can be composed of 10,000 to 1,000,000,000nucleotides in a long chain (Paux et al 2008). Typically eukaryotic cells (cells with nuclei) have large linear chromosomes and prokaryotic cells (cells without defined nuclei) have smaller circular chromosomes, although there are many exceptions to this rule. Furthermore, cells may contain more than one type of chromosome; for example, mitochondria in most eukaryotes and chloroplasts in plants have their own small chromosomes. The variations in chromosome number between species provide the basis for a range of studies in evolutionary cytology. In some cases there is even significant variation within species (Godfrey & Masters 2000). It is clear that changes in karyotype organization have effects on the evolutionary course of many species, but the significance of karyotype evolution is obscure (Maynard SJ 1998).

Changes during development. Some organisms go in for large-scale elimination of heterochromatin or other kinds of visible adjustment to the karyotype during development. In some species, as in many sciarid flies, entire chromosomes are eliminated during development (Goday & Esteban 2001). In some copepods and roundworms, such as Ascaris suum, portions of the chromosomes are cast away in particular cells. This process is a carefully organized genome rearrangement where new telomeres are constructed and certain heterochromatin regions are lost (Müller et al 1996, Wyngaard & Gregory 2001). In Ascaris suum, all the somatic cell precursors undergo chromatin diminution (Gilbert SF 2006).

Number of chromosomes. The number of chromosomes in the karyotype between (relatively) unrelated species is hugely variable. The low record is held by the nematode, Parascaris univalens, where the haploid n = 1; the high record would be somewhere amongst the ferns, with the Adder's Tongue Fern Ophioglossum ahead with an average of 1,262 chromosomes (Khandelwal S 1990). Top score for animals might be the short nose sturgeon, Acipenser brevirostrum, at a mere 372 chromosomes (Kim et al 2005). The existence of supernumerary or B chromosomes means that chromosome number can vary even within one interbreeding population; and aneuploids are another example, though in this case they would not be regarded

as normal members of the population. On the other hand, a spectacular example of variability between closely related species is the muntjac, which was investigated by Kurt Benirschke and his colleague Doris Wurster. The diploid number of the Chinese muntjac, Muntiacus reevesi, was found to be 46, all telocentric. When looked at the karyotype of the closely related Indian muntjac, Muntiacus muntjak, it was astonished to find it had female 2n = 6, male 2n = 7 chromosomes (Wurster & Benirschke 1970).

Chromosomal polymorphism. Some animal species are polymorphic for chromosome fusions or dissociations (Ford EB 1975). When this happens, the chromosome number is variable from one individual to another. Well-researched examples are the ladybird beetle, Chilocorus stigma, some mantids of the genus Ameles and European shrew Sorex araneus. There is some evidence from the case of the mollusc, Thais lapillus (the dog whelk) on the Brittany coast, that the two chromosome morphs are adapted to different habitats (White MJD 1973).

1.3. Chromosomal Abnormalities

Chromosomal abnormalities are disruptions in the normal chromosomal content of a cell, and are a major cause of genetic disorders (Fig. 1.1). In general, chromosome abnormalities can be classified as change in the number of chromosomes (numerical abnormalities) and change in the structure of chromosomes (structural abnormalities) (Gardner & Sutherland 1996).

In numerical chromosomal abnormalities, abnormal number of chromosomes is known as aneuploidy which occurs when an individual is either missing a chromosome from a pair (monosomy) or has more than two chromosomes of a pair (trisomy, tetrasomy, etc).

For structural chromosomal abnormalities, abnormal structure of chromosomes may include:
(1) deletions, a portion of the chromosome is missing or deleted.
(2) duplications, a portion of the chromosome is duplicated, resulting in extra genetic material.

Chromosomal Abnormalities			
Numerical Abnormalities		**Structural Abnormalities**	**Others**
Less	*More*		
Autosomes			
Monosomies/Deletion	**Trisomies**	**Deletions**	
(Chr 4) Wolf-Hirschhorn syndrome	(Chr 21) Down syndrome	(Chr 4) Wolf-Hirschhorn syndrome	Fragile X syndrome
(Chr 5) Cri du chat syndrome	(Chr 18) Edwards syndrome	(Chr 11) Jacobsen syndrome	Uniparental disomy
(Chr 7) Williams syndrome	(Chr 13) Patau syndrome	**Duplications**	Gonadal dysgenesis
(Chr 11) Jacobsen syndrome	(Chr 9) Trisomy 9	(Chr 17) Charcot-Marie-Tooth disease type 1A	
(Chr 17) Miller-Dieker/Smith-Magenis syndrome	(Chr 8) Warkany syndrome	**Translocations**	
(Chr 22) Di George's syndrome	(Chr 22) Cat eye syndrome	Reciprocal translocation	
(Chr 15) Angelman/Prader–Willi syndrome	(Chr 16) Trisomy 16	Robertsonian translocation	
		Inversions	
		Rings	
Sex-chromosomes		**Isochromosome**	
Monosomy	**Trisomy/Tetrasomy**		
(XO) Turner syndrome	(47,XXY) Klinefelter's syndrome		
	(48,XXYY)		
	(49,XXXXY)		
	(47,XXX) Triple X syndrome		
	(48,XXXX)		
	(49,XXXXX)		
	(47,XYY)		

Figure 1.1 Classifications of chromosomal abnormalities.

(3) translocations, when a portion of the chromosome is transferred to another chromosome. There are two main types of translocations: reciprocal translocation, segments from two different chromosomes have been exchanged; and Robertsonian translocation, an entire chromosome has attached to another at the centromere. In humans these only occur with chromosomes 13, 14, 15, 21 and 22.

(4) inversions: a portion of the chromosome has broken off, turned upside down and reattached, therefore the genetic material is inverted.

(5) rings, a portion of the chromosome has broken off and formed a circle or ring. This can happen with or without loss of genetic material.

(6) isochromosome, formed by the mirror image copy of the chromosome segment including the centromere.

Chromosome abnormalities usually occur when there is an error in cell division following meiosis or mitosis. The chromosome abnormalities occur in meiosis during formation of egg or sperm, are therefore not inherited and the abnormality is present in every cell of the body. Some abnormalities, however, can happen after conception, resulting in mosaicism. Such chromosome anomalies can be inherited from a parent or be *de novo*.

1.4. Aneuploidy in Organisms

Aneuploidy is the condition in which the chromosome number in the cells is not the typical number for the species. This would give rise to a chromosome abnormality such as an extra chromosome or one or more chromosomes lost. Abnormalities in chromosome number usually cause a defect in development.

Most organisms that reproduce sexually have pairs of chromosomes in each cell, with one chromosome inherited from each parent. Meiosis creates gametes (eggs or sperm) that have only one set of chromosomes. If the chromosome pairs fail to separate properly during cell division the egg or sperm may have a second copy of one of the chromosomes, it is known as nondisjunction (Fig. 1.2). This could arise from a failure of homologous chromosomes to separate in meiosis I, or the failure of sister chromatids to separate during meiosis II or mitosis. If such a gamete results in fertilization and an embryo, the resulting embryo may have an entire copy of the extra chromosome (Snustad & Simmons 2006).

The presence of three copies of a chromosome rather than the normal two is defined as trisomy. Trisomy is an aneuploidy occur with any chromosome, either in non-sex chromosomes (autosomal trisomies) or in sex chromosomes (sex-chromosome trisomies). Trisomy 16 is the most common trisomy in humans, occurring in more than 1% of pregnancies (Hassold et al, 1995). This condition, however, usually results in spontaneous miscarriage in the first trimester of pregnancy.

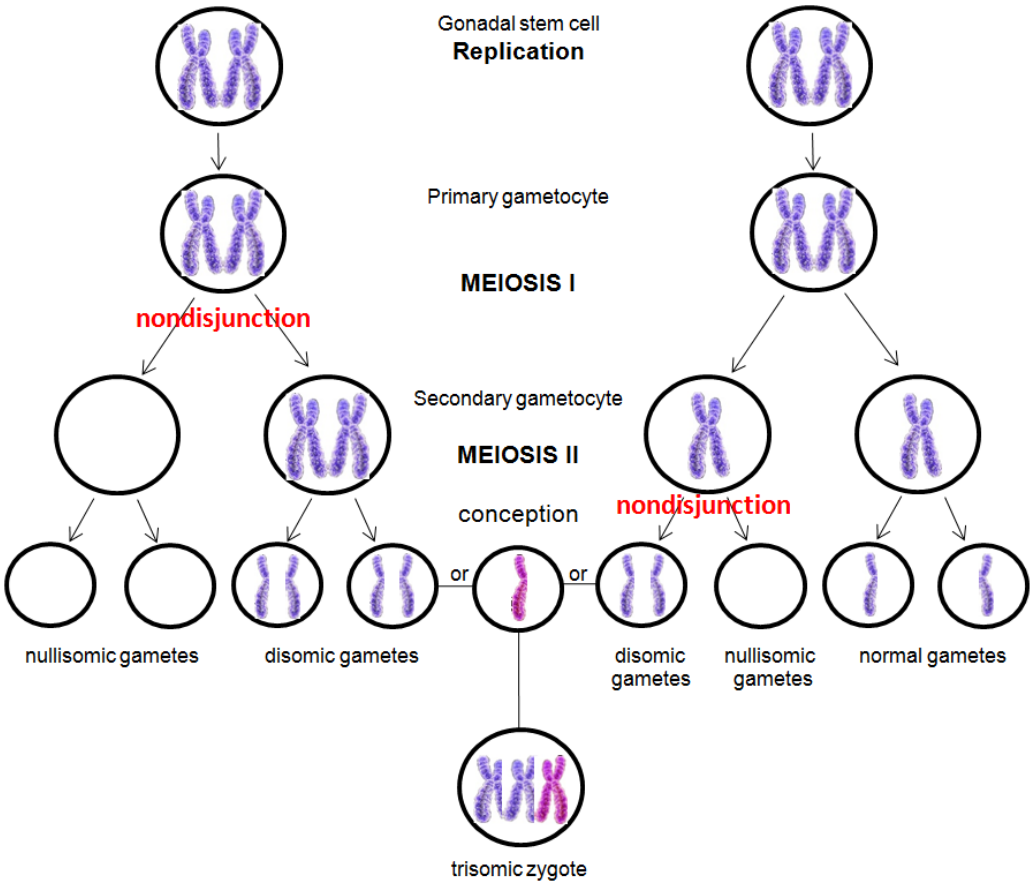

Figure 1.2 Nondisjunction of chromosomal abnormalities.

The most common types of autosomal trisomy that survive to birth in humans are trisomy of chromosome 21 which results in Down syndrome and trisomy of chromosome 18 which results in Edwards syndrome. In rare cases, a fetus with trisomy of chromosome 13 can survive, giving rise to Patau syndrome. Trisomy 12 (known as Chronic Lymphocytic Leukemia); Trisomy 9; Trisomy 8 (known as Warkany syndrome 2); and Trisomy 22 (Cat eye syndrome) are less common. Autosomal trisomies are usually associated with birth defects, mental retardation and shortened life expectancy. Sex-chromosomes trisomies can also occur, e.g. XXX (known as triple X syndrome); XXY (known as Klinefelter syndrome); and XYY (known as XYY syndrome).

Like mutations and other genetic defects, aneuploidy also occurs in animals, but usually the defective animals die after birth, are abandoned by the mother or, being incapable of getting its own food, starve to death, ensuring that the defect doesn't go through to the next generation,

unless the mutation becomes beneficial in some sort of way. Aneuploidy may occur within a group of closely related species in other organisms. Classic examples in plants are the genus Crepis, where the gametic haploid numbers form the series n = 3, 4, 5, 6, and 7; and Crocus, where every number from n = 3 to n = 15 is represented by at least one species. Evidence of various kinds shows that trends of evolution have gone in different directions in different groups (Stebbins & Ledley 1972).

1.5. Chromosome Drive and Evolution of Meiotic Nondisjunction

Meiotic nondisjunction is the failure of homologous chromosomes to segregate properly to opposite poles during meiosis resulting in the production of gametes that have an improper chromosome complement. When a normal gamete combines with a gamete that has an extra chromosome, the resulting zygote is trisomic (Koehler et al 1996, Risch et al 1986, Hassold et al 1985). Trisomy has been the focus of extensive medical research, but the molecular mechanism by which nondisjunction occurs is still not understood (Koehler et al 1996, Angell et al 1994, Orr-Weaver T 1996, Lamb et al 1996, Koehler et al 1996). One common feature to most autosomal trisomies is an increase in the frequency of trisomic pregnancies with increasing maternal age (Koehler et al 1996, Risch et al 1986, Hassold et al 1985). A complete explanation for this is still lacking, but at least two possibilities have been proposed (Zheng and Byers 1992, Henderson and Edwards 1968). One contends that the frequency of nondisjunction remains constant but that a screening mechanism becomes less effective at aborting trisomic zygotes in older females (Aymes and Lippman-Hand 1982). The other maintains that the frequency of nondisjunction increases with maternal age (Angell RR 1994). Past evidence has been indirect and inconclusive (Aymes and Lippman-Hand 1982, Stein 1986), but recent techniques have allowed a direct examination of the relationship between maternal age and the frequency of nondisjunction in oocytes. Results demonstrated that there is an increase in the frequency of nondisjunction with maternal age, and many researchers now argue for its importance in human trisomy, suggesting that a maternal screening mechanism is an unlikely or incomplete explanation. The issue, however, is not yet completely resolved.

Although these hypotheses center on the proximate cause of age-dependent trisomy, relatively little research addresses its evolutionary (ultimate) cause. Some evolutionary hypotheses have been suggested (Axelrod and Hamilton 1981, Kloss and Nesse 1992). One of the most commonly accepted hypothesis is chromosome drive (CD) hypothesis. The CD hypothesis asserts that homologous chromosomes are involved in an evolutionary game and that adaptive evolution of CD strategies results in the evolution of age-dependent nondisjunction and trisomy as a side effect. Unfortunately the hypothesis has not been examined in any detail to determine its adequacy. Until recently, Day and Taylor developed a more suitable model and explored the necessary conditions to explain maternal age-dependent trisomy (Day and Taylor 1998). The relationship between the decay of a female's reproductive potential and CD must exist for the CD hypothesis to work. With appropriate parameter values, including likelihood of female mortality *per se* and her reproductive system failure through ovarian cancer and/or cysts, a comparison of model predictions with empirical estimates for the age dependence of trisomy revealed a striking correspondence.

1.6. Trisomy 21 in Human - Down Syndrome

Trisomy 21 (an individual with three copies of chromosome 21, rather than two) is known as Down Syndrome, and is the most common autosomal trisomy.

Discovery. It is named after John Langdon Down, the British physician who described a set of children with common features who were distinct from other children with mental retardation in 1866 (Down JL 1866). Down was superintendent of an asylum for children with mental retardation in Surrey, England when he made the first distinction between children who were cretins (later to be found to have hypothyroidism) and what he referred to as "Mongoloids". Down based this unfortunate name on his notion that these children looked like people from Mongolia, who were thought then to have an arrested development. This ethnic insult came under fire in the early 1960s from Asian genetic researchers, and the term was dropped from scientific use. Instead, the condition became to call Down's syndrome. In the 1970s, an American revision of scientific terms changed it simply to Down syndrome, while it still is called Down's in the UK and some places in Europe.

In early twentieth century, there was much speculation of the cause of Down syndrome. The first people to speculate that it might be due to chromosomal abnormalities were Waardenburg (Waardenburg PJ 1932) and Bleyer (Bleyer A 1934) in the 1930s. But it wasn't until 1959 that Jerome Lejeune and Patricia Jacobs first determined the cause to be trisomy of the 21st chromosome (Lejeune et al 1959). Cases of Down syndrome due to translocation and mosaicism were described over the next three years (Lilenfeld & Benesch 1969).

Nondisjunction. Trisomy 21 is the cause of approximately 95% of observed Down syndromes, with 88% coming from nondisjunction in the maternal gamete and 8% coming from nondisjunction in the paternal gamete. The nondisjunction event is mainly meiotic. With nondisjunction, a gamete (a sperm or egg cell) is produced with an extra copy of chromosome 21; the gamete thus has 24 chromosomes. When combined with a normal gamete from the other parent, the embryo now has 47 chromosomes, with three copies of chromosome 21. A typical human karyotype is designated as 46,XX or 46,XY, indicating 46 chromosomes with an XX arrangement typical of females with extra copy of chromosome 21 [47,XX,+21] and 46 chromosomes with an XY arrangement typical of males with extra copy of chromosome 21 [47,XY,+21].

Translocation. The extra chromosome 21 material that causes Down syndrome may be due to a Robertsonian translocation in the karyotype of one of the parents. In this case, the long arm of chromosome 21 is attached to another chromosome, often chromosome 14 [45,XX,der(14;21)(q10;q10)]. A person with such a translocation is phenotypically normal. During reproduction, normal disjunctions leading to gametes have a significant chance of creating a gamete with an extra chromosome 21, producing a child with Down syndrome. Translocation in Down syndrome is often referred to familial Down syndrome. It is about 2–3% of observed cases of Down syndrome.

Mosaicism. Trisomy 21 is usually caused by nondisjunction in the gametes prior to conception, and all cells in the body are affected. However, when some of the cells in the body are normal and other cells have trisomy 21, it is called mosaic Down syndrome [46,XX/47,XX,+21]. This

can occur in one of two ways: a nondisjunction event during an early cell division in a normal embryo leads to a fraction of the cells with trisomy 21; or a Down syndrome embryo undergoes nondisjunction and some of the cells in the embryo revert to the normal chromosomal arrangement. There is considerable variability in the fraction of trisomy 21, both as a whole and among tissues. This is the cause of 1–2% of the observed Down syndromes.

Risk. The incidence of Down syndrome is estimated at one per 800 to one per 1000 births. Down syndrome occurs in all ethnic groups and among all economic classes. Researchers have established that the likelihood that a reproductive cell will contain an extra copy of chromosome 21 increases dramatically with a woman ages (Huether et al 1998). Therefore, an older mother is more likely than a younger mother to have a baby with Down syndrome. However, of the total population, older mothers have fewer babies; about 75% of babies with Down syndrome are born to younger women because younger women than older women have babies. Only about nine percent of total pregnancies occur in women 35 years or older each year, but about 25% of babies with Down syndrome are born to women in this age group. Many specialists recommend that women who become pregnant at age 35 or older undergo prenatal testing for Down syndrome.

The risk of Down syndrome rises with increasing maternal age (Fig. 1.3). The likelihood that a woman under 30 who becomes pregnant will have a baby with Down syndrome is less than 1 in 1,000, but the chance of having a baby with Down syndrome increases to 1 in 400 for women who become pregnant at age 35. The likelihood of Down syndrome continues to increase as a woman ages, so that by age 42, the chance is 1 in 60 that a pregnant woman will have a baby with Down syndrome, and by age 49, the chance is 1 in 12. But using maternal age alone will not detect over 75% of pregnancies that will result in Down syndrome. Paternal age, was suggested to increase the risk of Down syndrome, but recent large scale investigation refuted the association (Oliver et al 2009).

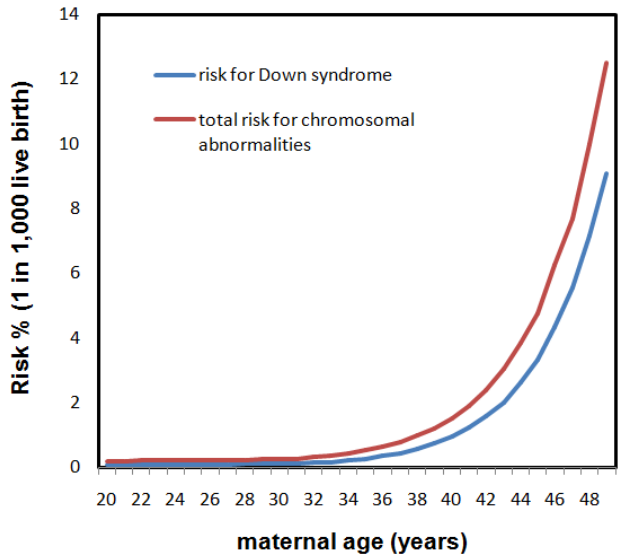

Figure 1.3 Risk of chromosomal abnormalities and Down syndrome in advanced maternal age.

Clinical Features. Over 80 physical and mental disorders can be presented in Down individuals. Common physical features of Down syndrome include microgenia, round face, macroglossia, epicanthic fold, wide palpebral fissures, brushfield spots, low set ear, flat occiput, shorter limbs, dermatoglyphics, hypotonia, and pronounced sandal gap (Fig. 1.4). Health concerns for individuals with Down syndrome include a higher risk for congenital heart defects, gastroesophageal reflux disease, secretory otitis media, obstructive sleep apnea, hypothyroidism, and leukaemia.

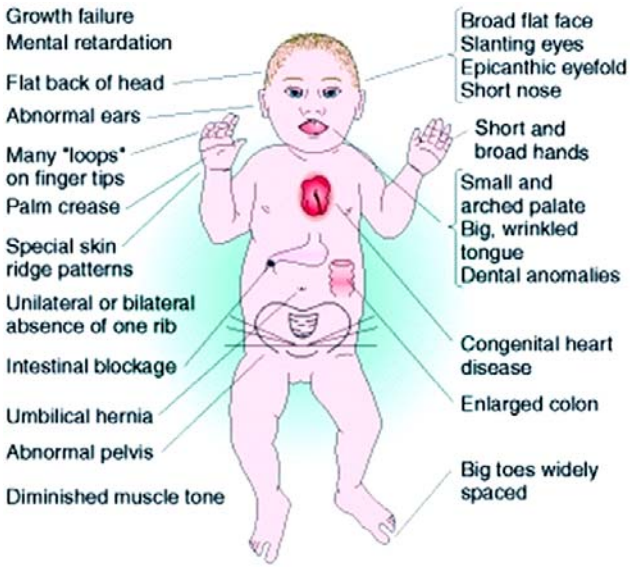

Figure 1.4 Clinical features of Down syndrome.

Chapter 2

Genomic and Developmental Implications of Gene Dosage Imbalance

2.1. Genome of Human Chromosome 21

Human chromosome 21 (HSA21) is one of the 23 pairs of chromosomes in humans. It is the smallest human autosome, representing about 1-1.5 percent of the total DNA in cells. It was the second HSA to be fully sequenced (Hattori et al 2000). Analysis of the contig revealed 127 known genes, 98 predicted genes and 59 pseudogenes by that time. Up to date, 48,129,895 base (~48 Mb) pairs had been sequenced, and 295,347 SNPs, 249 known protein-coding genes, 141 pseudogenes, 16 miRNA genes, 5 rRNA genes, 13 snRNA genes, 14 snoRNA genes, and 8 misc RNA genes had been deciphered (Ensembl Genome, assessed on 25.03.2010).

In HSA21, there is 10 kb intra-chromosomal duplication in the pericentromeric regions of the p- and q-arms. CpG island on the centromeric side of the duplication in the p-arm indicates an active gene in the vicinity of the duplicated regions. Another 200 kb duplication region is located in proximal and distal locations on 21q. It is characterized with 2 large inversions, several other rearrangements and several translocations or duplications within the duplicated units. Some paralogous regions between HSA21 and other chromosomal ends were identified, 100 kb on 21p shared with chromosomes 4, 7, 20 and 22, and 50 kb on 21q is shared with a segment on chromosome 16. Duplicated regions may mediate certain mechanisms involved in chromosomal rearrangement important for duplication, genetic recombination and chromosomal rearrangement.

Several anonymous loci for monogenic disorders and predispositions for common complex disorders have also been mapped to HSA21 earlier, and loss of heterozygosity has been observed in regions associated with solid tumors (Gilbert F 1997). There are 138 OMIM database had been linked and 90 human diseases had been identified in HSA21 (Tab 2.1). The greatest

Table 2.1 Disease map of human chromosome 21 (OMIM, assessed on 30.09.2010).

Start	Stop	Location	Gene	Symbol	Diseases
10906741	10990920	21p11	transmembrane phosphatase with tensin homology	TPTE	Down syndrome
14982498	15013906	21q11.2	POTE ankyrin domain family, member D	POTED	Prostate cancer
15481134	15579254	21q11.2	lipase, member I	LIPI	Hypertriglyceridemia, familial
15646120	15673707	21	ATP-binding cassette, sub-family C (CFTR/MRP), member 13	ABCC13	Leukemia
15857549	15918664	21q11	SAM domain, SH3 domain and nuclear localization signals 1	SAMSN1	Leukemia, multiple myeloma
16333556	16437126	21q11.2	nuclear receptor interacting protein 1	NRIP1	Hepatic steatosis, Infertile, Luteinized unruptured follicle syndrome
17102496	17252377	21q11.2	ubiquitin specific peptidase 25	USP25	Lung carcinoma
17912148	17912231	21	microRNA let-7c	MIRLET7C	Glioblastoma
17962557	17962645	21	microRNA 125b-2	MIR125B2	Prostate carcinoma, Glioblastomas, Cardiac hypertrophy, Neuroblastoma, Psoriasis, Breast cancer
18885330	18939276	21q21.1	coxsackie virus and adenovirus receptor	CXADR	Myocarditis, Dilated cardiomyopathy, Idiopathic left ventricular dysfunction
19641433	19775970	21q21.1	protease, serine, 7 (enterokinase)	PRSS7	Hypoproteinemia, Edema, Celiac disease
22370633	22911214	21q21.1	neural cell adhesion molecule 2	NCAM2	Down syndrome
26946292	26946356	21	microRNA 155	MIR155	B-cell lymphomas, Hodgkin lymphomas, Ancreatic carcinoma, Thyroid tumors
27107329	27144771	21q21.3	GA binding protein transcription factor, alpha subunit 60kDa	GABPA	Down syndrome
27252861	27543446	21q21.3	amyloid beta (A4) precursor protein	APP	Familial early/late-onset Alzheimer disease, Cerebral amyloid angiopathy
28290231	28339439	21q21.3	ADAM metallopeptidase with thrombospondin type 1 motif, 5	ADAMTS5	Chondroblastoma, Arthritis
30452873	30548204	21q22.3	chromosome 21 open reading frame 7	C21orf7	Breast carcinoma, Colon and prostatic adenocarcinoma
30909254	31312282	21q22.11	glutamate receptor, ionotropic, kainate 1	GRIK1	Uvenile absence epilepsy
32490736	32931290	21q22.11	T-cell lymphoma invasion and metastasis 1	TIAM1	Skin tumors
33031935	33041244	21q22.11	superoxide dismutase 1, soluble	SOD1	Familial amyotrophic lateral sclerosis, Microcephaly-cataract syndrome, Ribbing disease
33664124	33687095	21q22.1	melanocortin 2 receptor accessory protein	MRAP	Glucocorticoid deficiency
33947151	33957845	21	t-complex 10 (mouse)-like	TCP10L	Hepatoma
34001073	34100277	21q22.2	synaptojanin 1	SYNJ1	Down syndrome, Bipolar disorder
34398239	34401500	21q22.11	oligodendrocyte lineage transcription factor 2	OLIG2	Oligodendroglioma, Schizophrenia
34442573	34444726	21q22.11	oligodendrocyte transcription factor 1	OLIG1	Oligodendroglioma
34602231	34636827	21q22.11	interferon (alpha, beta and omega) receptor 2	IFNAR2	Hepatitis B
34638672	34669520	21q22.11	interleukin 10 receptor, beta	IL10RB	Early-onset severe enterocolitis, HBV persistence risk
34775202	34809828	21q22.11	interferon gamma receptor 2 (interferon gamma transducer 1)	IFNGR2	Atypical mycobacterial infection, familial
34876238	34915198	21q22.11	phosphoribosylglycinamide formyltransferase, phosphoribosylglycinamide synthetase, phosphoribosylaminoimidazole synthetase	GART	Down syndrome
34915350	34949812	21q22.11	SON DNA binding protein	SON	Down syndrome
34950211	34961014	21q22.1	downstream neighbor of SON	DONSON	Down syndrome
35014784	35261609	21q22.1-q22.2	intersectin 1 (SH3 domain protein)	ITSN1	Down syndrome
35445870	35478561	21q22.12	solute carrier family 5 (sodium/myo-inositol cotransporter), member 3	SLC5A3	Down syndrome
35736323	35743440	21q22.12	potassium voltage-gated channel, Isk-related family, member 2	KCNE2	Long QT Syndrome, Familial atrial fibrillation
35818988	35883613	21q22.12	potassium voltage-gated channel, Isk-related family, member 1	KCNE1	Down syndrome, Jervell and Lange-Nielsen Syndrome, Long QT Syndrome, Noise-induced hearing loss, Ervell & Lange-Nielsen Syndrome
35888782	35987382	21q22.12	regulator of calcineurin 1	RCAN1	Down syndrome, Cardiac hypertrophy
36160098	36421595	21q22.3	runt-related transcription factor 1	RUNX1	Acute myeloblastic leukemia, AD familial platelet disorder
37442285	37445462	21q22.13	carbonyl reductase 1	CBR1	Down syndrome, Breast cancer
37757689	37789125	21q22.13	chromatin assembly factor 1, subunit B (p60)	CHAF1B	Down syndrome
37832919	37852388	21q22.3	claudin 14	CLDN14	AR deafness, Kidney stones
38071991	38122510	21q22.13	single-minded homolog 2 (Drosophila)	SIM2	Down syndrome
38123189	38362503	21q22.13	holocarboxylase synthetase (biotin-(proprionyl-Coenzyme A-carboxylase (ATP-hydrolysing)) ligase)	HLCS	Early-onset multiple carboxylase deficiency, Holocarboxylase deficiency
38378863	38391959	21q22.2	Down syndrome critical region gene 6	DSCR6	Down syndrome

38437664	38445458	21q22.2	phosphatidylinositol glycan anchor biosynthesis, class P	PIGP	Down syndrome, Tongue malformation
38445571	38575408	21q22.2	tetratricopeptide repeat domain 3	TTC3	Down syndrome
38595726	38639833	21q22.2	Down syndrome critical region gene 3	DSCR3	Down syndrome
38739859	38887679	21q22.13	dual-specificity tyrosine-(Y)-phosphorylation regulated kinase 1A	DYRK1A	Down syndrome
38996785	39288696	21q22.13 -q22.2	potassium inwardly-rectifying channel, subfamily J, member 6	KCNJ6	Diabetic, Familial Parkinson disease
39426313	39457580	21q22.2	Down syndrome critical region gene 4	DSCR4	Down syndrome
39628664	39673748	21q22.2	potassium inwardly-rectifying channel, subfamily J, member 15	KCNJ15	Down syndrome, Type 2 diabetes mellitus
40177849	40196879	21q22.2	v-ets erythroblastosis virus E26 oncogene homolog 2 (avian)	ETS2	Down syndrome, Intestinal tumor, Acute myeloid leukemia M2
40547388	40555440	21q22.3	proteasome (prosome, macropain) assembly chaperone 1	PSMG1	Down syndrome
40714241	40721047	21q22.2	high-mobility group nucleosome binding domain 1	HMGN1	Down syndrome
40752213	40769815	21q22.3	tryptophan rich basic protein	WRB	Down syndrome, Congenital heart disease
41029254	41034815	21q22.3	UDP-Gal:betaGlcNAc beta 1,3-galactosyltransferase, polypeptide 5	B3GALT5	Gastrointestinal and pancreatic cancers
41239347	41301322	21q22.2	Purkinje cell protein 4	PCP4	Down syndrome
41384343	42219039	21q22.2	Down syndrome cell adhesion molecule	DSCAM	Down syndrome, Congenital heart disease
42539728	42648524	21q22.3	beta-site APP-cleaving enzyme 2	BACE2	Down syndrome, Breast cancer
42733950	42780869	21q22.3	myxovirus (influenza virus) resistance 2 (mouse)	MX2	Down syndrome
42792520	42831141	21q22.3	myxovirus (influenza virus) resistance 1, interferon-inducible protein p78 (mouse)	MX1	Down syndrome, Subacute sclerosing panencephalitis, Patchy alopecia areata
42836478	42880085	21q22.3	transmembrane protease, serine 2	TMPRSS2	Prostate cancer, AR hearing loss
43732163	43735706	21q22.3	trefoil factor 3 (intestinal)	TFF3	Colitis, Endometrial hyperplasia, Endometrial carcinomas, Breast cancer
43766466	43771208	21q22.3	trefoil factor 2	TFF2	Colitis, Breast cancer
43782391	43786644	21q22.3	trefoil factor 1	TFF1	Down syndrome, Breast cancer
43791999	43816200	21q22.3	transmembrane protease, serine 3	TMPRSS3	Childhood-onset deafness
43824019	43867774	21q22.3	ubiquitin associated and SH3 domain containing, A	UBASH3A	AR deafness, Immune disorder
43892596	43916401	21q22.3	radial spoke head 1 homolog (Chlamydomonas)	RSPH1	Immune disorder
44313378	44329773	21q22.3	NADH dehydrogenase (ubiquinone) flavoprotein 3, 10kDa	NDUFV3	Down syndrome, AR nonsyndromic deafness
44473301	44496040	21q22.3	cystathionine-beta-synthase	CBS	Homocystin-uria/emia, Ectopia lentis, Marfan syndrome, Generalized osteoporosis
44513066	44527688	21q22.3	U2 small nuclear RNA auxiliary factor 1	U2AF1	Progressive myoclonus epilepsy
44589141	44592913	21q22.3	crystallin, alpha A	CRYAA	Cataracts
44834395	44847002	21	salt-inducible kinase 1	SIK1	Heart diseases
45193831	45196259	21q22.3	cystatin B (stefin B)	CSTB	Myoclonic epilepsy
45432206	45526433	21q22.3	trafficking protein particle complex 10	TRAPPC10	Myoclonus epilepsy
45527208	45551063	21q22.3	PWP2 periodic tryptophan protein homolog (yeast)	PWP2	Down syndrome, Holoprosencephaly-1, Myoclonus epilepsy
45553494	45565605	21q22.3	chromosome 21 open reading frame 33	C21orf33	Autoimmune polyglandular disease type I
45666223	45682099	21q22.3	DNA (cytosine-5-)-methyltransferase 3-like	DNMT3L	ICF immunodeficiency syndrome
45705763	45718110	21q22.3	autoimmune regulator	AIRE	Autoimmune polyendocrinopathy syndrome type I
45719925	45747261	21q22.3	phosphofructokinase, liver	PFKL	Down syndrome
45773484	45862964	21q22.3	transient receptor potential cation channel, subfamily M, member 2	TRPM2	Oxidative stress, Inflammation
46269513	46293741	21q22.3	pituitary tumor-transforming 1 interacting protein	PTTG1IP	Pituitary tumor
46305868	46348753	21q22.3	integrin, beta 2 (complement component 3 receptor 3 and 4 subunit)	ITGB2	Down syndrome, Leukocyte adhesion deficiency
46825097	46933634	21q22.3	collagen, type XVIII, alpha 1	COL18A1	Ocular alterations, Knobloch syndrome type I , Pigment dispersion syndrome, Prostatic adenocarcinoma
47401663	47424963	21q22.3	collagen, type VI, alpha 1	COL6A1	Congenital heart defects, Ossification of the posterior longitudinal ligament of the spine, Bethlem Myopathy and Ullrich congenital muscular dystrophy, Multiple fibromatosis and articular dysplasia
47518033	47552763	21q22.3	collagen, type VI, alpha 2	COL6A2	AR myosclerosis
47556176	47575481	21q22.3	formiminotransferase cyclodeaminase	FTCD	Glutamate formiminotransferase deficiency, Megaloblastic anemia, Mental retardation
47608360	47648738	21q22.3	lanosterol synthase (2,3-oxidosqualene-lanosterol cyclase)	LSS	Cataracts
47744036	47865682	21q22.3	pericentrin	PCNT	Microcephalic osteodysplastic primordial dwarfism type II
47878890	47988600	21q22.3	DIP2 disco-interacting protein 2 homolog A (Drosophila)	DIP2A	Leukemia
48018531	48025035	21q22.3	S100 calcium binding protein B	S100B	Down syndrome, Alzheimer disease, Perinatal hypoxia-ischemia

impact of the HSA21 gene catalogue will be in accelerating the contribution of specific genes to the traits seen in Down syndrome.

2.2. Milestones of Genetic and Genomic Studies

Historical Development. Since the discovery in 1953 that Down syndrome occurs when there are three copies of HSA21, the chromosome's structure and gene content have been intensively studied (Fig. 2.1).

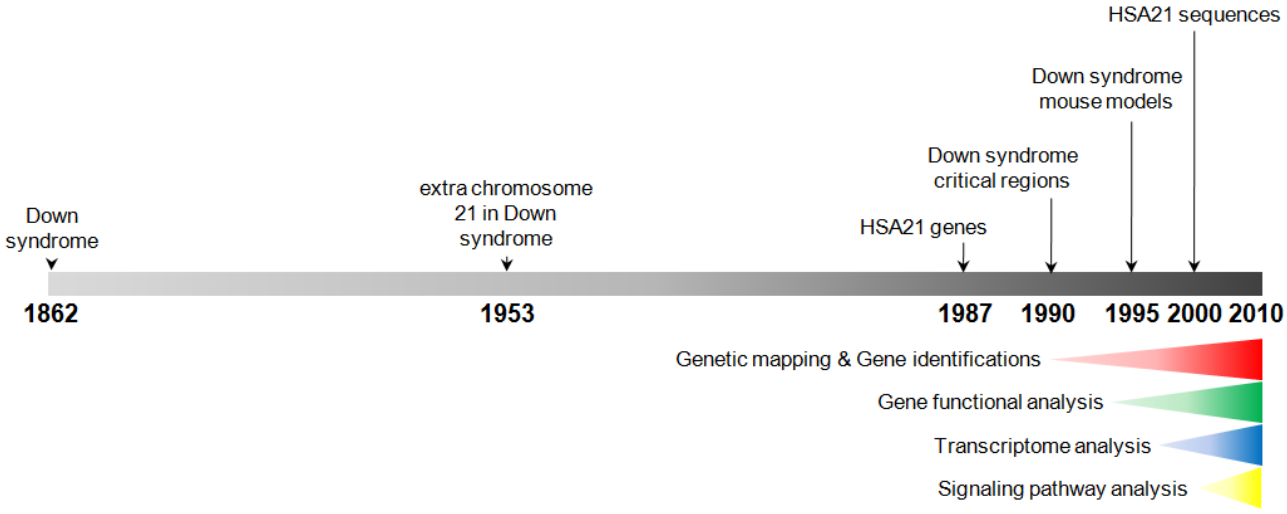

Figure 2.1 History of Down syndrome research

The exact mechanisms by which trisomy 21 produces phenotypical abnormalities are still not completely understood. However, it has been proposed that are resulted from the overexpression of the genes located in HSA21 due to the presence of the extra chromosome. Of particular interest are the genes located between bands 21q22.3–>ter, which code for 50–100 key proteins, including enzymes, membrane receptors, proto-oncogenes, and voltage-gated ionic channels named Down syndrome critical region (DSCR) (Koremberg et al 1992). Over the past few years, Down syndrome research has moved into the post genomic era, and a large amount of data on changes in RNA expression has being collected both for HSA21 genes and for the rest of the genome. In the coming years, an increased knowledge of the functional roles of HSA21 genes is expected. This should contribute to a better understanding of how gene overexpression affects the biological processes linked to the encoded protein products.

Animal Models. Down syndrome occurs in all human populations, and analogous effects have been found in other species such as chimpanzees (McClure et al 1969) and mice (Epstein et al 1985). HSA21 shows conserved syntenis to mouse chromosomes 3, 16, 17 and 10 (MMU3, MMU16, MMU17 and MMU10; Fig. 2.2), which has evolutionary translocations in the interval from zinc finger protein 295 (ZNF295) to ABCG1 (a member of the ATP-binding cassette family) and from KIAA0179 to 1-acylglycerol-3-phosphate O-acyltransferase 3 (AGPAT3).

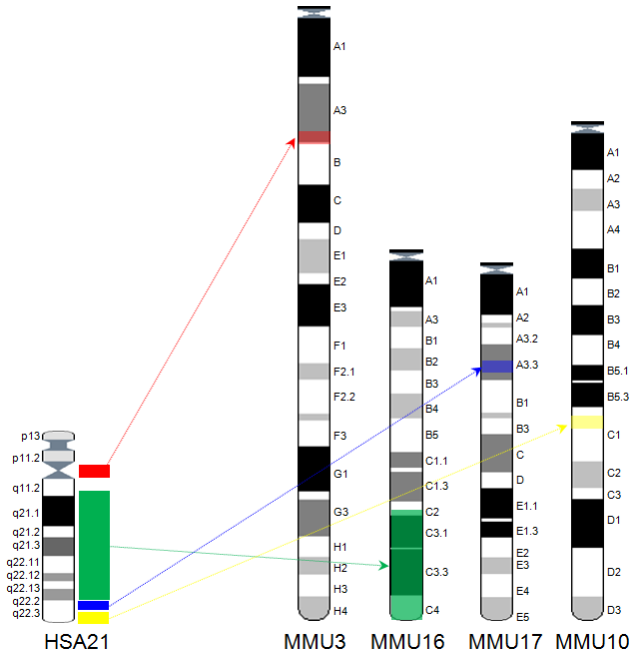

Figure 2.2 Synteny of human chromosome 21 and mouse chromosomes

The high degree of conservation between human and mouse is important, because comparing the two sequences is likely to increase the chance to pick out genes and other significant features from the welter of sequence information. The genes of DSCR have presented synteny along the mammalian evolution. Though DSCR is not necessary to generate the craniofacial phenotypes, is not sufficient to produce deficits in hippocampal function, but it is necessary for cognitive disabilities (Olson et al 2007). In mice, DSCR genes are located in the distal part of the MMU16. This is the genetic basis to propose mice with trisomy 16 as a model of Down syndrome (Epstein et al 1985). Segmental duplications of mouse MMU16 have been produced as mouse models to

study the pathogenesis of Down syndrome. The most widely studied of these, Ts65Dn (Reeves et al 1995), results in trisomy of ~17 Mb of MMU16, a region that contains 136 known genes [from mitochondrial ribosomal protein L39 (Mrpl39) to Znf295], 30 of which cannot be identified on HSA21. This interval contains 49 genes that are present on HSA21 but cannot be identified on MMU16. Another mouse model, Ts1Cje (Sago et al 1998), was caused by a translocation between MMU12 and MMU16 that resulted in a trisomic region of ~8.3Mb, which contains 97 HSA21 orthologous genes [from superoxide dismutase 1 (Sod1) to Znf295; Sod1 is functionally inactivated by the translocation], 15 of which cannot be identified on HSA21. There are 21 HSA21 genes in this interval that cannot be identified on MMU16. Though Ts65Dn and Ts1Cje have overlapping phenotypes that include learning deficits and craniofacial features, thought to model specific features of Down syndrome, both models never present with congenital heart defects as in Down syndrome unfortunately.

Limitations. Besides the constant feature of mental retardation, individuals with Down syndrome also frequently exhibit congenital heart disease, developmental abnormalities, dysmorphic features, early-onset Alzheimer's disease and increased risk for specific leukaemias, immunological deficiencies and other health problems. Ultimately, all these phenotypes are the result of the presence of three copies of genes on HSA21 instead of two. Data from transgenic mice indicate that only a subset of the genes on HSA21 may be involved in the specific phenotypes of Down syndrome.

Although it is difficult to select candidate genes for these phenotypes, some gene products may be more sensitive than others. These may include morphogens, cell adhesion molecules, components of multi-subunit proteins, ligands and their receptors, transcription regulators and transporters. The gene catalogue now allows the hypothesis-driven selection of different sets of candidates, which can then be used to study the molecular pathophysiology of the effects of extra chromosome in aneuploid trisomy. The complete catalogue will also provide the opportunity to search systematically for candidate genes without pre-existing hypotheses.

2.3. Global Gene Dosage Effects

Yet there are varying ideas about which genes are associated with particular features of Down syndrome, and the mechanisms by which an imbalance in the number of genes might produce the more than 80 physical and mental disorders. The presence of an extra copy of HSA21 genes predicts an increased expression for those genes in the trisomy in chromosome. In the simplest scenario, the overexpression of one specific gene would lead to the disturbance of a biological process and, as a result, a single gene would be responsible for each pathological feature of Down syndrome. However, it is more probable that the overexpression of several of the over 450 HSA21 genes would contribute to alter a functional pathway in a specific cell at a specific time. In some cases, functional interactions would result in additive or even synergistic effects, leading to signal amplification. In others, the positive effect of one gene might counteract the detrimental effects of other dosage-sensitive genes that act on the same pathway and, hence, result in no net change. Whatever the case might be, the final phenotypic outcome cannot be foreseen on the basis of analyzing the overexpression of single genes (Luna & Estivill 2006, Fig. 2.3).

Primary Gene Dosage. Conceptually, the most simple gene dosage imbalance is a proportionate (~1.5-fold) increase in products of the trisomic genes – the primary gene-dosage effect. There is long-standing, biochemical and genetic evidence for the existence of primary gene-dosage effects in HSA21-encoded enzymatic reactions in cells from individuals with Down syndrome (Epstein CJ 1986). The available transcriptome analyses of trisomic cells support the existence of a widespread (~50%) primary gene-dosage effect of trisomic genes in different tissues and in different developmental stages in both human (FitzPatrick et al 2002; Mao et al 2003) and mouse (Amano et al 2004; Kahlem et al 2004; Lyle et al 2004; Saran et al 2003).

Dosage Compensation. Dosage compensation occurs when the level of the trisomic gene product does not change compared with those of disomic cells. This phenomenon is a well-described feature of segmental aneuploidy in maize and Drosophila melanogaster (Birchler et al 2001). The transcriptome studies also provide evidence for the existence of dosage compensation in a subset (5-10%) of trisomic genes. The dosage compensation for individual genes appears to be both stage- and tissue-specific (Kahlem et al 2004; Dauphinot et al 2005). These effects are

presumably mediated by feedback at the level of transcription or mRNA stability; however, translational and posttranslational modifications might exist.

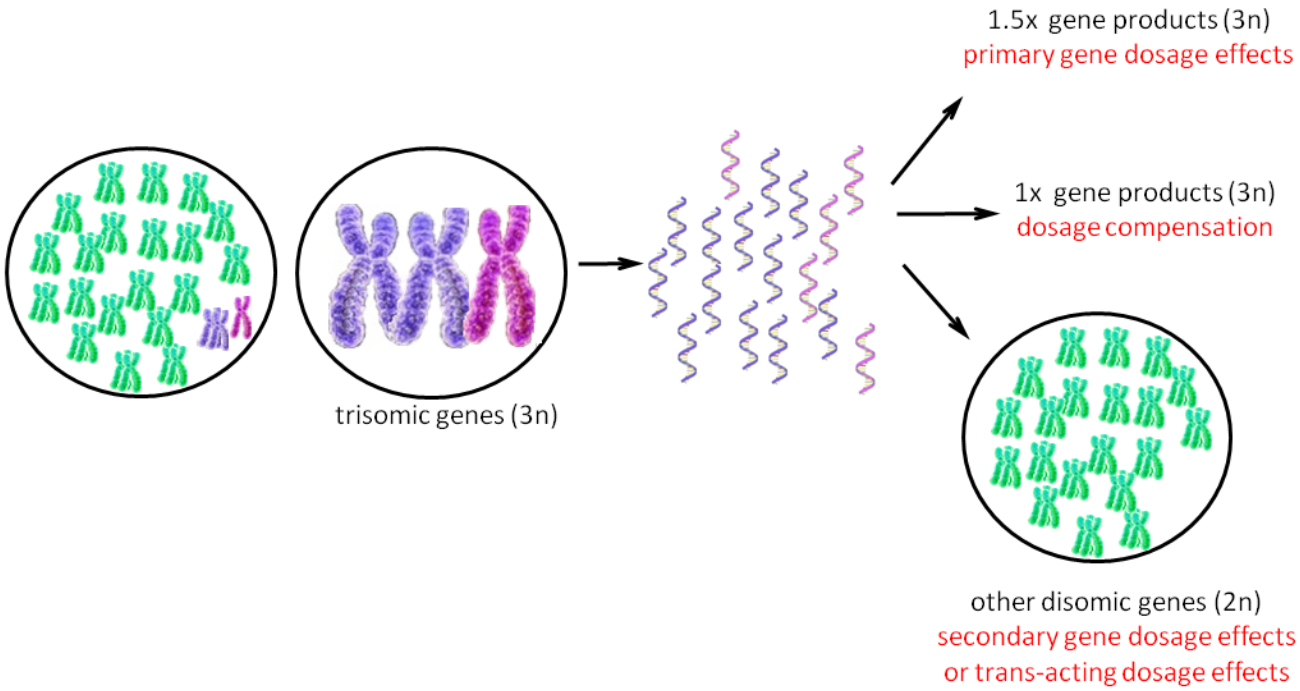

Figure 2.3 Gene dosage effects of autosomal trisomy. The extra chromosome (pink) will either have more gene products from the trisomic genes (blue) for primary gene dosage effects, same gene products for dosage compensation, or exert secondary gene dosage effects on other disomic genes (green) for trans-acting dosage effects.

Secondary Gene Dosage. It is easy to envisage an important consequence of primary gene dosage where the gene encodes a trans-acting factor because many of these function as transcription factors. A 1.5-fold increase of an individual trans-acting factor will result in a stoichiometric imbalance that might be detrimental to the function of target genes or pathways. Such secondary or trans-acting effects are likely to result in up- or down-regulation of disomic genes. Intrachromosomal trans-acting effects might be of greater phenotypic consequence than primary gene-dosage effects alone. There is now compelling evidence that the protein products of two genes on HSA21, Down syndrome candidate region 1 (DSCR1) and dual-specificity tyrosine-(Y)-phosphorylation regulated kinase 1A (DYRK1A), interact functionally, and that their increased dosage cooperatively leads to dysregulation of the signaling pathways that are controlled by the nuclear factor of activated T cells (NFAT) family of transcription factors, with

potential consequences or several organs and systems that are affected in Down syndrome individuals (Arron et al 2006). Nevertheless, tertiary (phenotypic) effects on disomic genes will be detected in all tissues when a morphological change becomes apparent. Thus, trans-acting effects cannot be differentiated from tertiary (phenotypic) effects without detailed knowledge of the morphology of the tissue being studied (FitzPatrick DR 2005).

Dosage Imbalance. In human triploidy, although neonatally lethal, is compatible with full-term gestation (Daniel et al 2001). In mouse, tetraploidy is compatible with survival to mid-gestation (Eakin & Behringer 2003). By contrast, individual trisomy of most autosomal chromosomes results in early pregnancy loss or failure to implant (Hassold et al 1980), suggesting that an imbalance of gene products is more important that the absolute dosage.

2.4. Neurodevelopmental Pathology and Mechanism

Down syndrome is the most common genetic cause of severe learning difficulties (Fig. 2.4). Individuals with Down syndrome tend to have a lower than average cognitive ability, often ranging from mild to moderate developmental disabilities and dysmorphic phenotypes. A small number have severe to profound mental disability (Rondal & Perera 2006).

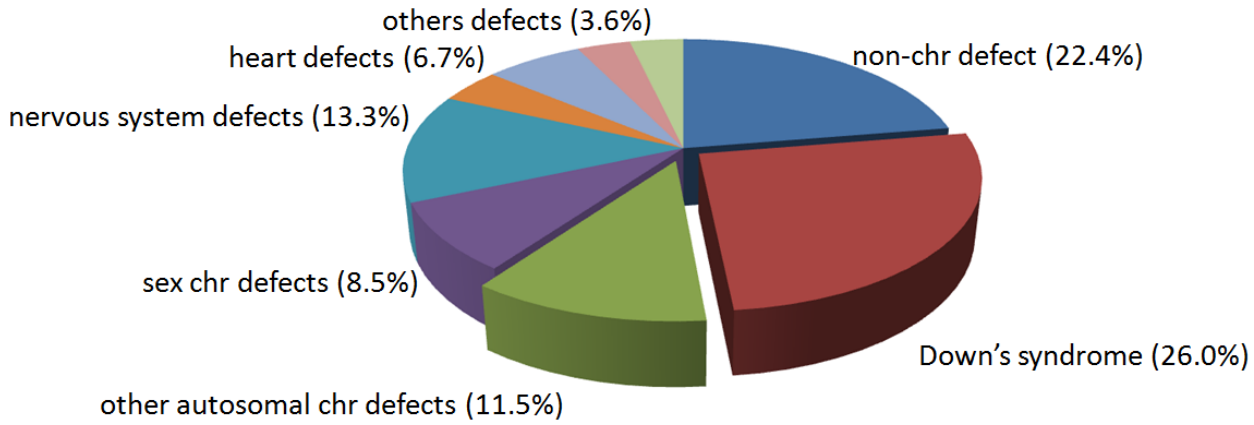

Figure 2.4 Risk of mental retardation

Pathology. The pathology of the brains in Down syndrome includes macroscopic, microscopic and biochemistry and functional changes (Table 2.2).

Table 2.2 Neurological and behavioral phenotypes in Down syndrome.

Macroscopic phenotypes
Early onset of Alzheimer's disease-like neurohistopathology
Altered shapes, number and density of dendrites, synapses and dendritic spines
Altered cortical layering
Hypoplasia of hippocampus and cortex, larger parahippocampus gyrus
Reduced cerebellum and volume of lobules VI-VIII
Microscopic phenotypes
Fewer neurons and lower neuronal density
Abnormal neuronal differentiation and synaptogenesis
Delayed myelination
Degeneration of basal forebrain cholinergic neurons
Biochemistry and function phenotypes
Neurotransmitter alterations
Impairment of prefrontal cortex and cerebellar function
Deficiency in language production, speech and articulation
Low intelligence quotient and cognitive impairment
Short-term and long-term memory deficits

Macroscopic changes of the central nervous system in Down syndrome reveal abnormal short and round brain with almost vertical occipital convexity. The superior temporal gyrus is narrow bilaterally in about half the cases, together with a larger parahippocampal gyrus and smaller hippocampus and neocortex. The brain stem and cerebellum are small in relation to the size of the cerebral hemispheres. It may relate to the impression of developing brain by retardation in the growth of the skull (Cairns NJ 1999). The abnormalities of brain development that result in learning disability and cognition impairment are compounded by the neuropathological changes that lead to Alzheimer disease in Down syndrome in later life (Malamud & Gaitz 1972). This neurodegeneration leads to loss of grey and white matter. The ventricles become enlarge and there is narrowing of the gyri (Fig. 2.5).

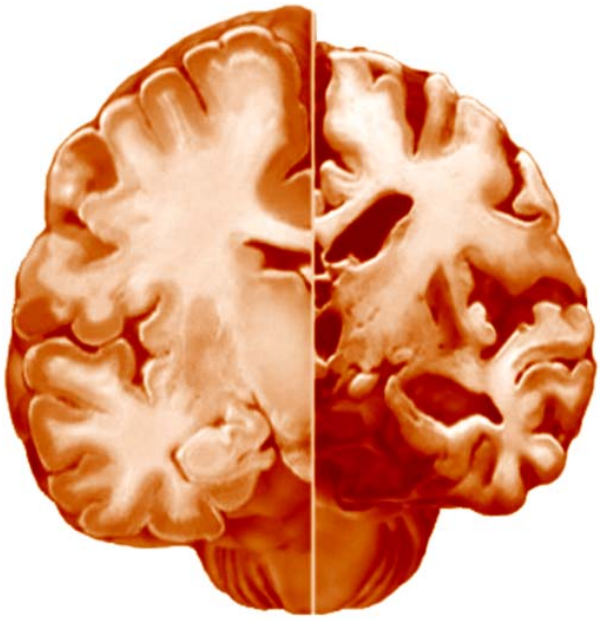

Figure 2.5 Pathology of brain in Down syndrome

Microscopic changes of the brain in Down syndrome are complex and variable. Additional to the decrease in brain size, neurofibrillary tangle and neuritic plaque formation are associated with neuronal loss. These 2 hallmark lesions-are associated with the pathological features observed in Alzheimer disease and complemented by granulovacuolar degeneration, Hirano bodies, neuronal loss, abnormalities of neuronal process and synapses, astrocytic and microglial response, and vascular changes in subtle and distribution differences amongst individuals. Lewy bodies in Down syndrome suggest common pathogenic mechanisms underlying aspects of neuronal degeneration in Parkinson's disease, Alzheimer's disease and Down syndrome (Esiri & Morris 1997).

Neuronal Loss. Mapping of neuronal loss in different regions of the brain of Down syndrome confined to the pyramidal and non-pyramidal cells of entorhinal cortex, hippocampus and associated neocortical regions. There is major loss in subcortical afferent connections based on reduced neurotransmitters acetylcholine, noradrenalin and serotonin. In the cortex somatostatin containing large pyramidal neurons are also affected. Compared with sporadic Alzheimer's disease, hippocampus neuronal loss was found to be greater in Down syndrome patients, where neocortical neuronal loss was less pronounced. It may be due to the compensatory mechanism

that appear in response to increased functional demands on remaining healthy neurons in Down syndrome (Mann DMA 1997). Lower neuronal counts in the hippocampus proper of fetuses with Down syndrome led to the hypothesis that the brain atrophy is mainly due to a congenital malformation (Sylvester PE, 1984). Though it is conceived that abnormal neuronal loss in the brain development in Down syndrome is involved, but there is no direct evidence yet. And also the molecular mechanism underlying the neuronal loss due to genomic implications of gene dosage imbalance remains to be elucidated.

Chapter 3

Gene Expression Studies

3.1 Advantages of the Global Gene Expression Analyses

Down syndrome represents the most common genetic cause of mental retardation in the human population. Brains of Down syndrome are characteristically small with additional gross morphological anomalies. Cerebellum, a critical organ for motor learning and event timing is also affected. Cerebellar volume is small in relation to brain volume and granule cell density is reduced. Anomalies of cortical lamination, clustering of neuronal cell bodies or dendritic arborisation provided potential physiological bases for Down syndrome cognition disorders. Linking Down syndrome mental retardation to gene-dosage imbalance is complex due to its possible multiple genetic causes and to the large number of genes affected by aneuploidy. Considering candidate genes requires looking primarily at the genes involved in (i) brain development including neurogenesis, neuronal differentiation, myelinization or synaptogenesis, (ii) neuronal activity, e.g. cell–cell communication and (iii) metabolic processes potentially harmful to the brain.

Given the large number of genes involved, determining which genes are overexpressed requires a large-scale approach, which is complicated by the small differences in expression level between normal and Down syndrome individuals predicted by gene dosage. Recently, several groups have contributed to progress in this area, by microarrays screening RNA from the brains of human fetuses with Down syndrome (Mao et al 2003) or a trisomic mouse model (Amano et al 2004), by a cDNA array containing mouse orthologs of HSA21 genes screening RNA from several tissues of a mouse model (Kahlem et al 2004), and, to circumvent the sensitivity of microarrays to detect genes expressed at low levels, by quantitative reverse-transcriptase-PCR analysis screening RNA from different tissues of a mouse model at different ages (Lyle et al 2004). The results of all four studies support the hypothesis that gene dosage effects exist in Down syndrome, but they also show that dosage effects may be specific to particular genes, alleles

and/or tissues, and that background and stochastic or transient effects may be confounding factors.

3.2 Limitations of Research Materials

Mao et al screened two Affymetrix oligonucleotide arrays with RNA from age-matched Down syndrome and euploid control fetuses at 17-20 weeks gestation (Mao et al 2003). They used RNA from four normal and four Down syndrome cerebrums and from four normal and four Down syndrome-derived astrocyte cell lines from cerebral cortex. Samples were analyzed individually in order to detect variation between individuals. From all analyses, a global increase in expression level of few HSA21 genes was observed in the Down syndrome samples compared to the euploid controls. The overall increase was consistent with predictions if gene expression followed gene dosage imbalance, but levels varied among individuals such that there were examples of individual genes showing no increase in comparison of individual Down syndrome-euploid pairs. Importantly, these variations in expression levels might be linked to phenotypic variations that would have been apparent at later developmental time points.

Regions of HSA21 are orthologous to segments of three mouse chromosomes: the centromere-proximal 30 Mb region of HSA21 up to and including the ZNF295 gene is orthologous to the telomeric region of MMU16 and the next two approximately 1-2 Mb segments of HSA21 are orthologous to regions of MMU17 and MMU10, respectively. Because of the large region of homology with MMU16, development of segmental trisomy mouse models for Down syndrome has focused on this region. Currently, the best mouse models of Down syndrome are the Ts65Dn mouse (Davisson and Costa 1999) and the Ts1Cje mouse (Sago et al 1998). Ts65Dn mice have three copies of 94 genes orthologous to HSA21 genes, contained within MMU16 from the Gabpa/App gene cluster to the distal telomere. Ts1Cje mice are trisomic for 71 orthologs of HSA21 genes, within MMU16 distal to (and not including) the Sod1 gene to the telomere.

Amano et al screened Affymetrix oligonucleotide arrays representing about 11,000 mouse genes with RNA from whole brains Ts1Cje mice at birth (Amano et al 2004). Only few genes within the trisomic segment showed detectable expression. Of these, most showed a mean increase in

expression level of about 1.5-fold in the trisomic mice, consistent with gene dosage effects. But out of all the possible trisomy:euploid comparisons, not all individual pairwise comparisons showed similar increases. Because these mice are maintained on C57BL/6J an inbred background, the only genetic contribution to expression differences is the trisomic segment. Also, similar to the results of Mao et al's study some non-trisomic genes showed altered expression levels.

Kahlem et al created custom arrays containing cDNAs for the orthologs of HSA21 genes that are trisomic in the Ts65Dn mouse (Kahlem et al 2004). Arrays were screened with Ts65Dn RNA from nine tissues, including cerebellum, cortex and midbrain, in each case pooling RNAs from four individuals, aged 3-4 months. Expression of most trisomic genes was detected in at least one of the nine tissues. In eight tissues, overall levels of expression were consistent with gene dosage, with trisomy:euploid ratios ranging from about 1.63 and about 1.73 in cortex and heart, respectively, to about 1.23 in kidney. Only muscle, with ratios of 1.16, failed to show notable gene-dosage effects. A small number of specific gene-tissue combinations deviated from dosage effects; few combinations showed unchanged or decreased ratios and the others showed ratios over 2.0.

Lyle et al used real-time RT-PCR for experiments with Ts65Dn mice (Lyle et al 2004). RNA from brain, liver, kidney, heart, muscle and lung of postnatal mice, and brain, liver, kidney and heart of 11-month-old mice were used, in each case pooling material from four trisomic or euploid male mice. Assays of the trisomic genes showed an overall mean expression ratio of approximately 1.5. There were statistically significant variations, however.

Many of the pathological traits of Down syndrome are likely to be linked to the alteration of pathways that are required for normal embryonic development. Brain development abnormalities contributing to the cognition phenotypes in Down syndrome are likely to arise during development and investigation at early stages is important, in particular neurogenesis and neural differentiation (Kahlem P 2006; Rachidi & Lopes 2007). Availability of human tissues is limited and most studies focused on adult or postnatal materials, and even amniocytes, placenta or fibroblast cell cultures. The variation of expression level for a given gene can change in the

different tissues, including brain, and during differential developmental stages. A precise definition of the appropriate developmental window is required for investigation and possible future intervention. Embryonic cells and tissues from human and mouse embryos will be the most suitable materials to understand the developmental mechanism of Down syndrome.

3.3 Importance of Data Analysis

Theoretically, the supernumerary copy of HSA21 is expected to result in a 50% increase in the level of transcripts of all genes in HSA21. However, it has been recently observed that there is not always a direct correlation between genomic imbalance (duplication) and transcript level of genes within the aneuploid segment, suggesting that complex molecular mechanisms regulate RNA transcription levels, probably protein translation levels as well (Lyle et al 2004).

An additional level of complexity comes from the recent observations of extensive gene-expression variation among unaffected individuals and that a significant fraction of this variation is controlled by genetic variation, either in cis or trans to the individual gene (Storey et al 2007, Cheung et al 2003, Monks et al 2004). There is also extensive expression variation for HSA21 genes, with some genes varying up to 40-fold among individuals (Deutsch et al 2005). These findings may have direct implications for the phenotypic variability of Down syndrome and underlie the need to re-evaluate our models of dosage imbalance and how they relate to human disorders. And such natural gene-expression variation in Down syndrome do modulate the outcome of gene-dosage imbalance as well (Prandini et al 2007). This suggests that precise data mining and systematic analysis are mandatory to understand the genomic implications of gene dosage imbalance in autosomal trisomy.

3.4 Aim of the study

The aim of the study was to investigate the genomic implications and its molecular mechanism of autosomal imbalance in early neurogenesis. Firstly, we employed large-scale gene expression approaches to profile the global transcriptome and proteome, through data mining and

bioinformatic analysis, in order to study the gene dosage imbalance in autosomal trisomy. Primary dosage effects, dosage compensation and secondary or trans-acting dosage effects were studied and detailed transcription networks were demonstrated. Secondly, we investigated the molecular regulation of neuronal differentiation of an aneuploid mouse ES clones containing extra HSA21. Differential transcriptomic and proteomic profiles were compared. Thirdly we also studied the molecular mechanism of the neural apoptosis in the aneuploid mouse ES clones containing with different number of human and mouse chromosomes. Last but not least, specific gene cluster and network and its potential evolutionary implications were speculated.

Chapter 4

Methodology

Down syndrome (DS) is a congenital disease caused by the trisomy of HSA21. It is characterized by distinct facial and other physical features, and mental retardation. The most commonly accepted hypothesis for the molecular origins of DS is that the extra HSA21 genes contribute to the DS phenotypes (Antonarakis et al 1998). It is also widely accepted that mental retardation in DS is mainly a consequence of brain developmental alternations in neurogenesis, neuronal differentiation, myelinization, and synaptogenesis (Coyle et al 1986; Becker et al 1991; Bahn et al 2002). Thus, the HSA21 genes with possible direct and indirect roles in brain development have become the focus of DS research. Molecular analyses using fetal or adult brain tissues or primary cultured neuronal cells from DS patients revealed spectrums of mis-regulated gene expression (Saran et al 2003; Engidawork & Luber 2003; Sawa A 2001). In these studies the aberrations were observed in well-differentiated neurons or in tissues that were contaminated by glial cells, however.

To understand the malformations in DS brain, a study of the early development of neurons and its differentiation process is mandatory. Inaccessibility *in utero* and difficulties in isolating neuronal stem cells have prevented study of early neuronal differentiation in DS patients. Recently, we successfully generated chimeric mice carrying an intact HSA21 as a freely segregated extra chromosome via microcell-mediated chromosome transfer (MMCT) into mouse embryonic stem (ES) cells (Shinohara et al 2001). These chimeric mice presented a wide variety of phenotypic traits of DS in humans, including impairment in learning and emotional behavior, and also hypoplastic thymus and cardiac defects. Delayed cardiogenesis was observed within the embryoid bodies of mouse ES cell lines containing a single HSA21 chromosome differentiated *in vitro* (Inoue et al 2000). We demonstrate the utility of aneuploid ES cell applied to the mouse PA6 stromal cell-derived inducing activity (SDIA)-induced neuron differentiation *in vitro* as a model to study the role of the additional HSA21 in DS neuronal development. Differentiation of ES cells on the feeder layer of PA6 mouse stromal cells results in extremely efficient neuronal

differentiation *in vitro* by SDIA (Kawasaki et al 2000). Increased susceptibility of the aneuploid cell lines to defective neurogenesis and neural apoptosis at the stage of neuronal stem cell differentiation *in vitro* using SDIA was observed (Kawasaki et al 2000; Kadota et al 2002).

In the first part of the study, we used cDNA microarray, derived from NIA 15K mouse cDNA clone set covering ESTs from pre- and peri-implantation embryos (see URL http://lgsun.grc.nia.nih.gov/cDNA/15k.html; Tanaka et al 2000), to compare the gene expression of the ES cell lines during neuronal differentiation *in vitro* in order to understand the molecular basis of the developmentally associated manifestations in DS neurogenesis. In an attempt to identify and confirm misregulated proteins as the functional output of aberrant mRNA information in early DS neuronal differentiation, we also conducted two-dimensional polyacrylamide gel electrophoresis (2-DE) protein separation to represent the distinctive proteomic signatures. Matrix-assisted laser desorption/ionization-time of flight (MALDI-TOF) mass spectrometry (MS) was then carried out to identify proteins corresponding to each distinctive protein spot. The identified proteins were compared with the RNA transcribed during neuronal differentiation *in vitro* in order to study the transcriptional translational regulations.

In the second part of the study, we hypothesized that imbalance in gene dosage caused by aneuploidy plays an important role in enhanced apoptosis during early neural differentiation *in vitro*, we constructed two aneuploidy mouse ES cell clones: one set of cell clones contained a single HSA21, HSA11, or HSA6p by the same MMCT method (Fourinier & Ruddle 1977; Koi et al 1989; Tomizuka et al 1997; Kugoh et al 1999), whereas the other contained MMU1, MMU11, MMU1+MMU8 and MMU8+MMU11 were isolated by sub-cloning parental ES cell clones. We investigated the enhanced apoptosis in autosomal imbalance during early neuronal differentiation *in vitro*, which are possibly associated with mental retardation. We then performed global gene expression analysis to reveal the underlying molecular mechanism that might be responsible for the enhanced apoptosis during early neurogenesis.

4.1. Chromosome Transfer

To study the gene dosage imbalance effects on autosomal trisomy in early neurogenesis, we employed chromosome transfer technology to transfer extra human or mouse chromosome(s) into mouse ES cell lines to create aneuploid clones.

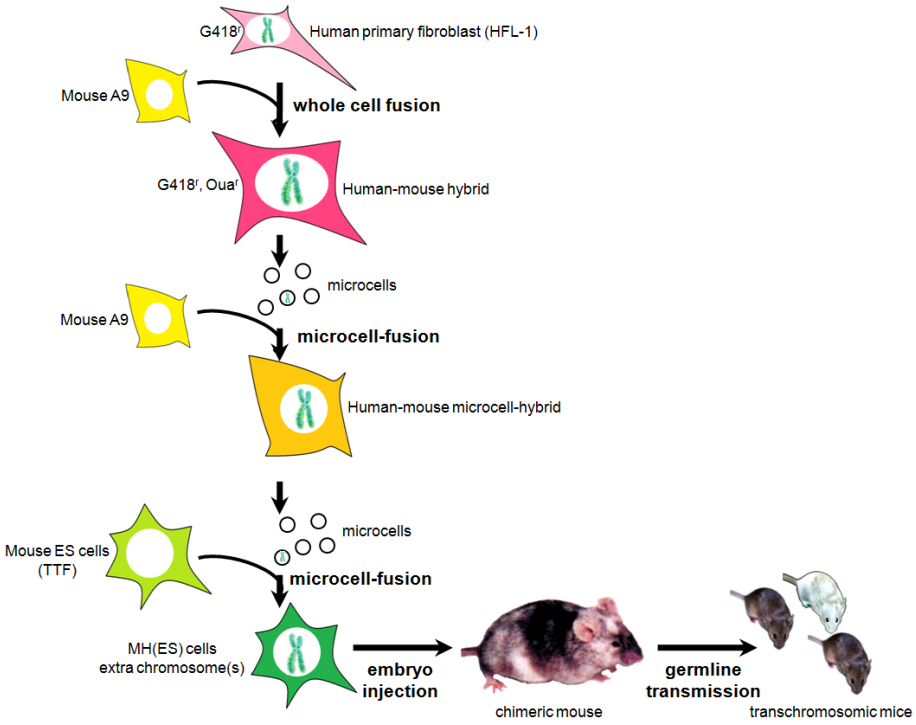

Figure 4.1 Microcell-mediated chromosome transfer. Extra chromosome from either human or mouse is transferred to embryonic stem cells containing extra chromosomes to produce chimeric and transchromosomic mice.

Chromosome(s) or chromosome fragment(s) was introduced into mouse ES cells by chromosome transfer and viable chimeric mice were generated (Tomizuka et al 1997; Shinohara et al 2001). Transferred chromosome(s) was stably retained; HSA & MMU genes were expressed in prolonged passages and also in proper tissue-specific manner in adult chimeric tissues; and even could be transmitted to the offspring through the germline.

ES Cell Culture. Parental undifferentiated ES cells E14, TT2F and TT2 cells and microcell hybrid clones TT2F/hChr (TT2F cell lines with additional/extra HSA) or TT2F/mChr (TT2F cell lines with additional/extra MMU) were used and maintained on mitomycin C (Sigma) treated

G418 resistant mouse embryonic fibroblasts (Gibco) as feeder layers in DMEM (Sigma) supplemented with 15% FBS (Hyclone), 1mM sodium pyruvate (Gibco), 0.1mM non-essential amino acids (Gibco), 0.1mM 2-mercaptoethanol (Sigma), 2mM L-glutamine (Gibco), and 1000U/ml LIF (Gibco), with or without 300lg/ml G418 (Gibco). EB5 cells (a kind gift of Dr Hitoshi Niwa, Osaka University) carry the blasticidin S-resistant selection marker gene driven by the Oct3/4 promoter (active under the undifferentiated status) were maintained in medium containing 20μg/ml blasticidin S to eliminate differentiated cells. EB5 is a subline derived from E14tg2a ES cells (Hooper et al 1987) and was generated by targeted integration of Oct-3/4-IRES-BSD-pA vector (Niwa et al 2000) into the Oct-3/4 allele.

Microcell Mediated Chromosome Transfer. Human or mouse chromosome(s) or chromosome fragment(s) derived from normal fibroblasts was introduced into mouse ES cells via microcell-mediated chromosome transfer (MMCT, Fournier & Ruddle 1977). Mouse ES cells (TT2, Lifetech Oriental) were harvested with trypsin, dispersed in ES medium with 18% FBS, and then washed twice with serum-free DMEM. Recipient ES cells ($1x10^7$ cells) were pelleted by centrifugation and overlaid with microcells or gamma-irradiated microcells purified from $1x10^8$ cells of donor A9 clones in serum-free DMEM, followed by re-centrifugation. The pelleted ES cells and microcell mixture was resuspended in 0.5ml of PEG (1:1.4) solution which was made by dissolving 5g of PEG1000 (Wako) in 7ml of serum-free DMEM containing 14% (v/v) of DMSO. After 1.5min at room temperature, 10ml of serum-free DMEM was added and centrifuged. The pellet was then resuspended in ES medium and plated onto three 10-cm dishes containing feeder layers (G418-resistant primary embryonic fibroblasts, Lifetech Oriental). G418 (300μg/ml, for A9/2-W23 and A9/14-C11) or puromycin (0.75μg/ml, for A9/22-G2) selection was performed 24h after microcell fusion. The resulting drug-resistant microcell hybrids were cloned between day 7 and day 9 after selection. Each clone was analysed by PCR using IGKC, IGHMC or IGLC primers (see Genomic DNA analysis). Fusion between microcells prepared from A9/2-W23 and TT2 resulted in six G418-resistant colonies. Four of the six clones retained the IGKC marker. Eleven G418-resistant colonies and four puromycin-resistant colonies were also isolated from the fusion experiments using microcells prepared from A9/14-C11 and A9/22-G2, respectively. All clones from A9/14-C11 retained the IGHMC marker and three of the four clones from A9/22-G2 retained the IGLC marker. Gamma-irradiated (30 Gy) microcells from

A9/14-C11 were also used and yielded four G418-resistant clones retaining the IGHMC marker. Representative microcell hybrids, MH(ES)2-1 from A9/2-W23, MH(ES)22-1 from A9/22-G2, MH(ES) 14-4 and MH(ES)14-5 from A9/14-C11, and MH(ES)14-6γ and MH(ES) 14-7γ from gamma-ray irradiated A9/14-C11 were further analysed and used to produce chimaeras. To introduce the hCF(2-W23) into XO-type ES cells (TT2-F, isolated from TT2; Lifetech Oriental), A9/2-W23P was used as a microcell donor (Table 4.1).

Table 4.1 Chromosome characteristics in aneuploid mouse embryonic stem cell clones

Mouse ES clones	Cells	Normal	Chromosome no.							Modal karyotypes (%)
	no.	cells (%)	37	38	39	40	41	42	>42	
E14-1	20	100				20				40,XY (100%)
E14-2	20	70	1	2	2	14	1			40,XY (70%)
E14(hChr11)-1*	20	0		2	2	2	14			An extra human chromosome 11 (70%)
E14(hChr11)-2	20	0	2			2	16			An extra human chromosome 11 (80%)
TT2F	90	76	1	6	68	8	5		2	39,XO (76%)
TT2F(hChr21)-10*	20	5		2	4	14				An extra human chromosome 21 (60%)
TT2F(hChr21)-11*	18	5			2	14	2			An extra human chromosome 21 (78%)
TT2F(hChr11)*	18	0		2		13	3			An extra human chromosome 21 (72%)
TT2F(hChr6p)*	20	0				15	5			An extra human chromosome 6 (75%)
TT2Fs-1	50	92	1	2	46	1				39,XO (92%)
TT2Fs-2	50	94		3	47					39,XO (94%)
TT2Fs-3	49	82		5	40				4	39,XO (82%)
TT2Fs(mChr1)**	50	12			6	38	6			40,XO+1 (76%)
TT2Fs(mChr8,17)**	49	8		1	4	13	31			41,XO+8,+17 (63%)
TT2Fs(mChr1,8)**	50	2			1	2	44	3		41,XO+1,+8 (88%)
TT2	120	66	5	2	14	79	19	1		40,XY (66%)
TT2s-1	42	70	2	1	3	33	2		1	40,XY (79%)
TT2s(mChrY)**	40	10	1	1	34	4				40,XY (85%)
TT2s(mChr8)-1**	41	7	4			3	34			41,XY+8 (83%)
TT2s(mChr8)-2**	41	7		1		3	37			41,XY+8 (90%)
TT2s(mChr8,17)**	42	5	2			2	1	36	1	41,XY+8, +17 (86%)

To confirm the ES cells containing the transferred HSA21, the genomic DNA analysis by PCR, Southern blot and FISH/SKY were performed.

Genomic DNA Analysis. PCR analyses were carried out using standard techniques. The following markers and primer pairs for HSA21 were used: D21S1904, 5'-ATGAGTTCAGTGTT TCATGGACACT-3' and 5'-AGCAAGATTACTTGTCTGGTTTCCC-3'; APP (GenBank accession no. SHGC-31514), 5'-CTGGGCAATAGAGCAAGACC-3' and 5'-ACCCATATTAT CTATGGACAATTGA-3', amplifies a 115 bp fragment; D21S260, 5'-AGCTGTTCATGCTTCC ATCT-3' and 5'-AGAGCCCAGAATATTGACCC-3', 270 bp; SOD1 (accession no. SHGC-

6902), 5'-ATTCTGTGATCTCACTCTCAGG-3' and 5'-TCGCGACTAACAATCAAAGT-3', 133 bp; CBR1 (accession no. J04056), 5'-GATCCTCCTGAATGCCTG-3' and 5'-GTAAATGC CCTTTGGACC-3', 245 bp; ETS2 (accession no. SHGC-6939), 5'-TCGTGGACACACACAGA CTA-3' and 5'-CTTTACAACGTCTCTTAGTCGG-3', 337 bp; D21S268, 5'CAACAGAGTGAG ACAGGCTC-3' and 5'-TTCCAGGAACCACTACACTG-3', 213 bp; COL18A1 (accession no. stSG1580), 5'-TTTATTTGCCTGTCTGAATTGG-3' and 5'-AAAGCAGCCACGAGGTGC-3', 227 bp; STCH (accession no. SHGC-10662), 5'-TTTTGTCTTAGGATTAGACGTGACC-3' and 5'-AGAACTGGGAAGTCTCATAACTGG-3', 215 bp; SIM2 (accession no. WI-22186), 5'GGG CCTCATGGTAAGAGTCA-3' and 5'-GAAAAATGTCGGTGGTATCTCC-3', 250 bp; ERG (accession no. M21535), 5'-AATGGCGTCAGCCTCTC C-3' and 5'CAGTTTGCCTTACGAGT GGTAGC-3', 254 bp; MX1 (accession no. WI-18875), 5'-TGGACTGACGACTTGAGTGC-3' and 5'-CTCATGTGCATCTGAGGGTG-3', 143 bp; PCP4 (accession no. WI-14954), 5'GAATTCACTCATCGTAACTTCATTT-3' and 5'-CCTTGTAGGAAGGTATAGACAATGG 3', 126 bp; PWP2 (accession no. SHGC-33273), 5'-GATCTTGACCGGGAAAAGGG-3' and 5'-AACAAGTGGCAAAATGCATAC-3', 150 bp; and GIRK2 (GIRK2F, 5'CCCAAAATACTACA CATCC-3' and GIRK2R, 5'-GTTTGTCTTCAGCTCACC-3', 266 bp). Amplifications were performed with an annealing temperature of 62°C for 30 cycles and the products were analyzed on a 3% agarose gel.

Southern Blotting. Retention of the transferred chromosome(s) in aneuploidy lines, Southern blotting and FISH analysis were carried out by standard methods. For Southern blot, digested DNA samples were electrophoresed through a 0.8% agarose gel and transferred to a Hybond N+ membrane (Amersham) in alkaline solution. The membrane was hybridized overnight at 65^{o}C with ^{32}P-labelled human L1 repeat probe (1.4 kb EcoRI-BamHI fragment purified from pKA19A plasmid) or human JK probe (1.8 kb SacI-SacI fragment) and washed twice at 65^{o}C in 0.1xSSC, 0.1% SDS for 30min. Radioactivity on the membrane was visualized by Image Analyzer BAS2000 (Fuji Photo Film).

FISH & SKY Analysis. ES cells were treated with 0.075M KCl and fixed in a 3:1 solution of methanol and acetic acid. For COT-1 painting, digoxigenin (Boehringer) labeled human COT-1 DNA (BRL) was used as a probe, and human-derived chromosomes were detected with anti-

digoxigenin-rhodamine (Boehringer) in mouse chromosomes stained with DAPI (Sigma). The probe for human IgK was prepared by biotinylating an equimolar mixture of human JK and CK (2.5 kb EcoRI-EcoRI fragment) genomic fragments (Fig. 4.2). For digital image microscopy, the Cytovision Probe system (Applied Imaging) was used.

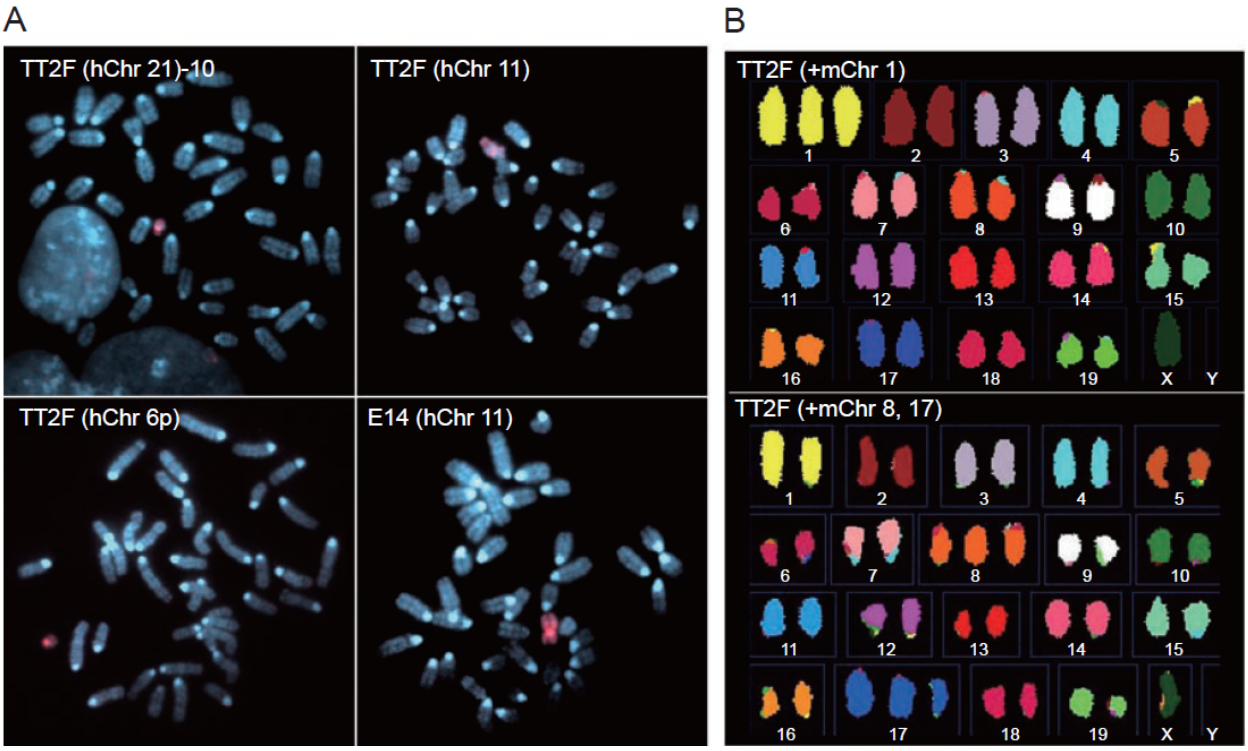

Figure 4.2 Chromosomal analysis of modal karyotypes of ES cells with various aneuploidies. (A) Transferred human chromosomes were detected by digoxigenin-labeled human Cot-1 DNA (red): TT2F (hChr 21)-10, TT2F (hChr 11) and TT2F (hChr 6p) contain human chromosome 21, 11 and 6p in parental TT2F, respectively, whereas E14 (hChr 11) contains human chromosome 11 in parental E14. The extra human chromosome was detected within the otherwise normal mouse karyotype of each ES cell. (B) SKY analysis revealed karyotypes of sub-cloned TT2F cell clones: TT2Fs (+mChr 1) shows a modal karyotype 40, XO +1, and TT2Fs (+mChr 8,17) a modal karyotype 41, XO +8, +17.

For two-colour FISH analysis, the IgK probe and the digoxigenin labeled COT-1 probe were used, and the hybridized probes were detected with FITC-avidin (Vector) and anti-digoxigenin-rhodamine, respectively. One round of amplification with biotinylated anti-avidin (Vector) and a second detection with FITC-avidin was performed in order to visualize the signal of IgK probe. Normal human metaphase spreads were prepared from peripheral blood lymphocytes for Alu-PCR painting. Generation of the Alu-PCR probe using CL1 and CL2 primers and the detection of the signal were performed. Signals were visualized by amplification with Texas red labeled

Anti-sheep IgG (H+L) (Vector) on human chromosomes stained with DAPI. Fibroblasts from the tail of 4-6 week old mice were cultured in DMEM containing 10% FCS and then used for metaphase chromosome preparation.

For SKY analysis, slides were processed using the ASI spectral mouse karyotyping kit (Applied Spectral Imaging (ASI, Carlsbad, CA) according to the manufacturer's instructions (Fig. 4.2). The slides were mounted in antifade reagent (ASI) and imaged using the SKY system with SkyView v.1.6 and Spectral Imaging v.3.0 (ASI).

4.2. Neuronal Differentiation

The aneuploid ES cells were induced and differentiated into neuronal lineage *in vitro* and the differentiating neurons were obtained for comparative studies in gene and protein expression profiling including global transcriptome and proteome analyses to investigate the genomic implications of autosomal imbalance.

Differentiation Cultures. ES cells were cultured to form colonies from a single cell on PA6 feeder cells. Neuronal differentiation of ES cells was performed by the Stromal Cell–Derived Inducing Activity (SDIA) as previously reported (Kawasaki et al 2000). Briefly, PA6 cells were cultured to confluence in a-MEM (Sigma), supplemented with 10% FBS and 2mM L-glutamine, and then used as feeder layers. ES cells were dissociated and plated on a gelatin-coated dish in stem cell medium for more than 30min to remove the mouse embryonic fibroblast feeder cells and 10^4–10^5 ES cells were plated on PA6 cells in 10cm dishes. The differentiation medium was G-MEM (Gibco) supplemented with 10% KSR (Gibco), 1mM sodium pyruvate, 0.1mM non-essential amino acids, 0.1mM of 2-mercaptoethanol, and 2mM L-glutamine. It was essential to remove serum from the media since the addition of FCS strongly inhibited neural differentiation. LIF also suppressed neural differentiation. ES cell colonies were grown at a density of 1×10^3 colonies per 3cm dish. Medium change was performed on day 4 and every other day following day 4. At the end of neuronal induction, differentiated neurons were isolated for subsequently analyses.

Dopamine Determination. To characterize the neurotransmitter metabolism of neuronal lineage, reverse phase–HPLC analysis of dopamine was performed by using an electrochemical detector (the Monoamine Analysis System, Eicom Corp., Kyoto, Japan). ES cells were cultured on PA6 for 8 days in differentiation medium and for an additional 6 days in G-MEM supplemented with N_2, 100μM tetrahydrobiopterin and 200μM ascorbate, 2mM glutamine, 1mM pyruvate, 0.1mM nonessential amino acids, and 0.1mM 2-ME. After rinsing twice with HBSS, cells were incubated with HBSS containing 56mM K^+ for 15min. The medium was then collected, stabilized with 0.4M perchloric acid and 5mM EDTA, and kept at −80°C until being used for analysis.

Immunocytochemistry. To localize the protein of neuronal lineage, immunohistochemistry was performed with the following antibodies against NCAM, TH, GAD (GABAergic marker), and VAChT (cholinergic marker) (Chemicon), TuJ (Babco), nestin (Pharmingen), GFAP and anti-synaptophysin (Sigma), RC2 and MF20 (Developmental Studies Hybridoma Bank), PDGFR alpha and Flk1, E-cadherin (Takara), Keratin 14 (Biomedia), serotonin (Dia Sorin), and DBH (PROTOS Biotech). ES cells differentiated in chamber slides (Nunc) for 0, 3, 6 or 8 days were fixed in 4% paraformamide, permeabilized in 0.2% Triton X-100 (Sigma), and treated in 1× Block-ace solution (Snow Brand Milk Products). FITC or Cy-3 conjugated secondary antibodies (Chemicon) were used and detected by a laser confocal microscope (Bio-Rad). Immunoreactivity of each antibody was confirmed with appropriate positive control tissues under the same conditions.

RT-PCR Analysis. To study the gene expression of neuronal lineage, total RNA was extracted using the RNeasy mini kit (Qiagen). After treatment of RNA with DNase (Nippon Gene), first strand cDNA was synthesized using 5μg total RNA with MMLV-RT (Gibco) and oligo(dT) primer (Roche), and 1/40 volume of cDNA was applied to PCR. The annealing temperature was 60°C for Nestin and 58°C for SIM2, Ncam-L1, and Gapdh. PCR cycles were 21, 27, 27, and 20 cycles for Nestin, SIM2, Ncam-L1, and Gapdh, respectively. Primer sequences were as follows: for Nestin, 5′-CCCTCTGGCACTGAGGACT-3′ and 5′-CAGCAGGCTGAGATGATGAG-3′; for SIM2, 5′-TCCCCCTAACCCCTATGAAC-3′ and 5′-GCAGTTCAGAGCCATGACAG-3′; for Ncam-L1, 5′-CTGTTTGGCAAGCCAGATTT-3′ and 5′-CTGTACTCGCCGAAGGTCTC-

3′; and for Gapdh, 5′-CCATCTTCCAGGAGCGAGA-3′ and 5′-TGTCATACCAGGAAATGA GC-3′. PCR products were separated by agarose gel electrophoresis and visualized with SYBR-green I nucleic acid staining solution (Takara) for high sensitivity detection.

Apoptosis. To count the apoptosis during neuronal differentiation, detection of DNA fragmentation using *in vitro* Terminal Deoxyncletidyl Transferase mediated dUTP Nick End labeling (TUNEL) of DNA were employed. The differentiated ES cells at D3 and D4 cultured in chamber slides were stained using the APOPtag red *in situ* apoptosis detection kit (Intergen). DNA was counter-stained with DAPI. Normal immunocytochemical staining following TUNEL detection was performed for double staining (Nestin/TUNEL). Apoptotic cell quantification was carried on by FACS scanning. Annexin-V was also used as early marker for apoptosis. Following dissociation of cells, parental euploid and aneuploid clones were subjected to FACS scanning analysis with FITC conjugated Annexin-V kits (MBL) according to the instruction manual. The apoptotic cell index (FITC positive/negative cells) was quantified using EPICS-XL software (Beckman Coulter).

4.3. Global Transcriptome & Proteome Analyses

ES cells from euploid and aneuploid clones cultured on PA6 feeder cells in a differentiation medium for 0, 2, 3, 4, and 6 days (D0, D2, D3, D4, and D6) were washed five times in PBS, dissociated by cell dissociation solution (Sigma), and passed through a cell strainer (Falcon) to remove any cell clumps. The resulting cell suspensions were used for either RNA extraction for transcriptome analysis or protein extraction for proteome analysis.

Microarray Gene Expression Profiling. Total RNA from ES cells on D0, D2, D3, D4, and D6 of differentiation was isolated from independent harvests using RNeasy mini kit (Qiagen), DNase treated (Nippon Gene), labeled with either Cy3 or Cy5, and competitively hybridized on cDNA mouse microarrays (Figure 4.3; NIG-NIA 15K cDNA mouse array sets; Tanaka et al 2000). Samples were examined in triplicate and analyzed pairwise (transchromosomic aneuploid clones verse parental euploid clones) at the same differentiation stage. The microarrays used for this study were constructed from a collection of NIA 15,012 mouse cDNA library, supplemented

with 976 control spots from Arabidopsis photosystem I chlorophyll a/b-binding protein and root cap 1, mouse transferring receptor, glyceraldehyde-3-phosphate dehydrogenase and b-actin as internal positive controls; poly(dA)45 oligonucleotide, Luciferase reporter pGL2, and novel Algae EST (CIB, NIG, Japan) as negative controls. Qualitative and quantitative assessments of performance for data acquisition, validation, and standardization were acquired from the exogenous Arabidopsis thaliana mRNA in intra-array and inter-array hybridizations with target RNA as external positive controls (Wang et al 2003).

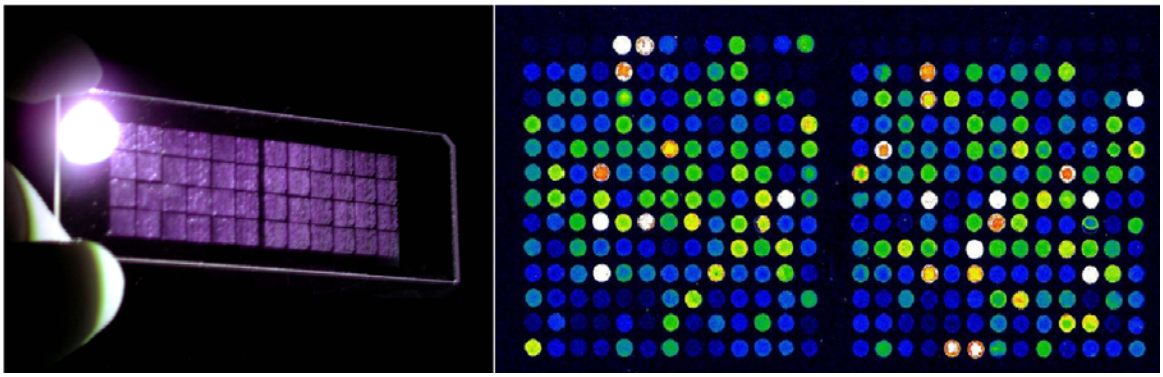

Figure 4.3 NIG-NIH 15K Mouse cDNA microarray (left panel) and representative subarray after hybridization (right panel).

Data collected from the hybridization were low-frequency algorithmic corrected in order to compensate for systemic variations. Less than 0.01% of genes were considered true outliers, with reproducible positive labeling in reverse fluorochrome hybridization. K-means hierarchical clustering was applied to the background subtracted, control spots calibrated, intra-array Lowess normalized, and intensity values log-transformed using an un-weighted pair-group method average (UPGMA) linkage and implemented by the CLUSTER and TREEVIEW programs (see URL, http://rana.lbl.gov/EisenSoftware.htm; Eisen et al 1998). Self-organizing maps (SOM) were employed to elucidate the possible biological relevant cluster during neuronal differentiation (Tamayo et al 1999). To calculate significant differential expression between the aneuploid clones and euploid clones, one-way ANOVA was performed. Pairwise bootstrap statistics were also performed to identify significantly differentially expressed clusters for individual genes. A 1.5-fold difference with p values less than 0.01 was considered as significant. Each of the mouse clones in the microarray was fully functional annotated (Kargul et

al 2002). The amount of expression in aneuploid clones was presented as the number of fold changes in logarithmic (base 2) intensity ratio to the control euploid clones.

To confirm the results of microarray, quantitative real-time RT-PCR was employed. Total RNA was isolated from ES cells after D3 of neuronal differentiation by SDIA treatment using an RNeasy Plus Mini Kit (Qiagen) and converted to cDNA using an oligo(dT)15 primer (Roche) and SuperScript III RT (Invitrogen). Real-time PCR was carried out using the ABI Prism 7900 Sequence Detection System and 2× converted SYBR Green PCR Master Mix reagent (PE Applied Biosystems) in 10-ml volume. b-actin was used as internal standard.

Comparative Proteomics. Protein extraction and 2 dimentional electrophoresis (2-DE) were performed as previously described (Toda et al., 1998; Nishigaki et al., 2002) with minor modifications. Briefly, each 10 mg of cell pellet samples from euploid TT2F clones and aneuploid TT2F/hChr21 clones (21–10, and 21–11) clones were lysed in 40ul of lysis buffer (7M urea, 2M thiourea, 0.5% CHAPS, 1.5% Triton X-100, 1% Pharmalyte (pH 3-10; Amersham Biosciences, NJ, USA), 10mg/ml DTT, 1ug/ml pepstatin, 1ug/ml leupeptin, 5ug/ml aprotinin, and 1mM PMSF with sonication. Following centrifugation, the supernatant was recovered and the protein concentration was estimated by dot blot staining. In the first dimension of isoelectric focusing, a 6ul aliquot of this supernatant was applied near the cathode wick of each 18cm Immobiline Gradient Gel pH 4–7 (Amersham Biosciences) and run under the protein IEF cell system (Bio-Rad, CA, USA). In the second dimension of SDS-PAGE, gels were equilibrated as described previously (Toda et al., 1998; Nishigaki et al., 2002). Gels were then placed on the top of the polyacrylamide gel (12%, 18×16.5×0.09cm) and run vertically in a glycine buffer system. After the second electrophoresis, gels were fixed in 50% methanol and 10% acetic acid for 30min, and protein spots were visualized by silver-staining reagent kit (Wako, Osaka, Japan) for 2-DE analysis. For peptide mass fingerprint, fixed gels were stained by SYPRO Ruby gel stain (Bio-Rad) according to the manufacturer's recommendations. SYPRO Ruby-stained images were scanned at excitation wavelength of 488 nm, and emission wavelength of over 550 nm on a Molecular Imager FX (Bio-Rad).

Protein spots were outlined and quantified using the PDQuest 7.1 software (Bio-Rad). Protein extracts from aneuploid TT2F/hChr21 clones (21–10 and 21–11) and euploid TT2F cells at the same differentiation stage were run in triplicate under the same conditions and were compared. Individual resolved protein features were enumerated and quantified on the basis of signal intensity. The quantity of individual spots (proteomic features) was expressed as a fractional intensity, relative to the sum of all detected features in that sample. Proteomic features common to individual images for euploid TT2F cells, and features common to individual images for aneuploid TT2F/hChr21 cells at D0, D3, D6, and D10 were identified. Next the two sets of proteomic features were compared with respect to the intensity for each spot. To minimize experimental dispersion of spot volumes among 2-DE gels, normalization was performed by taking the ratio of the intensity of each candidate spot to the total spot intensity. Only spots that showed more than two-fold differences in density after normalization, in any of the differentiation stage, were defined as altered. The identified features, especially those significantly expressed protein spots, were subjected to protein identification by proteolytic peptide fingerprinting method. Protein spots were excised using ProteomeWorks Spot Cutter (Bio-Rad). The separated protein spots were first in-gel digested with trypsin (Promega, WI, USA) according to the manufacturer's instructions. The digested peptide was directly mixed with an equal volume of 10 mg/ml cyano-4-hydroxy cinnamic acid and peptide mass spectra were obtained on an AXIMA-CFR MALDI-TOF MS (Shimadzu, Kyoto, Japan). Protein identification was carried out based on peptide match using Mascot Search program (http://www.matrixscience.com), referring the estimated molecular weight (MW) and pI value of the candidate match to the MW and pI value of the corresponding spot in the 2-DE gel.

To correlate the protein expression from results of proteome analysis with RNA expression, quantitative real-time RT-PCR was employed. Total RNA from D0, D3 and D6 harvested cells was extracted using the RNeasy mini kit (Qiagen, CA, USA). After treatment of RNA with DNase (Nippon Gene, Tokyo, Japan), first strand cDNA was synthesized using 5ug total RNA with MMLV-RT (Invitrogen) and random primer (Roche, Basel, Switzerland), and 1/80 volume of cDNA was applied to real-time PCR. Primer sequences designed with Primer Express 1.5 software. PCR was carried out in triplicate in a 10ul volume with 900nM forward and reverse primers using SYBR Green I Mastermix (Applied Biosystems, CA, USA) or Taqman Universal

PCR Mastermix, with ABI Prism 7900HT sequence detection. PCR cycling condition was 50°C for 2min, 40 cycles of 95°C for 15s, and 58°C for 1min. Dilutions of corresponding cDNA samples prepared from TT2F clones were used to construct a relative standard curve of critical threshold cycle for the target transcripts amplification. The amount of target mRNA expression in aneuploid TT2F/hChr21 clones was expressed as a number of fold difference relative to the control TT2F.

4.4. Quantitative & Functional Studies

The results from global transcriptome and proteome analyses on the genomic implications of autosomal imbalance will be validated and confirmed by further quantitative and functional studies as below.

Chimeric & Transchromosomal Mice. To confirm the microarray result and the molecular changes of autosomal imbalance for the neuropathogenesis in mice, brain tissues from the transchromosomal mice were obtained for quantitative real-time RT-PCR and *in situ* hybridization. One of the resultant puromycin-resistant MH(ES) clones, MH(ES)2-21, retained hCF(2-W23) and was used to produce chimeras. Ten to twenty MH(ES) cells from each cell line were injected into an 8-cell stage embryo derived from Jcl:MCH(ICR) mice (Crea Japan, Inc.). Injected embryos were then transplanted to the uteri or oviducts of pseudopregnant recipients and allowed to proceed to term delivery. Chimerism in resulting offspring was determined by the extent of coat pigmentation. The TT2 or TT2F line, derived from C57BL/6xCBA-F1 embryo, gives an agouti coat colour in an albino MCH(ICR) background. Three representative clones, ES(#21)-7, -10 and -11, were chosen from the panel of ES(#21) cells and used to produce viable chimeric mice. The ES(#21) cells were injected into 8-cell stage embryos of albino MCH(ICR) mice and the embryos were transplanted into the uteri or oviducts of pseudopregnant mice. Viable chimeric mice with varying levels of contribution of the ES cells were obtained. Among transplanted embryos, 1.7% (3/174) to 10.9% (20/183) produced live-born pups that survived >4 weeks, and 3.4% (9/266) to 9.3% (17/183) resulted in pre- and postnatal death. The latter is likely to be an underestimate, because some dead pups were likely to have been cannibalized before they could be ascertained. Based on coat color, ES(#21)-10 and -11 clones had an ability

to contribute to >90% in an albino MCH(ICR) background. ES(#21)-7 produced only low percentage chimeras (<50%) and these were not analyzed further. High level chimeras were produced more efficiently from clone ES(#21)-10 than from ES(#21)-11.

Human Fetal Brain. To confirm the molecular changes of autosomal imbalance for the neuropathogenesis in human, brain tissues from aborted human fetuses of controls and trisomy 13, 16 and 21 were obtained for quantitative real-time RT-PCR. Human ethics approvals (CRE-2003.139, CRE-2004.330 & UW 04-258 T/580, Appendix I - III) from the home institutions and hospitals were sought and informed written consent were obtained before operation. Trisomic condition was diagnosed by standard fetal cell culture and metaphase karyotype analysis for prenatal diagnosis. All subjects were underwent legal surgical termination of pregnancy by mechanical suction method without medical intervention before procedures. Fetal brain tissues were identified under disserting microscope and washed and snap frozen in liquid nitrogen prior to analysis.

Embryoid Body & Teratoma Formation. To confirm the morphological changes in undifferentiation state of the ES clones *in vitro*, embryoid bodies were cultured using the hanging drop culture method (Inoue et al 2000). Briefly, approximately 400 ES cells in 30 ml aliquots of differentiation medium, which consisted of ES culture medium without LIF, were placed on the undersurface of a petri dish lid, inverted and cultured for 3 days. The resulting EBs were transferred individually to separate wells of 24-well tissue culture plates (Costar). For the coculture of two EBs that were derived from different cell lines, one EB was allowed to attach to the bottom of 12-well plate (Costar) for 3 h, followed by the transfer of the second EB and attachment to a different position. Culture medium was changed every 2 days. To confirm the morphological changes during differentiation *in vivo*, subcutaneous injections of embryoid bodies in nude mice produced teratomas. 2×10^6 TT2F and TT2F/hChr21 cells were injected into CD-1 (ICR)-nu mice (Charles River, Yokohama, Japan). Five to six weeks after cell transplantation, the teratomas were fixed in 20% formalin and processed for paraffin sectioning to examine structures originating from all three germ layers.

Neuronal RNA interference. To confirm the candidate genes for the defective neuronal differentiation, RNA interference was employed to the ES cell culture and SDIA neuron lineage induction. The Stealth Select RNAi oligonucleotides for the targeted genes were synthesized by Invitrogen. BLOCK-iT RNAi Designer (Invitrogen), a web-based program for designing siRNA targets. The Stealth Select RNAi negative control Duplex was used as a control oligonucleotide. On D0 of neuronal differentiation, transfections were performed on ES cells on PA6 stromal cells using Lipofectamine 2000 (Invitrogen) following the manufacturer's protocol. Neural induction was carried out as above for neuronal differentiation for further functional analyses.

Chapter 5

Results

5.1 Gene Dosage of HSA21

Many genes with a potential impact on brain development have been localized to the distal arm of chromosome of HSA21 (Schapiro et al 1992). We predicted the gene expression of the HSA21 in TT2F/hChr21 clones in our mouse developmental cDNA microarray. The microarray library contains 56 HSA21 orthologs (<12.5% of current genes identified in the HSA21) where the mouse cDNA expressed tags covered over 80–85% homology of the human sequences (Tab. 5.1). These allowed us to investigate the contributions of the transferred HSA21 to the gene dosage imbalance of autosomal aneuploidy in mouse genome.

The gene expression profiling of the HSA21 genes in the aneuploid ES clones showed variable expression patterns (Fig. 5.1). There were both over-expression regions and under-expression regions along the HSA21 homologs. The over-expressed HSA21 genes were mainly distributed and highly up-regulated close to the centromere (equalivant to corresponding partial MMU3), between q11.2 and q21.2 regions (equalivant to corresponding partial MMU16) and between q21.3 and q22.3 regions (equalivant to corresponding partial MMU17 and MMU10). These regions are covered by DSCR loci contributing to many well characterized and uncharacterized phenotypes in Down syndrome (Tab. 5.1). On the other hand, the under-expressed HSA21 genes were scatterly involved in q11.2 (equalivant to corresponding partial MMU16) and between q21.3 and q22.3 regions (equalivant to corresponding partial MMU17 and MMU10) which were covered by other known loci contributing to many well characterised phenotypes in Down syndrome (Tab. 2.1).

High-stringency K-mean hierarchical clustering of the gene expression profilings of 56 HSA21 orthologs in TT2F/hChr21 clones during neuronal differentiation revealed 3 distinct gene clusters (Fig. 5.2).

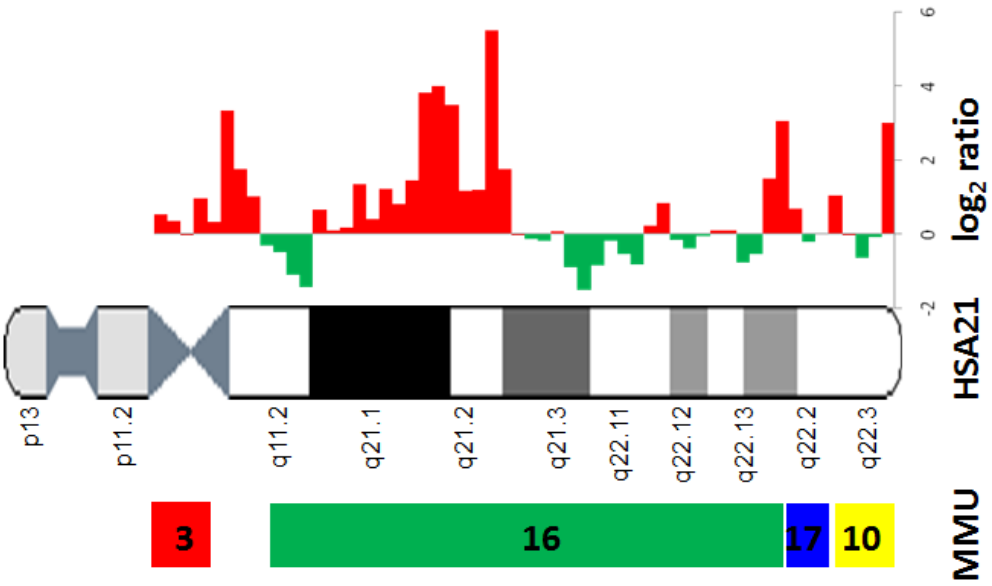

Figure 5.1 Expression of HSA21 homolog genes. The expression levels of the HSA21 genes corresponding to the mouse chromsomes MMU3, MMU16, MMU17 and MMU10 were shown and experssed in $\log_2$ ratios. Red bars are over-expressed and green are underexpressed genes along the chromosome HSA21.

5.1.1 Primary gene dosage effects

The first major cluster was identified as the primary gene dosage effect (Fig. 5.2 lowest panel). The expression of 30 (53.6%) "trisomic" genes were increased in average of 1.5254 fold, about 1.5-fold (Fig. 5.3). The extent of such primary dosage effects are similar to other studies (~50%). Functional annotation indicated that the primary gene dosage were mainly involved in matrix/structural proteins (36.7%), transcription/chromatin (16.7%) and signal transduction (13.3%) durign early neurogenesis. The "trisomic" genes for energy/metabolism; heat shock/stress; protein synthesis/translational were just less than 10% (Tab. 5.1). Amongst these genes, over-expression of App, Itsn1, and Mnb in differentiating TT2F/hChr21 cells was relevant to the published data using fetal brain tissue from DS patients (Engidawork & Lubec 2003, Tab. 5.6).

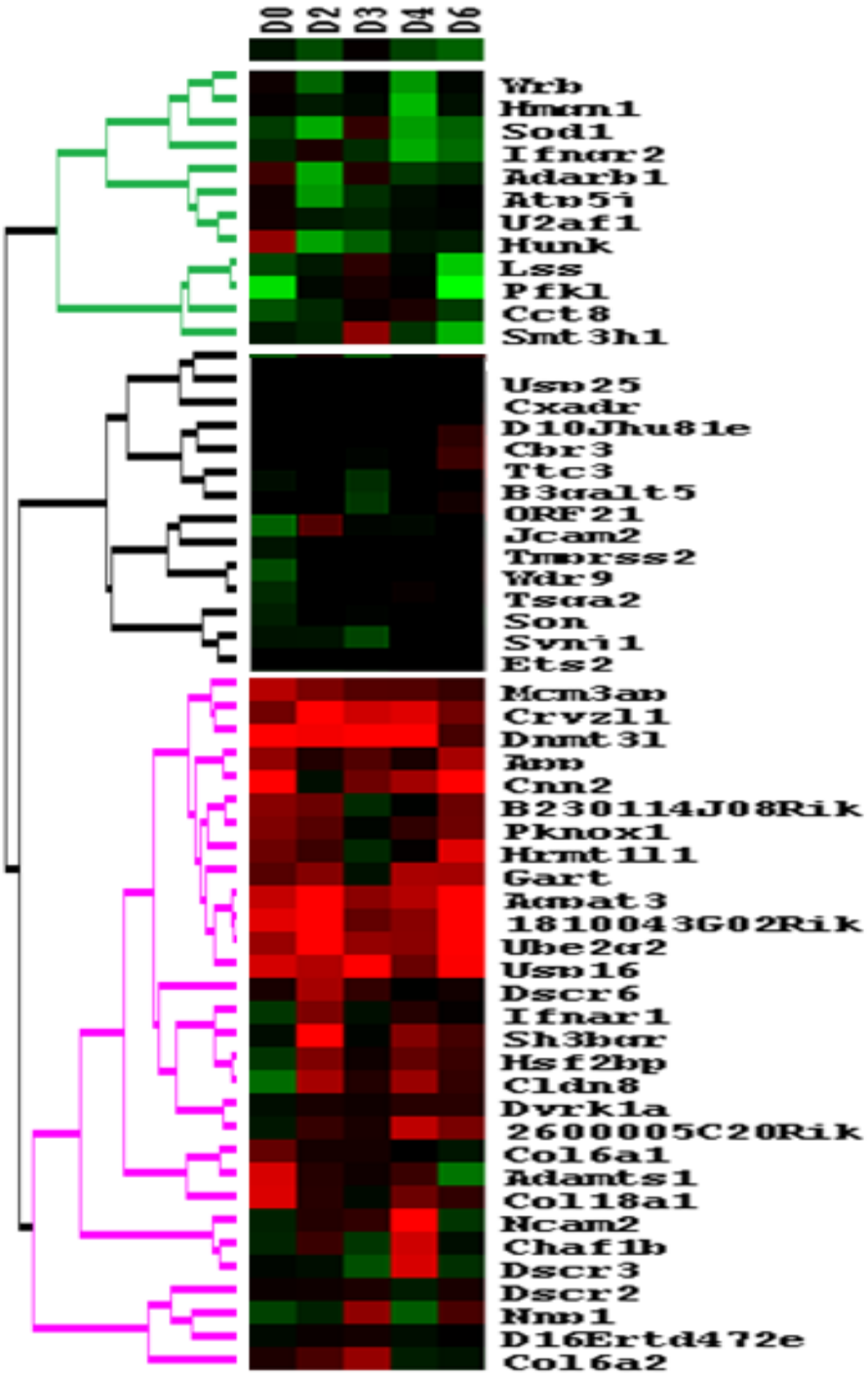

Figure 5.2 Gene dosage imbalance of HSA21 in autosomal trisomy. High-stringency K-mean hierarchical clustering of three biological replicated array experiments comparing TT2F/hChr21 cells to TT2F cells along the neruonal differentation from day 0 to day 6. Green dendogram indicates the decreased "trisomic" genes (reverse gene dosage effects), black dendogram indicates the unchanged "trisomic" genes (dosage compensation); pink dendogram indicates the increased "trisomic" genes (primary gene dosage effects). Gene list and annotation are shown in Table 5.1.

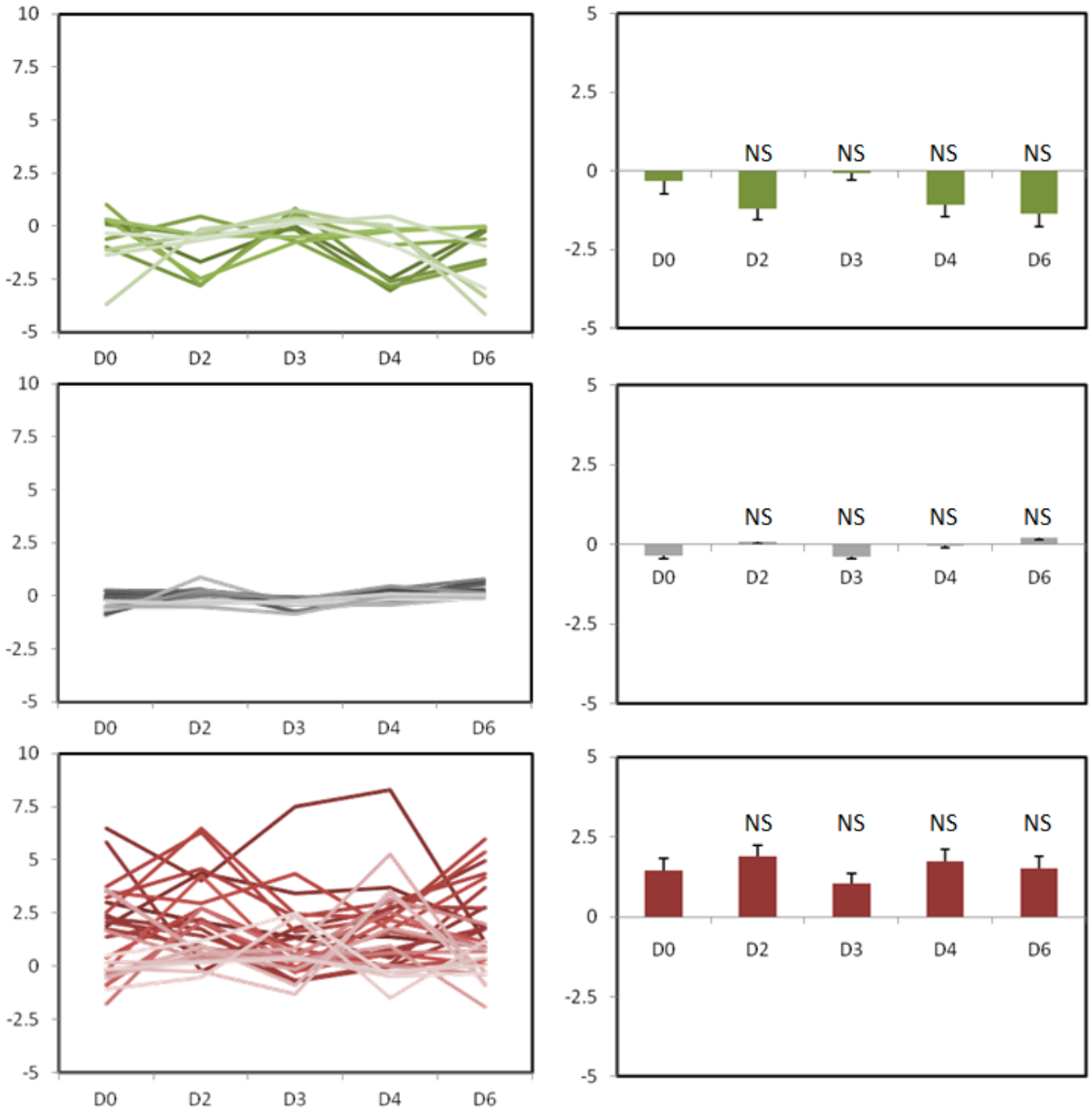

Figure 5.3 Gene dosage clusters of HSA21 in autosomal trisomy. Expression pattern changes of each cluster gene during neuronal differentiation are presented in left panels and mean expression levels of the cluster genes in different neuronal differentiation stages are presented in right panels. Green lines and bars indicate the decreased "trisomic" genes (reverse gene dosage effects), grey lines and bars indicate the unchanged "trisomic" genes (dosage compensation); and pink lines and bars indicates the increased "trisomic" genes (primary gene dosage effects). NS: no significant difference when compared with D0.

Table 5.1 HSA21 orthologs in NIA 15K mouse cDNA library

No.	Clone *	Gene	*Symbol*	Genbank Accession	Locus ^	Fx	Ontology #	mChr	cM	hChr	arm
Decreased Cluster:											
1	H3136F02	M. Tryptophan rich basic protein	*Wrb*	XM_148742.2	71446	M	integral to membrane	16	C4	21	q22.3
2	H3120G04	M. High mobility group nucleosomal binding domain 1	*Hmgn1*	NM_008251.1	15312	T	DNA packaging	16	69.8	21	q22.2
3	H3130B11	M. Superoxide dismutase 1, soluble	*Sod1*	BC032986.1	20655	H	oxidoreductase activity	16	61.00	21	q22.11
4	H3114F11	M. Interferon gamma receptor 2	*Ifngr2*	NM_008338.1	15980	S	hematopoietin cytokine receptor	16	63.30	21	q22.11
5	H3157B07	M. Adenosine deaminase ADAR2	*Adarb1*	AF525421.1	110532	T	dsRNA adenosine deaminase	10	41.40	21	q22.3
6	H3115C02	M. ATP synthase, H+ transporting, mitochondrial F0 complex subunit F	*Atp5j*	BC010766.1	11957	E	proton transport	9	4.00	21	q21.1
7	H3086D11	M. U2 small nuclear ribonucleoprotein auxiliary factor 35 kDa	*U2af1*	NM_024187.1	108121	P	ribonucleoprotein complex	17	A3.3	21	q22.3
8	H3010H08	M. Hormonally upregulated Neu-associated kinase	*Hunk*	NM_015755.1	26559	S	protein amino acid phosporylation	16	58.00	21	q22.1
9	H3037A02	M. Lanosterol synthase	*Lss*	NM_146006.1	16987	-	unknown	10	41.10	21	q22.3
10	H3025D11	M. Phosphofructokinase, liver, B-type	*Pfkl*	NM_008826	18641	E	glycolysis	10	41.70	21	q22.3
11	H3018A08	M. Chaperonin subunit 8	*Cct8*	NM_009840.1	12469	H	chaperone activity	16	A1	21	q22.11
12	H3023B05	M. SMT3 (supressor of mif two, 3) homolog 1 (S. cerevisiae)	*Smt3h1*	NM_019929.1	20610	H	chaperone activity	10	41.60	21	q22.3
Unchanged Cluster:											
13	H3152H01	M. Ubiquitin specific protease 25	*Usp25*	NM_013918	30940	P	ubiquitin-specific protease activity	16	-	21	q11.2
14	H3135F11	M. Coxsackievirus and adenovirus receptor	*Cxadr*	BC016457.1	13052	S	neural cell adhesion molecule	16	A1	21	q21.1
15	H3139H01	M. DNA segment, Chr 10, Johns Hopkins University 81 expressed	*D10Jhu81e*	NM_138601.1	28295	M	extracellular space	10	41.70	21	q22.3
16	H3049F02	M. Carbonyl reductase 3	*Cbr3*	XM_128324.2	109857	E	carbonyl reductase activity	16	67.20	21	q22.2
17	H3004A06	M. Tetratricopeptide repeat domain	*Ttc3*	NM_009441.1	22129	-	unknown	16	67.90	21	q22.2
18	H3104D12	M. UDP-Gal:betaGlcNAc beta 1,3-galactosyltransferase, polypeptide 5	*B3galt5*	AK004442.1	68871	E	galactosyltransferase activity	16	A1	21	q22.3
18	H3104D09	M. Open reading frame 21	*ORF21*	BC029101.1	224440	-	N-methyltransferase	16	A1	21	q22.13
20	H3109B09	M. Junction adhesion molecule 2	*Jcam2*	NM_023844	67374	M	extracellular space	16	A1	21	q21.2
21	H3037H01	M. Transmembrane protease, serine 2	*Tmprss2*	BC038393.1	268912	H	scavenger receptor	16	C2	21	q22.3
22	H3092A08	M. WD repeat domain 9	*Wdr9*	NM_145125.1	93871	T	Pol II promotor regulation	16	A1	21	q22.2
23	H3075A12	M. Testis specific gene A2	*Tsga2*	NM_025290.1	22092	C	meiosis	17	13.25	21	q22.3
24	H3094B06	M. Son cell proliferation protein	*Son*	NM_019973.1	20658	M	chitinase	16	64.00	21	q22.11
25	H3101D07	M. Synaptojanin 1 (Synaptic inositol-1,4,5-trisphosphate 5-phosphatase 1)	*Synj1*	XM_128379.2	106136	S	phospoinositide-mediated signaling	16	C3-C4	21	q22.2
26	H3028G09	M. E26 avian leukemia oncogene 2, 3' domain	*Ets2*	BC005486.1	23872	T	DNA binding	16	69.60	21	q22.2
Increased Cluster:											
27	H3031B12	M. Minichromosome maintenance deficient (S. cerevisiae) 3-associated protein	*Mcm3ap*	NM_019434.1	54387	M	nuclear protein export factor	10	C1	21	q22.3
28	H3123G05	M. Crystallin, zeta (quinone reductase)-like 1	*Cryzl1*	NM_133679.1	66609	E	NADPH:quinone reductase activity	16	A1	21	q21.3
29	H3094C02	M. DNA (cytosine-5-)-methyltransferase 3-like	*Dnmt3l*	XM_125698.2	54427	T	nuclear heterchromatin	10	41.60	21	q22.3
30	H3132G02	M. Amyloid beta (A4) precursor protein	*App*	NM_007471.1	11820	M	beta amyloid precursor protein	16	56.00	21	q21.3
31	H3039H01	M. Calponin 2	*Cnn2*	NM_007725.1	12798	M	calmodulin binding	10	C1	21	q11.1

32	H3137H08	M. RIKEN cDNA B230114J08 gene (B230114J08Rik)	*B230114 J08Rik*	NM_030018.1	77975	M	integral to membrane	16	A1	21	q22.11
33	H3129G08	M. Pbx/knotted 1 homeobox	*Pknox1*	NM_016670	18771	T	Pol II pormotor regulator	17	B-C	21	q22.3
34	H3059E02	M. Heterogeneous nuclear ribonucleoprotein methyltransferase-like 1 (S. cerevisiae)	*Hrmt1l1*	XM_122051.1	15468	T	methyltransferase	10	41.00	21	q22.3
35	H3047B10	M. Phosphoribosylglycinamide formyltransferase	*Gart*	NM_010256.1	14450	S	phosporibosylamine-glycine ligase	16	63.00	21	q22.11
36	H3158D09	M. 1-acylglycerol-3-phosphate O-acyltransferase 3	*Agpat3*	NM_053014.1	28169	E	phospholipid metabolism	10	41.80	21	q22.3
37	H3158A06	M. RIKEN cDNA 1810043G02 gene (1810043G02Rik)	*1810043 G02Rik*	NM_026431.1	67884	-	unknown	10	41.60	21	q22.3
38	H3154G06	M. Ubiquitin-conjugating enzyme E2G 2	*Ube2g2*	NM_0019803	22213	P	ubiquitin conjugating emzyme activity	10	41.60	21	q22.3
39	H3152C04	M. Ubiquitin specific protease 16	*Usp16*	NM_024258.1	74112	P	peptidase activity	16	A1	21	q22.11
40	H3111B09	M. Down syndrome critical region gene 6 DSCR6	*Dscr6*	NM_133229.1	170765	-	unknown	16	A1	21	q22.2
41	H3118F09	M. Interferon (alpha and beta) receptor	*Ifnar1*	NM_010508.1	15975	S	phosphoribosylamine-glycine ligase	16	63.20	21	q22.11
42	H3050D06	M. Partial mRNA for putative SH3BGR protein	*Sh3bgr*	AJ272170.1	50795	-	unknown	16	A1	21	q22.3
43	H3125B05	M. Heat shock transcription factor 2 binding protein	*Hsf2bp*	XM_128560.1	74377	H	chaperone activity	17	A3.3	21	q22.3
44	H3064H02	M. Claudin 8	*Cldn8*	NM_018778.1	54420	M	tight junction	16	A1	21	q22.11
45	H3027D04	M. DNA segment, Chr 16, ERATO Doi 272, expressed	*Dyrk1a*	XM_128336.2	13548	S	LAMMER dual specificity kinase	16	68.30	21	q22.13
46	H3020A05	M. RIKEN cDNA 2600005C20 gene (2600005C20Rik)	*2600005 C20Rik*	XM_128486.1	72462	T	nucleolar protein NOP52	17	B1	21	q22.3
47	H3151F07	M. Procollagen, type VI, alpha 1	*Col6a1*	NM_009933.1	12833	M	collagen	10	41.10	21	q22.3
48	H3034B07	M. mRNA for secretory protein containing thrombospondin motifs	*Adamts1*	D67076.1	11504	M	extracellular matrix degrading enzyme	16	53.40	21	q21.2
49	H3111D11	M. Procollagen, type XVIII, alpha 1	*Col18a1*	NM_009929.1	12822	M	collagen	10	41.30	21	q22.3
50	H3121A01	M. Neural cell adhesion molecule 2	*Ncam2*	NM_010954	17968	M	cell adhesion	16	56.00	21	q21.1
51	H3115E05	M. Chromatin assembly factor 1, subunit B (p60)	*Chaf1b*	NM_028083	72072	S	heterotrimeric G-protein complex	16	67.40	21	q22.13
52	H3007H01	M. Down syndrome critical region gene 3	*Dscr3*	NM_007834	13185	-	intracellular protein transport	16	A1	21	q22.2
53	H3129G11	M. Down syndrome critical region homolog 2	*Dscr2*	NM_019537.1	56088	M	membrane fraction	16	A1	21	q22.3
54	H3158F11	M. Similar to novel nuclear protein 1	*Nnp1*	BC022910.1	18114	T	nucleolar protein NOP52	10	C1	21	q22.3
55	H3025B10	M. DNA segment, Chr 16, ERATO Doi 472, expressed	*D16Ertd4 72e*	NM_025967.1	67102	-	unknown	16	A1	21	q21.1
56	H3152G04	M. Procollagen, type VI, alpha 2	*Col6a2*	NM_146007.1	12834	M	collagen	10	41.10	21	q22.3

* http://lgsun.grc.nia.nih.gov/cDNA/15k.html; ^ http://www.ncbi.nlm.nih.gov/LocusLink; # http://www.geneontology.org; Annotations: E, energy/metabolism; H, heat shock/stress; M, matrix/structural proteins; P, protein synthesis/translational; T, transcription/chromatin.

5.1.2 Dosage compensation

The second cluster was identified as the gene dosage compensation (Fig. 5.2 middle panel). The expression of 14 (25%) "trisomic" genes were unchanged compared with those of controls. The expression levels of the compensated "trisomic" genes were in average of -0.0906 fold, less than -0.1-fold (Fig. 5.3). The extent of such dosage compensation are relative higher than other studies (5-10% only). Functional annotation indicated that the reverse gene dosage effects were evenly involved in all kinds of gene functions for 15% each (Tab. 5.1).

5.1.3 Reverse gene dosage effects

The thrid cluster was identifed as novel reverse gene dosage affects (Fig. 5.2 upper panel). It has never been reported before. The expression of 12 (21.4%) "trisomic" genes were decreased in average of -0.8127 fold, less than -1.0-fold (Fig. 5.3). Under-expressions of Dscr3, Ets2, Hmgn1, SOD1, and CCT8 were found in contrast to what would be expected from a gene dosage effect (Engidawork & Lubec 2003). This further confirmed the extra load of gene copies is not always associated with gain in gene function. Again the functional annotation indicated that the reverse gene dosage effects were evenly involved in all kinds of gene functions for 15% each (Tab. 5.1).

5.2 Genomic Implication

5.2.1. Secondary gene or trans-acting dosage effects

To further investigate the contribution of "trisomic" genes in the the disomic genome, the secondary gene dosage or trans-acting effects, we measured the association strength of their gene expression using probabilistic clustering algorithms on 200 bootstrap datasets (Cheeseman & Stutz 1996) and illustrated by Terrain mountain plots for both positively and negatively correlated clusters between those HSA21 orthologs and expressed MMU transcripts during neuronal differentiation.

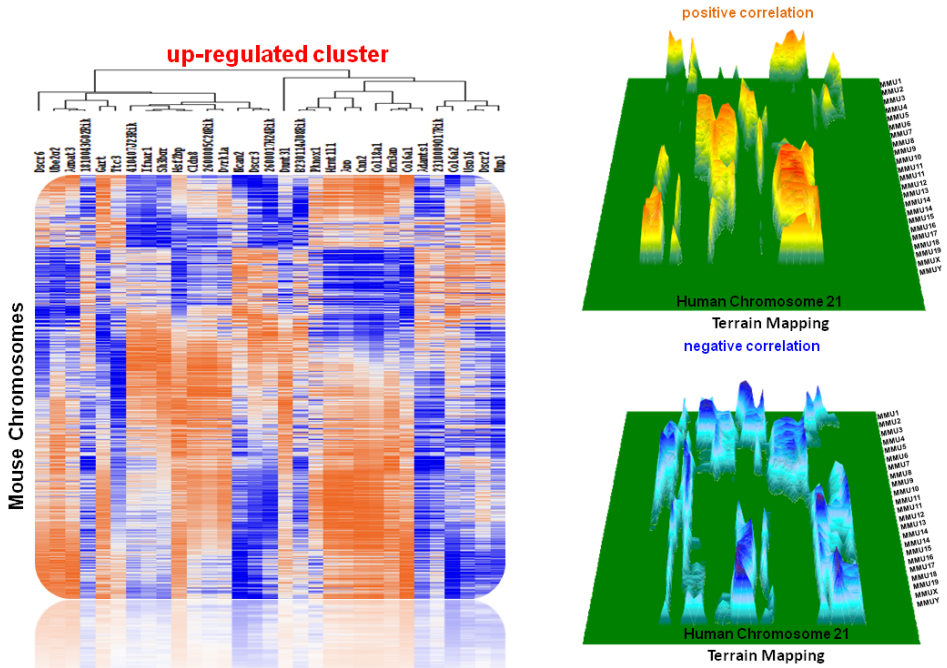

Figure 5.4 Correlation of primary gene dosage effects of HSA21 in autosomal trisomy. Terrain mountain plots is shown by probabilistic hierarchical clustering of HSA21 genes expression with mouse genes in other MMU chromosomes. Terrain peak hieght is referred to the correlation coefficient values of positively (upper panel) and negatively (lower panel) correlated expression.

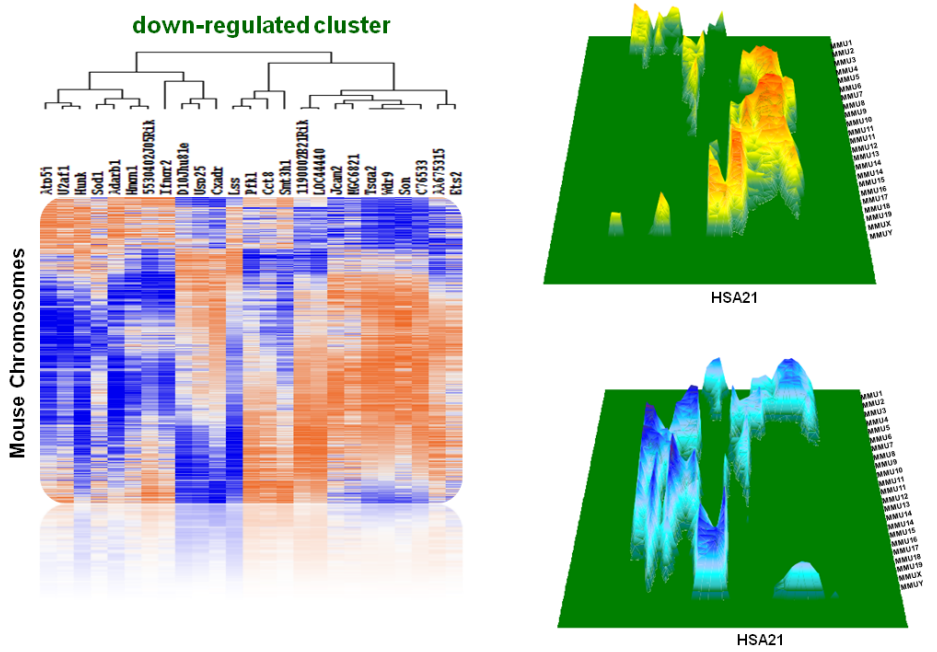

Figure 5.5 Correlation of reverse gene dosage effects of HSA21 in autosomal trisomy. terrain mountain plots is shown by probabilistic hierarchical clustering of HSA21 genes expression with mouse genes in other MMU chromosomes. terrain peak hieght is referred to the correlation coefficient values of positively (upper panel) and negatively (lower panel) correlated expression.

Figure 5.4 & 5.5 showed the correlation of increased (primary gene dosage effects) and decreased (reverse gene dosage effects) trisomic HSA21 gene clustered with disomic MMU gene expression, respectively. Either primary or reverse trisomic HSA21 genes has both positive and negative secondary or trans-acting gene dosage effects on the disomic genes. The effects by the primary gene dosage were mainly involved in the limited trisomic HSA21 genes on certain disomic genome, whilst the effects by the reverse gene dosage were randomly involved amongst the trisomic HSA21 genes on the disomic genome.

In order to further investigate the distribution of secondary or trans-acting genomic implications of the trisomic HSA21 gene dosage imbalance in the disomic genome, in particular focus on the primary gene dosage effects, we determined the significant associations between the up-regulated trisomic genes and the disomic genes and then plotted the correlation coefficient values along the mouse genome (Fig. 5.6). In total there were 118 significantly positively correlated genes and 47 significantly negatively correlated genes. It also demonstrated there was no obvious derivation on the secondary or trans-acting genomc implications. The secondary or trans-acting effects of primary HSA21 "trisomic" genes were rather evenly distributed thoughtout the mouse genome.

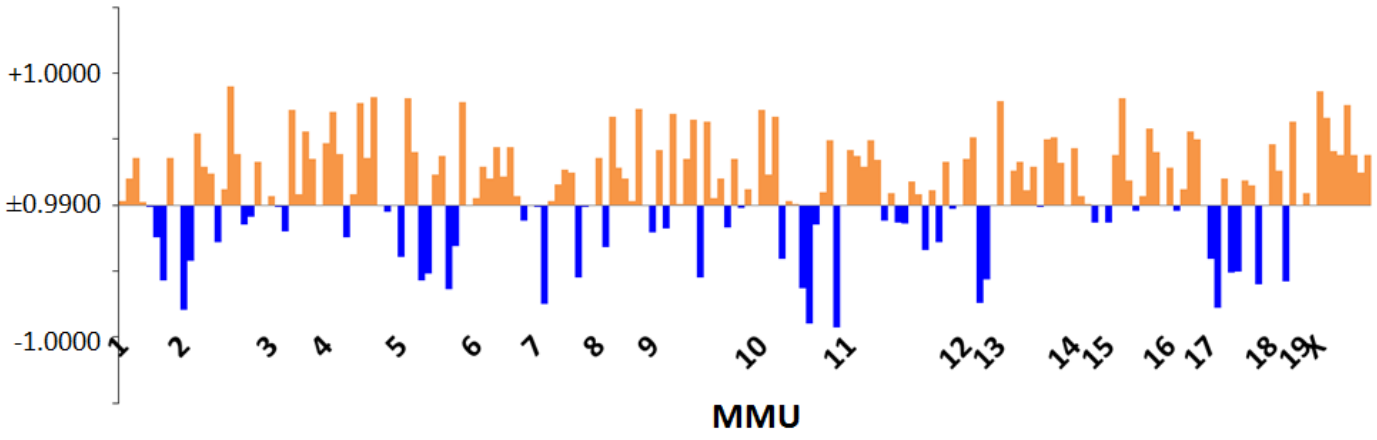

Figure 5.6 Correlation of secondary gene dosage effects of HSA21 in mouse genome. Correlation coefficient are plotted against the length of mouse genome. Only significant coefficient values between ±0.9900 and ±1.0000 are presented. Orange as positively correlated gene and blue as negative correlated genes.

And also such effects were not significantly correlated to the gene contents in each individual chromosome (Fig. 5.7). This indicates that an extra HSA21 in DS may nonselectively exert gene dosage phenomena on other chromosomal functions, resulting in more extensive secondary gene dosage or trans-acting outcomes.

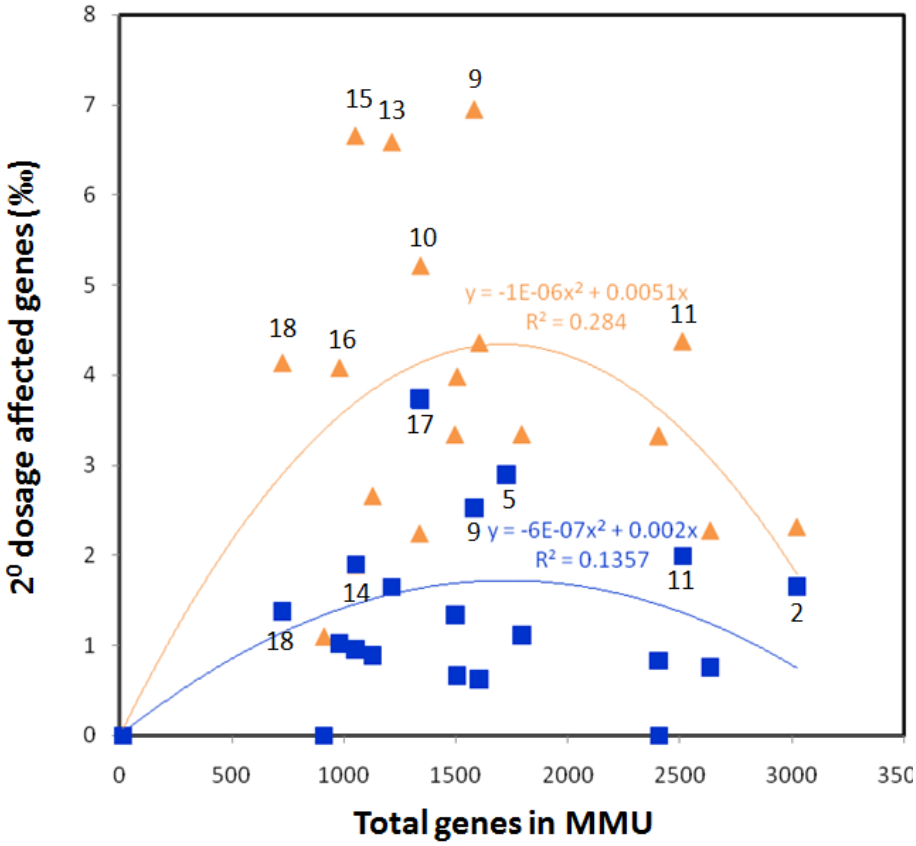

Figure 5.7 Association of gene numbers in the secondary gene dosage effects. Significantly correlated disomic genes in percentage 10^2% are plotted against the total number of genes in mouse genome. Orange as positively correlated gene and blue as negative correlated genes. The regression formula and coefficient and some of the MMU identifies are indicated.

5.2.2 Transcription networks

The significant secondary or trans-acting gene dosage effects of HSA21 trisomic genes on mouse genome were summarised in Table 5.2. Transcription networks were revealed from the most significant correlation coefficient calculation ($r>0.9900$, $p<0.01$) between trisomic HSA21 genes and the disomic MMU genes.

Table 5.2 Significant secondary affected genes

HSA21 Genes	MMU Genes	MMU Gene Name	mChrlocus	Correlation Coefficient	Gene Functions	Relevant Reports
2600017H24Rik	Gm3143	Predicted gene 3143	3-	0.9997	-	-
Dscr9 & Dscr2	Lmnb1	Lamin B1	18 D3	0.9996	intracellular|protein biosynthesis|ribosome|structural constituent of ribosome	impaired differentiation, increased polyploidy, and premature senescence; oligodendrocyte development and myelination (Vergnes et al 2004)
Hrmt1l1	Ctdsp1	Carboxy-terminal domain, RNA polymerase II, polypeptide A, small phosphatase 1	1 C3	0.9995	hydrolase and phosphatase activity	anti-neural function for neurogenesis (Visvanathan et al 2007)
Hsf2bp	C8714			0.9993	-	-
Dscr9 & Dscr2	Anxa4	Annexin A4	6 D1	0.9990	calcium binding	urinary bladder epithelium morphology and physiology (Hill et al 2008)
Dscr9 & Dscr2	Baiap2l1	Brain-specific angiogenesis inhibitor 1-associated protein 2-like protein 1	5 G2	0.9990	actin binding, cytoskelton adaptor, signal transduction\	brain-specific angiogenesis inhibitor
Hsf2bp	Pde8a	Phosphodiesterase 8A	7 D3	0.9989	hydrolase activity, signal transduction, DNA-dependent transcription regulation	testosterone synthesis (Vasta et al 2006)
Cldn8	2310001H12Rik	RIKEN cDNA 2310001H12 gene	5 F	0.9988	-	-
Gart	Cdk20	Cdk20 cyclin-dependent kinase 20	13 B3	0.9987	kinase, cell cycle, cell division, multicellular organismal development	promotes cardiac cell growth and survival (Qiu et al 2008)
Sh3bgr	Dlg2	Discs, large homolog 2 (Drosophila)	7 E1	0.9986	protein binding, neuronal ion channel and receptor clustering, synaptic tranmission, sensory perception of pain	rafts and postsynaptic densities of synaptic signaling complexes and contribute to molecular mechanisms of neuronal damage (Delint-Ramirez et al 2010, Zhang et al 2010)
Sh3bgr	D5Ertd577e	DNA segment, Chr 5, ERATO Doi 577, expressed	5 E3	0.9986	-	-
Hsf2bp & Cldn8	Wdr83	WD repeat domain containing 83	8 C3	0.9986	mRNA processing	renal protection (Hammerschmidt et al 2009)
Cldn8	Oxsm	3-Oxoacyl-ACP synthase, mitochondrial	14 A2	0.9986	lipid biosynthetic process	-
Cldn8	Zfp644	Zinc finger protein 644	5 E5	0.9986	-	-
Ifnar19 & Sh3bgr	C80915	Expressed sequence C80915	7	0.9902	-	-
Hsf2bp & Cldn8	Spin1	Spindlin 1	13 A5	0.9899	female meiosis, spindle	spermatogenesis, cell division and tumorigenesis (Zhang et al 2008, Yuan et al 2008)
Hsf2bp & Cldn8	Gtpbp10	GTP-binding protein 10 (putative)	5A1	0.9895	mitochondrion	-
Ifnar19 & Sh3bgr	Nfkb1	Nuclear factor of kappa light chain gene enhancer in B-cells 1, p105	3 G3	0.9895	apoptosis, transcription regulation, oxidative stress response, protein & DNA binding	apoptosis signaling in neurons degeneration (Wei et al 2010)
Col6a1	Rpp30	Ribonuclease P/MRP 30 subunit	19 C2	-0.9989	ribonuclease P for tRNA processing	-
Ncam8	Pdcl3	Phosducin-like 3	1 B	-0.999	apoptosis	modulates caspase activation to prevent cell death (Wilkinson et al 2004)
Ube2g2	Ptgr1	Prostaglandin reductase 1	4 C1	-0.9993	oxidoreductase	-
Sh3bgr	Rrm1	Ribonucleotide reductase M1	7 E3	-0.9993	RNA binding, DNA replication, protein modification, ubiquitin cycle, oxidoreductase	perturbation of regulatory networks in the cell cycle progression (Kawakami et al 2009)
Dscr9 & Dscr2	2610110G12Rik	RIKEN cDNA 2610110G12 gene	17 B3	-0.9996	unknown	-
Dnmt3l	Dcxr	Dicarbonyl L-xylulose reductase	11 E2	-0.9998	carbohydrate metabolic process	renal protection (Sudo et al 2005)
Ncam9	Tnrc6a	Trinucleotide repeat containing 6a	7 F3	-0.9999	regulation of translation	impairs RNAi and microRNA-induced gene silencing (Lian et al 2006)

significant positively correlated genes (top); negatively correlated genes (bottom)

The positively regulated targets with significant relevant molecular manifestation in DS included Lmnb1, Ctdsp1, Baiap2l1, Dlg2, and Nfkb1 genes. Duplication of the gene encoding lamin B1 (Lmnb1) with increased mRNA and protein levels has been shown to cause severe myelin loss in the brains of adult-onset autosomal dominant leukodystrophy patients. Similar to many neurodegenerative disorders, patients with adult-onset autosomal dominant leukodystrophy are phenotypically normal until adulthood and the defect is specific to the central nervous system despite the ubiquitous expression pattern of lamin B1 (Lin and Fu 2009). The anti-neural function of phosphatase Carboxy-terminal domain, RNA polymerase II, polypeptide A, small phosphatase 1 (Ctdsp1) during development and further the neuron-enriched miR-124 directly targets SCP1-3' untranslated region (UTR) to suppress SCP1 expression was demonstrated (Visvanathan et ala 2007). Baiap2l1 is Brain-specific Angiogenesis Inhibitor 1-Associated Protein 2-like protein 1. This gene encodes a member of the IRSp53/MIM homology domain (IMD) family. Members of this family can be subdivided in two groups, the IRSp53-like and MIM-like, based on the presence or absence of the Src homology 3 (SH3) domain. The protein encoded by this gene contains a conserved IMD, also known as F-actin bundling domain, at the N-terminus, and a canonical SH3 domain near the C-terminus, so it belongs to the IRSp53-like group. This protein is the substrate for insulin receptor tyrosine kinase and binds to the small GTPase Rac. It is involved in signal transduction pathways that link deformation of the plasma membrane and remodeling of the actin cytoskeleton. The scaffolding protein postsynaptic density (PSD)-93 (also called Discs, large homolog 2 (Drosophila), Dlg2) bind with N-methyl-D-aspartate receptor and neuronal nitric oxide (NO) synthase through its PDZ domains. PSD-93 deficiency reduced the amount of NMDAR subunits NR2A and NR2B in synaptosomal fractions from the cortical neurons and significantly prevented NMDA-stimulated increases in cyclic guanosine 3',5'-monophosphate and Ca^{2+} loading in the cortical neurons, suggesting that PSD-93 might contribute to molecular mechanisms of neuronal damage in the brain disorders (Zhang et al 2010). Nfkb1 involved in the degeneration of cochlea spiral ganglion neurons-apoptosis signaling (Wei et al 2010). All their roles in DS during brain development required to be confirmed.

The negatively regulated targets with significant relevant molecular manifestation in DS included Pdcl3, Rrm1, and Tnrc6a genes. Phosducin-like 3 (Pdcl3) is also called viral IAP-

associated factor (VIAF), a highly conserved ubiquitously expressed phosphoprotein with limited homology to members of the phosducin family that associates with baculovirus inhibitor of apoptosis (IAP). VIAF is a novel IAP-interacting factor that functions in caspase activation during apoptosis (Wilkinson et al 2004). Ribonucleotide reductase M1 (Rrm1) causes perturbation of regulatory networks in the cell cycle progression (Kawakami et al 2009). Trinucleotide repeat containing 6a (Tnrc6a) encodes a member of the trinucleotide repeat containing 6 protein family. The protein is highly similar to a human protein that functions in post-transcriptional gene silencing through the RNA interference (RNAi) and microRNA pathways. The human protein associates with messenger RNAs and argonaute proteins in cytoplasmic bodies known as GW-bodies or P-bodies, and inhibiting its expression delocalizes other GW-body proteins and impairs RNAi and microRNA-induced gene silencing (Lian et al 2006). Again all their roles in DS during brain development required further studies.

5.2.3 Phylogenetic analysis

Total brain volume is consistently reduced in DS, with a disproportionately greater reduction in the cerebellum (Davidoff LM 1928, Crome et al 1966). Furthermore, a significant reduction in granule cell density in the DS cerebellum has been reported for both human and Ts65Dn mouse model of DS (Baxter et al 2000). Regarding the development of the rhombencephalon in human embryos (Fig. 5.8), at Carnegie stage 8 (i.e., 23 days post-fertilisation), the neural groove can be detected in the neural plate as a very shallow sulcus bounded by neural folds. This is the first visible sign of the future nervous system (O'Rahilly and Müller 1981). The rostral part of the primitive neural tube will develop into the brain, while the caudal part develops into the spinal cord. During Carnegie stage 9 (i.e., 4 weeks post-fertilisation), the fusion of the neural folds in the cranial region and the closure of the rostral neuropore result in the division into 3 primary brain vesicles: the prosencephalon, the mesencephalon, and the rhombencephalon, which subsequently form the forebrain, midbrain and hindbrain, respectively (Müller and O'Rahilly 1983). The developing brain grows rapidly, and bends ventrally with the head fold, to form the cervical flexure at the junction of the rhombencephalon and spinal cord. Unequal growth in the rhombencephalon produces the pontine flexure in the opposite direction (O'Rahilly et al 1986),

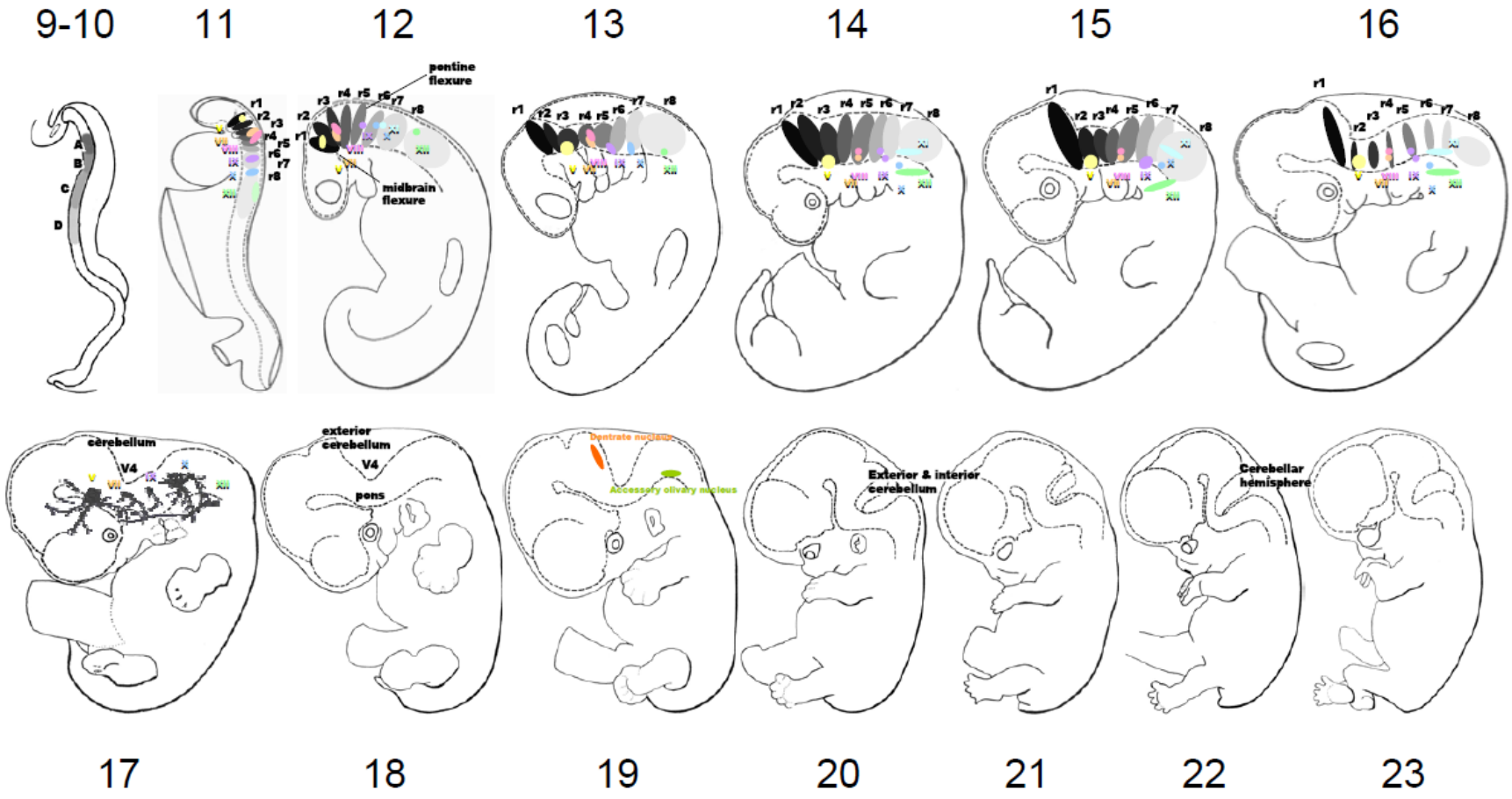

Figure 5.8 The developmental stages of the embryonic human brain. Embryo development is described according to Carnegie staging. The first 8 weeks of development (i.e., weeks after fertilisation) are subdivided into 23 stages based on external and internal morphological criteria. The development of the rhombomeres (A–D at stages 9–10; r1–r8 at stages 11–16) and the cranial ganglia (V–XII) of the rhombencephalon are labelled at the ventral and dorsal sides of the embryo, respectively. The majority of the cranial nerves that have developed by stage 17 are illustrated.

and thus divides the rhombencephalon into the caudal isthmus rhombencephali, the metencephalon, and the rostral myelencephalon during Carnegie stage 15 (i.e., 5 weeks post-fertilisation). The caudal part of the myelencephalon develops into the medulla oblongata whilst the walls of the metencephalon form the pons and the cerebellum.

In studying how genes and the genetic pathways that control neural development have evolved, Hox genes provide a starting point because they play a causal role in the regionalisation of the body plan of all bilaterally symmetric animals. All invertebrates examined today have at most one cluster of Hox genes, including the sister taxon of vertebrates, the cephalochordates. Vertebrates display variable, species-specific numbers of Hox gene clusters, which originated by successive duplications of a single ancestral complex (Fig. 5.9A and B). Even the primitive jawless vertebrates have at least three separate Hox gene clusters and teleosts have up to seven to eight Hox clusters. Such duplicated Hox clusters provided genetic opportunities for adaptive evolution. However, Hox cluster duplication did not play a role in the evolution of the affected clade. The most recent cluster duplication event documented is the one leading to the three additional Hox clusters in the teleost lineage. Teleost Hox genes are thus the best system to investigate the evolutionary forces acting on Hox genes after duplication. The rate of coding sequence evolution in duplicated Hox genes of teleosts has been shown to be increased compared to the unduplicated orthologs (Chiu et al 2000) and there is some evidence that duplicated Hox genes experienced directional selection (Peer et al 2001). Hence, the duplicated Hox genes became involved in adaptive evolutionary changes and played an active role in the evolution of the disparity and diversity of teleosts. The evolutionary sister of the Hox cluster, the ParaHox cluster, is believed to have resulted from the non-tandem duplication of a four gene ProtoHox cluster that gave rise to both the primordial Hox and ParaHox clusters (Brooke et al 1998). Hence, the Hox and ParaHox genes are the same evolutionary age (Fig. 5.9C).

The unique assignment of structural gene activation requires dividing the developing organism into smaller compartments or modules via the expression of developmental regulatory genes. More multiplied regulatory genes are expected than structural genes if the evolution of different organisms is controlled by the evolution of diversification of mechanisms regulating gene expression (Fritzsch B 1998). An example of this diversification and the possible increased

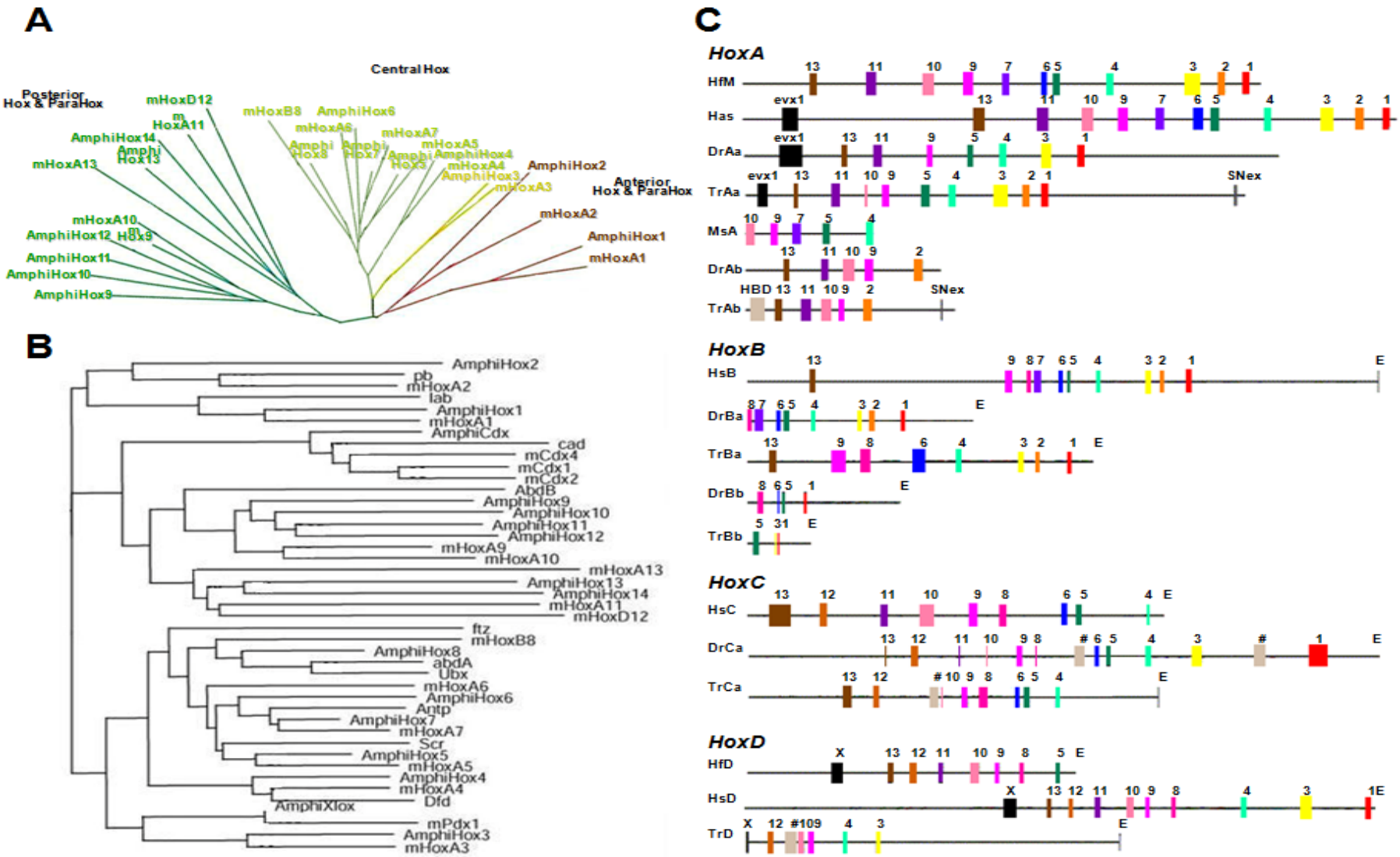

Figure 5.9 Molecular evolution of the Hox cluster. A. Unrooted neighbour-joining phylogenetic tree (scale 2cm = 0.1) and B. Rotted neighbour-joining the phylogenetic tree of the Hox/ParaHox clade. The tree was constructed from Hox and ParaHox cluster gene sequences and linkage data from mouse, amphioxus and Drosophila. C. Phylogenetic footprints in HoxA, HoxB, HoxC and HoxD clusters, Synteny of the Hox/ParaHox regions is shown in HsA Homo sapiens; HfM Heterodontus francisici; DrAa Danio rerio HoxAa; DrAb Danio rerio HoxAb; TrAb Takifugu rebripes and MsA Morone saxatilis. The phylogenetic tree was constructed using homeodomain sequences alone with methods of maximum arsimony (MP), neighbour joining (NJ) and quartet puzzling (QP). The alignment was constructed using the ClustalX programme and then was edited. NJ or MP trees were inferred by either ClustalX or MEGA 2.0 using Poisson model for amnio-acid evolution. A QP tree was inferred by TREE-PUXXLE 5.0 , using the JTT model with a Gamma distribution.

complexity of signalling systems is the family of nuclear receptors. The ability of their ligands to diffuse from a source to a target through membranes makes them ideal candidates to regulate developmental processes (Mangelsdorf et al 1995). In particular, Hox gene expression emerges in response to different concentrations of retinoic acid (RA), transduced by machinery regulation of RA receptors (RARα, β and γ). This, in turn, establishes rostrocaudal domains of gene expression, which are involved in rhombomere specification and in displaying different responses to dorsoventral signals that further refine the repertoire of cellular fates in rhombencephalon development (Gavalas A 2002). In insects, this family consists of one RXR-like receptor, ultraspiracle (usp), as well as three ecdysone receptor (EcR) isoforms encoded by a single gene (Bender et al 1997). In contrast, great extent of gene diversification and complexity are identified in mammals during evolution. Possible four RXR isoforms encoded by three genes, eight RAR isoforms encoded by three genes, and four thyroid hormone receptor (TR) isoforms encoded by two genes were proposed (Kastner et al 1995). These entire insect and vertebrate receptors signal through the formation of heterodimers between RXR and either RAR or TR. For signalling EcR/usp dimmers, possible number in flies is three, whereas thirty-two RXR/RAR and sixteen RXR/TR receptor heterodimers can exist in mammals. The complexity in this mammalian signaling system is sixteen times of that in flies (Bender et al 1997), but the the total number of genes in mammals may be only six times larger than in flies. Thus, at least these receptors genes show a disproportionate increase in numbers over the overall increase in gene numbers (Fritzsch B 1998).

On the other hand, the RAR/RXR family comprises hetermeric DNA binding proteins that recognize specific motifs within target genes called retinoic acid response elements (RAREs) (Mangelsdorf and Evans 1995). Numerous analyses have identified RAREs in the regulatory control regions of paralagous groups 1 and 4 Hox genes for direct response to RA signalling (Studer et al 1994). RAREs convey the ability to drive early abundant expression of the 3’ Hox genes within the neuroectoderm. RAREs establish the rostral limits of Hox gene expression and regulate the interpretation of positional information supplied by posteriorising signals from either the mesoderm or neural plate. The cis-regulatory mechanism for controlling Hox gene expression in the neuroepithelium, including a dependence upon retinoic acid signalling, has been highly conserved (Manzanares et al 2000). The cis-regulatory regions of 3’ genes in the

amphioxus Hox cluster, which are homologous to the 3' Hox genes in vertebrates, were linked to a lacZ reporter and assayed in transgenic mouse and avian embryos. Two regions designated Amphihox-1A and Amphihox-3b stimulated expression in the developing central nervous system. Amphihox-3b mediated expression in mouse and avian embryos up to an anterior r5/r6 boundary. Sequence analysis of Amphihox-1A revealed the presence of many putative RAREs and exogenous RA induces an anterior shift in Amphihox-1A expression. Amphihox-3b is also dependent upon RA signalling in the brain as reporter activity is downregulated by dominant negative RARa.

Several other transcription factors (i.e., Pax6, Tbr1, Emx1, Dlx2 and Nkx2.1) have been used to delineate the corresponding pallial domains of the developing chicken and mouse brains (Puelles et al 2000). In addition, the cadherins are expressed in peculiar combinations in more restricted regions and in specific neural circuits (Redies and Puelles 2001). Many of the genes, whose expression coincides with embryonic divisions, are also involved in the establishment and/or stabilisation of the divisions. Loss of gene function can cause partial or complete loss of the divisions. Same divisional origin, as developmental homology, does not imply same computational properties and should be considered functionally analogous. Many molecular mechanisms that underlie brain patterning are highly conserved in evolution. However, differences in the number of patterning genes are probably insufficient to account for the large differences in brain complexity between species.

5.3. Neural Differentiation

In this part, the genomic implications and its molecular network of autosomal imbalance in the aneuploid ES cells during neuronal differentiation were analyzed and compared.

5.3.1 Defective Neuron differentiation

To investigate the gene dosage effects of HSA21, two transchromosomal aneuploid clones, TT2F/hChr21-10 and TT2F/hChr21-11 were used. Parental euploid and transchromosomal aneuploid ES cell clones were both induced to neuronal lineage by SDIA for 6 days. ES cells

plated under serum free conditions on PA6 mouse stromal cell feeder layer differentiate along the default ectodermal pathway and then along the neuronal pathway as directed by SDIA of PA6. Neuron cells induced to differentiate from ES cells by SDIA were reported to contain naïve neural precursors that respond to patterning signals, directing a full dorsal–ventral range of neuroectodermal derivatives (Mizuseki et al 2003). In our experiment, two independently established TT2F/hChr21 clones 21–10 and 21–11, both producing the highest level of chimeras (Kadota et al 2002) and extending with a significant proportion of cells containing HSA21 (Shinohara et al 2001; Kadota et al 2002), were studied.

Defective Neurogenesis. Immunocytochemical analysis with anti-Nestin and TuJ antibodies illustrated the successful differentiation of both clones not only to neural stem cells but also to TuJ positive neurons (Fig. 5.10, Kadota et al 2002). Compared with the expression level, 21-10 and 21-11 clones have less Nestin and TuJ positive neurons than TT2F clones, indicating the neurogenesis in aneuploid clones were defective.

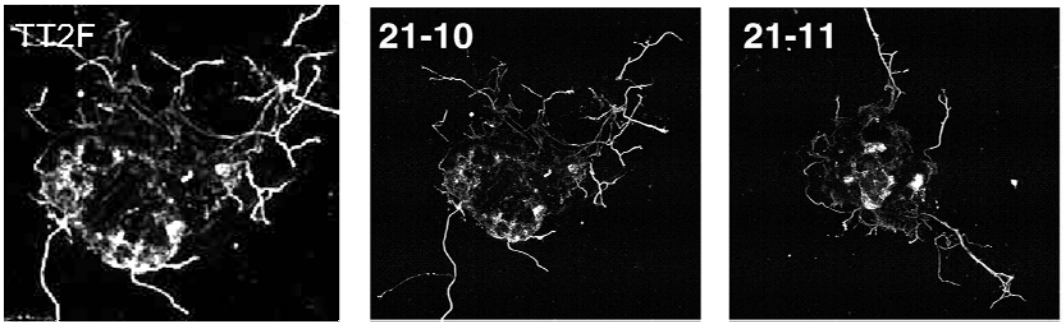

Figure 5.10 Immunocytochemistry of neuron marker TuJ in differentiating neurons. Euploid clone TT2F is compared with aneuploid clones 21-10 and 21-11.

The semi-quantitative RT-PCR analysis confirmed less Nestin mRNA expression starting from D4 of neuronal differentiation in the aneuplod clones (Fig. 5.11, Kadota et al 2002). Furthermore, the microarray gene expression profiles of the same neuronal-specific markers were compared between TT2F and TT2F/hChr21 cells during neuron differentiation (Tab. 5.3). Both differentiating cells from TT2F and TT2F/hChr21 clones expressed the neuronal stem cell markers Map2 and Tub, and were comparable to TT2F ($\log_2$ intensity ratios <0.20; Tab. 5.3).

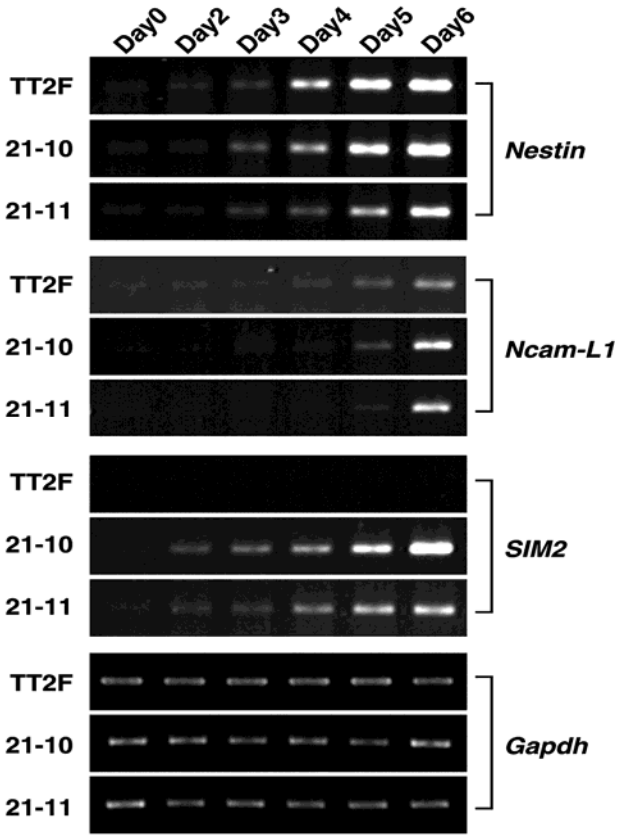

Figure 5.11 Expression of neuron markers during neuronal differentiation (day 0 to Day 6). Euploid clone TT2F is compared with aneuploid clones 21-10 and 21-11.

In contrast, expression of neuroectodermal marker Nes and neuronal differentiation marker Stmn2 in TT2F/hChr21 cells was relatively suppressed in neuronal stem cell stages on D2, D3, and D4 (Tab. 5.3). Even though the differences did not reach the statistical significance, this suggests that the differentiation process in TT2F cells with extra HSA21 was modified mainly in intermediate filament and microtubule destabilizing functions for neuron development.

Table 5.3 Neural expression of TT2F/hChr21 ES cells in neuronal differentiation

Gene	Clone	Symbol	Functions (annotation*)	Day 0	Day 2	Day 3	Day 4	Day 6
Microtubule-associated protein 2	H3040B05	*Map2*	Determining and stabilizing dentritic shape	0.11	0.06	0.16	0.14	0.15
Tubulin	H3043H01	*Tub*	Microtubule assembly	0.12	0.07	0.04	0.07	0.3
Nestin	H3040E02	*Nes*	Intermediate filament protein in neural tube	0.03	-0.49	-0.5	-0.34	0.54
Scgn-10-like protein	H3033G01	*Stmn2*	Microtubule-destabilizing phosphoproteins	0.13	-0.36	-0.3	-0.34	0.44

Data shown are mean $\log_2$ intensity ratios (TT2F/hChr21 to TT2F) of ES cell differentiation in days from triplicate microarray hybridization; positive value—up-regulation in TT2F/hChr21; negative value—down-regulation in TT2F/hChr21; and bold—significant differential expression ($p < 0:01$).

Differentiating neurons of euploid and aneuploid clones at different differentiation days were then collected for global gene expression profiling by microarray and for high throughput proteome separation and identification methods by 2D-PAGE & MALDI-TOF-TOF MS.

5.3.2 Differential gene expression

A 1.5-fold increase of an individual trans-acting factor will result in a stoichiometric imbalance that might be detrimental to the function of target genes or pathways. Such secondary or trans-acting effects are likely to result in up- or down-regulation of disomic genes. Of the 15,012 genes surveyed, only 57 (0.38%) genes significantly displayed a greater than 1.5-fold up-regulation or down-regulation in the differentiating TT2F/hChr21 cells relative to TT2F cells ($p < 0.01$). This confirms the intrachromosomal trans-acting effects might be of greater phenotypic consequence than primary gene-dosage effects alone.

For the functional annotation of these 57 significantly altered genes, a sequence of 29 genes were novel, hence their gene functions are still not very clear. Amongst the remaining 28 genes, 9 (32.1%) encode for protein and translational regulators; 6 (21.4%) encode for nuclear transcriptional factors; 5 (17.9%) encode for matrix and structural proteins; 5 (17.9%) encode for signal transduction mediators; 1 (3.6%) encodes for apoptosis-related protein; and 1 (3.6%) encodes for enzymes of energy and macromolecule metabolism (Tab. 5.4). This indicates that an extra HSA21 in the mouse genomic milieu primarily affects neuron differentiation by posttranscriptional and translational modification.

Herewith we found genes participating in mitoribosome ribonucleoprotein structure Mrpl10, RNA activating complex Snapc3, cotranslational targeting receptor Srprb, and spliceosome complex SF3a60 were significantly repressed from TT2F/hChr21 cells on D0 and sustained variable down-regulation along the subsequent stages of neuron differentiation. Later on however, the dysregulation in differentiation on D6 was mainly mediated by inhibition of another mitoribosome protein Mrps18a, and translation elongation factor Eef1g, by exaggeration of ubiquitin-dependent degradation protein Ubce8. This shift of translational regulation may suggest the underlying complexity of machinery mechanism.

Secondly, transcripts encoding for transcriptional factors also play an important role in the defective neuronal differentiation of TT2F/hChr21 clones. Signature proteins in modulating chromatin states Setdb1 and cell cycle checkpoint protein Klf4 were inhibited on D0, suggesting that DNA replication and cell proliferation were severely compromised in TT2F ES cells with HSA21. Nevertheless, developmental pluripotency by a RNA-binding domain Dppa5 was depressed on D6 in TT2F/hChr21 cells, whilst transcriptional factor for removal of deaminated cytosine Smug1 was significantly elevated.

Expression clusters of TT2F/hChr21 cells in neuron differentiation. We performed K-means hierarchical clustering to organize genes into a phylogenetic tree, identifying similarity in expression patterns in TT2F/hChr21 cells relative to control TT2F cells from D0 to D6 (Fig. 5.12A). Considering the influence of extra HSA21 in TT2F clones throughout the neuron differentiation process, we then employed SOM algorithms in fully functional annotated genes, including 847 (5.6%) upregulated and 282 (1.9%) down-regulated genes (Fig. 5.12B). The 1129 genes varying in at least one of the five stages of neuron differentiation were used to generate SOM. As a result, only 30 (2.7%) passed the variation filter and grouped into the 6 most prominent clusters (5 for up-regulation and 1 for down-regulation; Fig. 5.12C). Although generated without preconception, the clusters corresponded to the patterns of biological relevance in their gene functions (Tab. 4.5). Peak expression was detected with the transcripts related to apoptosis on D0 only; matrix and structural proteins on D2 and D6; protein synthesis and translation regulation on D4 only; and signal transduction on D2 and D4. This suggested that HSA21 affected the expression of TT2F ES cells in a periodic behavior in neuron differentiation in a stage-specific manner according to gene functional categorization; apoptosis-related genes being the most important manifestation in the beginning, then architecture proteins and signal transduction the second; and translational regulators thereafter. The vast majority of these clustered genes are regulated in cell differentiation and have been reported extensively, such as Col4a1, Map2k7, Vil2, Uchl3, Sh3d1B, Racgap1, Statip1, Mzf3, and Taf1a. Some are involved in neurite differentiation and neuronal growth, such as Syngr2, Dncic2, Eif3s7, and Peg3. Moreover, three enzymes involved in proline proteolytic metabolism, PRCP, PYCP1, and

Table 5.4 Differential expression of TT2F/hChr21 ES cells in neuronal differentiation

Gene	Clone	Symbol	Functions (annotation*)	mChr[a]	hChr & arm[a]	Day 0	Day 2	Day 3	Day 4	Day 6
Up-regulated genes										
Keratin complex 1, acidic, gene 18	H3007G06	*Krt1-18*	Type I intermediate filament chain keratin 18 (M)	15	12 q13	**1.67**	-0.29	0.11	0.82	1.2
Nuclear domain 10 protein	H3048G12	*NDP52*	Chromosome segregation ATPases (T)	11	17 q21.33	1	**1.84**	1.09	1.06	0.2
Karyopherin alpha 3	H3067H06	*Kpna3*	Nuclear pore complex (M)	14	13 q14.3	0.02	**1.8**	0.73	0.7	0.09
Non-kinase Cdc42 effector protein SPEC2	H3084G08	*SPEC2*	Protein binding (S)	11	5 q31.1	0.41	**1.62**	0.45	0.91	0.31
Homeobox protein NKX2.5	H3078E06	*NKX2.5*	cardiac developmental pathways (T)	14	— —	-0.11	1.24	0.33	**1.91**	0.43
PYRIN-containing APAF1like protein 4	H3080G03	*PYPAF4*	Neuronal apoptosis inhibitor protein (A)	13	19 q13.43	0.16	**1.36**	0.63	**1.83**	0.98
Spretus endogenous proviral sequence S3	H3028B08	*Ubce8*	Ubiquitin conjugation (P)	2	— —	-0.9	0.93	**1.25**	**1.8**	0.05
Claudin 6	H3076D06	*Cldn6*	Tight junction (M)	17	16 p13.3	-0.14	0.87	0.25	**1.68**	**1.45**
V kappa 2111 gene, partial	H3060E10	*Igk-V21-11*	Antigen binding and humoral immune response (O)	6	— —	0.1	1.05	1.15	**1.65**	0.89
Selective monofunctional uracil–DNA glycosylase	H3050H05	*Smug1*	Uracil–DNA glycosylase family (T)	15	12 q13.11–q13.3	-0.11	0.61	0.25	0	**1.84**
Down-regulated genes										
SET domain, bifurcated 1	H3036D03	*Setdb1*	Chromatin remodeling (T)	3	1 q21	**-4.62**	0.55	0.09	0.45	-0.02
Mitochondrial ribosomal protein L10	H3040B09	*Mrpl10*	Mitoribosome structure (P)	11	17 q21.32	**-4.59**	0.33	0.43	0.09	-0.04
General control of amino acid synthesis like 2	H3036D09	*Gcn5l2*	Transcription activation by c-myc transformation (P)	11	17 q21.32	**-4.39**	0.43	0.11	0.27	0.32
Tumor suppressor deleted in oral cancer related 1	H3036B12	*DOC-1R*	Cell growth inhibition (P)	19	11 q13	**-3.49**	0.26	0.05	0.06	0.12
Alkaline phosphatase 5	H3045A08	*Akp5*	Magnesium ion binding (E)	1	— —	**-3.29**	0.46	-0.31	0.13	0.5
Small nuclear RNA activating complex, Polypeptide 3	H3028H03	*SNAPC3*	DNA binding for snRNA transcription (P)	4	9 p22.2	**-2.54**	0.11	0.19	-0.01	0.12
Signal recognition particle receptor, B subunit	H3024H06	*Srprb*	Cotranslational targeting (P)	9	3 q22	**-2.48**	0.05	0.05	-0.09	-0.01
mRNA for splicing factor SF3a60	H3032D12	*SF3a60*	Spliceosome complex (P)	4	1 p34.2	**-2.45**	-0.12	0.08	-0.1	0.03
RAB17, member RAS oncogene family	H3028F06	*Rab17*	Small GTPase-mediated signal transduction (S)	1	2 q37.3	**-2.25**	0.05	0.16	-0.04	0.07
RalA-binding protein 1	H3065E01	*Ralbp1*	RLIP76-mediated transport of organic ions (S)	17	18 p11.3	**-1.74**	-0.08	-0.42	-0.05	0.5
Solute carrier family 35, member B1	H3028F09	*SLC35B1*	UDP-galactose transport activity (M)	17	17 q21.33	**-1.68**	0.55	0.25	0.34	0.55
Gutenriched Kruppel-like factor GKLF	H3015B01	*Klf4*	Cell cycle checkpoint protein (T)	4	9 q31	**-1.61**	0.72	0.31	-0.47	-1.02
Signal sequence receptor, delta	H3047A07	*Ssr4*	IDH3G for intra-cellular protein transport (S)	X	X q28	0.2	**-2.31**	-0.22	0.13	0.51
Arp2/3 complex subunit p21Arc	H3114D08	*Arpc3*	Actin polymerization (M)	5	12 q24.11	-0.05	-0.36	**-1.87**	-0.41	-0.04
Mitochondrial ribosomal protein S18A	H3044H01	*Mrps18a*	Mitoribosome structure (P)	17	6 p21.3	0.06	0.42	-0.18	0.22	**-3.26**
Eukaryotic translation elongation factor 1 gamma	H3079B04	*Eef1g*	Enzymatic delivery of aminoacyl	19	11 q12.3	0.02	0.68	0.16	0.7	**-2.72**
p116Rip	H3044H04	*Rhoip3*	tRNAs (P) Kinesin complex for	11	— —	0.43	0.22	-0.05	-0.01	**-2.37**
Developmental pluripotency associated 5	H3099F09	*Dppa5*	guanyl-nucleotide exchange (S) K homology RNA-binding domain (T)	16	— —	0.09	0.71	1.06	1.27	**-1.59**

Data shown are mean $\log_2$ intensity ratios (TT2F/hChr21 to TT2F) of ES cell differentiation in days from triplicate microarray hybridization; positive value—up-regulation in TT2F/hChr21; negative value—down-regulation in TT2F/hChr21; and bold—significant differential expression ($p < 0:01$). Annotation*: M—matrix/structural proteins; T—transcription/chromatin; S—signal/transduction; P—protein synthesis/translational; A—apoptosis; E—energy/metabolism; O—others. a mChr—mouse chromosome locus and hChr—human chromosome locus.

Timp2, which is necessary to achieve the physiologically active three-dimensional structure in a protein, were up-regulated in the same cluster.

Apoptosis. Not much of the literature focuses on the dysregulation of apoptosis processes in DS, except that insignificant changes in both pro-apoptotic and anti-apoptotic mechanisms have been found in fetal DS using microarray and proteomic approaches (Saran et al 2003; Engudwork et al 2001). However, an increased risk of apoptosis amongst the differentiating TT2F/hChr21 cells at the neuronal stem cell stage (D2–D5) was found (Kadota et al 2002). The decreased neuronal stem cell number in the population was relevant to the diminished neuronal markers Nes and Stmn2 (Tab. 5.4), as indicated above. Particularly, Bnip3, a dimeric mitochondrial protein with BH3 and transmembrane domains, associated with pro-apoptotic function even in the presence of BCL2, was up-regulated from D2 to D4 (Tab. 5.6). This implies that this specific apoptosis-related protein may respond to the transient increased risk of apoptosis in TT2F/hChr21 clones.

Signal transduction. The adaptors interact with effector molecules that are involved in a host of cellular processes. Disruption of such molecules or their interaction pathway may explain cell proliferation, differentiation, and migration abnormalities in DS brain, and probably in neurogenesis as well. Chaperone molecules for the elaborate regulation of fundamental cellular activities and differentiation of neurons, Ccs and Ywhag; and the signaling adaptor proteins, RACK, Crk, and Crkas, were inhibited in both differentiating TT2F/hChr21 clones and differentiated DS brain (Tab. 5.6). Synaptic markers Aplp2, Snap25bp, and Sept6; and downstream signaling of chemical transmission Gdi3 were up-regulated in TT2F/hChr21 clones, instead. The early induction of neurotransmitter release may be related to the disorganized emergence of lamination and abnormal neural networks seen in later DS brain (Golden & Hyman 1994).

Transcription and translation machinery. Modeling and wiring the neuron during differentiation depend on coordinated patterns of gene activation and repression, so do the brain development and differentiated neuronal functions. REST, a master negative transcriptional regulator of neurogenesis involved in brain development, neuronal plasticity, and synapse formation, was found to be repressed in neurospheres derived from fetal DS brain (Bahn et al

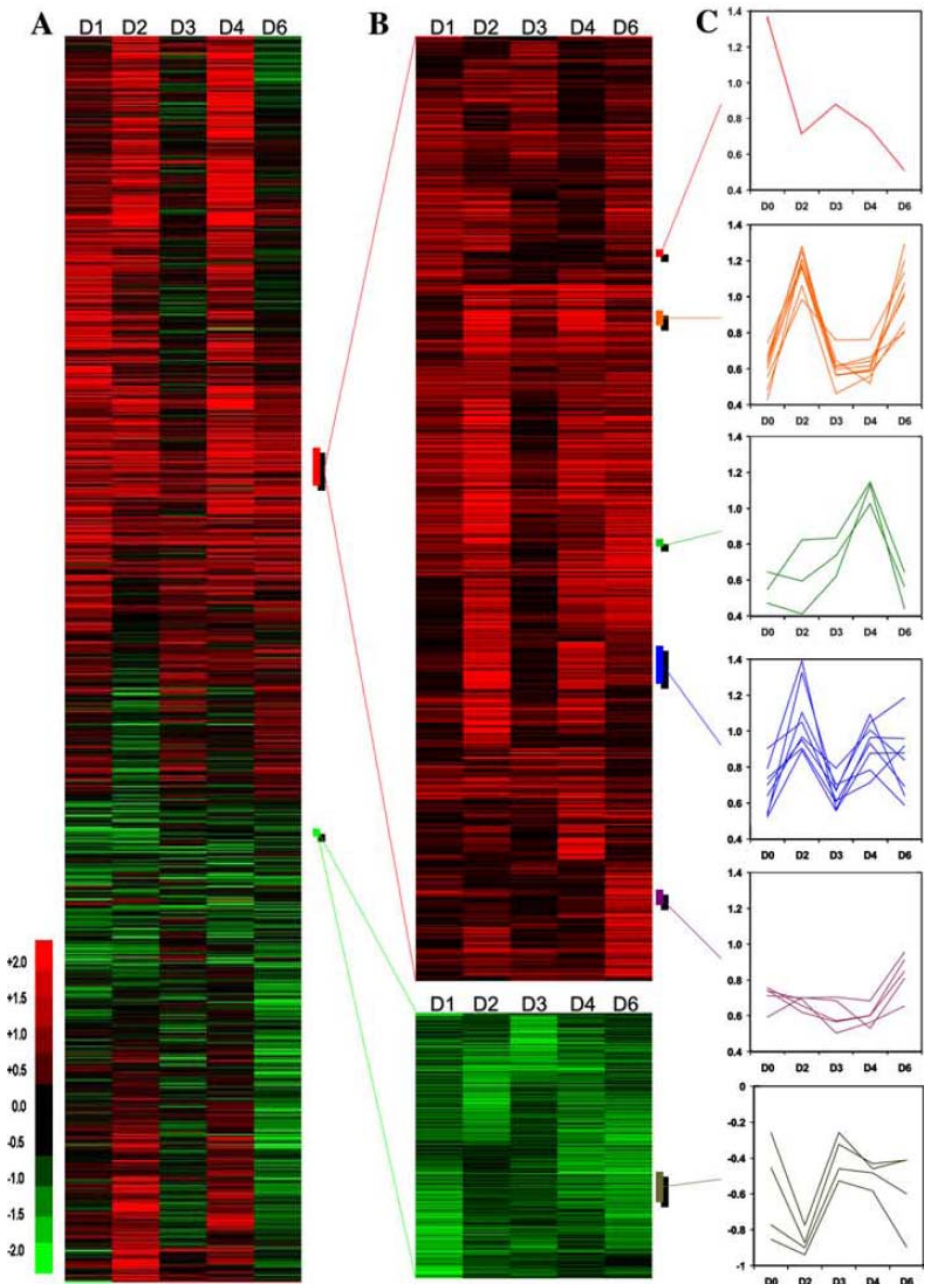

Figure 5.12. Molecular hierarchy of gene expression from TT2F/hChr21 clones in neuron differentiation. (A) High-stringency K-mean hierarchical clustering of three biological replicated array experiments comparing TT2F/hChr21 cells to TT2F cells. Each row represents a single cDNA clone on the array, whereas each column corresponds to prepared cells from TT2F/hChr21 and TT2F clones in 5 stages of differentiation (D0, D2, D3, D4, and D6). The results presented denote the ratio of hybridization of fluorescent cDNA (TT2F/hChr21 to TT2F cells) in a color scale extending from fluorescence ratios of 0.0625 to 4.0 (+2 to -2 in $\log_2$). Red refers to up-regulation in TT2F/hChr21 cells relative to TT2F cells and green refers to down-regulation in TT2F/hChr21cells relative to TT2F cells). (B) All up- and down-regulated genes of TT2F/hChr21 cells throughout neuron differentiation. SOM hierarchical clustering results are shown; red cluster as up-regulation and green clusters as down-regulation with the same color scale denotation as in (A). (C) Six characteristic SOM clusters of all up- and down-regulated genes. Novel genes are discarded, only functional annotated genes are presented as different expression patterns in different colors (Genelist is shown in Table 5.5). Figures show the fold changes of $\log_2$ intensity ratios, positive values as up-regulation and negative as down-regulation.

Table 5.5 Molecular hierarchy of gene expression from TT2F/hChr21 clones in neuron differentiation. Gene list of six SOM clusters from all up- and down-regulated genes. Coincidentally gene functional annotation shows the SOM clusters correspond to their biological relevance; red for apoptosis, orange for matrix/structural protein, green for protein/translation regulation, blue for signal/transduction, and purple for transcription/chromatin.

Gene	Clone	Symbol	Functions	mChr	hChr	& arm
Up-regulated clusters:						
feminization 1 b homolog	H3073H05	*Fem1b*	death receptor interacting protein	9	15	q22.31
alpha1 type IV collagen	H3159G06	*Col4a1*	extracellular matrix structure	8	13	q34-q35
MAP kinase kinase 7 gamma 2	H3124A09	*Map2k7*	microtubule associated protein	8	2	q34-q35
annexin A2	H3126C03	*Anxa2*	calcium-dependent phospholipid binding	9	15	q21-q22
synaptogyrin 2	H3133E09	*Syngr2*	membrane trafficking regulator	11	17	q25.3
annexin A4	H3087E01	*Anxa4*	membrane-related exocytosis/endocytosis	6	2	p13
dynein, cytoplasmic, intermediate chain 2	H3120F12	*Dncic2*	dynein complex for microtubule	2	2	q31.1
villin 2	H3156G10	*Vil2*	protein-tyrosine kinase substrate	17	6	q25.2-q26
eukaryotic translation initiation factor 3, subunit 7 zeta	H3149A12	*Eif3s7*	translation initiation factor	15	22	q13.1
ubiquitin carboxylterminal esterase L3	H3080A10	*Uchl3*	ubiquitin C-terminal hydrolase	14	13	q21.33
prolylcarboxypeptidase (angiotensinase C)	H3156F03	*PRCP*	lysosomal proX carboxy peptidase	-	11	q14
pyrroline 5 carboxylate reductase 1	H3120G09	*PYCR1*	osmoregulation	11	17	q25.3
tissue inhibitor of metalloproteinase 2	H3153C09	*Timp2*	metalloendopeptidase inhibitor	11	17	q25.3
Mpv17 transgene, kidney disease mutant	H3140G06	*Ssr2*	peroxisome	3	2	p23-p21
putative T1/ST2 receptor binding protein precursor	H3138E09	*Il1rl1l*	IL1 receptor activation	9	-	-
protein phosphatase 1D magnesiumdependent, delta isoform	H3156C03	*Ppm1d*	negative cell proliferation regulator	11	17	q23.3
SH3 domain containing protein SH3P18	H3128D06	*Sh3d1B*	kinesin complex for endocytosis	12	2	pter-p25.1
protein tyrosine phosphatase, receptor type, G	H3140G09	*Ptprg*	transmembrane receptor tyrosine protein	14	3	p21-p14
MgcRacGAP mRNA for GTPase activating protein	H3148G06	*Racgap1*	intracellular signaling cascade	15	12	q13.12
signal transducer/activator of transcription 3 interacting protein	H3147E03	*Statip1*	signal transductor	18	18	q12.2
Ran binding protein 2 gene	H3157C03	*Rbp2*	intracellular trafficking and secretion	-	2	q12.3
H1 histone family, member O, oocytespecific	H3059F06	*H1foo*	linker histone H1 family	6	3	q21.3
zinc finger protein	H3156C02	*Peg3*	TRAF family associated with NFKappaB	7	19	q13.4
KRAB zinc finger protein	H3139G05	*Mzf31*	nucleic acid binding	7	9	q22.31
nonPOU domaincontaining octamerbinding protein	H3149G03	*Nono*	pre-mRNA splicing factor	X	X	q13.1
E2Flike transcriptional repressor protein	H3126G09	*E2Fl2p*	cell cycle regulation	-	X	q26.2
Down-regulated cluster:						
ING1 protein	H3113C02	*Ing1*	negative regulator of cell proliferation	8	13	q34
TATA box binding protein-associated factor, RNA pol I, A	H3109C11	*Taf1a*	as SL1 for ribosomal RNA promoter	1	1	q42
seven transmembrane helix receptor	H3103B08	*FLJ31393*	G-protein couple receptor protien signaling	-	11	q12.1
heterogeneous nuclear ribonucleoprotein C	H3008F04	*Hnrpc*	RNA binding proteins	14	14	q11.2

2002). Not unlike the normal differentiation process in other cell types, REST was upregulated (Tab. 5.6), but one of the REST-regulated genes Stmn2 was negatively adjusted (Tab. 5.4) in the differentiating TT2F/hChr21 cells. On the other hand, the success or failure of a gene to be translated following transcription and splicing depends on the performance of a network of ribonucleoproteins (mRNPs) (Keene JD 2001). Besides ELAV/Hu proteins, Eif4e was down-regulated in TT2F/hChr21 clones. It proposes a potential mechanism for the dysregulation of genetic information between the genome and the proteome observed in DS.

Matrix and cytoskeleton proteins. There is growing evidence that cytoskeleton, microtubules, and actin filaments serve multiple roles in axonal transport, neuronal outgrowth, and motility in DS (Engidawork & Lubec 2003). Tubb and Dctn are important proteins that mediate microtubule-based functions in neuronal migration and intra-cellular transport. They were both down-regulated in differentiating TT2F/hChr21 clones and DS brain. This indicates that the disruption of structural and functional supply required for normal neuron growth and survival occurs in both differentiating and differentiated periods in DS.

Neuronal stem cells in TT2F/hChr21 clones versus fetal/adult brain with DS. Whether trisomy causes developmental perturbations that shift cell populations or disrupts the transcriptome of every cell, or both, it may be difficult to reverse these situations in adults. Analysis of gene expression profiles in the critical developmental stages at which the cells are generated and differentiate will help us to identify the most likely target for potential treatment. The clones used in this study were only composed of neuronal stem cells and neurons, and also the neuron differentiation process of ES cells *in vitro* is thought to be mimicking the neuron differentiation *in vivo*. The profile of gene expression in the differentiation of neuronal stem cells was expected to follow a quite different pattern from analyses using fetal or adult cells/tissues. We compared the discrepancy of the expressed transcripts in functional categories between the differentiating TT2F/hChr21 lines in our study and the other differentiated tissues or primary cultures published (Tab. 5.6; reviewed by Engidawork & Lubec 2003).

Table 5.6 Comparison of gene dosage in aneuploid neuronal stem cells and fetal/adult brain with DS.

Gene	Clone	Symbol	Function	Neuronal differentiation* D0	D2	D3	D4	D6	Fetal/Adult DS brain# RNA	(Reference)	pr	(Reference)
HSA21 gene expression:												
hippocampal amyloid precursor protein	H3132G02	*App*	Alzheimer's disaese	0.43	0.10	0.24	0.08	0.50	↑	Epstein 2001	↔	Engidawork et al 2001
Down syndrome critical region homolog 1	-	*Dscr1*	neurogenesis developmental regulation	-	-	-	-	-	↑	Fuentes et al 2000	-	-
Down syndrome critical region homolog 2	H3129G11	*Dscr2*	leucin-rich protein in membrane	0.04	0.04	0.08	-0.08	0.08	-	-	-	-
Down syndrome critical region gene a	H3007H01	*Dscr3*	retromer for protein tranfficking	-0.02	-0.04	-0.24	0.64	-0.14	-	-	-	-
Down syndrome critical region gene 6	H3111B09	*Dscr6*	membran matrix protein	0.07	0.49	0.15	-0.01	0.06	-	-	-	-
Ets avian erythroblastosis virus E2 oncogene homolog 2	H3028G09	*Ets2*	proto-oncogene	-0.18	-0.25	-0.16	0.06	0.02	↔	Baffico et al 1989	↔	Engidawork et al 2001
high mobility group protein 14	H3120G04	*Hmgn1*	nonhistone chromosomal protein	0.02	-0.08	-0.03	-0.55	-0.05	↑	Epstein 2001	↑	Epstein 2001
intersectin	H3150C12	*Itsn1*	synaptic vesicle recycling	0.75	1.15	0.32	0.81	1.02	↑	Pucharcos et al 1999	-	-
S100 calcium-binding protein beta	-	*S100b*	neuroptrophic agent	-	-	-	-	-	↑	Epstein 2001	↑	Griffin et al 1998
Cu-Zn superoxide dismutase	H3130B11	*Sod1*	oxidative stress	-0.18	-0.51	0.15	-0.47	-0.29	↑	de Haan et al 1997	↔	Gulesseria n et al 2001
procollagen, type VI, alpha 1	H3151F07	*Col6a1*	triple-helical-domain matrix protein	0.30	0.06	0.06	0.00	-0.06	-	-	↓	Engidawork et al 2001
Synaptojain	-	-	clathrin synatic endocytosis/signalling	-	-	-	-	-	-	-	↑	Arai et al 2002
neural cell adhesion molecule 2	H3121A01	*Ncam2*	neuronal cell adhesion	-0.10	0.11	0.14	0.95	-0.16	-	-	-	-
Cctq gene for chaperonin containing TCP-1 theta subunit	H3018A08	*CCT8*	molecular chaperon of T-complex protein 1	-0.24	-0.12	0.02	0.08	-0.17	-	-	↓	Yoo et al 2001
mnb protein kinase homolog mp86 (Dyrk)	H3061A08	*Mnb*	new dual protein kinase family	-0.10	0.53	-0.19	0.38	0.40	-	-	↑	Guimera et al 1999
Apoptosis:												
CPP32 apoptotic protease	H3088C12	*Casp3*	TNF-alpha-induced apoptotic pathway	0.09	-0.43	-0.07	-0.01	0.20	-	-	↔	Engidawork et al 2001
caspase 6	H3157C09	*Casp6*	transcriptional target of p53	0.54	0.52	0.52	0.50	0.53	-	-	-	-
caspase 8 associated protein 2	H3092E04	*Casp8ap2*	death-effector domain (DED) of caspase 8	-0.01	-0.03	0.10	0.63	0.44	-	-	-	-
caspase 9	H3124D04	*Casp9*	blocks apocytochrome c activation	0.39	0.71	0.10	0.51	0.24	-	-	-	-
caspase 12	H3131G02	*Casp12*	poly(Q) aggregate-mediated cell death	0.60	0.55	-0.01	0.54	0.47	-	-	-	-
Fas-associating protein with death domain	H3095D08	*Fadd*	death signaling from TNFRSF6/Fas-receptor	-0.17	0.01	-0.34	0.24	-0.15	-	-	↔	Engidawork et al 2001
Fas activated serine/threonine FAST kinase	H3140C01	*Fastk*	Fas receptor ligation phosphorylates TIA1	0.59	0.46	0.38	0.06	0.22	-	-	-	-
Bcl2/adenovirus E1B 19kD-interacting protein 2	H3123D10	*Bcl2l10*	mitochondrial membrane protein blocks cell death	0.25	0.05	-0.09	-0.25	-0.14	-	-	↔	Engidawork et al 2001
Bcl2-associated athanogene 1	H3083D06	*Bag1*	enhances the anti-apoptotic effects of BCL2	0.08	0.16	0.16	0.07	0.22	-	-	-	-
Bcl2-associated athanogene 2	H3003D08	*Bag2*	interact with Hsc70 ATPase domain	-0.32	0.09	-0.08	0.04	-0.44	-	-	-	-
Bcl2-associated athanogene 3	H3042D02	*Bag3*	interact with Hsc70 ATPase domain	0.31	-0.15	0.00	0.51	0.26	-	-	-	-
Bcl2-associated athanogene 4	H3042A05	*Bag4*	silenceing TNFR1 and modulating CD95	-0.08	0.32	-0.14	0.84	0.14	-	-	-	-
Bcl2-associated athanogene 5	H3086E09	*Bag5*	regulator of Hsp70	-0.06	-0.07	-0.02	-0.09	0.20	-	-	-	-
Bcl2-interacting killer-like	H3094H06	*Biklk*	cell-autonomous defect	0.10	0.61	-0.21	0.46	0.25	-	-	-	-
Bcl2/adenovirus E1B 19 kDa-interacting protein 1, NIP3	H3136C07	*Bnip3*	interacts E1B for protection	-0.24	0.42	0.49	0.22	-0.57	-	-	-	-
Bcl2/adenovirus E1B 19 kDa-interacting protein 3-like	H3016D08	*Bnip3l*	interacts E1B for protection	0.03	0.00	0.20	0.08	-0.06	-	-	-	-
Bcl-2-related ovarian killer protein-like-pending	H3081D02	*Bok*	apoptosis regulator	0.02	0.16	-0.14	0.04	0.12	-	-	-	-
cytoplasmic antiproteinase 3	-	*CAP*	serine proteinase inhibitor	-	-	-	-	-	-	-	↔	Engidawork et al 2001
annexin A5	H3016C05	*Anxa5*	phospholipase A2/protein kinase C inhibitory protein	0.86	-0.01	0.21	0.17	0.02	-	-	↔	Engidawork et al 2001
annexin A7	H3040G07	*Anxa7*	synexin mediates galectin-3 translocation	0.43	0.43	0.23	0.66	0.74	-	-	-	-
Signalling/Tranduction:												

amyloid precursor-like protein 2	H3108F12	*Aplp2*	Signal Transduction	0.01	0.14	-0.57	0.15	0.46	-	-	↓	Engidawork et al 2001
synaptosomal-associated protein, 23 kDa	H3083H12	*Snap23*	synaptobrevin/VAMP interaction	0.34	-0.43	-0.08	0.06	0.45	-	-	-	-
synaptosomal-associated protein, 25 kDa, binding protein	H3123D09	*Snap25 bp*	synaptic vesicle exocytosis	0.19	0.37	0.54	0.12	0.49	-	-	↓	Weitzdoerf er et al 2001
septin 2	H3152E11	*Sept2*	neural precursor cell developmentally down-regulated 5	0.16	0.01	0.47	-0.24	0.15	-	-	↔	Cheon et al 2001
septin 6	H3120G05	*Sept6*	GTP binding for cytokinesis	0.45	0.50	0.53	0.27	0.50	-	-	↓	Cheon et al 2001
septin 8	H3116H02	*Sept8*	ATP binding	0.03	0.19	0.01	0.15	0.13	-	-	-	-
septin 9	H3135D12	*Sept9*	DNA topoisomerase type II activity	0.62	-0.14	0.45	-0.31	0.47	-	-	-	-
partial 5-HT4 receptor gene, exons 2 to 5	H3068F12	*5-HT*	signal transduction	-0.11	1.09	0.34	0.65	0.69	-	-	↑	Bar-Peled et al 1991
14-3-3 sigma	H3121A08	*Ccs*	ubiquitous set of chaperone molecules	0.19	-0.12	-0.14	-0.07	-0.07	-	-	↓	Peyril et al 2002
14-3-3 gamma	H3014H04	*Ywhag*	intercellular signalling proteins	-0.37	-0.29	-0.02	-0.33	-0.28	-	-	↓	Peyril et al 2002
nucleoside diphosphate kinase	-	*NDK-B*	intermediate phgosphylated histidine residue	-	-	-	-	-	-	-	↓	Weitzdoerf er et al 2001
rab GDP-dissociation inhibitor beta	H3131H01	*Gdi3*	GTP/GDP cycling	0.74	0.01	0.27	-0.13	0.32	-	-	↓	Weitzdoerf er et al 2001
RACK-like protein	H3027G06	*RACK*	C2 domain of protein kinase Cb	0.21	-0.06	-0.11	0.26	-0.04	-	-	↓	Peyril et al 2002
Crk	H3083A04	*Crk*	recruiting proline-rich motif	0.12	-0.55	-0.20	0.12	-0.01	-	-	↓	Lubec et al 2003
v-crk-associated tyrosine kinase substR.e (Crkas),	H3109F03	*Crkas*	phospphorylated tryosine residues via SH2 domian	-0.15	0.45	-0.19	0.19	0.34	-	-	↓	Lubec et al 2003
Transcription & Translation:												
Ets avian erythroblastosis virus E2 oncogene homolog 2	H3028G09	*Ets2*	proto-oncogene and transcriptional factor	-0.18	-0.25	-0.16	0.06	0.02	↔	Baffico et al 1989	↔	Engidawork et al 2001
neural-restrictive silencer factor	H3153C03	*Rest*	Kruppel-type zinc finger transcription factor	0.05	-0.03	0.81	0.87	0.54	↓	Bahn et al 2002	-	-
Jun oncogene	H3058C09	*Jun*	enhancer binding protein, AP-1	0.17	0.25	-0.34	0.31	0.32	↓	Labudova et al 1999	-	-
nuclear factor-kB	-	*NFRKB*	specific RNA polymerase II transcription factor	-	-	-	-	-	↓	Labudova et al 1999	-	-
scleraxis	-	*SCX*	class II bHLH protein scleraxis	-	-	-	-	-	↑	Labudova et al 1999	-	-
eukaryotic translation initiation factor 1 alpha	H3091E09	*Eif1a*	binding of the 43S complex	-0.14	0.34	0.04	0.23	0.09	-	-	-	-
eukaryotic translation initiation factor 2 alpha kinase 4	H3125D04	*Eif2ak4*	protein amnio acid phosphorylation	0.13	0.54	0.01	0.18	0.10	-	-	-	-
eukaryotic translation initiation factor 2B	H3029H03	*Eif2b*	insulin-like growth factor 1-induction	0.16	0.09	0.04	0.16	0.19	-	-	-	-
eukaryotic translation initiation factor 2C, 1	H3114H07	*Eif2c1*	Argonaute family proteins in RNA interference	-0.03	-0.12	-0.21	-0.06	0.02	-	-	-	-
eukaryotic translation initiation factor 2, subunit 2	H3153F10	*Eif2s2*	form ternary complex with GTP and initiator tRNA	-0.27	0.03	0.02	0.07	-0.13	-	-	-	-
eukaryotic translation initiation factor 2, subunit 3, X-linked	H3086D04	*Eif2s3x*	GTP binding	-0.43	-0.33	-0.53	0.11	-0.05	-	-	-	-
eukaryotic translation initiation factor 3, subunit 1	H3017A04	*Eif3S1*	translation initiation regulation	-0.06	0.06	0.12	0.05	0.00	-	-	-	-
eukaryotic translation initiation factor 3, subunit 2	H3011F05	*Eif3s2*	TGFbeta receptor-interacting protein 1	0.03	-0.19	0.05	-0.10	-0.33	-	-	↔	Fredl et al 2001
eukaryotic translation initiation factor 3, subunit 3	H3155F12	*Eif3s3*	translation initiation regulation	0.31	0.09	0.29	-0.05	0.29	-	-	-	-
eukaryotic translation initiation factor 3 p42 subunit 4	H3110H12	*Eif3s4*	translation initiation regulation	-0.04	0.04	-0.19	-0.20	0.02	-	-	-	-
eukaryotic translation initiation factor 3, subunit 5	H3002D04	*Eif3s5*	translation initiation regulation	-0.14	-0.20	-0.17	-0.17	-0.35	-	-	↑	Lubec et al 2003
eukaryotic translation initiation factor 3, subunit 6	H3032B05	*Eif3s6*	bind complexes eIF3/COP9/26S	-0.19	-0.05	0.14	0.15	-0.12	-	-	-	-
eukaryotic translation initiation factor 3, subunit 7	H3149A12	*Eif3s7*	interact ternary complex eIF2/GTP/methionyl-tRNA	0.55	0.82	0.83	1.15	0.65	-	-	-	-
eukaryotic translation initiation factor 3, subunit 8	H3131B01	*Eif3S8*	translation initiation regulation	0.39	0.07	0.02	-0.05	0.25	-	-	-	-
eukaryotic translation initiation factor 3, subunit 9	H3017D08	*Eif3s9*	stabilizes initiator Met-tRNA binding to 40S subunits	-0.20	-0.24	-0.10	0.00	-0.05	-	-	-	-

eukaryotic translation initiation factor 4A1	H3011H05	*Eif4a1*	mediates interaction between mRNA and 40S	-0.17	0.06	-0.30	-0.22	0.07	-	-	↔	Fredl et al 2001
eukaryotic translation initiation factor 4A2	H3081A02	*Eif4a2*	conserved DEAD-box motif	-0.45	0.46	0.19	0.35	0.09	-	-	-	-
eukaryotic translation initiation factor 4B	H3050G08	*Eif4b*	translation initiation regulation	-0.60	-0.15	0.10	0.58	0.41	-	-	-	-
eukaryotic translation initiation factor 4E	H3089A10	*Eif4e*	associated with 4E-BP3	-0.11	-0.10	-0.01	0.67	-0.05	-	-	↔	Lubec et al 2003
eukaryotic translation initiation factor 4 gamma, 3	H3011D01	*Eif4g3*	MIF4G domain	-0.23	0.06	0.15	0.18	0.00	-	-	-	-
eukaryotic translation initiation factor 5	H3075C05	*Eif5*	IF2B/IF5 domain	-0.02	-0.01	0.13	-0.05	0.69	-	-	-	-
eukaryotic translation initiation factor 5A	H3124A10	*Eif5a*	stimulates ribosomal peptidyltransferase activity	0.55	0.02	0.39	-0.07	0.01	-	-	-	-
eukaryotic translation initiation factor 5B	H3128B06	*Eif5a2*	stimulates ribosomal peptidyltransferase activity	0.47	0.58	-0.04	-0.22	0.68	-	-	-	-
elongation factor	H3030H04	*Eef*	enzymatic delivery of aminoacyl tRNAs	-0.30	-0.18	0.02	-0.15	-0.11	-	-	-	-
elongation factor 1-alpha	H3153G04	*Eef1*	enzymatic delivery of aminoacyl tRNAs	0.08	0.02	0.24	-0.10	-0.48	-	-	-	-
eukaryotic translation elongation factor 1-alpha	H3140F07	*Eef1a1*	enzymatic delivery of aminoacyl tRNAs	-0.04	0.05	0.07	-0.14	-0.29	-	-	↓	Fredl et al 2001
eukaryotic translation elongation factor 1-beta	H3118G07	*Eef1b2*	enzymatic delivery of aminoacyl tRNAs	-0.14	-0.51	-0.27	-0.28	-0.54	-	-	↓	Fredl et al 2001
eukaryotic translation elongation factor 1-delta	H3005H10	*Eef1d*	guanine nucleotide exchange factor	-0.36	-0.15	0.02	-0.01	-0.52	-	-	-	-
eukaryotic translation elongation factor 1 epsilon 1	H3100H12	*Eef1e1*	glutathione S-transferase	-0.36	0.03	-0.47	0.02	0.11	-	-	-	-
eukaryotic translation elongation factor 1 gamma	H3079B04	*Eef1g*	enzymatic delivery of aminoacyl tRNAs	0.02	0.68	0.16	0.70	-2.72	-	-	-	-
elongation factor 2	H3129C01	*Eef2*	GTP-dependent translocation of nascent protein chain	0.02	0.15	0.21	-0.29	-0.32	-	-	↓	Fredl et al 2001
eukaryotic elongation factor-2 kinase	H3053H07	*Eef2k*	calmodulin-mediated signaling pathway	-0.01	0.43	0.14	0.36	0.65	-	-	-	-
elongation factor tu, mitochondrial precursor (p43)	-	*Ef-tu*	enzymatic delivery of aminoacyl tRNAs to ribosome	-	-	-	-	-	-	-	↓	Fredl et al 2001
Cytoskeletal proteins:												
tubulin alpha 1	H3043H01	*Tub*	microtubule assembly	0.12	0.07	0.04	0.07	0.30	-	-	-	-
class I beta-tubulin	H3029D06	*Tubb*	polymerizes to form microtubules	0.08	-0.12	0.14	-0.02	0.20	-	-	↓	Lubec et al 2003
synapsin I	H3028D10	*Syn1*	synaptogenesis/neurotransmitter release	-0.04	-0.19	-0.19	-0.19	-0.23	-	-	-	-
dynein, cytoplasmic, intermediate chain 2	H3120F12	*Dncic2*	dynein complex for microtubule	0.48	0.35	0.42	0.15	0.86	-	-	↔	Gulesserian et al 2002
dynactin 5	H3030D06	*Dctn5*	acetyltransferases isoleucine patch	-0.11	0.08	-0.05	-0.44	0.10	-	-	↓	LaMonte et al 2002
dynactin 6	H3103A08	*Dctn6*	adhesive properties to macromolecular proteins	0.05	-0.24	-0.06	-0.13	-0.11	-	-	↓	LaMonte et al 2002
moesin	H3044C12	*Msn*	ERM protein	0.53	0.96	0.13	0.42	0.58	-	-	↓	Lubec et al 2003
drebrin	H3124H11	*Dbn1*	actin-binding and -bunding	0.19	0.09	0.28	-0.25	0.29	-	-	↓	Weitzdoerfer et al 2001

[a] Data shown are mean $\log_2$ intensity ratios (TT2F/hChr21 to TT2F) of ES cell differentiation in days from triplicate microarray hybridization.
[b] pr, protein; ↑, increased; ↓, decreased; ↔, unchanged.

5.3.3 Differential proteome expression

To determine the gene dosage effects of an extra copy of HSA21 in the process of neuronal development in proteome expression, we compared the global protein expression patterns in the differentiating TT2F and TT2F/hChr21 cells by 2-DE analysis at D0, D3, D6 and D10 of differentiation. Proteins obtained from TT2F and TT2F/hChr21 clones (21–10 and 21–11) were resolved by 2-DE under the same experimental conditions and were detected by silver staining. Analysis by PDQuest 7.1 software detected over 1,400 protein spots in each gel, and the majority of them displayed comparable spotintensities between TT2F and TT2F/hChr21 cells. Following peptide mass fingerprinting and identification by Mascot Search Program, we only detected a total of 18 significantly altered proteins in TT2F cells with an extra HSA21 (Fig. 5.13 and Fig. 5.14). Included among these 18 proteins, were SOD1 and CCT8, which are gene products from the transferred HSA21. Of the other 16 proteins, six (37.5%) were matrix and structural proteins; three (18.8%) were heat shock/stress proteins; three (18.8%) were protein or translational regulators; two (12.5%) were nuclear transcriptional factors; and two (12.5%) were enzymes for energy and macromolecular metabolism (Tab. 5.7). Besides the gene products derived from HSA21, there were typically 7 proteins that were overexpressed and 9 proteins that were under-expressed significantly in TT2F/hChr21 cells compared with TT2F cells (Fig. 5.13 and Fig. 5.14). To determine the expression patterns of these altered proteins throughout neuronal differentiation, the corresponding spot intensities in the 2-DE gel were analyzed in TT2F and TT2F/hChr21 cells at D0, D3, D6 and D10 of differentiation (Tab. 5.7). Both protein subunits Atp6v1a1 and Atp6v1b2 of the vacuolar ATPase proton pump, which mediate acidification of intracellular organelles for energy production and convention, were over-expressed. Three proteins, AI850305, Eef1D and UchL1 that are involved in protein catabolism or translation regulation were under-expressed Heat shock proteins, Hsp84–1, Hsp70 and Hsp86–1, demonstrated a stage-specific suppression on D0, D3 and D6, respectively. However, Hsp84–1 protein expression did not change significantly in TT2F/hChr21 cells between D3 and D6. Splicing regulatory elements, HnrnpF and HnrnpC, displayed contradictory expression patterns of over-expression and underexpression respectively. Actin- (T-plastin and Vil2), filament-(Krt2– 8) and phospholipid-(Anxa4) related cytoskeleton proteins were over-expressed across

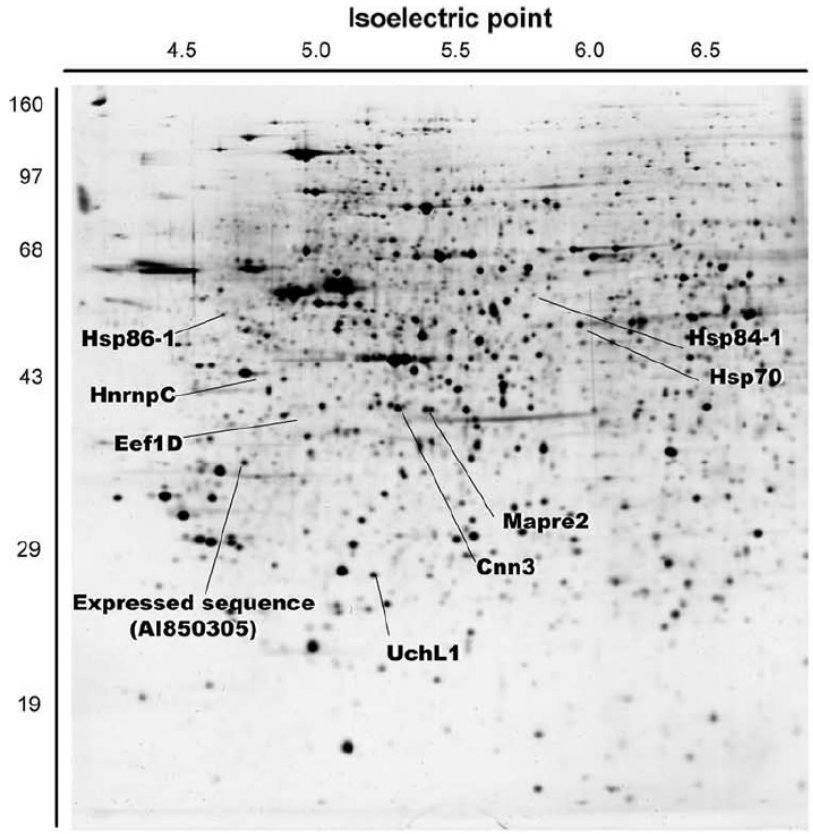

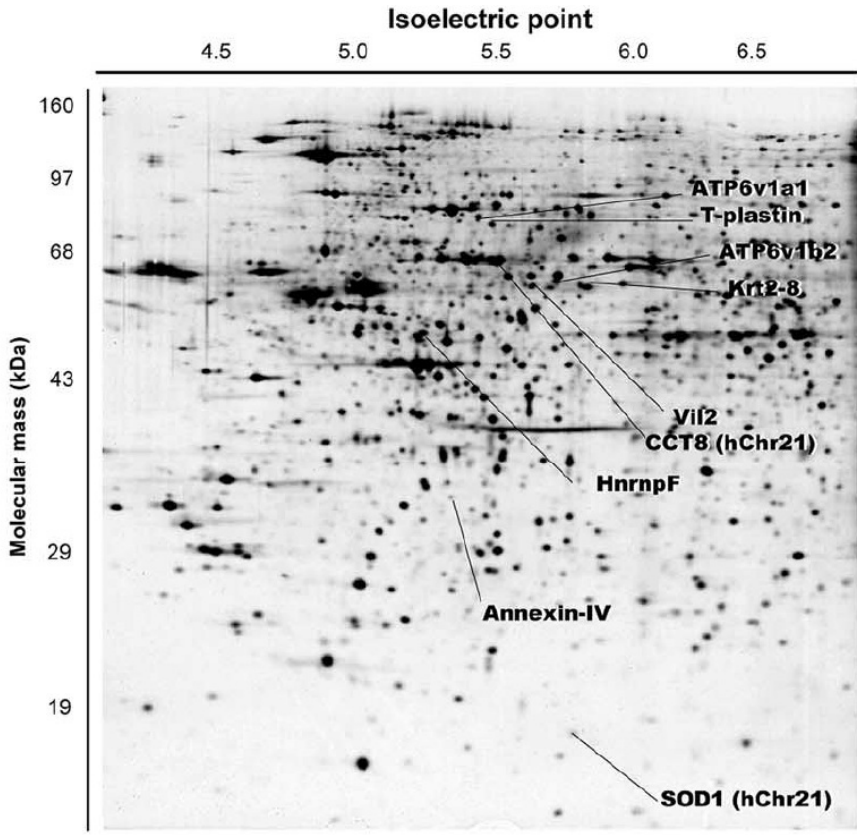

TT2F

symbol	Identification protein name	GenBank accession no.	Probability	Matching peptides (%)	Estimated MW9kDa)/pI	Sequence coverage (%)
Cnn3	calponin 3, acidic	AK005460	123	10 (63)	36.6/5.5	42
Eef1D	eukaryotic translation elongation factor 1 delta	AF304351	91	6 (86)	31.4/4.9	26
HnrnpC	heterogeneous nuclear ribonucleoprotein C	AF095257	92	11 (48)	33.1/4.9	34
Hsp70	heat shock protein, 70 kDa	AAC84169	73	10 (45)	70.3/5.5	16
Hsp84-1	heat shock protein, 84 kDa 1	gil28277018	70	8 (54)	43.8/5.2	18
Hsp86-1	heat shock protein, 86 kDa 1	J04633	119	11 (39)	39.6/4.7	36
Mapre2	microtubule-associated protein RP/EB family, member 2	AK038562	80	6 (50)	37.5/5.2	21
UchL1	ubiquitin carboxy-terminal hydrolase L1	AF172334	116	11 (23)	25.2/5.1	51
-	expressed sequence (AI850305)	BC022575	229	14 (77)	31.5/4.9	56

TT2F/hChr21

symbol	Identification protein name	GenBank accession no.	Probability	Matching peptides (%)	Estimated MW9kDa)/pI	Sequence coverage (%)
Anxa4	annexin A4	U72941	102	10 (48)	35.9/5.4	31
ATP6v1a1	ATPase, H+ transporting, V1 subunit A, isoform 1	BC038392	188	21 (60)	68.6/5.6	38
ATP6v1b2	ATPase, H+ transporting, V1 subunit B, isoform 2	BC012497	249	22 (61)	56.9/5.6	48
CCT8	chaperonin containing TCP1, subunit 8 (theta)	D13627	276	27 (55)	60.2/5.5	48
HnrnpF	Similar to heterogeneous nuclear ribonucleoprotein H1	gil20073357	114	18 (32)	37.2/5.7	47
Krt2-8	keratin complex 2, basic, gene 8	M22831	228	29 (45)	54.2/5.4	50
SOD1	superoxide dismutase 1, soluble	BC001034	81	10 (25)	15.9/5.7	44
T-plastin	T-plastin	gil13124445	75	7 (53)	70.8/5.6	14
Vil2	villin 2	X60671	174	30 (53)	69.4/5.8	46

Figure 5.13 2-DE protein patterns in TT2F and TT2F/hChr21 clones. TT2F and TT2F/hChr21 cells on D0, D3, D6 and D10 of neuron differentiation were separated by 2-DE and detected by silver staining under the same experimental conditions. Protein spots on each gel were located and compared. Spot densities were normalized by taking the ratio of the intensity of each candidate spot to the total spot intensity. Two-fold or greater change in spot density was defined as a significant alteration in protein expression. The indexed spots were subjected to MALDI-TOF-MS protein identification. The typical 2-DE image of D6 TT2F and TT2F/hChr21 (21–10) is shown. The spot densities of AI850305, Cnn3, Eef1D, HnrnpC, Hsp84-1, Hsp86-1, Hsp70, Mapre2 and UchL1 in TT2F gel were significantly higher, relative to TT2F/hChr21 (under-expression in TT2F/hChr21), whereas the spot densities of Annexin-IV, ATP6v1a1, ATP6v1b2, CCT8, HnrnpF, Krt-8, SOD1, T-plastin and Vil2 in TT2F/hChr21 gel were significantly increased, relative to TT2F (over-expression in TT2F/hChr21). Identified proteins are listed under the gel images with the output information from Mascot Search program.

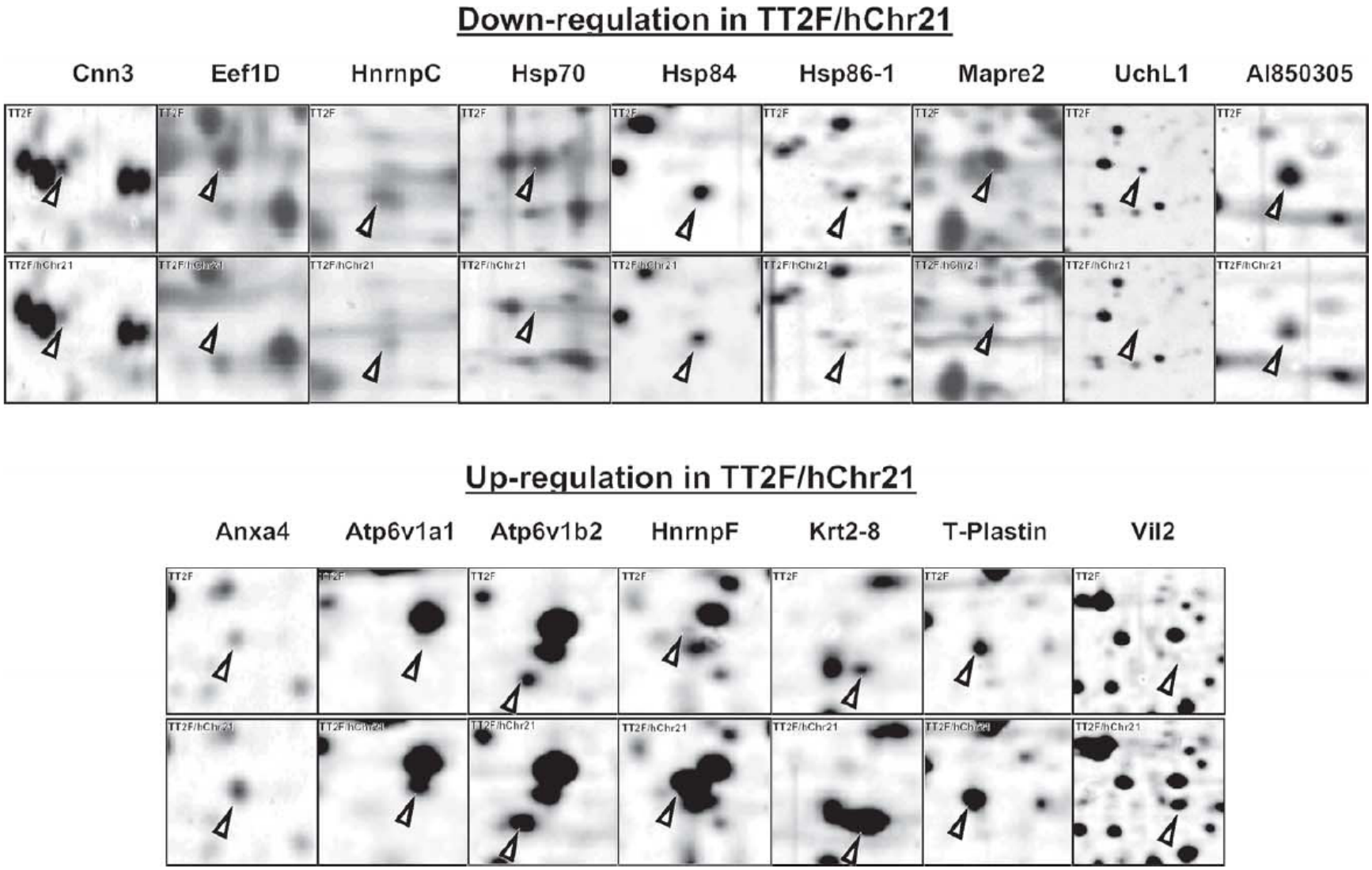

Figure 5.14. Close-up of areas of protein spots in both TT2F and TT2F/hChr21 gels of neuron differentiation. Under-expressed proteins (upper panels) and over-expressed proteins (lower panels) in TT2F/hChr21 cells are indicated by arrows. Images were enlarged from D0 (Cnn3, Eef1D, HnrnpC, Hsp84 and Mapre2), D3 (Hsp70) or D6 (AI850305, Hsp86-1, UchL1, Anxa4, Atp6v1a1, Atp6v1b2, HnrnpF, Krt2-8, T-plastin and Vil2) gels from either TT2F or TT2F/hChr21 (21–10).

Table 5.7. Results of protein expression in TT2F and TT2F/hChr21 clones in neuronal differentiation[a]

Proteins	Functions (Annotation*)		mChr[#]	hChr	& arm[#]	TT2F Day 0	TT2F Day 3	TT2F Day 6	TT2F Day 10	TT2F/hChr21 ^ Day 0	TT2F/hChr21 ^ Day 3	TT2F/hChr21 ^ Day 6	TT2F/hChr21 ^ Day 10
Over-expressed proteins:													
SOD1	copper, zinc superoxide dismutase activity	(H)	16	21	q22.11	NS	NS	NS	NS	**475.9**	**252.6**	**142.5**	**116.9**
HnrnpF	3' end pre-mRNA cleavage reaction	(T)	-	10	q11.21-q11.22	211.2	901.7	60.7	458.1	**1420.1**	812.2	**520.5**	**783.6**
T-plastin	non-hemopoietic lineage actin-binding proteins	(M)	X	X	q24	138.2	NT	350.4	341.4	**748.6**	NT	**845.5**	**918.5**
CCT8	chaperonin containing TCP1	(H)	16	21	q22.11	NS	NS	NS	NS	NS	NS	**1450.7**	**811.9**
Krt2-8	cytoskeleton organization and biogenesis	(M)	15	12	q13	NS	NS	356.0	301.3	NS	NS	**1961.1**	**1005.6**
ATP6v1a1	vacuolar proton pump for energy metabolism	(E)	16	3	q13.31	NT	NT	35.8	391.2	NT	NT	**151.7**	**817.8**
Anxa4	calcium-dependent phospholipid binding	(M)	6	2	p13	150.8	469.0	59.8	244.2	207.1	644.8	**222.0**	**442.5**
Vil2	as a protein-tyrosine kinase substrate in microvilli	(M)	17	6	q25.2-q26	NS	NS	326.8	123.5	NS	NS	**1057.6**	**367.0**
ATP6v1b2	vacuolar proton pump for energy metabolism	(E)	8	8	p22-p21	267.2	115.2	380.2	323.0	325.1	111.3	**764.3**	342.5
Under-expressed proteins:													
HnrnpC	nucleic acid binding	(T)	14	14	q11.21-q11.22	924.9	661.3	981.3	505.7	**517.6**	**279.9**	**615.6**	**303.6**
AI850305	UBP related cystein protease activity	(P)	19	-	-	245.4	353.2	1239.6	1456.3	**68.7**	297.6	**743.3**	**695.8**
Mapre2	signal transduction cascade downstream of the TCR	(M)	18	18	q12.2	1837.9	824.6	1161.0	111.3	**433.5**	573.6	**716.1**	**394.5**
Cnn3	actin binding in cytoskeleton	(M)	3	1	p22-p21	1131.0	306.7	425.2	124.4	**468.2**	260.8	**160.9**	**273.5**
Eef1D	enzymatic delivery of aminoacyl tRNAs to the ribosome	(P)	15	8	q24.3	997.6	NS	NS	NS	**457.2**	NS	NS	NS
Hsp84-1	Molecular chaperone, Hsp90 family	(H)	17	6	p12	147.2	323.3	313.7	744.6	**69.6**	480.8	400.0	**155.6**
UchL1	ubiquitin-dependent protein catabolism	(P)	5	4	p14	1001.5	970.5	1404.8	3426.2	1152.1	**467.3**	**828.1**	**1397.6**
Hsp70	preventing tau aggregation	(H)	17	6	p21.3	1073.9	1447.6	NS	NS	828.6	**623.2**	NS	NS
Hsp86-1	Molecular chaperone, Hsp90 family	(H)	12	14	q32.33	NT	NT	473.5	NS	NT	NT	**185.2**	NS

[a] Data shown are mean intensities of protein spots in different stages of neuron differentiation quantified by PDQuest 7.1 software from 2D-PAGE in triplicate.
* Annotation: E, energy/metabolism; H, heat shock/stress; hChr, human chromosome locus; M, matrix/structural proteins; P, protein synthesis/translational; T, transcription/chromatin.
# mChr, mouse chromosome locus; Red bold values, significant over-expression in TT2F/hChr21 (P<0.01); blue bold values, significant down-expression in TT2F/hChr21 (P<0.01); NS, no spot detected in 2D-PAGE and NT, not determined.

all stages of differentiation, whereas microtubule- (Mapre2) and calmodulin- (Cnn3) related architectural proteins were under-expressed.

RNA analysis using real-time quantitative RT-PCR. To study whether the alteration at the protein level is attributable to transcriptional or other regulatory mechanism, RNA quantitative analysis was carried out using real-time RT-PCR. Messenger RNAs from genes encoding the indexed proteins were amplified with the relevant cDNA for calibration and quantification. Comparison of the mRNA expression values and the protein expression values within the same cell lines was performed (Fig. 5.15). Expression data for vacuolar ATPase proton pump proteins, heat shock proteins and calmodulin-binding proteins were provided as microarray data from an independent study. The expression of Anxa4, Atp6v1a1, Atp6v1b2, Krt2–8, Vil2 (those proteins overexpressed in TT2F/hChr21 cells), and of HnrnpC, Mapre2, UchL1, AI850305 (those proteins under-expressed) were mostly consistent with their being transcribed to mRNA and translated to protein (Fig. 5.15). Cnn3, Eef1D, Hsp70, Hsp84, Hsp86, HnrnpF and T-plastin showed disagreement. We suggest that these proteins are subsequent to post-transcriptional regulation or complicated translational modification.

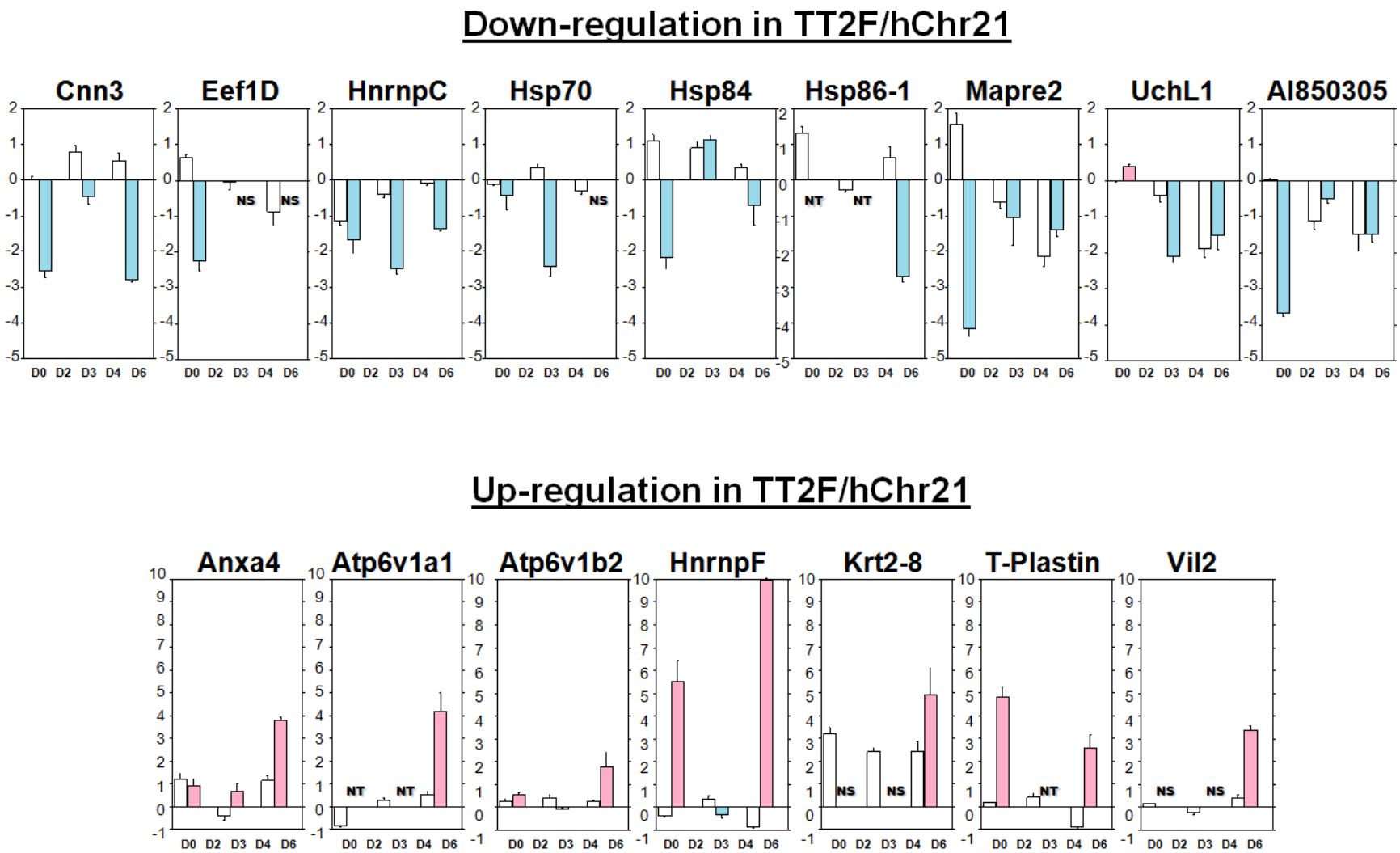

Figure .5.15 Protein and RNA expression of genes identified. RNA expression by real-time RT-PCR or microarray profiling, together with protein expression by 2-DE, was plotted against each differentiation stage (D0, D3 and D6). Significantly under-expressed proteins (upper panels) and over-expressed proteins (lower panels) in any stage of neuronal differentiation in TT2F/hChr21 cells are illustrated. Three independent experiment sets of TT2F cells and both 21-10 and 21-11 clones of TT2F/hChr21 cells were combined and compared. Fold changes in expression are displayed as $\log_2$ values of meansS.D. Empty bars refer to RNA expression and colour bars refer to protein expressions by 2-DE analysis. NS, no spot detected; NT, not determined, in 2-DE analysis.

5.4. Neural Apoptosis

In this part, we carried out global gene expression analysis to reveal the underlying molecular mechanism that might be responsible for the enhanced apoptosis during early neurogenesis.

5.4.1 Neuronal differentiation-associated apoptosis

The chromosome-aberrant ES cell clones contained HSA21, HSA11 or HSA6p were studied. HSA21, HSA11 or HSA6p were transferred into TT2F, whereas HSA11 was transferred by MMCT into E14. Chromosome-aberrant ES cell clones with mouse chromosome aneuploidy were constructed by sub-cloning normal TT2F cells (39, XO) derived from TT2 cells (40, XY). The passage number of ES clones used was unchanged throughout the experiment. Parental euploid and transchromosomal aneuploid embryonic stem cell clones were both induced to neuronal lineage by SDIA for 6 days. We investigated apoptosis during neurogenesis in parental and aneuploid clones by TUNEL staining. On the third day (D3) of neuronal differentiation on PA6, higher proportions of TUNEL-positive cells were observed in aneuploid than in normal ES cell clones (Fig. 5.16A).

Flow cytometry analysis revealed 11.1%, 4.3% and 10.5% apoptotic cells in parental E14-1, TT2F and TT2 cells, respectively. Further, the number of developing neural stem cells undergoing apoptosis significantly increased by one- to three-fold in all autosomal aneuploid ES cell clones compared with controls (Fig 5.16B). Single and double trisomy resulted in a similar increase in neuronal apoptosis. In contrast, no enhancement of apoptosis was observed after deletion of the Y chromosome (39, XO in TT2s(–mChr Y); Fig. 5.16B), suggesting that sex chromosome aneuploidy does not cause deterioration in neuronal apoptosis.

Further, we evaluated the enhanced apoptosis observed in aneuploid ES cell lines for its specific occurrence during neuronal differentiation. Because a highly efficient system of ES cell differentiation into a single lineage is not available except for neuronal differentiation, to confirm the morphological changes in undifferentiation state *in vitro* and *in vivo* we performed *in vivo* analysis by subcutaneous injection of ES cells into nude mice, which would lead to teratoma

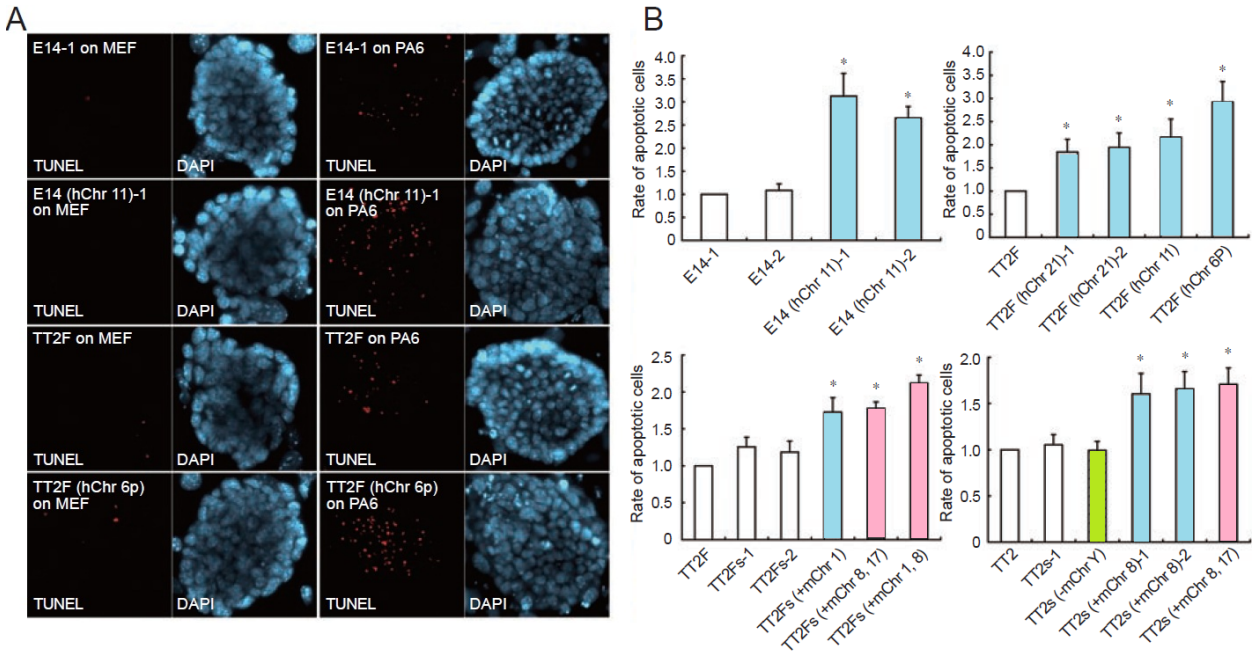

Figure 5.16 Detection of apoptotic cells in parental and chromosome-aberrant ES cells. (A) TUNEL assay in parental E14, E14 (hChr 11)-1, TT2F and TT2F (hChr 6p). ES cells with a normal karyotype showed a low level of apoptosis on PA6. (B) Quantitative analysis of apoptotic cells was performed by flow cytometry. Cells were subjected to staining with Annexin-V. Comparisons of normal and hChr.11 E14 clones, normal and hChr. 6P, 11, or 21 TT2F clones, as well as sub-cloned TT2F and TT2 clones are shown. The apoptotic rate of aneuploid clones was calculated on the basis of the apoptotic percentage of parental clones. Data are represented as the mean ± SD; n = three independent experiments, *P < 0.05 compared with control using Student's t-test.

formation with random differentiation. Transplanted aneuploid and euploid ES cells gave rise to typical teratomas after 5 weeks. Histological analyses showed that the tumors contained derivatives of all three embryonic layers including squamous epithelium, cartilage, skeletal muscle, osteoid tissue, glandular epithelium and ciliated epithelium (Fig. 5.17). Few apoptotic cells were noted in these differentiated areas or tissues. On the other hand, a large number of apoptotic cells were observed in the non-differentiated areas, consisting of cells with higher nuclear/cytoplasmic ratio. Importantly, no significant difference was noted in the rate of apoptotic cells between aneuploid and euploid ES cell lines (Fig. 5.17). Further, we evaluated apoptosis during embryoid body formation with random differentiation. Again, no significant difference was noted in the rate of apoptotic cells between aneuploid and euploid ES cell lines. These results suggest that the enhanced apoptosis observed in aneuploid ES cells is specific to neuronal differentiation. Nevertheless, we cannot exclude the possibility that enhanced apoptosis

may also occur in other cell lineages that were not reflected by the present assays.

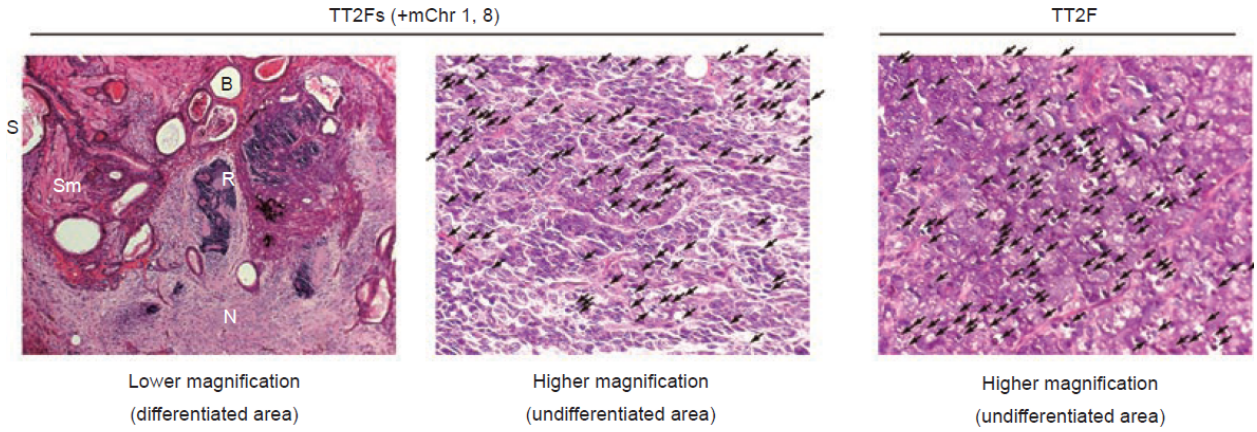

Figure 5.17 Histological analysis of teratomas derived from TT2Fs (+mChr 1, 8) and TT2F. Apoptotic cells were indicated by arrows. B, Bronchus; R, Rosette; Sm, Stratified muscle; N, Neuroid; S, Squamous cell.

5.4.2 Common down-regulated genes

To determine the underlying molecular mechanism involved in defective neuronal differentiation and enhanced apoptosis in autosome-imbalanced neural stem cells, we surveyed the expression patterns of more than 15,012 genes (Fig. 5.18). Although no cluster specific to aneuploid ES cells was observed in undifferentiated state, a differentially expressed cluster of 14 genes, which are commonly and significantly downregulated from D2 to D6 of neuronal differentiation (Fig 5.19 and Tab 5.8), was identified in both 40, XO (single trisomy of either mChr 1 or mChr 11) and 41, XO (double trisomy of either MMU1+8 or MMU8+17) clones (data available from CIBEX at http://cibex.nig.ac.jp/index.jsp).

(next page) Figure 5.18 High-stringency self-organizing maps (SOM) hierarchical clustering of biological replicated gene expression profiles. High-stringency hierarchical clustering of TT2F clones with autosomal imbalance during early neuronal differentiation by SOM analysis. Each row of the dentogram represents a single gene on the array, whereas each column corresponds to a prepared RNA population from TT2F clones (normal, 39,XO; single transferred mChr, 40,XO and double transferred mChr, 41,XO) at different stages of differentiation from D0, D2, D3, D4 and to D6. The results represent denote the ratio of hybridization of fluorescent labeled RNA in a color scale extending from hybridization intensity ratios of 0.0625 to 16 (+4 to -4 in $\log_2$). High-stringency hierarchical clustering of TT2F clones at D0 was shown (right). Red refers to up-regulation and green refers to down-regulation in individual fluorescent intensity of the differentiating neuron stem cells within the column relative to the average overall fluorescent intensity throughout differentiation. A small common differential under-expressed cluster from D2 to D6 of differentiation in both 40,XO and 41,XO clones is indicated.

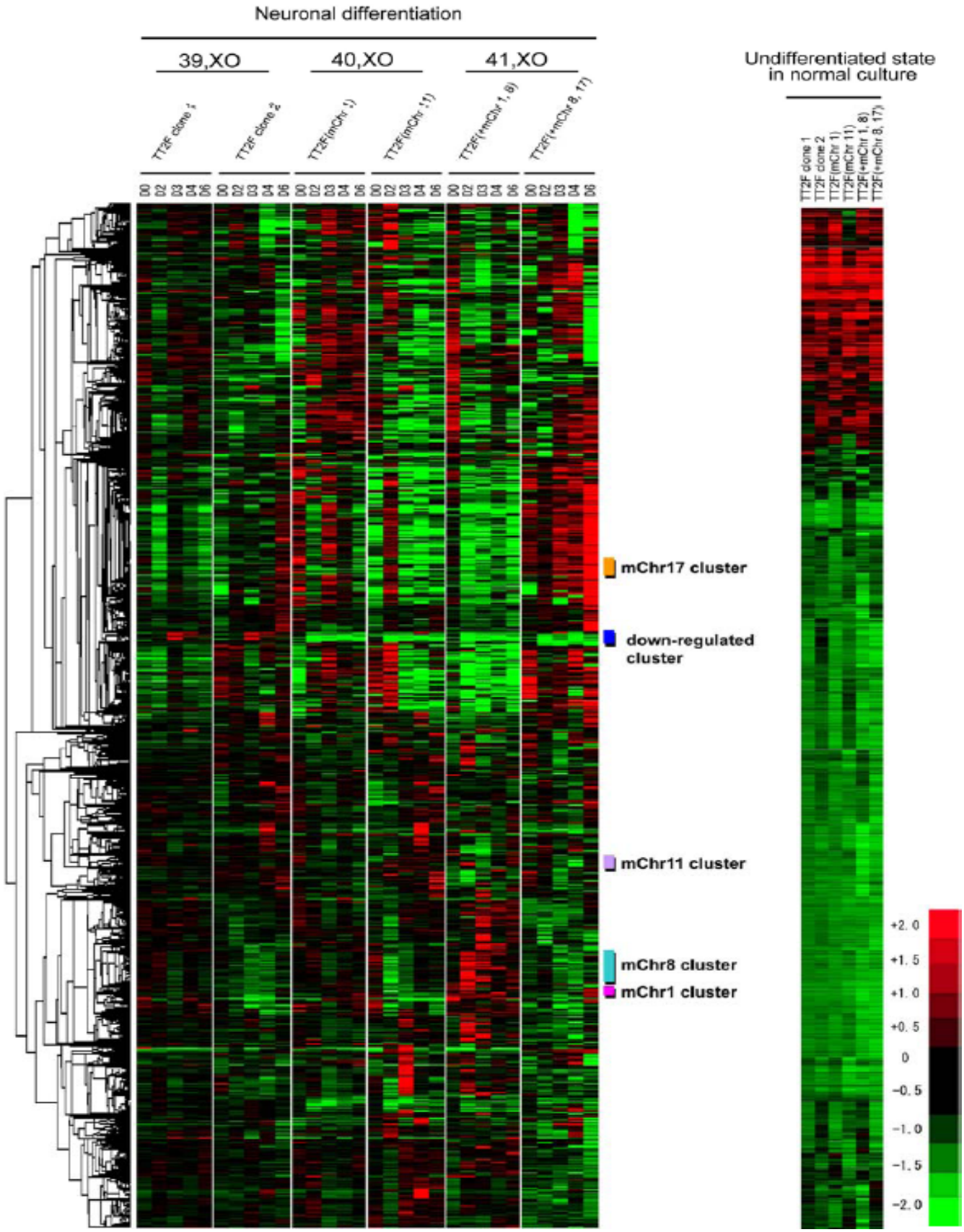
Neuronal differentiation
39,XO
40,XO
41,XO
T2F clone 1
T2F clone 2
T2F(mChr 1)
T2F(mChr 11)
T2F(+mChr 1, 8)
T2F(+mChr 8, 17)
D0
D2
D3
D4
D6
mChr17 cluster
down-regulated cluster
mChr11 cluster
mChr8 cluster
mChr1 cluster
Undifferentiated state in normal culture
T2F clone 1
T2F clone 2
T2F(mChr 1)
T2F(mChr 11)
T2F(+mChr 1, 8)
T2F(+mChr 8, 17)
+2.0
+1.5
+1.0
+0.5
0
−0.5
−1.0
−1.5
−2.0

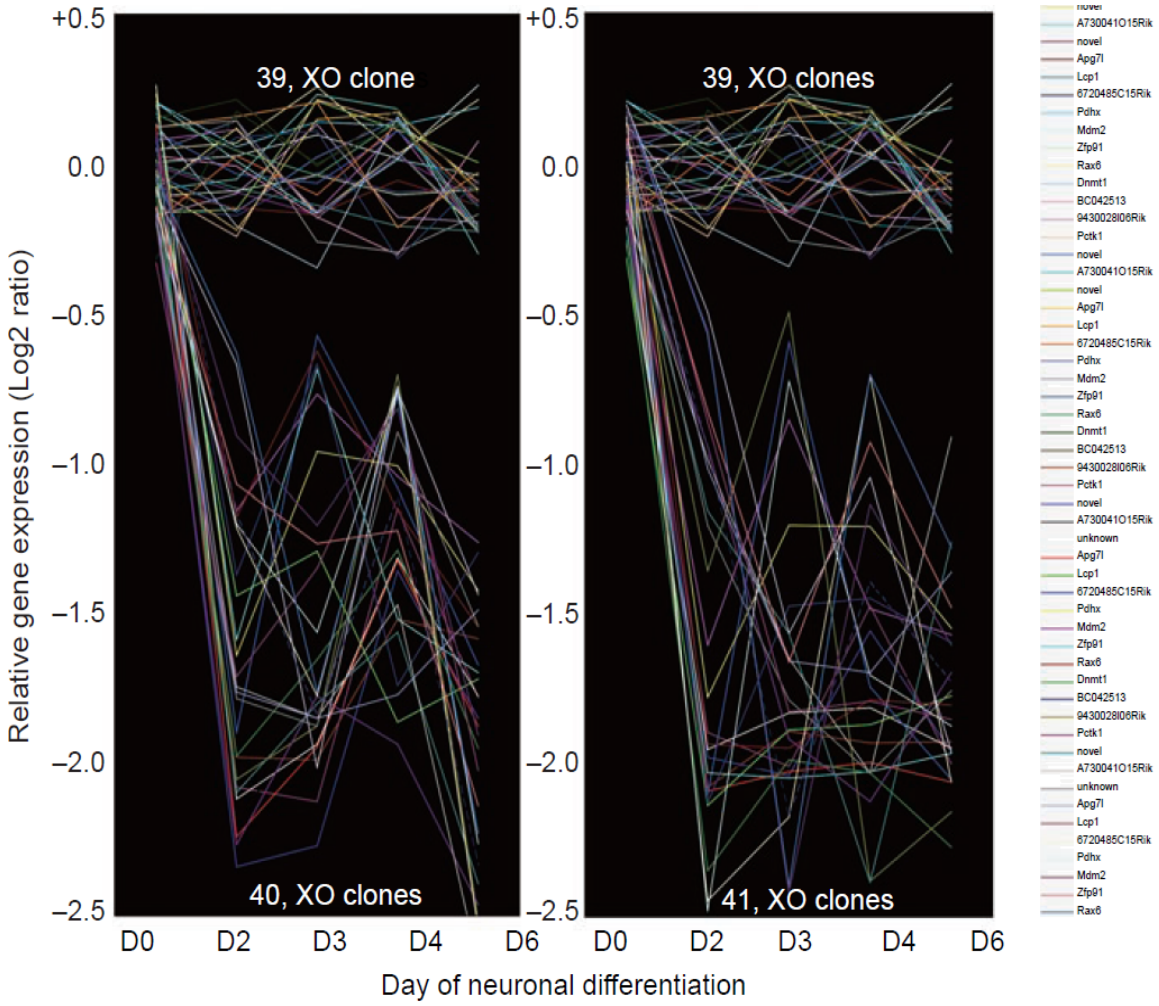

Figure 5.19 Identification of a gene cluster in autosome-imbalanced TT2F clones during early neuronal differentiation. Results from clustering analysis are shown. The dynamic changes in relative gene expression are plotted against the different days of neuronal differentiation. Significant expression suppression of the listed genes in 40, XO (lower left panel) and 41, XO (upper right panel) clones was observed compared with minor changes in expression profiles of 39, XO clones (upper left and right panels).

These genes locate to different chromosomes but not the trisomic chromosomes, suggesting that downregulation of these genes is caused by the aneuploidy status as secondary gene dosage or trans-acting effects. Of the 14 identified genes, 8 were already known, and quantitative real-time PCR analyses confirmed their down-regulation in aneuploid ES clones after induction of neuronal differentiation (Fig. 5.20A), which was not observed under normal conditions nor after induction of random differentiation in the embryoid body (Fig 5.20B).

Table 5.8 Commonly down-regulated genes in autosomal imbalanced TT2F clones during neuronal differentiation.

Gene (Symbol)	Gene Ontology	Accession	UniGene ID	Locus ID	mChr	40,XO (+mChr1 or 11)			41,XO (+mChr8,17 or 1,8)			40,XO (+hChr21)		
						M	B score	p value	M	B score	p value	M	B score	p value
RIKEN cDNA 9430028I06 gene	unknown	BG063914	Mm 216027	109245	3 G1	-1.773	4.549	0.00116	-1.773	3.883	0.00886	-0.814	1.363	0.00514
M. PCTAIRE-motif protein kinase 1 (Pctk1)	protein ser/thr kinase activity	BG063835	Mm 102574	18555	X 5.7 cM	-1.944	4.543	0.00143	-1.751	4.937	0.00036	-0.602	1.077	0.03599
NIA 15K cDNA H3011C07	unknown	-			-	-1.956	4.053	0.00654	-1.733	4.597	0.00107	-0.449	1.059	0.03684
RIKEN cDNA A730041O15 gene	unknown	BG063850	Mm 308396	269717	5 G2	-1.854	3.951	0.00833	-1.624	4.356	0.00233	-0.600	1.040	0.06598
NIA 15K cDNA H3011G04	unknown	-			-	-1.650	4.396	0.00233	-1.783	5.753	0.00018	-0.510	1.211	0.01457
S. cerevisiae autophay 7-like (Apg7l)	autophagy	BG063869	Mm 275332	74244	6 E3	-1.776	4.184	0.00376	-1.731	4.112	0.00475	-0.433	1.118	0.01885
M. lymphocyte cytosolic protein 1 (Lcp1)	actin filament binding	BG063844	Mm 153911	18826	14 42.0 cM	-1.516	4.202	0.00278	-1.744	4.097	0.00537	-0.499	1.041	0.04970
RIKEN cDNA 6720485C15 gene	kinase activity	BG063948	Mm 277449	68087	11 E1	-1.434	4.836	0.00045	-1.730	4.042	0.00671	-0.633	1.035	0.08054
M. pyruvate dehydrogenase complex, component X (Pdhx)	acyltransferase activity	-	Mm 315011	27402	2 E2	-1.345	4.660	0.00054	-1.560	3.996	0.00707	-0.666	1.024	0.08397
transformed M. 3T3 cell double minute 2 (Mdm2)	regulation of cell proliferation	BG064279	Mm 22670	17246	10 66.0 cM	-1.129	4.631	0.00098	-1.399	3.983	0.00797	-0.675	1.093	0.02828
M. zinc finger protein 91 (Zfp91)	nucleic acid binding	BG064217	Mm 290924	109910	19 7.0 cM	-1.393	4.189	0.00278	-1.615	3.967	0.00815	-0.617	1.246	0.00600
M. paired box gene 6 (Pax6)	DNA binding	BG064262	Mm 3608	18508	2 58.0 cM	-1.234	4.114	0.00475	-1.549	3.971	0.00806	-0.431	1.199	0.01114
M. DNA (cytosine-5-)-methyltransferase 1 (Dnmt1)	DNA methylation	BG063875	Mm 128580	13433	9 5.0 cM	-1.462	4.093	0.00600	-1.709	3.957	0.00824	-0.561	1.197	0.01371
M. cDNA sequence BC042513	unknown	BG063921	Mm 11186	215113	11 B5	-1.438	3.974	0.00806	-1.607	4.449	0.00170	-0.714	1.068	0.06255

M: Differential expression measurement: mean log2 ratios; B score: Log posterior odds score that the gene is differentially expressed (Statistics B); P value: probability analyses of the observed differential expression (Bootstrap test).

Figure 5.20 Quantitative real-time PCR results for the listed genes. (A) After neural differentiation induction, expression levels of target genes are significantly down-regulated in chromosome-aberrant compared with normal mouse ES cells. Error bars indicate standard deviation obtained from three independent experiments. The opened and closed bars represent normal and chromosome-aberrant ES cells, respectively. (B) In a random differentiation system during embryoid body formation, no alteration in expression levels of target genes was observed between chromosome-aberrant and normal mouse ES cells.

5.4.3 RNAi inhibits neurogenesis

To confirm the candidate genes for the neural apoptosis during neuronal differentiation, neuronal RNA interference *in vitro* was employed. We investigated the functional relationship between the eight identified genes and enhanced apoptosis during neuronal differentiation of ES cells, by RNAi experiments in parental TT2F clones. Transfection of each siRNA against these genes resulted in a dramatic and reproducible reduction in the levels of respective mRNAs compared with negative control. Further, similar to aneuploid ES cell clones, defective neurogenesis and enhanced apoptosis were observed in six of the knockdowns (Fig 5.21), suggesting that down-regulation of these genes is associated with enhanced apoptosis during neuronal differentiation. The precise mechanism by which the knockdown of these genes contributes to apoptosis, however, remains to be determined.

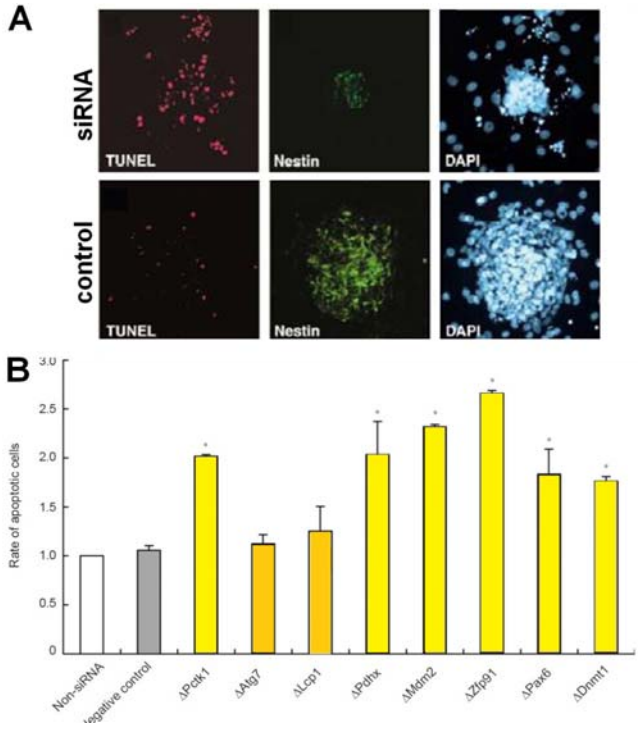

Figure 5.21 Dysregulated genes in early neuronal apoptosis. (A) Target gene knockdown mimics defective neurogenesis and apoptosis in aneuploid clones. siRNAs targeting eight genes were transfected into normal TT2F, followed by neuronal differentiation induction by SDIA treatment. (B) The graph compares the apoptosis rate between normal and siRNA-transfected TT2F during neurogenesis on D3. The white, closed and shaded bars represent non-treated, siRNA-transfected and negative control siRNA-transfected TT2F, respectively. Data are represented as mean ± SD; n=three independent experiments, *P<0.05 compared with control using Student's t-test.

5.4.4 Expression in fetal brain

Expression of the common down-regulated cluster genes were also suppressed in brain tissues of human trisomy 21 and trisomy 18 fetuses (Fig. 5.22). HSA21 transchromosomal mice derived from TT2F/hChr21 ES clones showed similar neuropathological characteristic as in Down syndrome, neurite plaque and neurofibrillary tangle were detected in the brain tissues (Fig. 5.23) and *in situ* expression of the common down-regulated cluster genes were also suppressed in different fetal brian regions (Fig. 5.24 - 5.27).

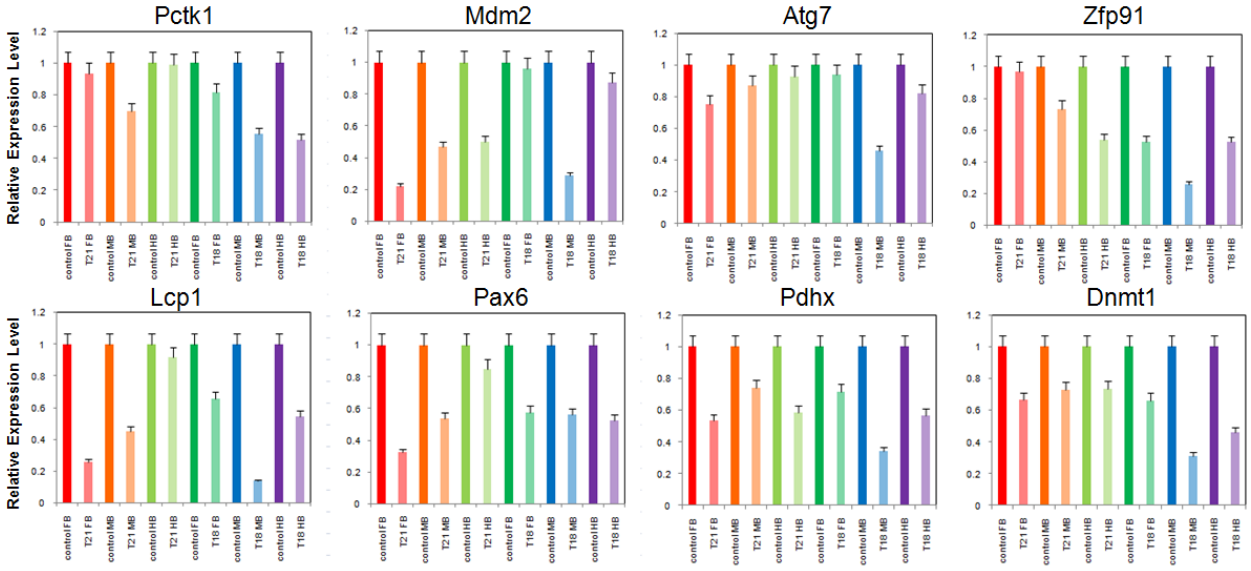

Figure 5.22 Expression of neural apoptotic genes in human fetal brain with autosomal trisomy. Relative mRNA expression were compared with normal gestational age matched brain tissues. T21, Trisomy 21; T18, Trisomy 18; FB, forebrain; MB, midbrain; HB, hindbrain.

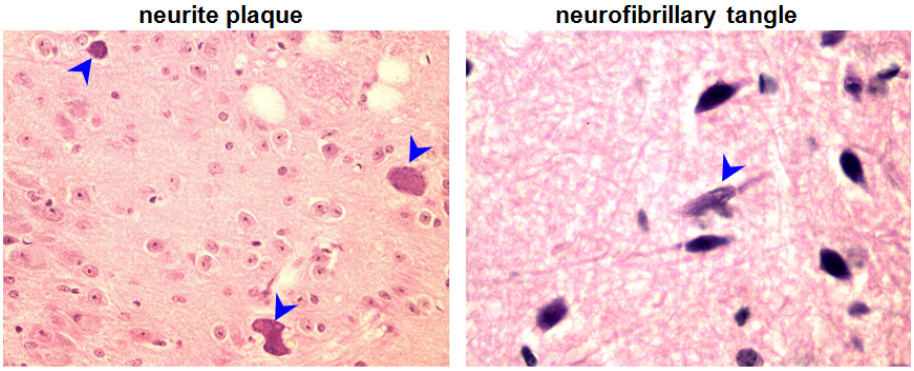

Figure 5.23 Neuropathology of HSA21 transchromosomal mouse brain. Representative pictures of neurite plaque (Left panel, arrows) and neurofibrillary tangle (right panel, arrow) are shown.

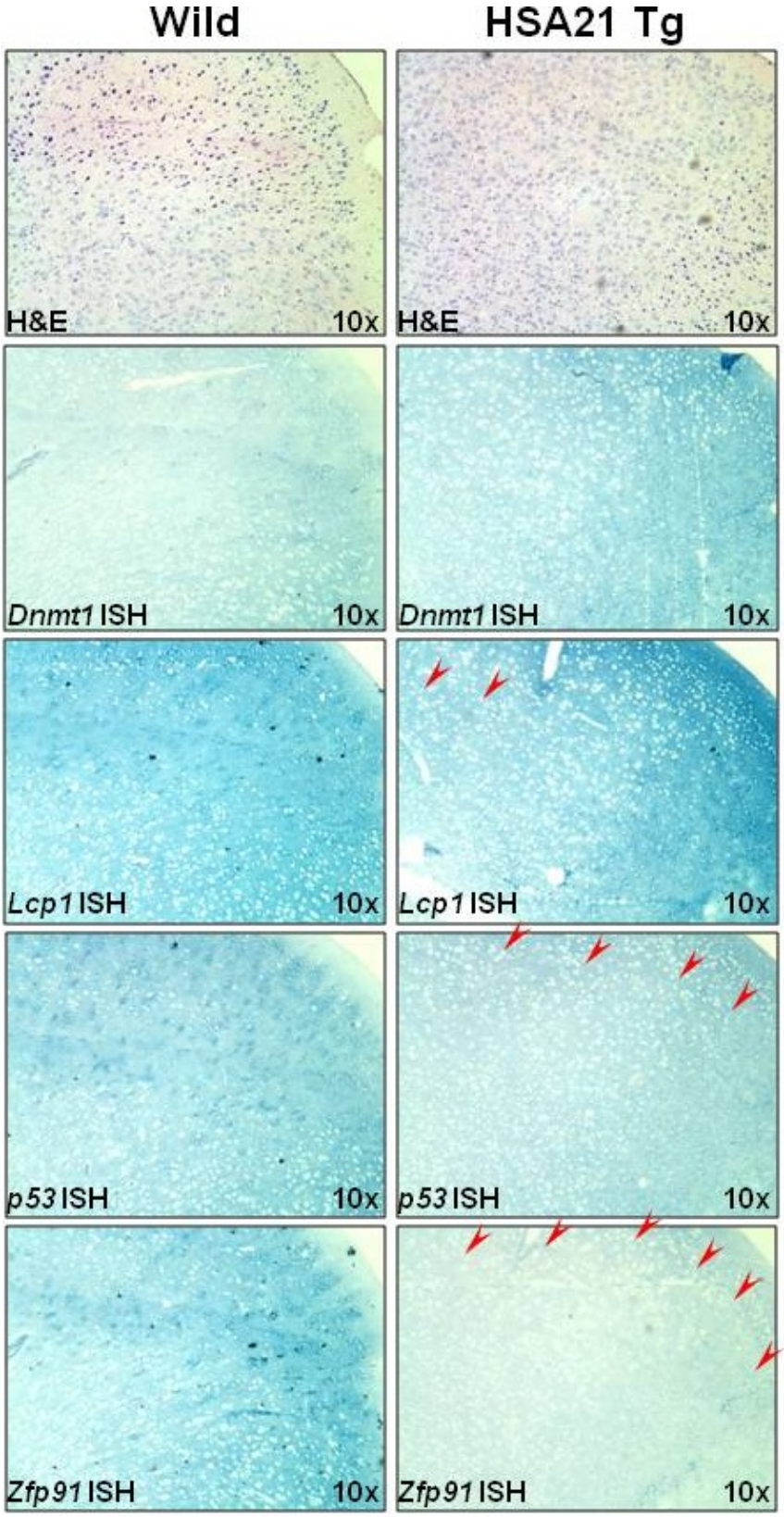

Figure 5.24 Dysregulated genes in cerebral cortex of HSA21 mice. Weak/no expression, red arrows.

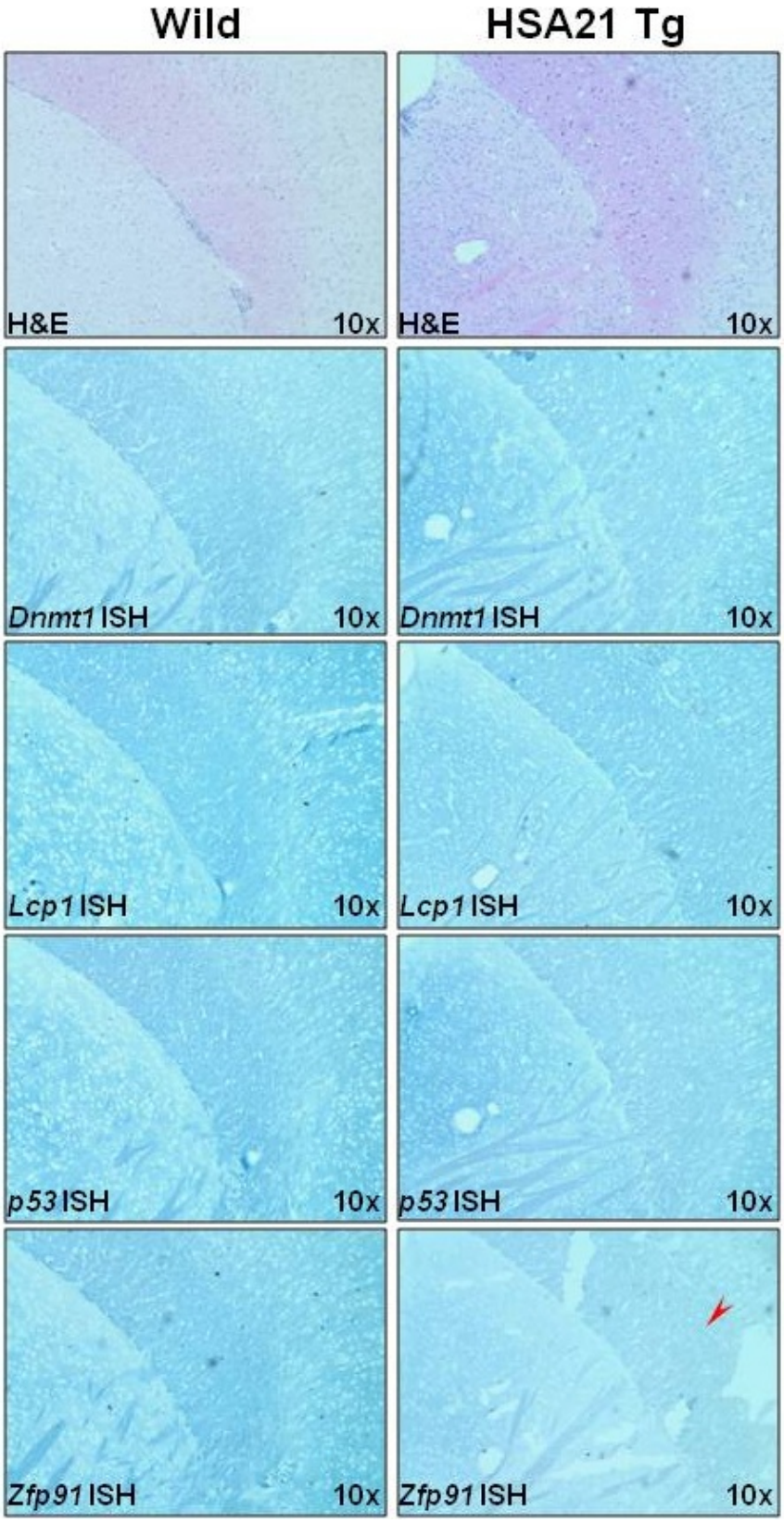

Figure 5.25 Dysregulated genes in corpus callosum of HSA21 mice. Weak/no expression, red arrows

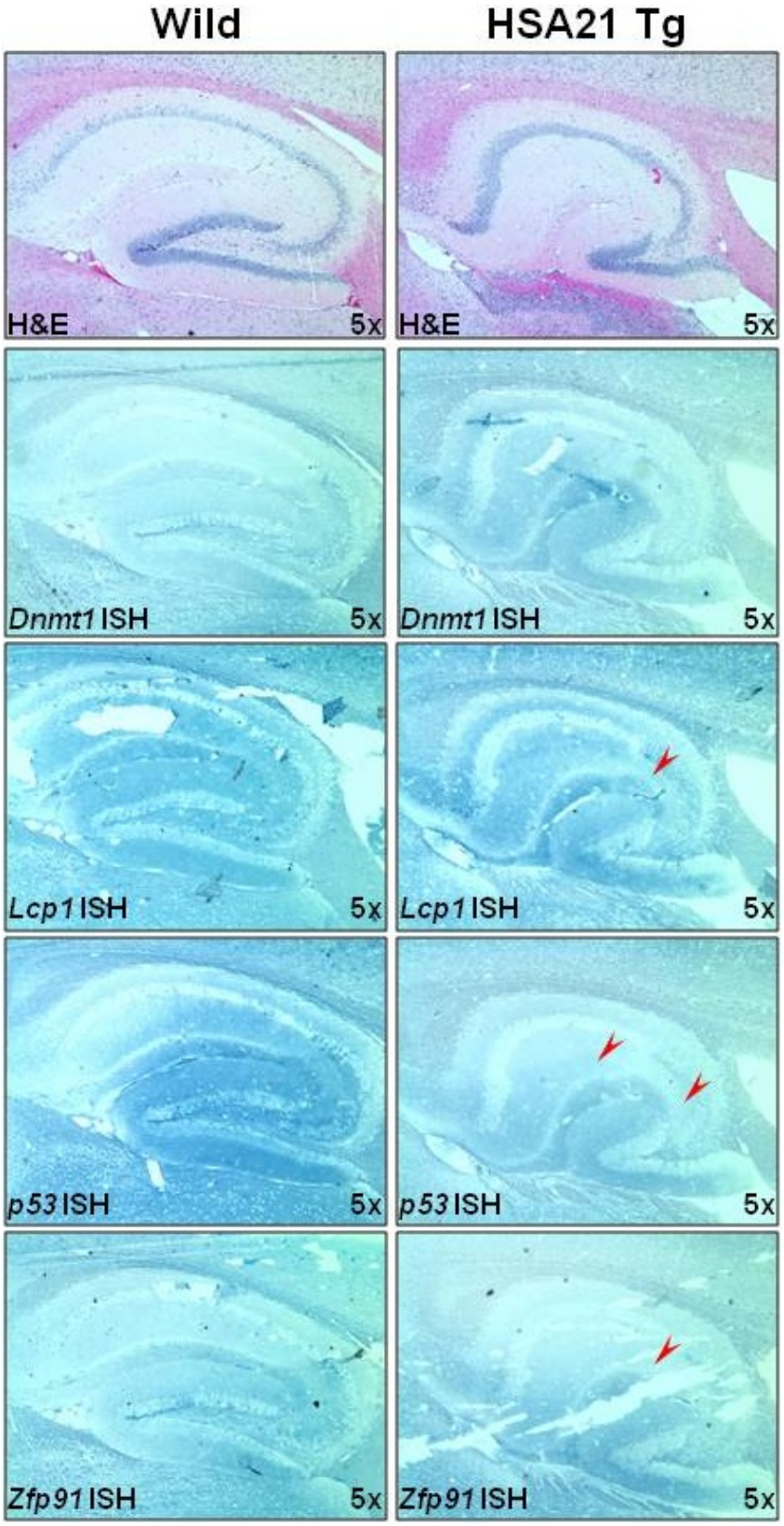

Figure 5.26 Dysregulated genes in hippocampus of HSA21 mice. Weak/no expression, red arrows

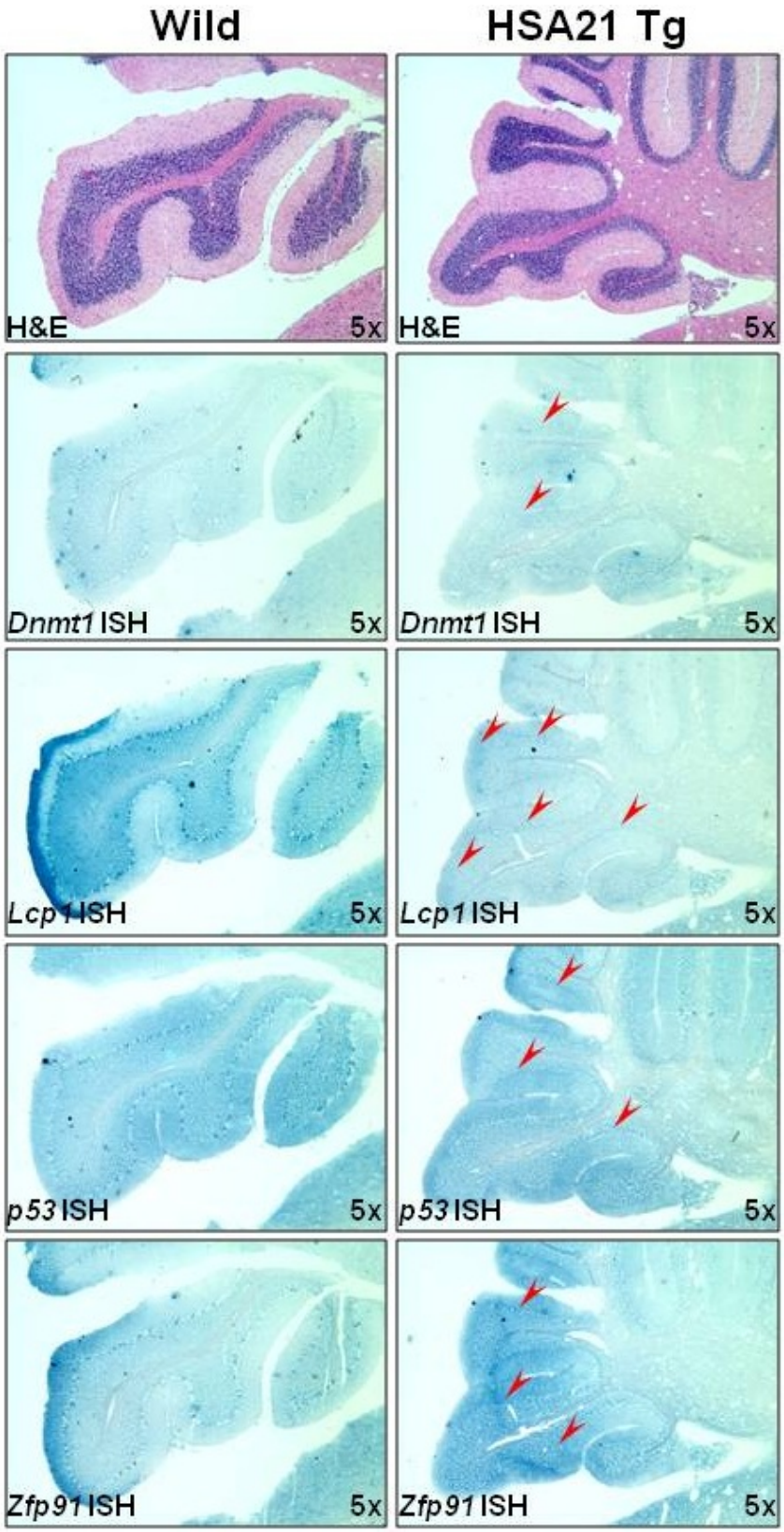

Figure 5.27 Dysregulated genes in cerebellum of HSA21 mice. Weak/no expression, red arrows

Chapter 6

Discussion

6.1. Genomic Implications

6.1.1. Large-scale studies of gene dosage effects

A DNA microarray is a multiplex technology used in molecular biology. It consists of an arrayed series of thousands of microscopic spots of DNA oligonucleotides, called features, each containing picomoles (10−12 moles) of a specific DNA sequence, known as probes (or reporters). This can be a short section of a gene or other DNA element that are used to hybridize a cDNA or cRNA sample (called target) under high-stringency conditions. Probe-target hybridization is usually detected and quantified by detection of fluorophore-, silver-, or chemiluminescence-labeled targets to determine relative abundance of nucleic acid sequences in the target. Since an array can contain tens of thousands of probes, a microarray experiment can accomplish many genetic tests in parallel. Therefore arrays have dramatically accelerated many types of investigation. DNA microarrays can be used to measure changes in expression levels, to detect single nucleotide polymorphisms (SNPs), and to genotype or resequence mutant genomes. The use of a collection of distinct DNAs in arrays for expression profiling was first described in 1987, and the arrayed DNAs were used to identify genes whose expression is modulated by interferon (Kulesh et al 1987). These early gene arrays were made by spotting cDNAs onto filter paper with a pin-spotting device. The use of miniaturized microarrays for gene expression profiling was first reported in 1995 (Schena et al 1995), and a complete eukaryotic genome (Saccharomyces cerevisiae) on a microarray was published in 1997 (Lashkari et al 1997).

Transcriptomics is an area of research characterizing the RNA transcribed from a particular genome under investigation. Although transcriptomes are more dynamic than genomic DNA, these molecules provide direct access to gene regulation. By measuring mRNA concentration levels is still a useful tool in determining how the transcriptional machinery of the cell is affected

in the presence of external signals (e.g. drug treatment), or how cells differ between a healthy state and a diseased state. The intrinsic experimental limitations of microarrays include low signal to noise ratios, cross-hybridization and semi-quantitation when compared with latest advanced technology for transcriptomic studies (Marioni et al 2008; Wang et al 2009). Nevertheless, NIH 15K mouse cDNA library restricted our gene expression microarray to detect all HSA21 orthologs and also whole mouse genome (Tanaka et al 2000). It only covered less than 12.5% of current genes identified in the HSA21.

Proteomics is the large-scale study of proteins, particularly their structures and functions (Anderson & Anderson 1998). Proteins are vital parts of living organisms, as they are the main components of the physiological metabolic pathways of cells. The term "proteomics" was first coined in 1997 to make an analogy with genomics (James P 1997). Two-dimensional gel electrophoresis, abbreviated as 2-DE or 2-D electrophoresis, is a form of gel electrophoresis commonly used to analyze proteins. Mixtures of proteins are separated by two properties in two dimensions on 2D gels. Protein mass spectrometry refers to the application of mass spectrometry to the study of proteins. Mass spectrometry is an important emerging method for the characterization of proteins. The two primary methods for ionization of whole proteins are electrospray ionization (ESI) and matrix-assisted laser desorption/ionization (MALDI). In the first, intact proteins are ionized by either of the two techniques described above, and then introduced to a mass analyzer. This approach is referred to as "top-down" strategy of protein analysis. In the second, proteins are enzymatically digested into smaller peptides using a protease such as trypsin. Subsequently these peptides are introduced into the mass spectrometer and identified by peptide mass fingerprinting or tandem mass spectrometry. Hence, this latter approach (also called "bottom-up" proteomics) uses identification at the peptide level to infer the existence of proteins.

The phenotypic abnormalities of DS are proposed to be resulted from the overexpression of the genes located in HSA21. Of particular interest are the genes located between 21q22.3->ter, which encode for 50-100 key proteins including enzymes, membrane receptors, proto-oncogenes, and voltage-gated ionic channels named DSCR (Koremberg et al 1992). However, the exact mechanism by which trisomy 21 produces the typical phenotypic abnormalities in

neurodevelopment and neurodegeneration are still not completely understood. It is because most of the genes in DSCR are not expressed in brains and have any neuron functions. Though 90 human diseases has been mapped in HSA21, only very few candidate HSA21 genes are associated with DS phenotypes, in particular abnormal brain development and neurodegeneration phenotypes (Table 2.1). Hence, the present genetic data cannot exclude the possibility that candidate genes responsible for DS phenotypes may reside outside the DSCR and even within the HSA21. To select a suitable target gene to study the molecular mechanism of neurodevelopmental abnormalities of DS is impossible before we have background information on the temporal and spatial expression data of candidate gene during neuronal differentiation and early brain development. Large-scale transcriptomic study will be the best approach to identify the most differentially expressed candidate gene for our study.

In our study, exploration of the overall mRNA expression by microarray analysis has revealed the aneuploid ES cells undergoing defective neuronal differentiation *in vitro*. The approach revealed the molecular signatures of defective neuronal differentiation with manifested posttranscriptional and translational modification in the same differentiation system (Wang et al 2004). These results suggested that the alteration exists as early as at the DS neuronal differentiation stage, which is probably related to a variety of biological dysfunctions in the subsequent developmental process. In an attempt to confirm and identify misregulated proteins as the functional output of aberrant mRNA information in early DS neuronal differentiation (Wang et al 2004), we conducted 2D-PAGE protein separation to represent the distinctive proteomic signatures between euploid and aneuploid clones. With the advent of proteomic techniques that allow high-throughput analysis of overall protein expression in particular tissues or cells, aberrant and specific brain proteins have been explored in DS or in DS with Alzheimer disease. Furthermore, autosomal imbalance commonly enhances apoptosis during early neuronal differentiation of mouse ES cells. By high throughput gene expression profiling we were able to identify the altered expression as a common cluster of genes related to the neual apoptosis during early neurogenesis. This indicates the advantage of conducting this kind of gene expression pattern profiling by both microarray and proteomic apprached in discovery of the important molecules or gene networks for further studies.

6.1.2. Aneuploid ES clones and Chromsome transfer

Molecular analyses using fetal or adult brain tissues or primary cultured neuronal cells from DS patients revealed spectrums of mis-regulated gene expression. In these studies the aberrations were observed in well-differentiated neurons or in tissues that were contaminated by glial cells, however. To understand the malformations in DS brain, a study of the early development of neurons and its differentiation process is mandatory. Inaccessibility in utero and difficulties in isolating neuronal stem cells have prevented study of early neuronal differentiation in DS patients. Recently, we successfully generated chimeric mice carrying an intact hChr21 as a freely segregated extra chromosome via MMCT into normal euploid mouse ES cell lines. These chimeric mice presented a wide variety of phenotypic traits of DS in humans, including impairment in learning and emotional behavior, and also hypoplastic thymus and cardiac defects. Delayed cardiogenesis was observed within the embryoid bodies of the aneuploid mouse ES cell lines containing extra chromosome differentiated *in vitro*. Increased susceptibility of the aneuploid cell lines to apoptosis at the stage of neuronal stem cell differentiation *in vitro* using mouse PA6-induced SDIA was also issued. In this study we demonstrate the utility of the aneuploid ES clones applied to the SDIA-induced neuron differentiation *in vitro* as a model to study the role of the autosomal trisomy in DS neuronal development during early neurogenesis.

On the other hand, homologous sets of transcription factors direct conserved tissue-specific gene expression, transcription factor–binding events may diverge rapidly between closely related species. Recently Wilson and coworkers used hepatocytes from an aneuploid mouse strain carrying HSA21 to determine, on a chromosomal scale, whether interspecies differences in transcriptional regulation are primarily directed by human genetic sequence or mouse nuclear environment (Wilson et al 2008). They showed that all transcription factor–binding locations, landmarks of transcription initiation, and the resulting gene expression observed in human hepatocytes were recapitulated across the entire HSA21 in the mouse hepatocyte nucleus. They concluded that it is the regulatory DNA sequence, rather than any other species-specific factor, that is the single most important determinant of gene expression. Hence in our study, the molecular regulation in the anueploid clones are driven largely by sequence, then the trisomic genes should be regulated just as they are in normal euploid clones, whereas if species-specific

developmental context, epigenetic factors, or differences in transcription factors themselves play a defining role, then the genes should most closely mimic their mouse orthologs.

6.1.3. Gene dosage imbalance and genomic adaptations

On average, the steady-state RNA levels of genes on HSA21 in trisomy is expected to be 1.5-fold higher than that in unaffected individuals. This is close to what we observed here: the mean overexpression of HSA21 genes was around 1.5-fold in trisomic ES clones. Interestingly, however, there are over 25% of genes were found to be significantly underexpressed in the trisomic clones when compared with in the euploid samples. Several mechanisms could explain this apparent discordance between the genomic dosage imbalance and the expression levels, such as negative feedback, epigenetic dosage compensation, and gene-expression variation. Because we and others previously reported extensive levels of inter-individual gene-expression variation of HSA21 genes. Though there is a wide distribution of CVs for HSA21 gene expression in both cell types (range 0.14–11), which is consistent with previously published data (Mao et al 2003, Lyle et al 2004), with ~75% of genes having a CV <0.5. Regression analysis clearly showed that genes with higher CV tended to be less overexpressed in DS samples, and/or total reversed, suggesting that gene-expression variation explains, to a certain extent, why many HSA21 genes are not significantly upregulated in trisomy 21.

Mutations can involve large sections of a chromosome becoming duplicated (usually by genetic recombination), which can introduce extra copies of a gene into a genome. In evolution, the most important role of such chromosomal rearrangements may be to accelerate the divergence of a population into new species by making populations less likely to interbreed, and thereby preserving genetic differences between these populations (Ayala and Coluzzi 2005). The two main mechanisms that produce evolution are natural selection and genetic drift. Natural selection is the process which favors genes that aid survival and reproduction. Genetic drift is the random change in the frequency of alleles, caused by the random sampling of a generation's genes during reproduction. Evolution influences every aspect of the form and behavior of organisms. Most prominent are the specific behavioral and physical adaptations that are the outcome of natural selection. These adaptations increase fitness for survival. Adaptation may cause either the gain of

a new feature, or the loss of an ancestral feature (Williams GC 1966). An interesting but still controversial idea is that some adaptations might increase the ability of organisms to generate genetic diversity and adapt by natural selection to increase the organisms' evolvability (Kirschner and Gerhart 1998).

Gene dosage imbalance could be a genomic adaptation to accept the additional chromosome with or without major phenotypic changes by gene-gene interaction and structural and functional modifications. Dosage compensation could be also one of the adaptation mechanism to remain unchanged, while primary and secondary gene dosage effects could be the passive and active adaptation mechanism to allow changes to take place for survival, respectively.

6.2. Neural Differentiation

Mental retardation, as the most common genetic cause of developmental disability in DS, represents a condition characterized by subnormal intellectual functioning and impaired adaptive behavior that become manifest during developmental years. The relationship between mental retardation and the trisomic condition of DS is complex. Conspicuous morphological abnormalities start to be apparent in brains of newborns and older infants with DS. They have shortened basilar dendrites, decreased number of spines with altered morphology, and defective cortical layering (Marin-Padilla M 1976; Takashima & Becker 1981; Becker et al 1986; Schmidt-Sidor et al 1990). In addition, relatively delayed myelination, fewer neurons, lower neuronal density and distribution, and abnormal synaptic and length have been demonstrated (Wisniewski & Schmidt-Sidor 1989; Wisniewski KE 1990). The literature indicates that there are a series of biochemical alterations occurring in fetal DS brain that could serve as substrate for these morphological changes (Engidawork & Lubec 2003). Our data demonstrated these biochemical alterations and subsequent morphological abnormalities may proceed by the underlying molecular changes as early as at the stage of neuron differentiation.

6.2.1. Defective neuronal differentiation in the automsomal trisomy

Neuronal differentiation was defective in this study, with evidence of transient impaired expression of neuronal differentiation and neuroectodermal markers. This manifestation is related to the dysregulated transcription program and post-transcriptional regulation in TT2F neuron differentiation with extra HSA21. Failure of the transcription and translation machinery early in life, essential for neuronal growth and differentiation, may reflect the impaired neurogenesis and brain development resulting in the deficient wiring of the brain in DS.

Interaction of trans-acting proteins, transcriptional factors, with the cis-regulatory sequences promotes a coordinated pattern of gene activation and repression in neuron development and its functional differentiation. REST is a repressor of transcription of multiple neuronal genes and mainly functions in non-neuronal cells and non-differentiated neuronal progenitor cells. REST regulated genes are also associated with synaptic plasticity in learning and memory (Sugiura & Mori 1995). Concerning REST's role as the silencer in neuron differentiation, over-expression of REST negatively suppressed the REST regulated gene Stmn2 in the differentiating TT2F/hChr21 cells. The expression of REST and its regulators is generally reduced in fetal DS brain (Bahn et al 2002). The loss of REST downstream regulation implies a complex mechanism of REST transcription in DS neurons in later life. Setdb1, which is a novel histone H3-specific methyltransferase interacting with Ets-related gene Erg in the control of cell growth and differentiation (Yang et al 2002); Klf4, the key p53-dependent G1/S cell cycle transcriptional factor for cell proliferation, differentiation, and apoptosis (Bieker JJ 2001); and also Esg1, an RNA-binding protein with posttranscription function in potential pluripotency and lineage specificity in stem cell and germ-lines (Tanaka et al 2002); are all inhibited during neuronal differentiation in TT2F/hChr21 cells.

Post-transcriptional/translational modification also regulates gene expression. The regulatory events, including RNA splicing, mRNA transport, stability/decay, and translation, play an important role in decisions to stabilize, degrade or translate the information in a message that can affect neuronal differentiation. Suppression of the differentiation-specific translational mechanism found in TT2F/hChr21 cells underlines the aberrant splicing, RNA stabilizing, and translation factors for the dysmorphogenesis in DS brain. For example, Mrpl10 is an essential mitochondrial ribosomal protein for neural crest cell migration and cell-fate determination

(Kirby et al 1995). Mrps18a is a putative substrate for Ca2þ/calmodulin-activated protein kinase II, activating signaling pathways through nerve growth factor and promoting axon outgrowth (Bonnington & McNaughton 2003; Hansen et al 2003). SNAPC3 binds to RNA polymerase II- and III-dependent small nuclear RNA gene promoters for essential cell viability, and targets heteromultimeric general transcriptional factors in control of cell proliferation and differentiation (Das & Bellofatto 2003).

Messenger RNA levels do not always correlate with protein levels, and lack of correlation between mRNA and protein levels warrants determination of protein level (Greenbaum et al 2003). The association of each mRNA with proteins results in the formation of heterogeneous complexes with diverse biophysical properties. The most obvious underlying mechanism is the ribonucleoprotein infrastructure, for example the dysregulation of Eif4e in the differentiating TT2F/hChr21 cells. Not unlike transcription, splicing, and polyadenylation, translation also involves combined interactions of RNAs and proteins, especially the circularization of the engaged mRNA mediated by interactions between Eif4e and Eif4g (Keene JD 2001). Eif4g was significantly suppressed when the neuron differentiation was established by D6 of TT2F/hChr21 cells (Tab. 4.1). These imply that the flow of genetic information between the genome and the proteome is disrupted and Eif4e and Eif4g may be regarded as the molecular pathogenesis of this discrepancy.

Elevated susceptibility of the differentiating TT2F/hChr21 cells to apoptosis at the neuronal stem cell stage was reported earlier (Kadota et al 2002). DNA damage and instability in the TT2F/hChr21 cells during neuronal differentiation is suggested by the activation of PRCP, PYCP1, and Timp2, which confer the essential conformational constraints of proline-containing peptide in normal biological processing (Vanhoof et al 1995); Peg3, which is a mediator between p53 and Bax in a neuronal cell death pathway (Johnson et al 2002); and SMUG1, which plays a role as uracil–DNA glycosylase and also acts as specific backup of DNA repair enzymes UNG2 in repair of 5-formyluracil and other oxidized and deaminated base lesions (Masaoka et al 2003). Apoptosis was first described as a phenomenon associated with developmental events, serving to match the neuron population to its target fields, and adjust the need for an initial progenitor pool for proper morphogenesis of the nervous system. Since the relative expression of growth-

survival and death-promoting factors influences a cell's commitment to death in response to an apoptosis stimulus, several lines of the apoptotic pathway were involved in the neuronal stem cell with extra HSA21 in the process of differentiation, which has not been found in differentiated fetal DS brain (Engidawork et al 2001). First, Fem1b conserves high homolog of the Caenorhabditis elegans sex-determination protein in the pathway of programmed cell death (Ventura-Holman et al 1998). The transient elevation of Fem1b in the beginning of differentiation programming may act as the trigger for neuron cell-fate determination. Second, up-regulated APP in TT2F/hChr21 cells can trigger neuronal death (Kienlen-Campard & Octave 2002). Third, PYPAF4, as a family member of PYRIN domain, assembles together with apoptosis-associated speck-like protein containing a caspase recruitment domain (ASC), and signals the activation of NF-jB and pro-caspase-1 (Grenier et al 2002). Also, Bnip3 is critical for homodimerization, proapoptotic function, and mitochondria targeting, even in the presence of Bcl2 (Ray et al 2000). Both expression of PYPAF4 and Bnip3 coincided with evidence of apoptosis at the neuronal stem cell stage in our TT2F/hChr21 cells.

6.2.2. Proteomic signatures and aberrations

With the advent of proteomic techniques that allow high-throughput analysis of overall protein expression in particular tissues or cells, aberrant and specific brain proteins have been explored in DS or in DS with Alzheimer disease. Decrease in ATP-sensitive potassium channels (Kim and Lubec 2001) and in stathmin, a ubiquitous phosphoprotein (Cheon et al 2001), increase in carbonyl reductase, alcohol dehydrogenase (Balcz et al 2001) and in nicotinic acetylcholine receptor β2 subunits (Engidawork et al 2001), were reported. Other specific proteins were altered in the fetal brains of DS patients. Decrease in synaptosomal associated protein 25 subunits, drebrin, nucleoside diphosphate kinase B, Rab GDP-dissociation inhibitor β subunit, and histidine triad nucleotide-binding protein,suggest the impairment of multiple transmembrane signaling and synaptic transmission pathways (Weitzdoerfer et al 2001). Misexpression of these proteins that play crucial roles in neuro-morphogenesis and neurogenic cascades appears to be the biological mechanism responsible for the pathogenesis of mental retardation and premature development of Alzheimer disease in DS. However, the aberrations of protein expression in

well-differentiated neurons, or in fetal or adult DS brain tissues that also contains glial cells, are expected to be different from the aberrations in the developing neuron itself.

Human genes on the transferred chromosome 21 were also expressed in TT2F/hChr21 cells during neuronal differentiation. Among the 225 genes on hChr21, only CCT8 and SOD1 proteins were identified in our study. In our previous study, genes on the introduced human chromosome were expressed in appropriate tissue specific manners in mouse models containing human chromosome 2, 14 and 21 (Tomizuka et al., 1997; Shinohara et al., 2001), or in culture (Kadota et al., 2002), suggesting that the detection sensitivity of 2-DE gel analysis limited to highly abundant proteins such as housekeeping genes; the restricted isoelectric conditions between pH 4–7, and the MW range between 15 and 150 kDa; indistinguishable human/mouse protein sequence homolog; and comigration of different hChr21 proteins in the 2-DE gel could have probably lowered the assay specificity for hChr21 genes. Moreover, inverse dosage effect on hChr21 genes and their mouse counterparts that decreases the expression level of each gene copy to achieve dosage compensation (Birchler et al., 2001), might be affecting our assay sensitivity to detect proteins derived from hChr21. In any case, it is apparent that SOD1 and CCT8 proteins are highly represented in neuronal cells, suggesting these two genes from hChr21 are good candidates involved in the defective neuronal development in fetal DS brain, directly or by trans-acting genes on other chromosomes.

CCT8 is the Θ subunit of the T-complex protein one (TCP-1) which is a molecular chaperon essential for cell growth, assists in the folding of proteins in the eukaryotic cytosol, and has previously been reported to be dysregulated in adult DS brain (Yoo et al., 2001). The molecular function of the subunit CCT8 itself is unknown; however, the target protein of the molecular chaperon TCP-1 is thought to be diverse due to its composition of CCT subunits, suggesting the over-expression of a single subunit resulting in the functional conversion of the TCP-1. It has also been suggested that TCP-1 plays an important role in the recovery of cells from protein damage by assisting in the folding of proteins under stress conditions (Yokota et al., 2000).

SOD1 is a CuZn-superoxide dismutase located within the DS critical region. SOD1 is a key enzyme in the metabolism of oxygen free radicals or reactive oxygen species by catalyzing the

dismutation of superoxide anions to hydrogen peroxide. In the fetal DS brain, SOD1 activity is elevated, which may lead to the overproduction of hydrogen peroxide. Indeed, neurons in DS exhibit a three- to four-fold increase in intracellular reactive oxygen species (Brooksbank and Balazs, 1984). On the other hand, increased generation of mutant SOD1 shows a cytoskeleton dependent defect in neurite outgrowth and viability (Lee et al., 2002); however, de novo peptide sequencing is necessary to confirm this possibility in our system.

By successful survey and comparison of the overall protein expressed between TT2F and TT2F/hChr21 cells in neuronal differentiation, we have identified nine up-regulated and seven down-regulated proteins that were altered in TT2F/hChr21 cells compared with TT2F cells. More than half of them were mostly consistent between the amounts of RNA transcript compared with the amounts of proteins, including cytoskeleton proteins, chaperone proteins, translation regulators, energy metabolism enzymes and transcriptional mediators.

6.2.3. Transcriptional and translational machinery

Transcriptional mediators Heterogeneous nuclear ribonucleoproteins (hnRNPs) are RNA binding proteins that associate with heterogeneous nuclear RNAs (hnRNAs) in the nucleus and stabilize the hnRNA secondary structure for nucleosome assembly, pre-mRNA processing, mRNA metabolism and transport (Dreyfuss et al 1993). HnrnpF binds to DNA at a promoter via an oligo (dG)-motif and is associated with RNA polymerase II. Evidence for an association between a splicing factor, HnrnpF and TAT-binding protein demonstrated the essential factor needed for transcription initiation in splicing machinery prior to transcriptional elongation (Yoshida et al 1999). HnrnpF has been shown to be a neuralspecific pre-mRNA splicing factor (Min et al 1995), and was over-expressed in TT2F/hChr21 cells, suggesting this mechanism is enhanced. However, another hnRNP subfamily protein HnrnpC was under-expressed in TT2F/hCh21 cells. HnrnpC has been implicated in a variety of processes including splicing, polyadenylation, and RNA turnover. Null mutation of HnrnpC gene in mice results in the failure to develop beyond E6.5, suggesting a nonredundant function of this gene essential to development (Williamson et al 2000). Moreover, other hnRNP proteins hnRNP-A2/B1 have been reported to be altered in fetal DS brain (Kim et al 2001), which suggests that the misregulation of RNA processing is one of

the general cellular malfunctions that might be responsible for the neurodegenerative condition in DS.

The ubiquitin–proteasome proteolytic pathway is involved in an important non-lysosomal proteolytic pathway for highly selective turnover of cellular proteins, both under basal metabolic and under stress conditions. Recently there has been increasing interest in the proteasome because of its possible role in neuron degeneration and death. Altered expression of de-ubiquitinating enzymes may contribute to the neurodegenerative condition in DS. The under-expressed protein AI850305, the nomenclature of which has recently been updated as Otub1 protein, is predicted to have cysteine protease activity and belongs to the ubiquitin-specific protease family (NCBI LocusLink Report; http://www.ncbi.nlm.nih.gov/LocusLink/index.html, ID: 107260). UchL1 is a developmentally regulated neuron and neuroendocrine cell-specific ubiquitin C-terminal hydrolase family, regulating cell cycle progression and neurite differentiation (Trowern et al 1996), which has also been identified as causative gene in Parkinson disease, causing massive loss of dopaminergic neurons in the pars compacta of the substantia nigra (Vaughan et al 2001). In fact, UchL1 gene encodes two opposing enzymatic activities, either in accumulation of α-synuclein or in dimerization-dependent ubiquityl ligase, and the latter is known to play a role in proteasomal protein degradation required for neuronal health and survival (Liu et al., 2002). Eef1D is a subunit of the eukaryotic elongation factor-1 complex. Elongation factor-1 functions in delivery of aminoacyl tRNA to the ribosome for mRNA translation and perinuclear localization in protein synthesis. Eef1D undergoes developmental regulation with perdurable phosphorylation memory signal in early embryonic development (Minella et al 1998). Decrease in Eef1D may affect neurite maturation and transformation in the early phase of neuron differentiation. Thus, the misregulation of protein synthesis and translation machinery might be responsible for neurodegeneration in DS.

In this part of the study, we found the complex network of molecular changes in neuronal stem cells with extra HSA21 for the defective neuron differentiation mechanism by locus-specific disturbance of chromosome imbalance and various HSA21 gene dosage effect, including primary, secondary and reverse dosage effects and dosage conpensation. We demonstrated the chromosomal imbalance associated molecular deteriorations in the post-transcription and

translation mechanism, and also specific gene expression hierarchy of HSA21 gene dosage effects on neuron outgrowth, migration, and differentiation. These could serve as substrates for functional changes preceding the morphological abnormalities in DS that are unequivocally apparent following birth. It will also be possible to discuss how these factors may be relevant to manipulating neuron stem cells to express the normal neural induction, neural fate stabilization, and neuron differentiation for stem cell therapy to DS patients in future.

6.2.4. Gene dosage effects on neural differentiation

The identification of genes on HSA21 and the elucidation of their functions encoded by these genes have been a major challenge for the human genome project as well as for research in DS. Over-expression of HSA21 genes is believed to be responsible for the mental retardation and other phenotypic abnormalities of DS, but gene dosage effect applies to some gene products but not to others.

APP, the precursor of b-amyloid protein, which is considered to be the major pathogenic molecule in Alzheimer's disease, is up-regulated during neuron differentiation. DS is also characterized by premature Alzheimer's disease-like neuropathology, including bamyloid plaque, neurofibrillary tangles, and neuronal loss, known to supervene later in life. Even though there is the lack of detectable difference in protein expression between control and DS fetal brains (Engidawork et al 2001), evidence of neuronal death triggered by APP in neuron differentiation could be related (Kienlen-Campard & Octave 2002). The long isoform of Itsn1 is brain specific, taking part in synaptic vesicle recycling activities and is widely expressed in both proliferating and differentiating neurons (Pucharcos et al 1999). Itsn1, an adaptor protein involved in clathrin-mediated endocytosis, activates mitogenic signaling pathways with its conserved Eps homology (EH) domains as well as additional protein recognition motifs (adams et al 2000). However, the SH3 domains of Itsn1 have been proved to inhibit coated-vesicle formation *in vitro* (Simpson et al 1999), in which Itsn1 is over-expressed in the brain of DS fetuses compared with controls (Pucharcos et al 1999), and also in differentiating TT2F neuronal stem cells with extra HSA21. Mnb is the ortholog of the formerly characterized minibrain gene of Drosophila (Tejedor et al 1995). Mnb is over-expressed in DS embryonic brain (Guimera et al

1999) and differentiating TT2F/hChr21 cells, and is expressed in neural progenitor cells related to the cell determinant of neurogenesis resulting in a decrease in the number of neurons (Hammerle et al 2002). It is also involved in the dramatic cessation of dendrite growth during late development in DS brain (Hammerle et al 2003).

In contrast to what would be expected in gain of function from the extra HSA21 gene load, decreased Ets2 message was found in temporal and frontal lobes of DS patients (Greber-Platzer et al 1999), and in the differentiating TT2F/hChr21 clones. Knockout of Ets2 expression shows non-hematopoietic defects related to extraembryonic development and neurogenesis (Bartel et al 2000), suggesting specific neurodegenerative processes and deteriorated plasticity of the brain taking place in DS. Dscn3 is in one of the DS critical regions, with domains of vacuolar protein sorting-associated protein 26 (Vps26), which plays a role in retromer-mediated endosome-to-Golgi retrieval (Reddy & Seaman 2001). The detailed biological function of Dscn3 in DS brain is still not very clear, it down-regulates in differentiating TT2F/hChr21 clones, however. Hmgn1 promotes interaction with 14-3-3 proteins impeding the reentry of proteins into the nucleus during mitosis (Prymakowska-Bosak et al 2002) and enhances the rate of DNA repair in chromatin (Birger et al 2003). Under-expressed Hmgn1, together with 14-3-3, in the differentiating TT2F/hChr21 cells implies the possibility of abolished chromatin binding and inhibited nuclear transport in DS brain for neuron proliferation. Whilst SOD1 catalyzes the dismutation of superoxide radicals and neutralizes the oxidative metabolites. The increased activity of SOD1 might not be linked to its over-expression in DS brain (Gulesserian et al 2001). It is probably attributed to enzymatic modification and suggests it is the consequence of low levels of reducing agents and enzymes involved in the removal of hydrogen peroxide, rather than an antecedent of oxidative stress. SOD1, positively mediated by transcriptional factor Elk1 and negatively by YY1 (Chang et al 1999), can maintain expression of nitric oxide synthase for potential neuronal differentiation, and prevent nitric oxide cytotoxicity (Takikawa et al 2001). SOD1 transcript is down-regulated, as is Elk1, in the differentiating TT2F/hChr21 cells. This implies a potential defect in neurite outgrowth and associates with neuronal death, as in mutant SOD1 (Lee et al 2002). CCT8, as a chaperonin containing TCP1, which was first identified in the mouse as relevant for tailless and embryonic lethal phenotypes, encodes a molecular

chaperon for actin and tubulin for cell division (Iijima et al 1998). Down-regulation of CCT8 in the differentiating TT2F/hChr21 cells may interfere with neuronal outgrowth and proliferation.

There are several transcription factor genes that are triplicated in DS individuals and mouse models that are known to be essential for specification of various cell types. Basic helix-loop-helix (bHLH) transcription factors Olig1 and Olig2 have been implicated in oligodendrogenesis and neurogenesis (Takebayashi et al 2000; Lu et al 2002; Zhou and Anderson 2002). 1.7- and 1.5-fold increases in Olig1 and Olig2 expression using real-time RT-PCR were detected in the Ts65Dn forebrain at E14.5 and the increases were associated with the Ts65Dn inhibitory neuron phenotype (Chakrabarti et al 2010). Unfortunately our microarray did not contain Olig1 and Olig2 probes. Comparison in the expression levels of these 2 genes in the aneuploid and euploid differentiating neurons were not determined due to restricted coverage. Currently whole mouse genome microarray is very commonly used for transcriptomic studies and also RNA sequencing technology is now available with absolute quantitation, deep coverage and base level resolution in understanding how different alleles of a gene are expressed. The full coverage of HSA21 of other mouse genome will allow us to detect and compare the expression levels of trisomic HSA21 and disomic MMU genes in the aneuploid and euploid differentiating neurons.

6.3. Neural Apoptosis

It is becoming widely accepted that apoptosis may be responsible for neuronal death in degenerative diseases of the adult and aging brain. There is also evidence to indicate that the expression of apoptosis regulatory proteins is altered in the brain of DS individuals (Busciglio & Yankner 1995; de la Monte et al 1998; Nagy & Esiri 1997; Sawa et al 1997). These finding lead to the hypothesis that neuronal death in DS occurs via an apoptotic mechanism. The phenomena, however, that trigger neurodegeneration are still much debated. *In vitro* evidence has suggested that the main factor responsible for neuronal death is the accumulation of β-amyloid, due to the over-expression of its precursor protein. Another hypothesis argues for the importance of reactive oxygen species in neuronal detah. However, the *in vivo* findings do not entirely support either theories (Nagy ZS 1999).

6.3.1. Common molecular gene cluster

Here, we present evidence suggesting that specific ES cell aneuploidy is not directly related to enhanced apoptosis at the early stage of neural stem cell differentiation *in vitro*. Owing to the involvement of a large number of genes in neuronal differentiation, an additional or missing chromosome in any chromosome pair carrying these genes may affect neuronal differentiation and result in apoptosis. Alternatively, an abnormal total number of chromosomes results in non-specific genetic imbalance, which may also induce enhanced apoptosis at the early stage of neural stem cell differentiation. This study suggests that autosomal imbalance triggers apoptosis during early neuronal differentiation by altering the expression of a set of genes, which were identified as a common cluster and reported to be involved in cell proliferation, as well as neurite outgrowth and differentiation.

This cluster includes 2 novel genes, 4 ESTs and 8 known genes, which are also down-regulated in the aneuploid 40,XO clones with single transferred HSA21 in previous chapter. The 4 known genes are mainly transcription factors related to cell proliferation, neurite outgrowth and differentiation, including mouse double minute 2 (Mdm2), autophagy 7-like (Apg7l), lymphocyte cytosolic protein 1 (L-plastin, Lcp1), human zinc finger protein 91 homolog (ZFP91), DNA methyltransferase (cytosine-5) 1 (Dnmt1), paired box gene 6 (Pax6), PCTAIRE protein kinase 1 (Pctk1), and pyruvate dehydrogenase complex, component X (Pdhx).

Mdm2 is a transcriptional target of tumor protein p53, the encoded protein is a nuclear phosphoprotein E3 ubiquitin ligase binds and inhibits transactivation of p53 (Hipfner et al 1998). p53 transcription factor activates target genes that promote cell-cycle arrest or apoptosis in response to cellular stresses, while Mdm2 maintains low levels of p53 by targeting the protein for degradation by the proteasome, and by directly blocking p53 transcriptional activity. Down-regulation of Mdm2 in both aneuploid 40,XO and 41,XO clones can suppress the Mdm2-mediated p53 transcriptional silencing and degradation, leads to cell-cycle arrest and apoptosis in the differentiating neurons.

Apg7l was identified based on homology to Pichia pastoris GSA7 and Saccharomyces cerevisiae APG7 during autophagy, which is a process for the bulk degradation of proteins in fusion of peroxisomal and vaculuolar membranes during survival under starvation, cell differentiation and development (Mizushima et al 1998). The whole process is highly conserved as macroautophagy in higher eukaryotic cells. Apg7l protein shows homolog to the ATP-binding and catalytic sites of the E1 ubiquitin activating enzymes essential in the formation of pre-autophagosomal membrane conjugate with Apg12-Apg5 (human apoptosis specific protein homolog) in autophagy. Inhibition of Apg7l expression in aneuploid clones suppress the autophagic cell death but may have unanticipated effect of promoting apoptosis in the affected neural stem cells. A group of severe inherited neurodegenerative disorders and neuronal ceroid-lipofuscinosis involve active autophagy-derived lysosomal degradation during neuronal development.

Lcp1 is an actin-crosslink protein for cellular organization and reorganization of the focal adhesion. Reduced Lcp1 expression interferes with these processes in inhibiting the cellular proliferation activity and restores the cell-cell adhesion and cell-extracelllar matrix interactions leading to the reduction of invasive and migratory properties (Matsudaira P 1988). Lcp1 is highly abundant cellular proteins with differentiation-specific isoforms (Lin et al 1988), its involvement in both tissue differentiation and neoplastic transformation suggested that Lcp1 plays critical roles in oncogenesis as an important constituent in the normal development of tissue, and in normal cell proliferation and migration, which was down-regulated in the aneuploid clones.

ZFP91, contains C2H2 type domains for nucleic acid-binding proteins, plays an important role in leukemia cell proliferation and anti-apoptosis in human (Unoki et al 2003). In mouse, Zfp91 generally expresses in the developing central nervous system (Mouse Genome Informatics at http://www.informatics.jax.org.). Down-regulation of Zfp91 explains the enhanced premature apoptosis by inhibiting proliferation in the aneuploid 40,XO and 41,XO clones. Whereas, co-transcription of upstream Zfp91 and ciliary neurotrophic factor (Cntf) encoding the same protein has been observed (Saotome et al 1995). Cntf, suppressed in the aneuploid clones as well, is a neurotrophic factor for neurotransmitter synthesis, neurite outgrowth and neuron progenitor

differentiation (Stockli et al 1989), which is related to the lower neuronal density and distribution, and abnormal synaptic length and transmission in the brain of aneuploidy.

Dnmt1 has a role in the establishment and regulation of tissue-specific patterns of methylated cytosine residues. Longer Dnmt1 isoform found in somatic cells was important in maintaining methylation of intracisternal A-type particle (IAP) during gastulation by suppressing IAP expression and the potential for mutagenesis by retrotransposition. Functional rescue of Dmnt1 mutant embryonic stem cells, as in the down-regulated Dmnt1 aneuploid clones, that contain highly demethylated genomic DNA and fail to differentiate normally was shown (Tucker et al 1996). It suggests that aberrant methylation patterns are associated with certain human tumors and developmental abnormalities.

Pax6 encodes paired box gene 6, one of many human homologues of the Drosophila melanogaster gene prd and also contains a homeobox domain. Both domains are known to bind DNA, and function as regulators of gene transcription. Pax6 is a potent neurogenic determinant in precursors of the dorsal telencephalon during brain development. It is required for most of the neurogenesis in both cerebral cortex and neurosphere-derived ES cells towards neurogenesis (Hack et al 2004). Defective neuronal differentiation is consistent with depression of the Pax6 expression in aneuploid clones.

The protein encoded by Pctk1 belongs to the cdc2/cdkx subfamily of the ser/thr family of protein kinase in control of individual phase transitions of cell cycle. Pctk1 plays a role in signal transduction cascades in neurite outgrowth and terminally differentiation in the developing brain tissues (Besset Besset et al 1999), however it is suppressed in aneuploid clones. Pctk1 is also thought to escape X inactivation located in Xp11.3-Xp11.23, a hotspot for mental retardation and neurogenetic disorders (Thiselton et al 2002).

The mammalian pyruvate dehydrogenase complex differs from the complex in Escherichia coli by the presence of a 53kD protein that has been labeled component protein X, i.e. Pdhx, which involves the acyltransferase activity for electron transportation in mitochondrion. Missing the X component in the enzyme is identified in a known genetic defect presented with psychomotor,

ataxia and familial mentally retardation (Robinson et al 1990). The direct mission of Pdhx in neuronal functions and its association with mental incapacitation in autosomal imbalance requires further evaluation as implied in development of the neurological deficit.

6.3.2. Underlying mechanism

We suggest that dysregulation of these genes leads to excess apoptosis during early neurogenesis by altering the cell cycle progression and differentiation program. Alternatively, these genes could be components of a pathway unidentified to date, the disturbance of which leads to apoptosis in early neuronal differentiation. In particular, genes identified as down-regulated in aneuploid ES clones are located at different chromosomal positions in the genome, showing that trisomy triggers the dysregulation of disomic genes (Vacik et al 2005; Mao et al 2003; Lyle et al 2004; FitzPatrick DR 2005). Aneuploidy associated down-regulation of the 14 common genes is possibly due to the effect of putative genes that monitor genomic imbalance (Devlin et al 1988; Guo & Birchler 1994; Niehrs & Pollet 1999). In addition, aneuploidy for various chromosomes should also modify the expression of different groups of target genes, thus producing unique phenotypes.

Apoptosis occurs naturally during normal development, and a number of studies have reported the importance of cell death during neural development in mammals (Oppenheim RW 1991; Thomaidou et al 1997). Recently, several groups have shown the important role of the caspase family in apoptosis associated with neural development. In particular, studies showed that caspase 3 is crucial during the developmental period and under pathological conditions such as cerebral ischemia (Nicholson DW 1999; Porter & Janicke 1999; Zheng et al 1999). A few studies reported the involvement of Sonic hedgehog (Shh) in the ongoing neurogenesis in postnatal rodent brains (Lai et al 2003; Machold et al 2003; Ahn & Joyner 2005). Further, a study in Ts65Dn mice showed a substantially reduced mitogenic response to Hedgehog signaling (Roperr et al 2006). These molecular mechanisms are possibly linked to the enhanced apoptosis induced by aneuploidy during early neurogenesis. It would also be important to understand the functional roles of the identified cluster of down-regulated genes, for example, by further in-depth analysis in knockout mice. Further studies are also required to better understand whether the enhanced

apoptosis we have observed is caused by an increase in naturally occurring apoptosis or by an additional pathway not observed during normal neural development.

Our results show that autosomal imbalance commonly enhances apoptosis during early neuronal differentiation of mouse ES cells, and alters the expression of a common cluster of genes. In addition, this effect is possibly limited to autosomes as no enhancement of apoptosis was observed in TT2s cells with a missing sex chromosome. We identified a gene cluster underlined the common molecular mechanism of neural apoptosis during early neurogenesis. These findings are consistent with the suggested relationship between dysregulated developmental apoptosis in early neurogenesis and mental retardation in patients with autosomal aneuploidy.

6.4. Gene Clusters and Networks

Since the discovery of the chromosomal anomaly causing DS, one major goal has been to characterize the number and the nature of genes involved in the determinism of the pathology. Often referred to as a gene-dosage effect, the initial pathogenic scenario could either result from the cumulative effects of a large number of genes whose individual contribution would not produce a strong phenotype in a trisomic situation, or from a small set of tightly regulated genes for which a non-diploid status would alter cascades of key developmental pathways, or from a combination of both events. A recent comparative study of craniofacial skeleton dysmorphologies between mice carrying MMU16 segments of variable lengths in triplicate demonstrated that the genes located in the DSCR were not sufficient to produce the DS facial phenotype modeled in the mouse (Olson et al 2004). DS phenotype is likely to result from complex genetic interactions probably not restricted to a segment of the triplicated chromosome, but rather involving primarily HSA21 genes and expanding to larger genetic networks. The understanding of the molecular mechanisms causing DS relies in fine on the integration of multilevel molecular data (transcriptome, proteome, metabolome amongst others) and also the deciphering of the genetic networks affected by the massive gene dosage imbalance as a result of trisomy 21.

Hierarchical clustering is a statistical method for finding relatively homogeneous clusters. Hierarchical clustering consists of two separate phases (Johnson SC 1967). Initially, a distance matrix containing all the pairwise distances between the genes are calculated. Pearson's or Spearman's correlation are often used as dissimilarity estimates, but other methods, like Manhattan distance or Euclidian distance can also be applied. If the genes on a single chip are to be clustered, the Euclidian distance is the correct choice, since at least two chips are needed for calculation of any correlation measures. After calculation of the initial distance matrix, the hierarchical clustering algorithm either (A) joins iteratively the two closest clusters starting from single data points (agglomerative, bottom-up approach), or (B) partitions clusters iteratively starting from the complete set (divisive, top-down approach). After each step, a new distance matrix between the newly formed clusters and the other clusters is recalculated. Hierarchical cluster analysis methods include: single linkage (minimum method, nearest neighbor); complete linkage (maximum method, furthest neighbor); and average linkage, such as UPGMA.

Most cell-fate decisions in mammalian cells are not controlled by one single pathway alone. Rather, the combinatorial and quantitatively different activation of signalling pathways seems to determine the cellular response. Large-scale analysis of gene expression networks is required to identify the target genes. One of the major bottlenecks in understanding how signalling networks control gene expression is the link between transcription factors and their target genes. Despite intense methodological work, it is still problematic to predict which transcription factor controls which gene. Pathway analysis, after determining a list of genes involved in a given biological process, map these genes to known pathways and Gene Ontology terms and determine i.e. which pathways are overrepresented in a given set of genes. In our study we are able to calculate the highest signficant candidate genes associated with the secondary or trans-acting gene dosage effects by the aneuploid trisomy. Such algorithm allow further discriminatory gene expression, annotation enrichment, gene-gene interaction, and signaling network analyses which is impossible determined by a single experiment. It further indicates that importance of large-scale gene expression for data mining and analysis in producing and interpreting the data through bioinformatic methods to goal for the biological information for further studies.

6.5. Evolutionary Implications

Since human samples were not feasible in current study, we took advantage of an ideal system: a mouse model of Down syndrome in which mouse cells contain a copy of HSA21 in addition to the complete mouse genome. In these cells, the human DNA sequence is placed in an otherwise murine context, including all external and cellular cues as well as regulatory proteins. This unquie system has been proven that its regulation of the genes on HSA21 in these mouse cells is mainly determined by the human DNA sequence, or by the mouse cellular environment and transcriptional machinery. It also calls into question one of the basic tenets of comparative genomics: that evolutionary conservation can serve as the primary tool for finding functional sequences. Clearly, nonconserved sequences are responsible for the observed functional differences in binding and expression of human and mouse genes in the same cells. Thus, although many conserved noncoding sequences are functional, and interspecies comparisons can help us to identify these motifs, narrowing our attention only to these sequences in an incomplete understanding of the regulatory code. Indeed, this approach guarantees missing the species-specific regulatory instructions that make us different from mice.

In our study, the system allows us to ask an otherwise impossible question: how the gene dosage imbalance is affected by an external extra copy of the genetic materials in the individuals. The data interpretation has taken account of the evolution implication of difference of the human homologs in mosue genome but precautious should be drew from the other potential unknown genetic effects due to the technology of chromosome transfer in the anueploid ES clones, such as epigenetic modification of the genes in the transferred chromosome and the host chromosomes.

Chapter 7

Conclusions

Autosomal trisomy is a numerical chromosomal anomaly involved one extra copy of an autosomal chromosome. Trisomy 21, known as DS, is the most common autosomal trisomy at birth, the only one for which individuals survive beyond childhood. It is associated with mental developmental failure followed by processes of neurodegeneration. All individuals present various extent and severity of cognitive impairment and behavioural phenotype. Relationship between intellectual disabilities and autosomal trisomic conditions is not clear. Central working hypothesis in autosomal trisomy research relies on gene dosage imbalance results from increased gene expression on the extra chromosome. Recently large-scale gene expression analyses in adult and postnatal tissues from human subjects and mouse models of DS were reported. However, investigating molecular mechanism for neuropathological abnormalities affected by autosomal trisomy primarily in early brain development, in particular neurogenesis and neuronal differentiation, is lacking.

Theoretically, the supernumerary copy of HSA21 in DS is expected to result in a 50% increase in the level of transcripts of all genes in HSA21. However, it is not always a direct correlation between genomic imbalance and transcript level of genes within the aneuploid segment, suggesting complex genomic implications. There is also extensive expression variation for HSA21 genes in DS, suggesting that precise data mining and systematic analysis are mandatory to understand the genomic implications of gene dosage imbalance in autosomal trisomy.

In our study, we aimed to investigate the genomic implications and its molecular mechanism of autosomal imbalance in early neurogenesis. A large-scale gene expression approaches to profile the global transcriptome and proteome, through data mining and bioinformatic analysis, were employed in order to study the gene dosage imbalance in autosomal trisomy. A mouse embryonic stem cell line containing single HSA21 differentiated to neurons *in vitro* was used to study the genomic and developmental implications of autosomal imbalance in neural

differentiation, apoptosis and development. Impaired neuronal differentiation in aneuploid clone were observed. Transcriptome analysis using microarray and proteome analysis for global gene and protein expression profiling revealed the complex network of molecular changes in aneuploid clones with defective neuronal differentiation. Primary and secondary gene dosage effects and dosage compensation in aneuploid clones were confirmed in early neurogenesis, but we the first time identified the reverse gene dosage effects. The specific gene networks by HSA21 gene dosage effect and locus-specific disturbance of chromosome balance in the affected genome as secondary or trans-acting gene dosage effects were also identified.

We demonstrated the chromosomal imbalance associated molecular deteriorations in the post-transcription and translation mechanism, and also specific gene expression hierarchy of HSA21 gene dosage effects on neuron outgrowth, migration, and differentiation. With several mouse embryonic stem cell lines containing extra copy of different mouse autosomal chromosome(s), we showed autosomal imbalance enhances apoptosis during early neuronal differentiation of mouse ES cells, and alters the expression of a common gene expression cluster specific to autosomal imbalance, but not to sex-chromosomal imbalance. These genes were significantly down-regulated in brain tissues of trisomic human fetuses and chimeric mice with human chromosome. These findings are consistent with the suggested relationship between dysregulated developmental apoptosis in early neurogenesis and neurodevelopmental manifestations in patients with autosomal aneuploidy. Therefore, gene dosage imbalance of autosomal trisomy affects both trisomic and disomic gene and protein expression during early neurogenesis and neuronal differentiation. The autosomal imbalance is associated with general neuronal loss though a common molecular mechanism for neural apoptosis during neural differentiation.

DS phenotype is likely to result from complex genetic interactions probably not restricted to a segment of the triplicated chromosome, but rather involving primarily HSA21 genes and expanding to larger genetic networks. Understanding of the molecular mechanisms causing DS relies on the integration of multilevel molecular data (transcriptome, proteome, metabolome amongst others) and the deciphering of the genetic networks affected by the massive gene dosage imbalance as a result of trisomy 21. Our study also showed that data mining and bioinformatic

analysis are essential to interpret and integrate the biological information from the gene clusters and networks.

The results of the study could serve as substrates for functional changes preceding the morphological abnormalities in DS that are unequivocally apparent following birth. There is no doubt that the development of new therapies would greatly improve the quality of life of patients with DS. It will be possible to discover how these factors may be relevant to manipulate neuron stem cells to express the neural induction, neural fate stabilization, and neuron differentiation for stem cell therapy to DS patients in near future.

References

Adams A, Thorn JM, Yamabhai M, Kay BK, O'Bryan JP. Intersetin, an adaptor protein involved in clathrin-mediated endocytosis, activates mitrogenic signaling pathways. J Biol Chem 2000; 275: 27414–27421.

Ahn S, Joyner AL. In vivo analysis of quiescent adult neural stem cells responding to Sonic hedgehog. Nature 2005; 437: 894-897.

Amano K, Sago H, Uchikawa C, Suzuki T, Kotliarova SE, Nukina N, Epstein CJ, Yamakawa K. Dosage-dependent over-expression of genes in the trisomic region of Ts1Cje mouse model for Down syndrome. Hum Mol Genet 2004; 13: 1333–1340.

Anderson NL, Anderson NG. Proteome and proteomics: new technologies, new concepts, and new words. Electrophoresis 1998; 19(11): 1853–1861.

Angell RR, Xian J, Keith J, Ledger W, Baird DT. First meiotic division abnormalities in human oocytes: mechanism of trisomy formation. Cytogenet Cell Genet 1994; 65: 194–202.

Angell RR. Aneuploidy in older women. Higher rates of aneuploidy in oocytes from older women. Hum Reprod 1994; 9: 1199–1200.

Antonarakis SE, Lyle R, Dermitzakis ET, Reymond A, Deutsch S. Chromosome 21 and down syndrome: from genomics to pathophysiology. Nat Rev Genet 2004; 5: 725–738.

Antonarakis SE. 10 years of genomics, chromosome 21, and Down syndrome. Genomics 1998; 51: 1–16.

Ar Peled O, Korkotian E, Segal M, Groner Y. Constitutive overexpression of Cu/Zn superoxide dismutase neurons. Proc Natl Sci USA 1996; 93: 8530-8535.

Arai Y, Ijuin T, Takenawa T, Becker LE, Takashima S. Excessive expression of synaptojanin in brains with Down syndrome. Brain Dev 2002; 24: 67–72.

Arron JR, Winslow MM, Polleri A, Chang CP, Wu H, Gao X, Neilson JR, Chen L, Heit JJ, Kim SK, Yamasaki N, Miyakawa T, Francke U, Graef IA, Crabtree GR. NFAT dysregulation by increased dosage of DSCR1 and DYRK1A on chromosome 21. Nature 2006; 441: 595–600.

Axelrod R, Hamilton WD. The evolution of cooperation. Science 1981; 211: 1390–1396.

Ayala FJ, Coluzzi M. Chromosome speciation: humans, Drosophila, and mosquitoes. Proc Natl Acad Sci USA 2005; 102(Suppl 1): 6535–6542.

Aymes S, Lippman-Hand A. Maternal-age effect in aneuploidy: does altered embryonic selection play a role? Am J Hum Genet 1982; 34:558.

Baffico M, Perroni L, Rasore-quartino A, Scartezzini P. Expression of the human ETS-2 oncogene in normal fetal tissues and in the brain of a fetus with trisomy 21. Hum. Genet. 1989; 83: 295–296.

Bahn S, Mimmack M, Ryan M, Caldwell MA, Jauniaux E, Starkey M, Svendsen CN, Emson P. Neuronal target genes of the neuron-restrictive silencer factor in neurospheres derived from fetuses with Down's syndrome: a gene expression study Lancet 2002; 359: 310–315.

Balcz B, Kirchner L, Cairns N, Fountoulakis M, Lubec G. Increased brain protein levels of carbonyl reductase and alcohol dehydrogenase in Down syndrome and Alzheimer's disease. J Neural Transm 2001; 61: 193–201.

Bar-Peled O, Gross-Isseroff T, Ben-Hur H, Hoskins I, Groner Y, Biegon A. Fetal human brain exhibits a prenatal peak in the density of serotonin 5-HT1A receptors. Neurosci Lett 1991; 127: 173–176.

Bartel FO, Higuchi T, Spyropoulos DD. Mouse models in the study of the Ets family of transcription factors. Oncogene 2000; 19: 6154–6443.

Baxter LL, Moran TH, Richtsmeier JT, Troncoso J, Reeves RH. Discovery and genetic localization of Down syndrome cerebellar phenotypes using the Ts65Dn mouse. Hum Mol Genet 2000; 9: 195-202.

Becker L, Mito T, Takashima S, Onodera K. Growth and development of the brain in Down syndrome. In: The Morphogenesis of Down syndrome. Epstein CH Ed., Wiley-Liss, New York. 1991, p133–152.

Becker LE, Armstrongm DL, Chan F. Dendritic atrophy in children with Down's syndrome Ann Neurol 1986; 20: 520– 532.

Bender M, Imam FB, Tallot WS, Ganetzky B, Hogness DS. Drosophila ecdysone receptor mutations reveal functional differences among receptor isoforms. Cell 1997; 91: 777-788.

Besset V, Rhee K, Wolgemuth DJ. The cellular distribution and kinase activity of the Cdk family member Pctaire1 in the adult mouse brain and testis suggest functions in differentiation. Cell Growth Differ 1999; 10: 173-181.

Bieker JJ. Kruppel-like factors: three fingers in many pies. J Biol Chem 2001; 276: 34355-34358.

Birchler JA, Bhadra U, Bhadra MP, Auger DL. Dosage-dependent gene regulation in multicellular eukaryotes: implications for dosage compensation, aneuploid syndromes, and quantitative traits. Dev Biol 2001; 234: 275–288.

Birger Y, West KL, Postnikov YV, Lim JH, Furusawa T, Wagner JP, Laufer CS, Kraemer K, Bustin M. Chromosomal protein HMGN1 enhances the rate of DNA repair in chromatin. EMBO J 2003; 22: 1665–1675.

Bleyer A. Indications that mongoloid imbecility is a gametic mutation of degressive type. Am J Dis Child 1934; 47 : 342-348.

Bonnington JK, McNaughton PA. Signalling pathways involved in the sensitization of mouse nociceptive neurons by nerve growth factor. J Physiol 2003; 551(Pt 2): 433–446.

Boschan C, Borchert A, Ufer C, Thiele BJ, Kuhn H. Discovery of a functional retrotransposon of the murine phospholipid hydroperoxide glutathione peroxidase: chromosomal localization and tissue-specific expression pattern. Genomics 2002; 79: 387–394.

Britto J, Tannahill D, Keynes R. A critical role for sonic hedgehog signaling in the early expansion of the developing brain. Nat Neurosci 2002; 5: 103–110.

Brooke NM, Garcia-Fernandez J, Holland PWH: The ParaHox cluster is an evolutionary sister of the Hox gene cluster. Nature 1998; 392: 920-922.

Busciglio J, Yankner BA. Apoptosis and increased generation of reactive oxygen species in Down's syndrome neurons in vitro. Nature 1995; 378: 776-779.

Cairns NJ. Neuropathology. J Neural Transm 1999; 57(Suppl): 61-74.

Chakrabarti L, Best TK, Cramer NP, Carney RSE, Isaac JTR, Galdzicki Z, Haydar TF. Olig1 and Olig2 triplication causes developmental brain defects in Down syndrome. Nature Neurosci 2010; 13: 927-934.

Chang MS, Yoo HY, Rho HM. Positive and negative regulatory elements in the upstream region of the rat Cu/Znsuperoxide dismutase gene. Biochem J 1999; 339: 335–341.

Cheeseman P, Stutz J. In: Advances in Knowledge Discovery and Data Mining. Fayyad UM Ed., MIT Press, Cambridge, MA. 1996, p.153–180.

Cheon MS, Fountoulakis M, Dierssen M, Ferreres JC, Lubec G. Expression profiles of proteins in fetal brain with Down syndrome. J Neural Transm 2001; 61 Suppl.: 311–319.

Cheung VG, Conlin LK,Weber TM, Arcaro M, Jen KY,Morley M, Spielman RS. Natural variation in human gene expression assessed in lymphoblastoid cells. Nat Genet 2003; 33: 422–425.

Chiu CH, Nonaka D, Xue L, Amemiya CT, Wagner GP: Evolution of Hoxa-11 in lineages phylogenetically positioned along the fin-limb transition. Mol Phyogenet Evol 2000; 17: 305-316.

Coyle JT, Oster-Granite ML, GearhartJD. The neurobiologic consequences of Down syndrome Brain Res Bull 1986; 16: 773–787.

Crome L, Cowie V, Slater E. A statistical note on cerebellar and brain stem weight in mongolism. J Ment Defic Res 1966; 10: 69-72.

Daniel A, Wu Z, Bennetts B, Slater H, Osborn R, Jackson J, Pupko V, Nelson J, Watson G, Cooke-Yarborough C, Loo C. Karyotype, phenotype and parental origin in 19 cases of triploidy. Prenat Diagn 2001; 21: 1034–1048.

Das A, Bellofatto V. RNA polymerase II-dependent transcription in trypanosomes is associated with a SNAP complex like transcription factor. Proc Natl Acad Sci USA 2003; 100: 80–85.

Dauphinot L, Lyle R, Rivals I, Dang MT, Moldrich RX, Golfier G, Ettwiller L, Toyama K, Rossier J, Personnaz L, Antonarakis SE, Epstein CJ, Sinet PM, Potier MC. The cerebellar transcriptome during postnatal development of the Ts1Cje mouse, a segmental trisomy model for Down syndrome. Hum Mol Genet 2005; 14: 373–384.

Davidoff LM. The brain in mongolian idiocy. Arch Neurol Psychiatr 1928; 20: 1229-1257.

Davisson MT, Costa ACS. Mouse models of Down syndrome. In: Mouse Models in the Study of Genetic Neurological Disorders. Volume 9 of Advances in Neurochemistry. Edited by Popko B. New York: Plenum Press; 1999, 297-327.

Day T, Taylor PD. Chromosomal drive and the evolution of meiotic nondisjunction and trisomy in humans. Proc Natl Acad Sci USA 1998; 95: 2361-2365.

de Haan JB, Cristiano F, Iannello RC, Kola I. Cu/Zn-superoxide dismutase and glutathione peroxidase during aging. Biochem Mol Biol Int 1995; 35(6): 1281-1297.

de Haan JB, Wolvetang EJ, Cristiano F, Iannello R, Bladier C, Kelner MJ, Kola I. Reactive oxygen species and their contribution to pathology in Down syndrome. Adv Pharmacol 1997; 38: 379–402.

de la Luna S, Estivill X. Cooperation to amplify gene-dosage-imbalance effects. Trends Mol Med. 2006; 12(10): 451-454.

de la Monte SM, Sohn YK, Ganju N, Wands JR. P53- and CD95-associated apoptosis in neurodegenerative diseaeses. Lab Invest 1998; 78: 401-411.

Delint-Ramirez I, Fernández E, Bayés A, Kicsi E, Komiyama NH, Grant SG. In vivo composition of NMDA receptor signaling complexes differs between membrane subdomains and is modulated by PSD-95 and PSD-93. J Neurosci 2010; 30(24): 8162-8170.

Deutsch S, Lyle R, Dermitzakis ET, Attar H, Subrahmanyan L, Gehrig C, Parand L, Gagnebin M, Rougemont J, Jongeneel CV, Antonarakis SE. Gene expression variation and expression quantitative trait mapping of human chromosome 21 genes. Hum Mol Genet 2005; 14: 3741–3749.

Devlin RH, Holm DG, Grigliatti TA. The influence of wholearm trisomy on gene expression in Drosophila. Genetics 1988; 118: 87-101.

Down JL. Observations on an Ethnic Classification of Idiots. London Hospital Reports. 1866; 3: 259-262.

Dreyfuss G, Matunis MJ, Pinol-Roma S, Burd CG. hnRNP proteins and the biogenesis of mRNA. Annu Rev Biochem 1993; 62: 289–321.

Eakin GS, Behringer RR. Tetraploid development in the mouse. Dev Dyn 2003; 228: 751–766.

Eisen MB, Spellman PT, Brown PO, Botstein D. Cluster analysis and display of genome-wide expression patterns. Proc Natl Acad Sci USA 1998; 95: 14863–14868.

Engidawor E, Balic N, Juranville JF, Fountoulakis M, Lubec G. Unaltered expression of Fas, caspase 3, Bcl-2, and annexins in brain of fetal Down syndrome: evidence against increased apoptosis. J Neural Transm 2001; 61 Suppl.: 149–162.

Engidawork E, Balic N, Fountoulakis M, Dierssen M, Graber-Platzer S, Lubec G. b-Amyloid precursor protein, ETS-2 and collagen alpha 1 (VI) chain precursor, encoded on chromosome 21, are not overexpressed in fetal brain Down syndrome: further evidence against gene dosage effect. J Neural Transm Suppl 2001; 61: 335–346.

Engidawork E, Gulesserian T, Balic N, Cairns N, Lubec G. Changes in nicotinic acetylcholine receptor subunits expression in brain of patients with Down syndrome and Alzheimer's disease. J Neural Transm 2001; 61: 211–222.

Engidawork E, Lubec G. Molecular changes in fetal Down syndrome brain. J Neurochem. 2003; 84: 895–904.

Epstein CJ, CoxDR, Epstein LB. Mouse trisomy 16: an animal model of human trisomy 21 (Down syndrome). Ann NY Acad Sci 1985; 450: 157.

Epstein CJ. In: The Consequences of Chromosomal Imbalance: Principals, Mechanisms, and Models, Cambridge University Press. 1986.

Epstein J. Down syndrome. In: The Metabolic and Molecular Bases of Inherited Disease. Scriver CL, Sly WS, Childs B, Beaudet AL, Valle D, Kinzler KW, Vogelstein B Eds., McGraw Hill Inc, New York. 2001, p.1223–1256.

Esiri MM, Morris JM. In: The neuropathology of demintia. Cambridge University Press, Cambridge. 1997.

FitzPatrick DR, Ramsay J, McGill NI, Shade M, Carothers AD, Hastie ND. Transcriptome analysis of human autosomal trisomy. Hum Mol Genet 2002; 11: 3249–3256.

FitzPatrick DR. Transcriptional consequences of autosomal trisomy: primary gene dosage with complex downstream effects. Trends Genet 2005; 21: 249-253.

Ford EB. Polymorphism: when two or more clearly different phenotypes exist in the same interbreeding population of a species. Ecological genetics, 4th ed. 1975.

Fournier RE, Ruddle FH. Microcell-mediated transfer of murine chromosomes into mouse, Chinese hamster, and human somatic cells. Proc Natl Acad Sci USA 1977; 74: 319−323.

Freidl M, Gulesserian T, Lubec G, Fountoulakis M, Lubec B. Deterioration of the transcriptional splicing and elongation machinery in brain of fetal Down syndrome. J Neural Transm 2001; 61 Suppl.: 47–57.

Fritzsch B: Of mice and genes: evolution of vertebrate brain development. Brain Behav Evol 1998; 52: 207-217.

Fuentes JJ, Genesca L, Kingsbury TJ, Cunningham KW, Perez-Riba M, Estivill X, de la Luna S. DSCR1, over-expressed in Down syndrome, is an inhibitor of calcineurin-mediated signaling pathways. Hum Mol Genet 2000; 9: 1681–1690.

Gardner RJM, Sutherland GR. In: Chromosome Abnormalities and Genetic Counseling. Gardner RJM Ed. 2nd ed. New York: Oxford University Press. 1996.

Gavalas A. ArRAnging the hindbrain. Trends Neursci 2002; 25: 61-64.

Gilbert F. Disease genes and chromosomes: disease maps of the human genome. Chromosome 21. Genet Test 1997; 1 (4): 301–306.

Gilbert SF. Developmental biology. Sinauer Associates, Stamford CT. 8th ed, Chapter 9. 2006.

Goday C, Esteban MR. Chromosome elimination in sciarid flies. Bioessays 2001; 23: 242–250.

Godfrey LR, Masters JC. Kinetophore reproduction theory may explain rapid chromosome evolution. Proc Natl Acad Sci U S A. 2000; 97: 9821–9823.

Golden JA, Hyman BT. Development of the superior temporal neocortex is anomalous in trisomy 21. J Neuropathol Exp Neurol 1994; 53: 513–520.

Greber-Platzer S, Schatzmann-Turhani D, Cairns N, Balcz B, Lubec G. Expression of the transcription factor ETS2 in brain of patients with Down syndrome—evidence against the overexpression-gene dosage hypothesis. J Neural Transm 1999; 57 Suppl.: 269–281.

Greenbaum D, Colangelo C, Williams K, Gerstein M. Comparing protein abundance and mRNA expression levels on a genomic scale. Genome Biol 2003; 4: 117.1–117.8.

Grenier JM, Wang L, Manji GA, Huang WJ, Al-Garawi A, Kelly R, Carlson A, Merriam S, Lora JM, Briskin M, DiStefano PS, Bertin J. Functional screening of five PYPAF family

members identifies PYPAF5 as a novel regulator of NF-jB and caspase-1. FEBS Lett 2002; 530: 73–78.

Griffin WST, Sheng JG, McKenzie LE, Royston MC, Gentleman SM, Mrak RE. Life-long over-expression of S100b in Down's syndrome: implications for Alzheimer's pathogenesis. Neurobiol Aging 1998; 19: 401–405.

Guimera J, Casas C, Estivill X, Pritchard M. Human minibrain homologue (MNBH/DYRK1): characterization, alternative splicing, differential tissue expression, and overexpression in Down syndrome. Genomics 1999; 57: 407–418.

Gulesserian T, Engidawork E, Fountoulakis M, Lubec G. Antioxidant proteins in fetal brain: superoxide dismutase-1 is not over-expressed in fetal Down syndrome. J Neural Transm 2001; 61 Suppl.: 71–84.

Gulesserian T, Kim SH, Fountoulakis M, Lubec G. Aberrant expression of centractin and capping proteins, integral constituents of the dynactin complex, in fetal Down syndrome brain. Biochem Biophys Res Commun 2002; 291: 62–67.

Guo M, Birchler JA. Trans-acting dosage effects on the expression of model gene systems in maize aneuploids. Science 1994; 266: 1999-2002.

Hack MA, Sugimori M, Lundberg C, Nakafuku M, Gotz M. Regionalization and fate specification in neurospheres: the role of Olig2 and Pax6. Mol Cell Neurosci 2004; 25: 664-678.

Hammerle B, Carnicero A, Elizalde C, Ceron J, Martinez S, Tejedor FJ. Expression patterns and subcellular locatozation of the Down syndrome candidate protein MNB/DYRK1A suggest a role in late neuronal differentiation. Eur J Neurosci 2003; 17: 2277–2286.

Hammerle B, Vera E, Spreicher S, Arencibia R, Martinez S, Tejedor FJ. Mnb/Dryk1A is transiently expressed and asymmetrically segregated in neural progenitor cells at the transition to neurogenic divisions. Dev Biol 2002; 246: 259–273.

Hammerschmidt E, Loeffler I, Wolf G. Morg1 heterozygous mice are protected from acute renal ischemia-reperfusion injury. Am J Physiol Renal Physiol 2009; 297(5): F1273-1287.

Hansen MR, Bok J, Devaiah AK, Zha XM, Green Sh. Ca2+/calmodulin-dependent protein kinase II and IV both promote survival but differ in their effects on axon growth in spiral ganglion neurons. J Neurosci Res 2003; 72: 169–184.

Hassold T, Chen N, Funkhouser J, Jooss T, Manuel B, Matsuura J, Matsuyama A, Wilson C, Yamane JA, Jacobs PA. A cytogenetic study of 1000 spontaneous abortions. Ann Hum Genet 1980; 44: 151–178.

Hassold T, Chiu D. Maternal age-specific rates of numerical chromosome abnormalities with special reference to trisomy. Hum Genet 1985; 70: 11–17.

Hassold T, Merrill M, Adkins K, Freeman S, Sherman S. Recombination and maternal age-dependent nondisjunction: molecular studies of trisomy 16. Am J Hum Genet. 1995; 57(4): 867–874.

Hattori M, Fujiyama A, Taylor TD, Watanabe H, Yada T, Park HS, Toyoda A, Ishii K, Totoki Y, Choi DK, Groner Y, Soeda E, Ohki M, Takagi T, Sakaki Y, Taudien S, Blechschmidt K, Polley A, Menzel U, Delabar J, Kumpf K, Lehmann R, Patterson D, Reichwald K, Rump A, Schillhabel

M, Schudy A, Zimmermann W, Rosenthal A, Kudoh J, Schibuya K, Kawasaki K, Asakawa S, Shintani A, Sasaki T, Nagamine K, Mitsuyama S, Antonarakis SE, Minoshima S, Shimizu N, Nordsiek G, Hornischer K, Brant P, Scharfe M, Schon O, Desario A, Reichelt J, Kauer G, Blocker H, Ramser J, Beck A, Klages S, Hennig S, Riesselmann L, Dagand E, Haaf T, Wehrmeyer S, Borzym K, Gardiner K, Nizetic D, Francis F, Lehrach H, Reinhardt R, Yaspo ML; Chromosome 21 mapping and sequencing consortium. The DNA sequence of human chromosome 21. Nature 2000; 405(6784): 311-319.

Henderson SA, Edwards RG. Chiasma frequency and maternal age in mammals. Nature 1968; 217: 22–28.

Hill WG, Meyers S, von Bodungen M, Apodaca G, Dedman JR, Kaetzel MA, Zeidel ML. Studies on localization and function of annexin A4a within urinary bladder epithelium using a mouse knockout model. Am J Physiol Renal Physiol 2008; 294(4): F919-927.

Hipfner DR, Cohen SM. Connecting proliferation and apoptosis in development and disease. Nat Rev Mol Cell Biol 2004; 5: 805-815.

Hooper M, Hardy K, Handyside A, Hunter S, Monk M. HPRT-deficient (Lesch-Nyhan) mouse embryos derived from germline colonization by cultured cells. Nature 1987; 326: 292–295.

Huether CA, Ivanovich J, Goodwin BS, Krivchenia EL, Hertzberg VS, Edmonds LD, May DS, Priest JH. Maternal age specific risk rate estimates for Down syndrome among live births in whites and other races from Ohio and metropolitan Atlanta, 1970-1989. J Med Genet 1998; 35 (6): 482–490.

Hussain SP, Amstad P, He P, Robles A, Lupold S, Kaneko I, Ichimiya M, Sengupta S, Mechanic L, Okamura S, Hofseth LJ, Moake M, Nagashima M, Forrester KS, Harris CC. p53-induced up-regulation of MnSOD and GPx but not catalase increases oxidative stress and apoptosis. Cancer Res 2004; 64(7): 2350-2356.

Iijima M, Chimizu H, Tanaka Y, Urushihara H. A Dictyostelium discoideum homologue to Tcp-1 is essential for growth and development. Gene 1998; 213: 101–106.

Ijdo JW, Baldini A, Ward DC, Reeders ST, Wells RA. Origin of human chromosome 2: an ancestral telomere-telomere fusion. Proc Natl Acad Sci U S A. 1991; 88: 9051–9055.

Imai H, Hirao F, Sakamoto T, Sekine K, Mizukura Y, Saito M, Kitamoto T, Hayasaka M, Hanaoka K, Nakagawa Y. Early embryonic lethality caused by targeted disruption of the mouse PHGPx gene. Biochem Biophys Res Commun 2003; 305: 278–286.

Imai H, Nakagawa Y. Novel function of mitochondrial phospholipid hydroperoxide glutathione peroxidase as anti apoptotic factor. Seikagaku 2000; 72: 1344–1348.

Inoue T, Shinohara T, Takehara S, Inoue J, Kamino H, Kugoh H, Oshimura M. Specific impairment of cardiogenesis in mouse ES cells containing a human chromosome 21. Biochem Biophys Res Commun 2000; 273: 219–224.

James P. Protein identification in the post-genome era: the rapid rise of proteomics. Quarterly reviews of biophysics 1997; 30(4): 279–331.

Jiao X, Trifillis P, Kiledjian M. Identification of target messenger RNA substrates for the murine deleted in azoospermia-like RNA-binding protein. Biol Reprod 2002; 66: 475–485.

Johnson MD, Wu X, Aithmitti N, Morrison RS. Peg3/Pw1 is a mediator between p53 and Bax in DNA damage-induced neuronal death. J Biol Chem 2002; 277: 23000–23007.

Johnson SC. Hierarchical Clustering Schemes. Psychometrika 1967; 2: 241-254.

Jones SN, Roe AE, Donehower LA, Bradley A. Rescue of embryonic lethality in Mdm2-deficient mice by absence of p53. Nature 1995; 378: 206–208.

Kadota M, Shirayoshi Y, Oshimura M. Elevated apoptosis in pre-mature neurons differentiated from mouse ES cells containing a single human chromosome 21. Biochem Biophys Res Commun 2002; 299: 599-605.

Kahlem P, Sultan M, Herwig R, Steinfath M, Balzereit D, Eppens B, Saran NG, Pletcher MT, South ST, Stetten G, Lehrach H, Reeves RH, Yaspo ML. Transcript level alterations reflect gene dosage effects across multiple tissues in a mouse model of Down syndrome. Genome Res 2004; 14: 1258–1267.

Kahlem P. Gene-dosage effect on chromosome 21 transcriptome in trisomy 21: implication in Down syndrome cognitive disorders. Behav Genet 2006; 36(3): 416-428.

Kargul GJ, Dukekula DB, Qian Y, Lim MK, Jaradat SA, Tanaka TS, Carter MG, Ko MSH. Verification and initial annotation of the NIA mouse 15K cDNA set. Nat Genet 2002; 28: 17–18.

Kastner P, Mark M, Chambon P. Nonsteroid nuclear receptors: what are genetic studies telling us about their role in real life? Cell 1995; 83: 859-869.

Kavli B, Sundheim O, Akbari M, Otterlei M, Nilsen H, Skorpen F, Aas PA, Hagen L, Krokan HE, Slupphaug G. hUNG2 is the major repair enzyme for removal of uracil from U:A matches U:G mismatches, and U in single-stranded DNA, with hSMUG1 as a broad specificity backup. J Biol Chem 2002; 277: 39926–39936.

Kawakami Y, Yoshida K, Yang JH, Suzuki T, Azuma N, Sakai K, Hashikawa T, Watanabe M, Yasuda K, Kuhara S, Hirabayashi Y, Furuya S. Impaired neurogenesis in embryonic spinal cord of Phgdh knockout mice, a serine deficiency disorder model. Neurosci Res 2009; 63(3): 184-193.

Kawasaki H, Mizuseki K, Nishikawa S, Kaneko S, Kuwana Y, Nakanishi S, Nishikawa SI, Sasai Y. Induction of midbrain dopaminergic neurons from ES cells by stromal cell-derived inducing activity. Neuron 2000; 28: 31–41.

Kazuki Y, Hoshiya H, Kai Y, Abe S, Takiguchi M, Osaki M, Kawazoe S, Katoh M, Kanatsu-Shinohara M, Inoue K, Kajitani N, Yoshino T, Shirayoshi Y, Ogura A, Shinohara T, Barrett JC, Oshimura M. Correction of a genetic defect in multipotent germline stem cells using a human artificial chromosome. Gene Ther 2008; 15: 617-624.

Kazuki Y, Shinohara T, Tomizuka K, Katoh M, Ohguma A, Ishida I, Oshimura M. Germline transmission of a transferred human chromosome 21 fragment in transchromosomal mice. J Hum Genet 2001; 46: 600-603.

Keene JD. Ribonucleoprotein infrastructure regulating the flow of genetic information between the genome and the proteome. Proc Natl Acad Sci USA 2001; 98: 7018–7024.

Kelner MJ, Montoya MA. Structural organization of the human selenium-dependent phospholipid hydroperoxide glutathione peroxidase gene (GPX4): chromosomal localization to 19p13.3. Biochem Biophys Res Communs 1998; 249: 53–55.

Khandelwal S. Chromosome evolution in the genus Ophioglossum L. Botanical Journal of the Linnean Society 1990; 102: 205–217.

Kienlen-Campard P, Octave JN. Correlation between betaamyloid peptide production and human APP-induced neuronal death. Peptides 2002; 23: 1199–1204.

Kim DS, Nam YK, Noh JK, Park CH, Chapman FA. Karyotype of North American shortnose sturgeon Acipenser brevirostrum with the highest chromosome number in the Acipenseriformes. Ichthyological Research 2005; 52 (1): 94–97.

Kim SH, Dierssen M, Ferreres JC, Fountoulakis M, Lubec G. Increased protein levels of heterogeneous nuclear ribonucleoprotein A2/B1 in fetal Down syndrome brains. J Neural Transm 2001; 61 Suppl.: 273–280.

Kim SH, Lubec G. Brain alpha-endosulfine is manifold decreased in brains from patients with Alzheimer's disease: a tentative marker and drug target. Neurosci Lett 2001; 310: 77–80.

King RC, Stansfield WD, Mulligan PK. In: A dictionary of genetics. 7th Ed, Oxford U.P Oxford & New York. 2006, p. 242.

Kirby ML, Cheng G, Stadt H, Hunter G. Differential expression of the L10 ribosomal protein during heart development. Biochem Biophys Res Commun 1995; 212: 461–465.

Kirschner M, Gerhart J. Evolvability. Proc Natl Acad Sci USA 1998; 95(15): 8420–8427.

Kloss RJ, Nesse RM.Trisomy: Chromosome competition or maternal strategy? Increase of trisomy incidence with increasing maternal age does not result from competition between chromosomes. Ethol Scciobiol 1992; 13: 283-287.

Knopp EA, Arndt TL, Eng KL, Caldwell M, LeBoeuf RC, Deeb SS, O'Brien KD. Murine phospholipid hydroperoxide glutathione peroxidase: cDNA sequence, tissue expression, and mapping.Mamm Genome 1999; 10: 601–605.

Koehler KE, Boulton CL, Collins HE, French RL, Herman KC, Lacefield SM, Madden LD, Schuetz CD, Hawley RS. Spontaneous X chromosome MI and MII nondisjunction events in Drosophila melanogaster oocytes have different recombinational histories. Nat Genet 1996; 14: 406–413.

Koehler KE, Hawley RS, Sherman S, Hassold T. Recombination and nondisjunction in humans and flies.Hum Mol Genet 1996; 5: 1495–1504.

Koi M, Shimizu M, Morita H, Yamada H, Oshimura M. Construction of mouse A9 clones containing a single human chromosome tagged with neomycin-resistance gene via microcell fusion. Jpn J Cancer Res 1989; 80: 413-418.

Koremberg JR, Bradley C, Disteche CM. Down syndrome: molecular mapping of the congenital heart disease and duodenal stenosis. Am J Hum Genet 1992; 50: 294.

Kugoh H, Mitsuya K, Meguro M, Shigenami K, Schulz TC, Oshimura M. Mouse A9 cells containing single human chromosomes for analysis of genomic imprinting. DNA Res 1999; 6: 165-172.

Kulesh DA, Clive DR, Zarlenga DS, Greene JJ. Identification of interferon-modulated proliferation-related cDNA sequences. Proc Natl Acad Sci USA 1987; 84(23): 8453–8457.

Labudova O, Kitzmueller E, Rink H, Cairns N, Lubec G. Gene expression in fetal Down syndrome brain as revealed by subtractive hybridization. J Neural Transm 1999; 59; Suppl.: 125–136.

Lai K, Kaspar BK, Gage FH, Schaffer DV. Sonic hedgehog regulates adult neural progenitor proliferation in vitro and in vivo. Nat Neurosci 2003; 6: 21-27.

Lamb NE, Freeman SB, Savage-Austin A, Pettay D, Taft L, Hersey J, Gu Y, Shen J, Saker D, May KM, Avramopoulos D, Petersen MB, Hallberg A, Mikkelsen M, Hassold TJ, Sherman SL. Susceptible chiasmate configurations of chromosome 21 predispose to non-disjunction in both maternal meiosis I and meiosis II. Nat Genet 1996; 14: 400–405.

LaMonte B, Wallace KE, Holloway BA, Shelly SS, Ascano J, Tokito M, Van Winkle T, Howland DS, Holzbaur ELF. Disruption of dynein/dynactin inhibits axonal transport in motor neurons causing late-onset progressive degeneration. Neuron 2002; 34: 715–727.

Lashkari DA, DeRisi JL, McCusker JH, Namath AF, Gentile C, Hwang SY, Brown PO, Davis RW. Yeast microarrays for genome wide parallel genetic and gene expression analysis. Proc Natl Acad Sci USA 1997; 94(24): 13057–13062.

Lee KW, Kim HJ, Sung JJ, Park KS, Kim M. Defective neurite outgrowth in aphidicolin/camp-induced motor neurons expressing mutant Cu/Zn superoxide dismutase. Int J Dev Neurosci 2002; 20: 521–526.

Lejeune J, Gautier M, Turpin R. Étude des chromosomes somatiques de neuf enfants mongoliens. Comptes Rendus de l'Académie des Sci 1959; 248 : 1721-1722.

Lian S, Jakymiw A, Eystathioy T, Hamel JC, Fritzler MJ, Chan EK. GW bodies, microRNAs and the cell cycle. Cell Cycle 2006; 5(3): 242-245.

Lickert H, Cox B, Wehrle C, Taketo MM, Kemler R, Rossant J. Dissecting Wnt/-catenin signaling during gastrulation using RNA interference in mouse embryos. Development 2005; 132: 2599–2609.

Lilienfeld AM, Benesch CH. Down syndrome is caused by translocations or by mosaicism. In: Epidemiology of Mongolism. Baltimore: Johns Hopkins Press, 1969, p.2.

Lin CS, Aebersold RH, Kent SB, Varma M, Leavitt J. Molecular cloning and characteristization of plastin, a human leukoctye protein expressed in transformed human fibroblasts. Mol Cell Biol 1988; 8: 4659-4668.

Lubec B, Weitzdoerfer R, Fountoulakis M. Manifold reduction of moesin in fetal Down syndrome brain. Biochem Biophys Res Commun 2003; 286: 1191–1194.

Lu QR, Sun T, Zhu Z, Ma N, Garcia M, Stiles CD, Rowitch DH. Common developmental requirement for Olig function indicates a motor neuron/oligodendrocyte connection. Cell 2002; 109: 75–86.

Lyle R, Gehrig C, Neergaard-Henrichsen C, Deutsch S, Antonarakis SE. Gene expression from the aneuploid chromosome in a trisomy mouse model of Down syndrome. Genome Res 2004; 14: 1268–1274.

Machold R, Hayashi S, Rutlin M, Muzumdar MD, Nery S, Corbin JG, Gritli-Linde A, Dellovade T, Porter JA, Rubin LL, Dudek H, McMahon AP, Fishell G. Sonic hedgehog is required for progenitor cell maintenance in telencephalic stem cell niches. Neuron 2003; 39: 937-950.

Maele-Fabry GV, Delhaise F, Picard JJ. Morphogenesis and quantification of the development of post-implantation mouse embryo. Toxicol In Vitro 1990; 4: 149–156.

Malamud N, Gaitz CM. In: Aging and the brain. Plenum Press, New York. 1972.

Mangelsdorf DJ, Evans RM. The RXR heterodimers and ophan receptors. Cell 1995; 83: 841-850.

Mangelsdorf DJ, Thummel C, Beato M, Herrlich P, Schutz G, Kastner P, Mark M, Chambon P, Evans RM. The nuclear receptor superfamily: the second decade. Cell 1995; 83: 835-839.

Manzanares M, Wada H, Itasaki N, Trainor PA, Krumlauf R, Holland PW. Conservation and elaboration of Hox gene regulation during evolution of the vertebrate head. Nature 2000; 408: 854-857.

Marioni JC, Mason CE, Mane SM, Stephens M, Gilad Y. RNA-seq: An assessment of technical reproducibility and comparison with gene expression arrays. Genome Research 2008; 18: 1509-1517.

Mao R, Zielke CL, Zielke HR, Pevsner J. Global up-regulation of chromosome 21 gene expression in the developing Down syndrome brain. Genomics 2003; 81: 457–467.

Marin-Padilla M. Pyramidal cell abnormalities in the motor cortex of a child with Down's syndrome. J Comp Neurol 1976; 167: 63–75.

Masaoka A, Matsubara M, Hasegawa R, Tanaka T, Kurisu S, Terato H, Ohyama Y, Karino N, Matsuda A, Ide H. Mammalian 5-formluracil–DNA glycosylase in repair of 5-formyluracil and other oxidized and deaminated base lesions. Biochemistry 2003; 42: 5003–5012.

Matsudaira P. Modular organization of actin crosslinking proteins. Trends Biochem Sci 1991; 16: 87-92.

Maynard SJ. Evolutionary genetics. 2nd ed, Oxford. 1998. p.218-219.

McClure HM, Belden KH, Pieper WA, Jacobson CB. Autosomal trisomy in a chimpanzee: resemblance to Down's syndrome. Science 1969; 165 (897): 1010–1012.

McKee AE, Minet E, Stern C, Riahi S, Stiles CD, Silver PA. A genome-wide in situ hybridization map of RNA-binding proteins reveals anatomically restricted expression in the developing mouse brain. BMC Dev Biol 2005; 5: 14.

Miller OJ, Therman E. In: Human Chromosomes. Miller OJ Ed. 4th ed. New York: Springer. 2001.

Min H, Chan RC, Black DL The generally expressed hnRNP F is involved in a neural-specific pre-mRNA splicing event. Genes Dev 1995; 9: 2659–2671.

Minella O, Mulner-Lorillon O, Bec G, Cormier P, Belle R. Multiple phosphorylation sites and quaternary organization of guaninenucleotide exchange complex of elongation factor-1 (EF-1betagammadelta/ValRS) control the various functions of EF-1alpha. Biosci Rep 1998; 18: 119–127.

Mizuseki K, Sakamoto T, Watanabe K, Muguruma K, Ikeya M, Nishiyama A, Arakawa A, Suemori H, Nakatsuji N, Kawasaki H, Murakami F, Sasai Y. Generation of neural crestderived peripheral neurons and floor plate cells from mouse and primate embryonic stem cells. Proc Natl. Acad Sci USA 2003; 100: 5828–5833.

Mizushima N, Noda T, Yoshimori T, Tanaka Y, Ishii T, George MD, Klionsky DJ, Ohsumi M, Ohsumi Y. A protein conjugation system essential for autophagy. Nature 1998; 395: 395-398.

Momand J, Wu HH, Dasgupta G. MDM2--master regulator of the p53 tumor suppressor protein. Gene 2000; 242(1-2): 15-29.

Monks SA, Leonardson A, Zhu H, Cundiff P, Pietrusiak P, Edwards S, Phillips JW, Sachs A, Schadt EE Genetic inheritance of gene expression in human cell lines. Am J Hum Genet 2004; 75: 1094–1105.

Montes de Oca Luna R, Wagner DS, Lozano G. Rescue of early embryonic lethality in mdm2-deficient mice by deletion of p53. Nature 1995; 378: 203–206.

Müller F, Bernard V, Tobler H. Chromatin diminution in nematodes. Bioessays 1996; 18: 133–138.

Müller F, O'Rahilly R. The first appearance of the major divisions of the human brain at stage 9. Anat Embryol (Berl) 1983; 168: 419–432.

Müller F, O'Rahilly R. The timing and sequence of appearance of neuromeres and their derivatives in staged human embryos. Acta Anat (Basel) 1997; 158: 83–99.

Nagy ZS, Esiri MM. Apoptosis-realted protein expression in the hippocampus in Alzheimer's disaese. NeurobiolAging 1997; 18: 565-571.

Nagy ZS. Mechanisms of neuronal death in Down's syndrome. J Neural Transm 1999; 57 Suppl: 233-245.

Nakamura A, Sato K, Hanyu-Nakamura K. Drosophila cup is an eIF4E binding protein that associates with Bruno and regulates oskar mRNA translation in oogenesis. Dev Cell 2004; 6: 69–78.

Nicholson DW. Caspase structure, proteolytic substrates, and function during apoptotic cell death. Cell Death Differ 1999; 6: 1028-1042.

Niehrs C, Pollet N. Synexpression groups in eukaryotes. Nature 1999; 402: 483-487.

Niessing D, Blanke S, Jackle H. Bicoid associates with the 5-cap-bound complex of caudal mRNA and represses translation. Genes Dev 2002; 16: 2576–2582.

Niwa H, Miyazaki J, Smith AG. Quantitative expression of Oct-3/4 defines differentiation, dedifferentiation or self-renewal of ES cells. Nat Genet 2000; 24: 372–376.

Nomura K, Imai H, Koumura T, Arai M, Nakagawa Y. Mitochondrial phospholipid hydroperoxide glutathione peroxidase suppresses apoptosis mediated by a mitochondrial death pathway. J Biol Chem 1999; 274: 29294–29302.

O'Rahilly R, Müller F, Bossy J. Atlas des stades du développement des formes exterieures del'encéphale chez l'embryon humain. Arch Anat Histol Embryol 1986; 69: 3–39.

O'Rahilly R, Müller F. The early development of the hypoglossal nerve and occipital somites in staged human embryos. Am J Anat 1984; 169: 237–257.

O'Rahilly R, Müller F. The first appearance of the human nervous system at stage 8. Anat Embryol 1981; 163: 1-13.

O'Rahilly R. The optic, vestibulocochlear, and terminal-vomeronasal neural crest in staged human embryos. In: Second Symposium on Eye Structure. Rohen JW Ed., Stuttgart, Schattauer. 1965.

Okado N. Onset of synapse formation in the human spinal cord. J Comp Neurol 1981; 201: 211–219.

Oliver TR, Bhise A, Feingold E, Tinker S, Masse N, Sherman SL. Investigation of factors associated with paternal nondisjunction of chromosome 21. Am J Med Genet A. 2009; 149A(8): 1685-1690.

Olson LE, Richtsmeier JT, Leszl J, Reeves RH. A chromosome 21 critical region does not cause specific down syndrome phenotypes. Science 2004; 306:.687–690.

Olson LE, Roper RJ, Sengstaken CL, Peterson EA, Aquino V, Galdzicki Z, Siarey R, Pletnikov M, Moran TH, Reeves RH. Trisomy for the Down syndrome ''critical region'' is necessary but not sufficient for brain phenotypes of trisomic mice. Human Mol Genet 2007; 16: 774–782.

Oppenheim RW. Cell death during development of the nervous system. Annu Rev Neurosci 1991; 14: 453-501.

Orr-Weaver T. Meiotic nondisjunction does the two-step. Nat Genet 1996; 14: 374–376.

Paux E, Sourdille P, Salse J, Saintenac C, Choulet F, Leroy P, Korol A, Michalak M, Kianian S, Spielmeyer W, Lagudah E, Somers D, Kilian A, Alaux M, Vautrin S, Bergès H, Eversole K, Appels R, Safar J, Simkova H, Dolezel J, Bernard M, Feuillet C. A Physical Map of the 1-Gigabase Bread Wheat Chromosome 3B. Science 2008; 322 (5898): 101–104.

Pearson PL. In: Encyclopedia of Genetics. Brenner S, Miller JH Eds. Vol. 4. London: Academic Press. 2001, p.2056-2058.

Peer YVD, Taylor JS, Meyer A: The ghost of selection past: rates of evolution and functional divergence of anciently duplicated genes. J Mol Evol 2001; 53: 436-446.

Perrone-Bizzozero N, Bolognani F. Role of HuD and other RNA-binding proteins in neural development and plasticity. J Neurosci Res 2002; 68: 121–126.

Peyril A, Weitzdoerfer R, Gulesserian T, Fountoulakis M, Lubec G. Aberrant expression of signaling-related proteins 14-3-3 gamma and RACK1 in fetal Down syndrome brain (trisomoy 21). Electrophoresis 2002; 23: 152–157.

Pfeifer H, Conrad M, Roethlein D, Kyriakopoulos A, Brielmeier M, Bornkamm GW, Behne D. Identification of a specific sperm nuclei selenoenzyme necessary for protamine thiol cross-linking during sperm maturation. FASEB J 2001; 15: 1236–1238.

Porter AG, Janicke RU. Emerging roles of caspase-3 in apoptosis. Cell Death Differ 1999; 6: 99-104.

Prandini P, Deutsch S, Lyle R, Gagnebin M, Delucinge Vivier C, Delorenzi M, Gehrig C, Descombes P, Sherman S, Dagna Bricarelli F, Baldo C, Novelli A, Dallapiccola B, Antonarakis

SE.Natural gene-expression variation in Down syndrome modulates the outcome of gene-dosage imbalance. Am J Hum Genet 2007; 81(2): 252-263.

Prymakowska-Bosak M, Hock R, Catez F, Lim JH, Birger Y, Shirakawa H, Lee K, Bustin M. Mitotic phosphorylation of chromosomal protein HMGN1 inhibits nuclear import and promotes interaction with 14.3.3 proteins. Mol Cell Biol 2002; 22: 6809–6819.

Pucharcos C, Fuentes JJ, Casas C, de la Luna S, Alcabtara S, Arbones ML, Soriano E, Estivill X, Pritchard M. Alu-splice cloning of the human intersectin (ITSN), a putative multivalent binding protein expressed in proliferating and differentiating neurons and over-expressed in Down syndrome. Eur J Hum Genet 1999; 7: 704–712.

Puelles L, Kuwana E, Puelles E, Bulfone A, Shimamura K, Keleher J, Smiga S, Rubenstein J: Pallial and subpallial derivatives in the embryonic chick and mouse telencephalon, traced by the expression of the genes Dlx-2, Emx-2, Nkx-2.1, Pax-6 and Tbr-1. J Comp Neurol 2000; 424: 409-438.

Puglisi R, Tramer F, Panfili E, Micali F, Sandri G, Boitani C. Differential splicing of the phospholipid hydroperoxide glutathione peroxidase gene in diploid and haploid male germ cells in the rat. Biol Reprod 2003; 68: 405–411.

Qiu H, Dai H, Jain K, Shah R, Hong C, Pain J, Tian B, Vatner DE, Vatner SF, Depre C. Characterization of a novel cardiac isoform of the cell cycle-related kinase that is regulated during heart failure. J Biol Chem 2008; 283(32): 22157-22165.

Rachidi M, Lopes C. Mental retardation in Down syndrome: from gene dosage imbalance to molecular and cellular mechanisms. Neurosci Res 2007; 59(4): 349-369.

Ray R, Chen G, Vande Velde C, Cizeau J, Park JH, Reed JC, Gietz RD, Greenberg AF. BNIP3 heterodimerizes with Bcl-2/Bcl-X (L) and induces cell death independent of a Bcl-2 homology 3 (BH3) domain at both mitochondrial and nonmitochondrial sites. J Biol Chem 2000; 275: 1439–1448.

Reddy JV, Seaman MN. Vps26p, a component of retromer, directs the interactions of Vps35p in endosome-to-Golgi retrieval. Mol Biol Cell 2001; 12: 3242–3256.

Redies C, Puelles L: Modularity in vertebrate brain development and evolution. BioEssays 2001; 23: 1100-1111.

Reeves RH, Irving NG, Moran TH, Wohn A, Kitt C, Sisodia SS, Schmidt C, Bronson RT, Davisson MT. A mouse model for Down syndrome exhibits learning and behaviour deficits. Nat Genet 1995; 11: 177–184.

Risch N, Stein Z, Kline J, Warburton D. The relationship between maternal age and chromosome size in autosomal trisomy. Am J Hum Genet 1986; 39: 68–78.

Robinson BH, MacKay N, Petrova-Benedict R, Ozalp I, Coskun T, Stacpoole PW. Defects in the E2 lipoyl transacetylase and the X-lipoyl containing component of the pyruvate dehydrogenase complex in patients with lactic acidemia. J Clin Invest 1990; 85: 1821-1824.

Rondal JA, Perera J. In: Down Syndrome: Neurobehavioural Specificity. West Sussex, England. John Wiley & Sons Ltd. 2006.

Roper RJ, Baxter LL, Saran NG, Klinedinst DK, Beachy PA, Reeves RH. Defective cerebellar response to mitogenic Hedgehog signaling in Down syndrome mice. Proc Natl Acad Sci USA 2006; 103: 1452-1456.

Sago H, Carlson EJ, Smith DJ, Kilbridge J, Rubin EM, Mobley WC, Epstein CJ, Huang TT. Ts1Cje, a partial trisomy 16 mouse model for Down syndrome, exhibits learning and behavioral abnormalities. Proc Natl Acad Sci U S A 1998; 95: 6256–6261.

Saotome Y, Winter CG, Hirsh D. A widely expressed novel C2H2 zinc-finger protein with multiple consensus phosphorylation sites is conserved in mouse and man. Gene 1995; 152: 233-238.

Saran NG, Pletcher MT, Natale JE, Cheng Y, Reeves RH. Global disruption of the cerebellar transcriptome in a Down syndrome mouse model. Hum Mol Genet 2003; 12: 2013–2019.

Sawa A, Oyama F, Cairns NJ, Amano N, Matsushita M. Aberrant expression of bcl-2 gene family in Down's syndrome brains. Brain Res Mol Brain Res 1997; 48: 53-59.

Sawa A. Alteration of gene expression in Down's syndrome (DS) brains: its significance in neurodegeneration. J Neural Transm 2001; 57 Suppl.: 361–371.

Sawa A. Neuronal cell death in Down's syndrome. J Neural Transm 1999; 57: 87-97.

Schapiro MB, Haxby JV, GradyCL. Nature of mental retardation and dementia in Down syndrome: study with PET, CT, and neuropsychology. Neurobiol Aging 1992; 13: 723– 734.

Schena M, Shalon D, Davis RW, Brown PO. Quantitative monitoring of gene expression patterns with a complementary DNA microarray. Science 1995;270(5235): 467–470.

Schmidt-Sidor B, Wisniewski KE, Shepard TH, Sersen EA. Brain growth in Down syndrome subjects 1–22 weeks of gestation age and birth to 60 months. Clin Neuropathol 1990; 4: 181–190.

Schnabel D, Salas-Vidal E, Narvaez V, Sanchez-Carbente Mdel R, Hernandez-Garcia D, Cuervo R, Covarrubias L. Expression and regulation of antioxidant enzymes in the developing limb support a function of ROS in interdigital cell death. Dev Biol 2006; 291: 291–299.

Shinohara T, Tomizuka K, Miyabara S, Takehara S, Kazuki Y, Inoue J, Katoh M, Nakane H, Iino A, Ohguma A, Ikegami S, Inokuchi K, Ishida I, Reeves RH, Oshimura M. Mice containing a human chromosome 21 model behavioral impairment and cardiac anomalies of Down's syndrome. Hum Mol Genet 2001; 10: 1163-1175.

Simpson F, Hussain NK, Qualmann B, Kelly RB, Kay BK, McPherson PS, Schmid SL. SH3-domain-containing proteins function at distinct steps in clathrin-coated vesicle formation. Nat Cell Biol 1999; 1: 119–124.

Singer HS, Tiemeyer M, Hedreen JC, Gearthart J, Coyle JT. Morphological and neurochemical studies of embryonic brain in murine trisomy 16. Dev Brain Res 1984; 15: 155.

Sinha S. Anti-oxidant gene expression imbalance, aging and Down syndrome. Life Sci 2005; 76(12): 1407-1426.

Snustad DP, Simmons MJ. In: Principles of Genetics. 4th ed. Hoboken: John Wiley & Sons, Inc. 2006.

Stebbins G, Ledley Jr. Chromosomal evolution in higher plants. Nelson, London. 1972, p.18.

Stebbins GL. Variation and evolution in plants. Chapter XII: The Karyotype. Columbia University Press New York. 1950

Stein Z, Stein W, Susser M. Attrition of trisomies as a maternal screening device. An explanation of the association of trisomy 21 with maternal age. Lancet 1986; 8487: 944–947.

Stockli KA, Lottspeich F, Sendtner M, Masiakowski P, Carroll P, Gotz R, Lindholm D, Thoenen H. Molecular cloning, expression and regional distribution of rat ciliary neurotrophic factor. Nature 1989; 342: 920-923.

Storey JD, Madeoy J, Strout JL, Wurfel M, Ronald J, Akey JM. Gene-expression variation within and among human populations. Am J Hum Genet 2007; 80: 502–509.

Studer M, Popperl H, Marshall H, Kuroiwa A, Krumlauf R. Role of a conserved retinoic acid response element in rhombomere restriction of Hoxb-1. Science 1994; 265: 1728-1732.

Sudo T, Ishii A, Asami J, Uematsu Y, Saitoh M, Nakamura A, Tada N, Ohnuki T, Komurasaki T, Nakagawa J. Transgenic mice over-expressing dicarbonyl/L-xylulose reductase gene crossed with KK-Ay diabetic model mice: an animal model for the metabolism of renal carbonyl compounds. Exp Anim 2005; 54(5): 385-394.

Sugiura Y, Mori N. SCG10 expresses growth-associated manner in developing rat brain, but shows a different pattern to p19/stathmin or GAP-43. Dev Brain Res 1995; 90: 73–91.

Sylvester PE. Ammon's horn or hippocampus sclerosis without epilepsy in mental handicap. Br J Psychiatry 1984; 144: 538-541.

Takashima S, Becker LE, Armstrong DL, Chan F. Abnormal neuronal development in the visual cortex of the human fetus and infant with Down's syndrome. A quantitative and qualitative Golgi studies. Brain Res 1981; 225: 1–21.

Takebayashi H, Yoshida S, Sugimori M, Kosako H, Kominami R, Nakafuku M, Nabeshima Y. Dynamic expression of basic helix-loop-helix Olig family members: implication of Olig2 in neuron and oligodendrocyte differentiation and identification of a new member, Olig3. Mech. Dev. 2000; 99: 143–148.

Takikawa M, Kato S, Esumi H, Kurashima Y, Hirano A, Asayama K, Nakashima K, Ohama E. Temporospatial relationship between the expressions of superoxide dismutase and nitric oxide synthase in the developing human brain: immunohistochemical and immunoblotting analyses. Acta Neuropathol 2001; 102: 572–580.

Tamayo P, Slonim D, Mesirov J, Zhu Q, Kitareewan S, Dmitrovsky E, Lander ES, Golub TR, Interpreting patterns of gene expression with self-organizing maps: methods and application to hematopoietic differentiation. Proc Natl Acad Sci USA 1999; 96: 2907–2912.

Tanaka TS, Jaradat SA, Lim MK, Kargul GJ, Wang XH, Grahovac MJ, Pantano S, Sano Y, Piao Y, Nagaraja R, Doi H, Wood III WH, Becker KG, Ko MSH. Genome-wide expression profiling of mid-gestation placenta and embryo using 15,000 mouse developmental cDNA microarray, Proc Natl Acad Sci USA 2000; 97: 9127–9132.

Tanaka TS, Kunath T, Kimber WL, Jaradat SA, Stagg CA, Usuda M, Yokota T, Niwa H, Rossant J, Ko MSH. Gene expression profiling of embryo-derived stem cell reveals candidate genes associated with pluripotency and lineage specificity. Genome Res 2002; 12: 1921–1928.

Tejedor F, Zhu XM, Kaltenbach E, Ackermann A, Baumann A, Canal I, Heisenberg M, Fischbach KF, Pongs O. Minibrain: a new protein kinase family involved in postembryonic neurogenesis in Drosophila. Neuron 1995; 14: 287–301.

Thiselton DL, McDowall J, Brandau O, Ramser J, d'Esposito F, Bhattacharya SS, Ross MT, Hardcastle AJ, Meindl A. An integrated, functionally annotated gene map of the DXS8026-ELK1 interval on human Xp11.3-Xp11.23: potential hotspot for neurogenetic disorders. Genomics 2002; 79: 560-572.

Thomaidou D, Mione MC, Cavanagh JF, Parnavelas JG. Apoptosis and its relation to the cell cycle in the developing cerebral cortex. J Neurosci 1997; 17: 1075-1085.

Tomizuka K, Yoshida H, Uejima H, Kugoh H, Sato K, Ohguma A, Hayasaka M, Hanaoka K, Oshimura M, Ishida I. Functional expression and germline transmission of a human chromosome fragment in chimaeric mice. Nat Genet 1997; 16(2): 133-143.

Trowern AR, Laight R, MacLean N, Mann DA. Detection of neuron-specific protein gene product (PGP) 95 in the rat and zebrafish using anti-human PGP95 antobodies. Neuroscience 1996; 210: 21–24.

Tucker KL, Talbot D, Lee MA, Leonhardt H, Jaenisch R. Complementation of methylation deficiency in embryonic stem cells by a DNA methyltransferase minigene. Proc Natl Acad Sci USA 1996; 93: 12920-12925.

Uchida M, Tokunaga T, Aizawa S, Niwa K, Imai H. Isolation and nature of mouse embryonic stem cell line efficiently producing female germ-line chimeras. Anim Sci Technol (Jpn) 1995; 66: 361-367.

Unoki M, Okutsu J, Nakamura Y. Identification of a novel human gene, ZFP91, involved in acute myelogenous leukemia. Int J Oncol 2003; 22: 1217-1223.

Ursini F, Bindoli A. The role of selenium peroxidases in the protection against oxidative damage of membranes. Chem Phys Lipids 1987; 44: 255–276.

Ursini F, Heim S, Kiess M, Maiorino M, Roveri A, Wissing J, Flohe L. Dual function of the selenoprotein PHGPx during sperm maturation. Science 1999; 285: 1393–1396.

Vacík T, Ort M, Gregorová S, Strnad P, Blatny R, Conte N, Bradley A, Bures J, Forejt J. Segmental trisomy of chromosome 17: a mouse model of human aneuploidy syndromes. Proc Natl Acad Sci USA 2005; 102: 4500-4505.

Vanhoof G, Goossens F, de Meester I, Hendriks D, Scharpe S. Proline motifs in peptides and their biological processing. FASEBJ 1995; 9: 736–744.

Vasta V, Shimizu-Albergine M, Beavo JA. Modulation of Leydig cell function by cyclic nucleotide phosphodiesterase 8A. Proc Natl Acad Sci U S A 2006; 103(52): 19925-19930.

Ventura-Holman T, Seldin MF, Li WH, Maher JF. The murine Fem1 gene family: homologs of the Caenorhabditis elegans sex-determination protein FEM-1. Genomics 1998; 54: 221–230.

Vergnes L, Péterfy M, Bergo MO, Young SG, Reue K. Lamin B1 is required for mouse development and nuclear integrity. Proc Natl Acad Sci U S A 2004; 101(28): 10428-10433.

Visvanathan J, Lee S, Lee B, Lee JW, Lee SK. The microRNA miR-124 antagonizes the anti-neural REST/SCP1 pathway during embryonic CNS development. Genes Dev 2007; 21(7): 744-749.

Waardenburg PJ. Das menschliche Auge und seine Erbanlagen. The Hague: Martinus Nijhoff, 1932, p.44.

Wang CC, Chu KO, Chong WS, Li WY, Pang CP, Shum AS, Lau TK, Rogers MS. Tea epigallocatechin-3-gallate increases 8-isoprostane level and induces caudal regression in developing rat embryos. Free Radic Biol Med 2007; 43: 519–527.

Wang CC, Hwang JS, Rogers MS, Gojobori T, Ikeo K. Triple hybridization: a new implementation of microarray profiling, In: EUROMEDLAB 2003. Monduzzi Editore SpA Eds., MEDIMOND, Italy. 2003, p. 975–978.

Wang CC, Kadota M, Nishigaki R , Kazuki Y, Shirayoshi Y, Rogers MS, Gojobori T, Ikeo K, Oshimura M. Molecular hierarchy in neurons differentiated from mouse ES cells containing a single human chromosome 21. Biochem Biophys Res Commun 2004; 314: 335-350.

Wang CC, Shum ASW, Leung MBW, Hwang JS, Rogers MS, Gojobori T, Ikeo K. Microarray analysis of differential gene expression in embryos of diabetic mice. In: EUROMEDLAB 2003. Monduzzi Editore SpA (Eds.), MEDIMOND, Italy. 2003, p.979–981.

Wang Z, Gerstein M, Snyder M. RNA-Seq: a revolutionary tool for transcriptomics. Nature Reviews Genetics 2009; 10: 57-63.

Webster PJ, Liang L, Berg CA, Lasko P, Macdonald PM. Translational repressor bruno plays multiple roles in development and is widely conserved. Genes Dev 1997; 11: 2510–2521.

Wei L, Ding D, Salvi R. Salicylate-induced degeneration of cochlea spiral ganglion neurons-apoptosis signaling. Neuroscience 2010; 168(1): 288-299.

Weitzdoerfer R, Dierssen M, Fountoulakis M, Lubec G. Fetal life in Down syndrome starts with normal neuronal density but impaired dendritic spines and synaptosomal structure. J Neural Transm 2001; 61 Suppl.: 59–70.

Weitzdoerfer R, Fountoulakis M, Dierssen M, Lubec G. Aberrant expression of dihydropyrimidinase-related proteins-2-3, and -4 in fetal Down syndrome brain. J Neural Transm 2001; 61 Suppl.: 95–107.

Weitzdoerfer R, Stolzlechner D, Dierssen M, Ferreres J, Fountoulakis M, Lubec G. Reduction of nucleoside diphosphate kinase B, Rab GDP-dissociation inhibitor beta and histidine triad nucleotidebinding protein in fetal Down syndrome brain. J Neural Transm 2001; 61: 347–359.

White MJD. The chromosomes. 6th ed, Chapman & Hall, London. 1973.

Wilkinson DG. (Ed) In: Situ Hybridisation, IRL Press, Oxford, 1992, p.75–83.

Wilkinson JC, Richter BW, Wilkinson AS, Burstein E, Rumble JM, Balliu B, Duckett CS. VIAF, a conserved inhibitor of apoptosis (IAP)-interacting factor that modulates caspase activation. J Biol Chem 2004; 279(49): 51091-51099.

Williams GC. Adaptation and natural selection: a critique of some current evolutionary thought. Princeton. In: Evolutionary adaptation is a phenomenon of pervasive importance in biology. 1966, p5.

Williamson DJ, Banik-Maiti S, DeGregori J, Ruley HE. hnRNP C is required for postimplantation mouse development but Is dispensable for cell viability. Mol Cell Biol 2000; 20: 4094–4105.

Wilson MD, Barbosa-Morais NL, Schmidt D, Conboy CM, Vanes L, Tybulewicz VL, Fisher EM, Tavaré S, Odom DT. Species-specific transcription in mice carrying human chromosome 21. Science 2008; 322(5900): 434-438.

Wisniewski KE. Down syndrome children often have brain with maturation delay, retardation of growth, and cortical dysgenesis. Am J Med Genet 1990; 7: 274–281.

Wurster DH, Benirschke K. Indian Muntjac, Muntiacus muntjak: a deer with a low diploid number. Science 1970; 168: 1364-1366.

Wyngaard GA, Gregory TR. Temporal control of DNA replication and the adaptive value of chromatin diminution in copepods. J Exp Zool. 2001; 291: 310–316.

Xiong SB, Van Pelt CS, Elizondo-Fraire AC, Liu G, Lozano G. Synergistic roles of Mdm2 and Mdm4 for p53 inhibition in central nervous system development. Proc Natl Sci USA 2006; 103(9): 3226-3231.

Yang L, Xia L, Wu DY, Wang H, Chansky HA, Schubach WH, Kickstei DD, Zhang Y. Molecular cloning of ESET, a novel histone H3-specific methyltransferase that interacts with ERG transcription factor. Oncogene 2002; 21: 148–152.

Yant LJ, Ran Q, Rao L, Van Remmen H, Shibatani T, Belter JG, Motta L, Richardson A, Prolla TA. The selenoprotein GPX4 is essential for mouse development and protects from radiation and oxidative damage insults. Free Radic Biol Med 2003; 34: 496–502.

Yoo BC, Fountoulakis M, Dierssen M, Lubec G. Expression patterns of chaperone proteins in cerebral cortex of the fetus with Down syndrome: dysregulation of T-complex protein 1. J Neural Transm 2001; 61 Suppl.: 321–334.

Yoshida T, Makino Y, Tamura T. Association of the rat heterogeneous nuclear RNA-ribonucleoprotein F with TATA-binding protein. FEBS Lett 1999; 457: 251–254.

Yuan H, Zhang P, Qin L, Chen L, Shi S, Lu Y, Yan F, Bai C, Nan X, Liu D, Li Y, Yue W, Pei X. Overexpression of SPINDLIN1 induces cellular senescence, multinucleation and apoptosis. Gene 2008; 410(1): 67-74.

Zhang KM, Wang YF, Huo R, Bi Y, Lin M, Sha JH, Zhou ZM. Characterization of Spindlin1 isoform2 in mouse testis. Asian J Androl 2008; 10(5): 741-748.

Zhang M, Xu JT, Zhu X, Wang Z, Zhao X, Hua Z, Tao YX, Xu Y. Postsynaptic density-93 deficiency protects cultured cortical neurons from N-methyl-D-aspartate receptor-triggered neurotoxicity. Neuroscience 2010; 166(4): 1083-1090.

Zheng C, Byers B. Oocyte selection: a new model for the maternal-age dependence of Down syndrome. Hum Genet 1992; 90: 1–6.

Zheng TS, Hunot S, Kuida K, Flavell RA. Caspase knockouts: matters of life and death. Cell Death Differ 1999; 6: 1043-1053.

Zhou Q, Anderson DJ. The bHLH transcription factors OLIG2 and OLIG1 couple neuronal and glial subtype specification. Cell 2002; 109: 61–73.

香港中文大學醫學院
Faculty Of Medicine
The Chinese University Of Hong Kong

醫院管理局
新界東醫院聯網
Hospital Authority
New Territories East Cluster

Joint CUHK – New Territories East Cluster Clinical Research Ethics Committee
香港中文大學--新界東醫院聯網 臨床研究倫理 聯席委員會

Secretary of the Clinical Research Ethics Committee c/o
Centre for Clinical Trials and Epidemiological Research, Faculty of Medicine, The Chinese University of Hong Kong, 5th Floor, School of Public Health, Prince of Wales Hospital.
Tel : (852) 2252 8717 Fax : (852) 2645 3098

To: Prof. Chi Chiu Wang
Dept. of Obstetrics & Gynaecology
Prince of Wales Hospital

19 May 2003

Ethics Approval of Research Protocol

CREC Ref:	**CRE-2003.139**
Date of Approval:	**19 May 2003***
Protocol Title:	**Molecular Neurogenesis in Down's Syndrome**
Investigator(s):	**Chi Chiu WANG, Michael Scott ROGERS and Kazuho IKEO and Takashi GOJOBORI**
Proposed Start Date:	**30 June 2003**
Proposed End Date:	**30 June 2004**

I write to inform you that ethics approval has been given to you to conduct the captioned study in accordance with the following document(s) submitted:

- Protocol
- Patient Informed Consent form in English and Chinese version

This ethics approval* will be valid for 12 months. Application for further renewal can be made by submitting the Renewal and Research Progress Report Form to the CREC. It will be much appreciated if the completion of the project will be reported to the Committee in due course.

The Joint CUHK-NTEC Clinical Research Ethics Committee serves to ensure that research complies with the Declaration of Helsinki, ICH GCP Guidelines, local regulations, HA and University policies.

(Prof. Joseph Lau)
Secretary, Joint CUHK-NTEC
Clinical Research Ethics Committee

c.c. Mrs. Alice Yip – RTAO (Ref: Direct Grant 2002/2003)
Encl: CREC/CT0001 – w.e.f. 4/2003 (for HA employee concerned ONLY)
JL/ci

香港中文大學醫學院
Faculty Of Medicine
The Chinese University Of Hong Kong

醫院管理局
新界東醫院聯網
Hospital Authority
New Territories East Cluster

Joint The Chinese University of Hong Kong – New Territories East Cluster Clinical Research Ethics Committee
香港中文大學–新界東醫院聯網 臨床研究倫理 聯席委員會

Secretary of the Clinical Research Ethics Committee c/o Centre for Epidemiology and Biostatistics,
Faculty of Medicine, The Chinese University of Hong Kong, 5th Floor, Postgraduate Education Centre, Prince of Wales Hospital.
Tel : (852) 2252 8717 ~~Fax : (852) 2615 3098~~ Fax No.: 2646 6653

To: Prof. Chi Chiu WANG (Principal Investigator)
Dept. of Obstetrics and Gynaecology
Prince of Wales Hospital

5 October 2004

Ethics Approval of Research Protocol

CREC Ref. No.:	**CRE-2004.330**
Date of Approval:	**05 October 2004***
Protocol Title:	**Evaluation of Functional Genetic Analysis in Fetus With Down's Syndrome for Prenatal Genetic Counseling**
Investigator(s):	**PWH/ TYH - Chi Chiu WANG, Elizabeth Tak Kwong LAU, Tze Kin LAU and Mary Hoi Yin TAN**

I write to inform you that ethics approval has been given to you to conduct the captioned study in accordance with the following document(s) submitted:

- Protocol
- Patient Information Sheet in English and Chinese Version
- Patient Informed Consent Form in English and Chinese Version

This ethics approval* will be valid for 12 months. Application for further renewal can be made by submitting the Renewal and Research Progress Report Form to the CREC. It will be much appreciated if the completion of the project will be reported to the Committee in due course.

The Joint CUHK-NTEC Clinical Research Ethics Committee serves to ensure that research complies with the Declaration of Helsinki, ICH GCP Guidelines, local regulations, HA and University policies.

(Prof. Joseph Lau)
Secretary, Joint CUHK-NTEC
Clinical Research Ethics Committee

c.c. Mrs. Alice Yip – RTAO (Ref. HHSRF)
JL/ci

香港大學
University of Hong Kong
香港大學及醫管局港島西醫院聯網研究倫理委員會

醫院管理局
HOSPITAL AUTHORITY

Institutional Review Board of the University of Hong Kong/
Hospital Authority Hong Kong West Cluster (HKU/HA HKW IRB)

Address: Rm 901, Administration Block, QMH Tel 2855 3351 2855 3923 2855 4086 Fax 2855 4735

Dr. Cora Ngai
Dept. of O&G
Queen Mary Hospital

02-Nov-04

Dear Dr. Ngai,

IRB Reference Number: **UW 04-258 T/580**

The HKU/HA HKW IRB* is authorized by the Cluster Chief Executive [and the University of Hong Kong, Faculty of Medicine] to review and monitor clinical research. It serves to ensure that research complies with the Declaration of Helsinki and acts in accordance to ICH GCP guidelines, local regulations and HA [and the University] policy. It has the authority to approve, require modifications in (to secure approval), or disapprove research. This Committee has power to terminate/suspend a research at any time if there is evidence to indicate that the above principles and requirements have been violated.

Professor CL Lai, Chairman and Dr. Kathryn Tan, Deputy Chairman of the HKU/HA HKW IRB have reviewed/approved, as appropriate, your submission on the date shown below by an expedited process. You are also required to adhere to the conditions listed.

Date of expedited review	:	02-11-2004 (Date/Month/Year)
Protocol title	:	Evaluation of functional genetic analysis in fetus with Down's syndrome (DS) for prenatal counselling
Study site(s)	:	Tsan Yuk Hospital
Document(s) approved	:	01. Clinical research ethics review application form
	:	02. Amended study protocol version 2 dated 24/09/2004
	:	03. Amended patient information sheet; version 2 - English and Chinese
	:	04. Consent form (for fetal/blood cell study); version 2 - English and Chinese
	:	05. Consent form (for termination of pregnancy); version 2 - English and Chinese
Document(s) reviewed	:	06. Short CV of Co-investigator (Dr. Ronald Wang)

Conditions : 1. Do not deviate from, or make changes to the study protocol without prior written IRB approval, except when it is necessary to eliminate immediate hazards to research subjects or when the change involves only logistical or administrative issues.

2. Report the following to HKU/HA HKW IRB: (i) study protocol or consent document change (use 'HKU/HA HKW IRB RE001F7'), (ii) serious adverse event (use 'HKU/HA HKW IRB RE001F8'). (iii) study progress (use 'HKU/HA HKW IRB RE001F9a')* (iv) new information that may be relevant to a subject's willingness to continue participation in the study.

3. Report first study progress to HKU/HA HKW IRB at a 12-monthly interval until study closure.

(Mr. Chris Yip)
Secretary
HKU/HA HKW IRB

c.c.: Dr. Ronald Wang, Assistant Professor, Dept O&G, Prince of Wales Hospital

THE CHINESE UNIVERSITY OF HONG KONG

MEMO

	Professor Christopher J Haines Chairman		Professor WANG Chi Chiu Dept of Obstetrics & Gynaecology
From	Animal Experimentation Ethics Committee	*To*	Faculty of Medicine
Ref.			
Tel. No.	2632 2800	*Your Ref.*	
Date	June 5, 2003	*dated*	

Animal Experimentation Ethics Approval

I am pleased to confirm that the Animal Experimentation Ethics Committee agrees to grant ethical approval for your research project entitled "Molecular neurogenesis in Down's Syndrome" (Ref No. 03/008/MIS).

Thank you for your attention.

Professor Christopher J Haines

cc Dr Anthony James, Laboratory Animal Services Centre

CJH/JC/cp

THE CHINESE UNIVERSITY OF HONG KONG
UNIVERSITY SAFETY & ENVIRONMENT OFFICE

Tel: 2609 7864
Fax: 2603 6862

MEMO

To : Prof. Chi Chiu Wang
Department of Obstetrics & Gynaecology

c.c. : Research & Technology Administration Office

From : S.K. Lam
Safety Manager & Chief Laboratory Safety Officer

Date : 6 May 2003

Subject: Your Direct Grant Application for 2003/2004
"Molecular Neurogenesis of Down's Syndrome"

Dear Prof. Wang

I am pleased to advise that the following safety approvals have been allocated to the above grant.

(a) Chemical Safety: approved/C/DG 2003/2004
(b) Biological Safety: not required
(c) Ionizing Radiation Safety: not required
(d) Non-ionizing Radiation Safety: not required

The assessments have been made principally on the information supplied and signed for by yourself.

The experimentation stages etc will always be subject to strict safety, environmental and waste requirements. You are encouraged to approach the USEO for any assistance should you feel it is required.

May I take this opportunity of wishing you success with the above project.

S.K. Lam
Safety Manager & Chief Laboratory Safety Officer

SKL/jk